



University
of Glasgow

Duffy, Margaret R. (2012) *Investigation and manipulation of adenovirus interactions with host proteins*. PhD thesis.

<http://theses.gla.ac.uk/3582/>

Copyright and moral rights for this thesis are retained by the author

A copy can be downloaded for personal non-commercial research or study

This thesis cannot be reproduced or quoted extensively from without first obtaining permission in writing from the Author

The content must not be changed in any way or sold commercially in any format or medium without the formal permission of the Author

When referring to this work, full bibliographic details including the author, title, awarding institution and date of the thesis must be given

**Investigation and manipulation of adenovirus
interactions with host proteins**

Margaret R. Duffy

BSc. (Hons)

**Submitted in fulfilment of the requirements for the
Degree of Doctor of Philosophy**

Institute of Cardiovascular and Medical Sciences
College of Medicine, Veterinary & Life Sciences
University of Glasgow

May 2012

© Margaret R. Duffy 2012



Author's Declaration

I declare that this thesis has been written entirely by myself and is a record of work performed by myself with the exception of Home Office licensed procedures (Dr. Alan Parker and Dr. Katie White), Figure 3.10, Figure 3.11 (Prof. John McVey) and Figure 5.21 (Dmytro Kovalskyy). This thesis has not been submitted previously for a higher degree. The research was carried out in the Institute of Cardiovascular and Medical Sciences, University of Glasgow, under the supervision of Prof. Andrew Baker.

Margaret R. Duffy

May 2012

Acknowledgements

Firstly, I would like to thank my supervisor Prof. Andy Baker for all his advice and guidance throughout my PhD. I'm extremely grateful to have had such a great opportunity and good experiences over the past three and a half years.

I would like to especially thank Dr. Alan Parker and Dr. Angela Bradshaw for the support they have given me from the very first day I started my project to the last. They were always there to offer advice and I'm so appreciative to them both for all their help.

Thanks to all the other members of the Baker group, in particular Lynda Coughlan, Nicola Britton and Gregor Aitchison for always offering a helping hand. I am also very grateful to Prof. John McVey for his advice and for taking the time to teach me new techniques.

Thanks to the girls in the office, Lynsey Howard, Wendy Crawford, Aiste Monkeviciute and especially Emily Ord, whose friendship, even in the case of a lunch time emergency, made the worst days something to laugh at! To all my friends and family who have always been there for me.

Most of all thank you Dave, for the constant ability to put a smile on my face, for the hugs, and for supporting me so much throughout my PhD. You have been amazing.

This thesis is dedicated to my Mam and Dad for their unwavering faith in me always. Thank you both for everything.

Table of Contents

Author's Declaration	ii
Acknowledgements	iii
Table of Contents	iv
List of Figures	x
List of Tables.....	xiii
List of Publications	xiv
List of Abbreviations.....	xv
Abstract	xxiv
Chapter 1	1
1.1 Introduction.....	2
1.2 Adenoviruses	5
1.3 Adenoviral structure	6
1.3.1 Outer capsid	6
1.3.2 Inner core	8
1.4 Ads as gene delivery vectors	10
1.5 Ad gene therapy – the highs and the lows	12
1.6 Ad interactions with host proteins	15
1.6.1 Coxsackie virus and adenovirus receptor.....	15
1.6.2 The role of the immune system.....	18
1.6.2.1 Innate immunity	18
1.6.2.2 Adaptive immunity	20
1.6.3 Blood components.....	21
1.6.3.1 Erythrocytes	21
1.6.3.2 Platelets	23
1.6.3.3 Lactoferrin.....	24
1.6.3.4 Complement proteins	24
1.6.3.5 Blood factors	25
1.7 A critical role for coagulation factor X in determining the Ad5 liver tropism.....	28
1.8 FX Gla domain mediates binding to Ad5	29
1.9 FX binds directly to the Ad5 hexon.....	30
1.10 FX binds to hexon HVRs.....	31
1.11 Ad:FX complex binding to hepatocytes	34
1.12 Post-binding events via the FX infectivity pathway.....	35
1.13 Methods of manipulation of the Ad:FX interaction	36

1.13.1	Genetic modification of the Ad hexon to prevent FX binding.....	36
1.13.2	Polymer-conjugated Ad complexes shield the vector from FX.....	38
1.13.3	Adaptor molecules	40
1.13.4	Pharmacological agents to prevent Ad transduction.....	40
1.14	Future of Ad-based gene therapy.....	43
1.15	Aims of this thesis	44
Chapter 2	45
2.1	Chemicals	46
2.2	Proteins	46
2.3	Plasmid DNA constructs.....	46
2.4	Antibodies.....	46
2.5	Cell culture materials.....	47
2.6	Tissue culture.....	47
2.7	Maintenance of established cell lines	47
2.8	Cryopreservation.....	47
2.9	Cloning procedures.....	48
2.9.1	Plasmid preparation.....	48
2.9.2	Small scale preparation of plasmid DNA	49
2.9.3	Large scale preparation of plasmid DNA.....	49
2.9.4	Generation of glycerol stocks.....	50
2.9.5	Site-directed polymerase chain reaction mutagenesis.....	50
2.9.5.1	Step 1: Plasmid preparation	52
2.9.5.2	Step 2: Temperature cycling	52
2.9.5.3	Step 3: Digestion	53
2.9.5.4	Step 4: Transformation.....	53
2.9.6	Design of mutagenic oligonucleotide primers	53
2.9.7	Cloning FX SP mutant cDNA into pcDNA3.1+zeocin	54
2.9.7.1	Step 1: Excision of FX SP mutant cDNA from the pMK-RQ_FX SP mutant plasmid.....	55
2.9.7.2	Step 2: Ligation of the FX SP mutant cDNA into the pSCb plasmid.....	56
2.9.7.3	Step 3: Excision of the FX SP mutant cDNA from the pSCb plasmid and ligation into pcDNA3.1+zeocin	57
2.9.7.4	Step 4: Investigating the efficiency of FX SP mutant cDNA ligation into pcDNA3.1+zeocin.....	57
2.10	DNA sequencing.....	59
2.10.1	Sequencing PCR	59
2.10.2	Sequencing reaction purification.....	59

2.11	Recombinant FX production	60
2.11.1	Differential pH transient transfections	60
2.11.2	Determining optimal concentration of zeocin.....	60
2.11.3	Generation of FX stable cell lines.....	60
2.12	Human FX ELISA	61
2.13	rFX purification	62
2.14	Activation of rFX.....	62
2.15	Surface plasmon resonance analysis.....	63
2.15.1	Analysis of purified FX fractions.....	63
2.15.2	Analysis of rFX binding to Ad5 hexon.....	63
2.15.3	Analysis of pharmacological compounds binding to FX and Ad5 binding to FX in the presence of compounds.....	64
2.16	Protein extraction.....	64
2.17	Determination of protein concentration in cells	64
2.18	Electrophoresis	65
2.18.1	SDS-PAGE.....	65
2.18.2	Coomassie blue staining.....	65
2.18.3	Western immunoblotting.....	65
2.19	Adenovirus production	66
2.19.1	Recombinant Ad5 production	66
2.19.2	Ad5 purification using caesium chloride (CsCl) gradient.....	67
2.20	Virus titration by end-point dilution assay	68
2.21	Quantification of virus particles	68
2.22	Adenovirus infection	69
2.22.1	Virus cell binding.....	69
2.22.2	DNA extractions.....	69
2.22.3	Quantitative PCR for quantifying Ad genomes	70
2.22.4	Fluorescence activated cell sorting (FACS) analysis of virus:cell binding	70
2.22.5	Virus cell transduction in the presence of rFX.....	71
2.22.6	Virus cell transduction in the presence of pharmacological agents.....	71
2.22.7	β -galactosidase transgene quantification	71
2.22.8	GFP transgene quantification.....	72
2.22.9	Luciferase transgene quantification	72
2.23	Investigating intracellular Ad5 transport.....	72
2.23.1	Fluorescently labelling vectors	72
2.23.2	Cell trafficking of fluorescently labelled vectors.....	73
2.24	Immunocytochemistry	74

2.25	Quantification of Ad5 colocalisation with the MTOC	75
2.26	Analysis of Ad5 attachment <i>ex vivo</i>	75
2.27	MTT assay.....	75
2.28	RNA extractions	76
2.29	DNase treatment of RNA.....	76
2.30	cDNA synthesis	76
2.30.1	QPCR for quantification of cellular genes.....	77
2.31	High throughput screening	77
2.31.1	Compound library	77
2.31.2	Production of compound library dilution plates.....	78
2.31.3	Seeding cells.....	78
2.31.4	Screening the compound library	78
2.31.5	Fixing cells from the HTS screen.....	79
2.31.6	Using the IN Cell Analyser 2000 to capture screen images.....	81
2.31.7	Analysing the screen images and acquiring screen data	82
2.32	Animals.....	83
2.32.1	<i>In vivo</i> administration of Ad5	83
2.32.2	Quantification of adenoviral transgene expression.....	84
2.33	Statistical analysis.....	84
Chapter 3	85
3.1	Introduction.....	86
3.2	Results	92
3.2.1	Generation of FX plasmid constructs.....	92
3.2.2	Cloning FX SP mutant into pcDNA3.1+zeocin.....	94
3.2.3	Producing recombinant FX protein.....	96
3.2.4	Purification and validation of rFX protein.....	98
3.2.5	Assessment of the biological activity of rFX.....	98
3.2.6	Mutating residues in the FX HBPE has no effect on FX binding to Ad5 hexon	102
3.2.7	FX dose response	102
3.2.8	Effect of the FX SP domain mutations on Ad5:FX binding to HSPGs	106
3.2.9	The FX SP domain mutations decrease FX-mediated Ad5 cell binding	106
3.2.10	The FX SP domain mutations inhibit FX-mediated Ad5 cell binding, internalisation and cytosolic transport	110
3.2.11	The FX SP domain mutations decrease FX-mediated Ad5 transduction compared to WT rFX	113

3.2.12	Effects of single and double amino acid mutations in the SP domain on FX-mediated Ad5 gene transfer	115
3.2.13	Role of HBPE on FX-mediated cell binding <i>ex vivo</i>	116
3.3	Discussion.....	120
Chapter 4	127
4.1	Introduction.....	128
4.2	Results	132
4.2.1	Role for PKA, PI3K and p38MAPK in FX-mediated Ad5 intracellular transport.....	132
4.2.2	Screening a library of kinase inhibitors for effects on FX-mediated Ad5 gene transfer.....	132
4.2.3	Effect of ER-27319 on FX-mediated Ad5 cell attachment and intracellular transport.....	139
4.2.4	Effect of the Syk inhibitor BAY 61-3606 on FX-mediated Ad5 infectivity ..	144
4.2.5	Syk gene and protein expression.....	144
4.2.6	Mechanism of action of ER-27319	148
4.2.7	ITAM-containing viral proteins	149
4.2.8	ITAM containing cellular proteins.....	152
4.2.9	Ezrin, radixin and moesin gene expression.....	153
4.2.10	Effects of ER-27319 on ERM protein expression	154
4.3	Discussion.....	159
Chapter 5	169
5.1	Introduction.....	170
5.2	Results	175
5.2.1	Design and optimisation of an assay compatible with HTS	175
5.2.2	Plates – 384-well assay format to increase assay robustness.....	175
5.2.3	Cells – optimal seeding densities	175
5.2.4	Control-based method of normalisation.....	176
5.2.5	Designing robotic liquid handling protocols.....	176
5.2.6	Design of imaging analysis conditions	179
5.2.6.1	Acquiring	179
5.2.6.2	Analysis.....	180
5.2.7	Assay validation.....	184
5.2.8	HTS to identify inhibitors of FX-mediated Ad5 gene transfer	188
5.2.9	Enhancers of FX-mediated Ad5 gene transfer	188
5.2.10	HTS quality control.....	192

5.2.11	Secondary screening of compounds.....	195
5.2.12	Effects of preliminary hits on cell viability	195
5.2.13	Manual testing of preliminary HTS hits.....	199
5.2.14	IC ₅₀ determination of the candidate hit compounds.....	202
5.2.15	Effect of candidate hit compounds on FX-mediated Ad5 intracellular transport	202
5.2.16	Structural analysis and determination of hit compounds	206
5.2.17	Assessing the activity of hit T5424837 analogues.....	209
5.2.18	Assessing the activity of hit T5660138 analogues.....	213
5.2.19	Assessing the activity of hit T5550585 analogues.....	217
5.2.20	Investigation of compound effect on Ad5:FX binding	221
5.2.21	Effect of hit compounds on FX-mediated Ad5 cellular binding.....	224
5.2.22	Effect of compounds on CAR-mediated Ad5 transduction	224
5.2.23	Effect of compounds on Ad5 transduction <i>in vivo</i>	226
5.2.24	Effect of compounds on Ad5 liver accumulation <i>in vivo</i>	226
5.3	Discussion.....	229
Chapter 6	237
List of References	245
Appendices	277

List of Figures

Figure 1.1. Gene therapy clinical trials summarised by indication.....	4
Figure 1.2. Gene therapy clinical trials summarised by vector.....	5
Figure 1.3. Ad capsid structure.	7
Figure 1.4 Facets of the Ad icosahedron capsid	8
Figure 1.5. Transcription of the Ad genome.....	9
Figure 1.6. Liver cells and Ad5 hepatic uptake.	14
Figure 1.7. Critical features of the Ad fiber.....	17
Figure 1.8. <i>In vivo</i> Ad5 interactions with host factors.	27
Figure 1.9. Coagulation factor X.....	28
Figure 1.10. Analysis of Ad5 hexon binding to FX by cryoelectron microscopy.	32
Figure 1.11. Model view of Ad5:FX interaction.	33
Figure 1.12. Tropism modifying strategies.....	42
Figure 2.1 Overview of the Stratagene QuikChange site-directed mutagenesis method..	52
Figure 2.2. Strategy for cloning FX SP mutant into pcDNA3.1+zeocin.	58
Figure 2.3. Purification of Ad5 by CsCl gradient.	68
Figure 2.4. SAMI Workstation EX Software screening protocols.....	80
Figure 2.5. Determining the field of view using the IN Cell Analyser 2000.....	81
Figure 2.6. IN Cell Analyser 2000 preview scan.	82
Figure 3.1. Coagulation cascade.	87
Figure 3.2. Mechanism of action of heparin.	88
Figure 3.3. Residues to which NAPc2 and Ixolaris bind.	91
Figure 3.4. Amino acids residues for mutagenesis studies.	93
Figure 3.5. Cloning of the FX SP mutant sequence into pcDNA3.1+zeocin.	95
Figure 3.6. Generating stable cell lines.....	97
Figure 3.7. Purification and validation of rFX.....	99
Figure 3.8. Validation of purified rFX.....	100
Figure 3.9. Activation of rFX.....	101
Figure 3.10. HBPE mutations have no effect on rFX binding to Ad5 hexon.	103
Figure 3.11. Anti-FX antibody binding to rFX bound to Ad5 hexon.	104
Figure 3.12. FX dose response.....	105
Figure 3.13. Role of the HBPE in the FX SP domain in Ad5 binding to HSPGs.....	108
Figure 3.14. Role of the FX SP domain in Ad5 cell binding	109

Figure 3.15. Role of the FX HBPE in Ad5 cellular trafficking.	111
Figure 3.16. Role of the FX HBPE in Ad5 accumulation at the MTOC.	112
Figure 3.17. Role of the FX HBPE in Ad5 gene transfer.	114
Figure 3.18. Ribbon diagram of the FX.	115
Figure 3.19. Effect of single and double point HBPE mutations on Ad5 gene transfer. ...	117
Figure 3.20. Effect of mutations on Ad5 binding to liver sections <i>ex vivo</i>	118
Figure 3.21. Quantification of Ad5 binding to liver sections <i>ex vivo</i>	119
Figure 3.22. Sequence alignments of human FX, FVII, FIX and protein C.	125
Figure 3.23. Sequence alignments of human FX and murine FX.	126
Figure 4.1. Ad5 infectivity pathway.	131
Figure 4.2. Ad5 transport in the presence of PKA, PI3K and p38 MAPK inhibitors.	134
Figure 4.3. Effect of kinase inhibitors on FX-mediated Ad5 gene transfer.	135
Figure 4.4. Effect of ER-27319 on cell viability after 48 h.	138
Figure 4.5. Effect of ER-27319 on Ad5 binding to SKOV3 cells.	140
Figure 4.6. Effect of ER-27319 on FX-mediated Ad5 trafficking in A549 cells.	141
Figure 4.7. Effect of ER-27319 on FX-mediated Ad5 trafficking in SKOV3 cells.	142
Figure 4.8. Effect of ER-27319 on Ad5 colocalisation with the MTOC.	143
Figure 4.9. Effect of ER-27319 on cell viability after 4 h.	143
Figure 4.10. Effect of BAY 61-3606 on FX-mediated Ad5 intracellular transport.	145
Figure 4.11. Effect of BAY 61-3606 on FX-mediated Ad5 transduction.	146
Figure 4.12. Syk kinase expression in SW620, A549 and SKOV3 cells.	147
Figure 4.13. Mechanism of action of ER-27319 in mast cells.	148
Figure 4.14. Ad5 hexon ITAMs.	151
Figure 4.15. Schematic of ERM activation.	153
Figure 4.16. ERM gene expression in A549 and SKOV3 cells.	155
Figure 4.17. Ezrin, radixin and moesin protein expression in SKOV3 cells.	156
Figure 4.18. Effect of ER-27319 on ERM proteins expression and FX-mediated Ad5 cellular trafficking.	157
Figure 4.19. Spleen tyrosine kinase.	161
Figure 4.20. Compound structure.	168
Figure 5.1. Steps of the HTS process.	171
Figure 5.2. Effect of DMSO on SKOV3 cell viability and assay activity.	178
Figure 5.3. Assay plate layout.	179
Figure 5.4. Design of image analysis conditions – signal window.	181

Figure 5.5. Design of image analysis conditions – defining non viable cells.....	182
Figure 5.6. Testing screening control conditions.....	183
Figure 5.7. Principle component analysis of the compound library.	186
Figure 5.8. 80 compound screen in SKOV3 cells to validate the HTS method.....	187
Figure 5.9. HTS of the Pharmacological Diversity Drug-like Set.	189
Figure 5.10. HTS inhibitors of FX-mediated Ad5 gene transfer.	190
Figure 5.11. HTS enhancers of FX-mediated Ad5 gene transfer.....	191
Figure 5.12. Plate positional effects.....	194
Figure 5.13. Secondary screen.	196
Figure 5.14. Preliminary hits.....	197
Figure 5.15. Effects of preliminary hits on cell viability.	198
Figure 5.16. Manual testing of preliminary hits.....	200
Figure 5.17. Structures of the 5 candidate hit compounds.....	201
Figure 5.18. IC ₅₀ determination of the candidate hit compounds.	203
Figure 5.19. Effects of candidate hits on FX-mediated Ad5 intracellular trafficking.	204
Figure 5.20. Effect of candidate hits on Ad5 colocalisation with the MTOC.	205
Figure 5.21. Structural alignments.....	208
Figure 5.22. Assessing the activity of T'837 analogues.	210
Figure 5.23. Chemical structures of T'837 analogues.	211
Figure 5.24. IC ₅₀ determination of compound T'837 and analogues.....	212
Figure 5.25. Assessing the activity of T'138 analogues.	214
Figure 5.26. Chemical structures of T'138 analogues.	215
Figure 5.27. IC ₅₀ determination of compound T'138 and analogues.....	216
Figure 5.28. Assessing the activity of T'585 analogues.	218
Figure 5.29. Chemical structures of T'585 analogues.	219
Figure 5.30. IC ₅₀ determination of compound T'585 and analogue.....	220
Figure 5.31. SPR analysis of compound binding to FX.....	222
Figure 5.32. Effect of compounds on Ad5 binding to FX by SPR.	223
Figure 5.33. Effect of compounds on FX-mediated Ad5 binding to SKOV3 cells and transduction in A549 cells	225
Figure 5.34. Effect of hit compounds on <i>in vivo</i> Ad5 transduction in MF1 mice.	227
Figure 5.35. Liver Ad5 accumulation and transduction at 48 h <i>in vivo</i>	228
Figure 5.36. Cell-based assay development.....	230
Figure 5.37. Graphical review of the HTS.....	232

List of Tables

Table 1.1. Classification of Ad serotypes.	6
Table 2.1. Cell lines and media used.	48
Table 2.2. Mutagenic oligonucleotide primers.	54
Table 2.3. Primer design.	55
Table 2.4. Antibodies used in experimental procedures.	74
Table 3.1. Amino acid residues of FX and FXa to which NAPc2 or Ixolaris bind.	90
Table 3.2. Primer design.	94
Table 3.3. Concentration of rFX protein.	116
Table 4.1. Kinase inhibitor library.	136
Table 4.2. ITAM containing viral proteins.	150
Table 4.3. Searching the Ad proteome for ITAMs.	150
Table 4.4. ITAM-containing cellular proteins.	152
Table 5.1. Traditional screening assay versus the HTS format.	184
Table 5.2. Summary of compounds enhancing FX-mediated Ad5 gene transfer.	188
Table 5.3. HTS data quality control review.	193

List of Publications

Articles

Duffy MR, Parker AL, Bradshaw AC, Baker AH (2012). Manipulation of adenovirus interactions with host factors for gene therapy applications. *Nanomedicine* 7(2): 271-288 [Appendix 2].

Duffy MR, Bradshaw AC, Parker AL, McVey JH, Baker AH (2011). A Cluster of Basic Amino Acids in the Factor X Serine Protease Mediates Surface Attachment of Adenovirus/FX Complexes. *Journal of Virology* 85(20): 10914-10919 [Appendix 3].

Bradshaw AC, Parker AL, **Duffy MR**, Coughlan L, van Rooijen N, Kähäri V-M, et al. (2010). Requirements for Receptor Engagement during Infection by Adenovirus Complexed with Blood Coagulation Factor X. *PLoS Pathogens* 6(10): e1001142

Abstracts

- **Duffy MR**, Kalkman E, Baker AH (2012). Identification of a Novel Small Molecule Inhibitor of FX-Mediated Ad5 Gene Transfer for Gene Therapy Applications. *Molecular Therapy*. Oral presentation at the American Society of Gene and Cell Therapy 2012.
- **Duffy MR**, Bradshaw AC, Parker AL, McVey JH, Baker AH (2011). A Cluster of Basic Amino Acids in the Factor X Serine Protease Mediates Surface Attachment of Adenovirus:FX Complexes. *Human Gene Therapy*. Oral presentation at ESGCT and BSGT Collaborative Congress 2011. The Fairbairn Award winner.
- **Duffy MR**, Kalkman E, Baker AH (2011). Identification of a Small Molecule Inhibitor of Ad5:FX Gene Transfer. *Human Gene Therapy*. Poster presentation at the ESGCT and BSGT Collaborative Congress 2011.
- **Duffy MR**, Bradshaw AC, Parker AL, McVey JH, Baker AH (2011). Basic residues in the heparin-binding proexosite of the factor X serine protease domain mediate Ad5:FX complex binding to hepatocytes. *Molecular Therapy*. Oral presentation at the American Society of Gene and Cell Therapy 2011.
- **Duffy MR**, Bradshaw AC, Parker AL, McVey JH, Baker AH (2010). Modification of the factor X serine protease domain ablates heparan sulphate proteoglycan engagement by Ad5/FX Complexes. *Human Gene Therapy*. Oral presentation at the German Society of Gene Therapy Conference (DG-GT) 2010.

List of Abbreviations

4G3	Monoclonal anti-human FX antibody
Å	Angstroms
A549 cells	Adenocarcinomic human alveolar basal epithelial cells
AAV	Adeno-associated virus
ABCG2	Adenosine triphosphate-binding cassette protein G2
Ad	Adenovirus
Ad5	Adenovirus serotype 5
ADA	Adenosine deaminase
AdKO1	CAR-binding ablated Ad5 vector
ADME	Absorption, distribution, metabolism, and excretion
ADP	Adenovirus death protein
AIDS	Acquired immune deficiency syndrome
ANOVA	Analysis of variance
Apo	Apolipoprotein
ATP	Adenosine triphosphate
BAP	Biotin acceptor peptide
BCA	Bicinchoninic acid assay
BLV	Bovine leukemia virus

Bp	Base pair
BSA	Bovine serum albumin
C3	Complement component 3
CAR	Coxsackie virus and adenovirus receptor
CD	Cytosine deaminase
cDNA	Complementary deoxyribonucleic acid
CHO cells	Chinese hamster ovarian cells
CMV	Cytomegalovirus
CPE	Cytopathic effects
CR1	Complement receptor 1
CRA _d	Conditionally replicating adenovirus
Cryo-EM	Electron cryomicroscopy
CsCl	Caesium chloride
DAF	Decay accelerating factor
DAPI	4',6-diamidino-2-phenylindole
DBP	DNA binding protein
DC-SIGN	Dendritic cell-specific intercellular adhesion molecule-3-grabbing non-integrin
DMEM	Dulbecco's Modified Eagle Medium
DMSO	Dimethyl sulfoxide

DNA	Deoxyribonucleic acid
dsDNA	Double-stranded deoxyribonucleic acid
EBV	Epstein–Barr virus
ECL	Enhanced chemiluminescent
EGF	Epidermal growth factor
ELISA	Enzyme-linked immunosorbent assay
ERK	Extracellular-signal-regulated kinases
ERM	Ezrin, radixin and moesin
FACS	Fluorescence activated cell sorting
FB	Factor B
FC	Fluorocytosine
FCS	Fetal calf serum
FC ϵ RI	Fc ϵ receptor I, high affinity receptor for IgE
FITC	Fluorescein isothiocyanate
FIX	Blood coagulation factor IX
FVIIa	Activated blood coagulation factor VII
FX	Blood coagulation factor X
FXa	Activated blood coagulation factor X
GCV	Ganciclovir

GDFX	Gla domainless factor X
GFP	Green fluorescent protein
Gla	Glutamic acid
GM-CSF	Granulocyte macrophage colony-stimulating factor
GMP	Good manufacturing practice
GTP	Guanosine triphosphate
HBE	Heparin-binding exosite
HBPE	Heparin-binding proexosite
HCV	Hepatitis C virus
HEK cells	Human embryonic kidney cells
HepG2 cells	Hepatic carcinoma cell line
HRP	Horseradish peroxidase
HS	Heparan sulphate
HSPG	Heparan sulphate proteoglycans
HTS	High throughput screen
HVR	Hypervariable region
IC ₅₀	Half maximal inhibitory concentration
ICC	Immunocytochemistry
IgG	Immunoglobulin G

IgM	Immunoglobulin M
IL	Interleukin
ITAM	Immunoreceptor tyrosine-based activation motif
ITR	Inverted terminal repeat
K_2	Association rate constant
KC	Kupffer cell
Kd	Dissociation constant
kDa	Kilodalton
KKTK	Amino acid sequence of putative HSPG binding site in Ad5 fiber
KSHV	Kaposi's sarcoma-associated herpesvirus
L	Litre
LB	Luria Broth
LDL	Low density lipoprotein
LMO2	LIM domain only 2
LRP	Lipoprotein receptor-related protein
M	Molar
MAPK	Mitogen-activated protein kinase
MLP	Major late promoter
MMTV	Mouse mammary tumor virus

MPEG	Monomethoxy polyethylene glycol
mRNA	Messenger ribonucleic acid
MTOC	Micotubule organising centre
MTT assay	3-(4,5-Dimethylthiazol-2-yl)-2,5-diphenyltetrazolium bromide, cell viability assay
N/A	Non-applicable
NAb	Neutralising antibody
NAPc2	Nematode Anticoagulant Protein c 2
NK cell	Natural killer cell
NPC	Nuclear pore complex
NS	Non-significant
NTR	Nitroreductase
OCT	Optimum cutting temperature
ORF	Open reading frame
PBS	Phosphate buffered saline
PCA	Principle component analysis
PCR	Polymerase chain reaction
Pd FX	Plasma derived factor X
PEG	Polyethylene glycol
PFA	Paraformaldehyde

Pfu	Plaque-forming unit
PI3K	Phosphoinositide 3-kinase
PIP ₂	Phosphatidylinositol 4,5-bisphosphate
PKA	Protein kinase A
Pol	Polymerase
Poly(I)	Polyinosinic acid
PRR	Pattern-recognition receptor
QPCR	Quantitative polymerase chain reaction
RAG-1	Recombination-activating gene-1
Rb	Retinoblastoma
rFX	Recombinant factor X
RGD	Arginine-glycine-aspartic acid motif, α_v integrin binding site in the penton base
RID	Receptor internalisation and destruction
RLU	Relative light unit
RU	Response unit
SAP	Shrimp alkaline phosphatase
SAR	Structure activity relationship
ScFV	Single-chain antibody variable fragments
SCID	Severe combined immunodeficiency

SDS PAGE	Sodium dodecyl sulphate polyacrylamide gel electrophoresis
SEM	Standard error of the mean
SH2	Src Homology 2
SIV	Simian immunodeficiency virus
SKOV3 cells	Human ovary adenocarcinoma cell line
SP mutant	Factor X containing seven amino acid mutations in the heparin binding proexosite of the serine protease domain
SP	Serine protease
SPR	Surface plasmon resonance
SSPEG	Succinimidyl succinate-monomethoxy polyethylene glycol
SW620 cells	Human colorectal adenocarcinoma cells
Syk	Spleen tyrosine kinase
TAP	Tick anticoagulant peptide
TCA	Trichloroacetic acid
TCID ₅₀	50% Tissue Culture Infectious Dose
TK	Thymidine kinase
TMPEG	Tresyl-monomethoxy polyethylene glycol
TP	Terminal protein
TRITC	Tetramethyl rhodamine isothiocyanate
Vp	Virus particle

vWF	von Willebrand factor
WDI	World Drug Index
WT	Wild-type
X-bp	Factor X-binding protein
ZAP-70	Zeta-chain-associated protein kinase 70
β -gal	β -galactosidase
γ c	Common cytokine receptor γ chain gene

Abstract

Adenoviruses are the most commonly used vectors for clinical gene therapy applications, accounting for 24% of all clinical trials to date, the majority of which are based on Ad serotype 5 (Ad5). However, the high prevalence of neutralising antibodies and a range of “off target” interactions result in liver sequestration, hepatic transduction and decreased circulation times. Such interactions include Kupffer cell uptake and binding to blood components such as erythrocytes, platelets, complement and coagulation factors. Recent studies have shown that hepatocyte transduction by Ad5 is mediated by a high-affinity interaction between coagulation factor X (FX) and the Ad5 major capsid protein hexon, with FX bridging the virus to heparan sulphate proteoglycans (HSPGs) on the cell surface. This thesis has focused on gaining a greater understanding of the Ad5:FX pathway and potential strategies for its manipulation.

FX, a key component of the blood coagulation system, is a zymogen of a vitamin K-dependent serine protease that is primarily synthesised in the liver and circulates in the bloodstream at 8-10 µg/ml. It is composed of a light chain consisting of a domain rich in γ -carboxylated glutamic acid (Gla) residues, two epidermal growth factor-like domains and a serine protease (SP) heavy chain. The Gla domain of FX binds to the virion by docking in the cup formed by each hexon trimer, whilst the SP domain tethers the Ad5:FX complex to the hepatocyte surface through binding HSPGs. Previously, it was demonstrated that pharmacological blockade of the heparin-binding proexosite (HBPE) in the SP domain prevents FX-mediated cell binding. Here, the specific residues of FX which mediate Ad5 attachment to HSPGs were identified. Employing mutagenesis techniques each of the seven basic residues R93, K96, R125, R165, K169, K236 and R240 that were previously shown to bind heparin, were converted to alanine. This mutated FX was termed “SP mutant”. Stable cell lines were generated to constitutively produce the wild-type and SP mutant rFX protein in the presence of vitamin K. The conditioned media was affinity purified using a FX specific mouse monoclonal antibody 4G3 coupled to sepharose. The rFX proteins were quantified by ELISA, had the predicted molecular weight of 59 kDa and were biologically active, as shown by conversion to FXa in the presence of tissue factor and FVIIa. Surface plasmon resonance (SPR) analysis demonstrated the SP mutations had no effect on FX-specific binding to the Ad5 hexon. However the proexosite mutations ablated FX-mediated Ad5 cell surface binding, internalisation, cytosolic transport and gene transfer as shown by confocal microscopy, qPCR and quantification of transgene expression. Assessing the involvement of rFX with single (R125A) and double

(R93A_K96A, R165A_K169A and K236A_R240A) point mutations in the SP domain, indicated the residues exhibit different levels of contribution to Ad5:FX complex binding to HSPGs. The seven SP mutations also inhibited FX-mediated Ad5 binding to mouse liver sections *ex vivo*. Taken together, this study uncovered that basic residues within the HBPE of FX have a fundamental role in Ad5:FX complex engagement with HSPGs at the surface of target cells. This study contributes to the existing knowledge of the FX-mediated Ad5 transduction pathway.

Whilst the classical *in vitro* CAR-mediated Ad5 infection mechanism has been extensively studied, the post-binding events governing FX-mediated Ad5 intracellular transport and gene expression have not been fully characterised. This study employed a panel of small molecule inhibitors of cellular kinases *in vitro* to investigate cellular and signalling events occurring during FX-mediated Ad5 infection. Blockade of protein kinase A, p38 mitogen-activated protein kinase and phosphatidylinositol 3-kinase significantly hindered efficient Ad5 intracellular trafficking and colocalisation with the microtubule organising centres (MTOC), as shown by confocal microscopy, indicating their fundamental involvement in the pathway. Screening a library of 80 diverse kinase inhibitors for effects on FX-mediated gene transfer, highlighted the compound ER-27319 had the ability to prevent Ad5 transduction *in vitro*. Previous work reported that ER-27319 acts by binding to the immunoreceptor tyrosine based activation motif (ITAM) of the FcεRI receptor gamma subunit in mast cells to prevent spleen tyrosine kinase (Syk) activation. Here, this compound had no effect on FX-mediated cell binding but substantially disrupted intracellular transport at 3 h in the absence of toxicity. It was postulated that this effect may be due to ER-27319 binding to a viral or cellular ITAM-containing protein involved in viral trafficking. Sequence analysis of the Ad capsid proteome for ITAM-like motifs ((D/E)-x-x-Y-x-x-(L/I)-(x_{n=6-8})-Y-x-x-(L/I)) identified two motifs on the hexon. However neither followed that reported for the FcεRI gamma subunit, instead of the conventional 6-8 amino acid residues between the two Y-x-x-I/L, the hexon ITAM-like sequences expressed 17 or 22 amino acids. Alternatively the ITAM-containing cellular proteins, ezrin, radixin and moesin (ERM) were investigated. The ERM family are key regulators of the cell cortex, capable of interacting with both the plasma membrane and filamentous actin. However, in the time frame imposed by this study this hypothesis could not be studied in depth, but warrants further research to investigate whether ERM proteins have a novel role in FX-mediated Ad5 intracellular trafficking.

A wide range of approaches have been investigated to detarget Ad5 from the liver. In this thesis, a pharmacological strategy to preclude FX-mediated liver gene transfer was implemented. A high throughput screening platform was developed to identify a novel small molecule(s) to manipulate the Ad5:FX infection pathway. In addition to the value of such an agent in the gene therapy setting, it may also have potential to treat life-threatening disseminated Ad infections in immunocompromised individuals. Using a fluorescence and cell-based *in vitro* high throughput assay 10,240 small molecules were screened using the Pharmacological Diversity Drug-like Set library. Initial screening identified 288 compounds that reduced FX-mediated Ad5 gene transfer by > 75% without causing toxicity. Upon further analysis, three compounds, T5424837, T5550585 and T5660138 were identified as consistently ablating Ad5 transduction both in the absence and presence of FX and all had IC₅₀ values < 5.5 μM. These compounds did not directly interfere with Ad5 binding to FX, instead they primarily caused a post-binding stage block of the Ad infection pathway and all affected optimal virus trafficking to the MTOC, as demonstrated by SPR, flow cytometry and confocal microscopy. The candidate molecules have common structural features and fall into the “one pharmacophore” model. Focused mini-libraries were generated relating to these molecules and structure-activity relationship analysis was performed. *In vitro* screening of the analogues revealed novel hits with similar or improved activity, thereby further validating the initial hits and pharmacophore model. Six compounds, T5550585, its analogue T5572402, T5660138, its analogue T5660136, T5424837 and its analogue T5677956 were tested *in vivo*. 10 μM T5660138 substantially reduced Ad5 liver accumulation 48 h post-injection and, in addition to its closely related analogue T5660136, significantly reduced transgene expression at 48 h post-intravenous administration of a high viral dose (1 x 10¹¹ vp/mouse). Therefore, this study identifies novel small molecule inhibitors of circulating Ad5 infection.

Through investigation and manipulation of Ad5 interactions with host proteins the work presented here, increases the understanding of the key *in vivo* Ad5:FX tropism determining pathway. In summary, in this thesis the mechanism of FX-mediated Ad5 complex binding to hepatocytes was dissected and potent inhibitors of this important Ad5 infectivity pathway both *in vitro* and *in vivo* were identified. This data may contribute to the optimisation of Ad vectors for gene therapy applications and potentially the advancement of anti-adenoviral drug development.

Chapter 1

Introduction

1.1 Introduction

Gene therapy is a rapidly advancing area of preclinical and clinical research, holding immense promise for the future of modern medicine. In the most basic sense, it is a technique for correcting defective genes responsible for disease development. This may involve substituting the mutated gene with a functional copy, alternatively it can entail the delivery of genes to stimulate an immune response, to produce a therapeutic protein or suicidal genes to induce cell death. Gene therapy shows exciting potential to provide novel, selective, beneficial and even curative treatments for a wide range of inherited and acquired diseases which currently lack effective medication. In many respects the ultimate success of this approach is defined by the delivery vector, the route of vector administration, accessibility of the target cells or tissue and the stability of transgene expression. Viruses have evolved sophisticated mechanisms over millennia to deliver their genomic payload into host cells. Of the available vectors for gene therapy applications, engineered viruses are often the most efficient for the transfer of such genetic material to cells.

The first approved human therapeutic gene therapy clinical trial came in 1990 (Blaese *et al.*, 1995). This phase I study was aimed at treating the rare autosomal recessive disorder, severe combined immunodeficiency (SCID) caused by a genetic deficiency of adenosine deaminase (ADA), a key enzyme in purine metabolism (Blaese *et al.*, 1995; Cristalli *et al.*, 2001). Lack of ADA leads to the accumulation of the ADA substrate 2'-deoxyadenosine and its subsequent conversion to the toxic compound deoxyadenosine triphosphate in T cells, thereby disabling the immune system (Cohen *et al.*, 1978; Hirschhorn, 1983). The gene therapy clinical study employed a retroviral vector for the *ex vivo* delivery of ADA complementary DNA into the T lymphocytes of two patients suffering from the disorder (Blaese *et al.*, 1995). Although the clinical response was limited, in a ten year follow up approximately 20% of the first patient's lymphocytes still carried and expressed the ADA gene, indicating the long lasting effects in the absence of toxicity (Muul *et al.*, 2003). This positive first step highlighted the potential of the therapy (Muul *et al.*, 2003).

Later, a clinical trial was performed for the treatment of X-linked SCID, an inherited disorder caused by mutations in the common cytokine receptor γ chain gene (γc) located on chromosome X, preventing T and natural killer (NK) cell differentiation (Fischer, 2000). CD34+ bone marrow stem cells were transduced with a retroviral vector, encoding the wild-type version of the γc cytokine receptor gene (Cavazzana-Calvo *et al.*, 2000; Hacein-

Bey-Abina *et al.*, 2002). Patients demonstrated sustained T cell and NK cell reconstitution, which were present within normal ranges for the majority of the patients. (Cavazzana-Calvo *et al.*, 2000; Hacein-Bey-Abina *et al.*, 2002). However, five of the nineteen participants across the two trial centres in London and Paris, developed treatment-related leukaemia 2-6 years following the trial due to retroviral insertional mutagenesis (Hacein-Bey-Abina *et al.*, 2008; Howe *et al.*, 2008). Detailed mapping of the retroviral integration sites indicated insertional transactivation of the LIM domain only 2 (LMO2) proto-oncogene, and additional sites close to BMI1 (involved in transcriptional control) and CCND2 (a cell-cycle protein) led to leukaemogenesis (Hacein-Bey-Abina *et al.*, 2008; Howe *et al.*, 2008). Whilst this study demonstrated the potential of such an approach to restore T cell immunity, it raised serious concerns regarding the toxicity of retrovirus-based vectors for gene therapy. The detailed analysis of these adverse effects, the mapping of the retroviral integration profiles and the use of safer vectors will help to avoid such events.

In parallel to the progression of gene therapy, major advances in the field of recombinant DNA technology were being made, and there came a greater understanding of our genetic makeup. Over a decade has passed since scientists announced the initial draft of the human genome (Lander *et al.*, 2001). Mapping over 3 billion base pairs and identifying 25,000 genes, it was a breakthrough which offered an unrivalled resource for understanding the basis of genetic disorders and complex diseases. The human genome project widened the scope of genetic targets, meaning the identification of suitable therapeutic genes was no longer a limiting factor, and as a result the perspectives broadened. In recent years, a great deal of work has focused on the treatment of cancer, currently accounting for 64.6% of clinical trials (www.wiley.com/legacy/wileychi/genmed/clinical/), whilst promise has been realised for a variety of other conditions, as diverse as cardiovascular disease (Jessup *et al.*, 2011), human immunodeficiency virus infection (Barouch *et al.*, 2012) and blindness (Vandenberghe *et al.*, 2011) amongst others (Figure 1.1). Recently, a study by Nathwani *et al.* demonstrated the success of a gene therapy approach for the treatment of haemophilia B, an X-linked bleeding disorder, caused by a mutation in the gene for coagulation factor IX (FIX) (Nathwani *et al.*, 2011). Six patients with severe haemophilia B were administered an adeno-associated virus (AAV) expressing the human FIX transgene, resulting in a sufficient increase in FIX expression levels to improve the bleeding phenotype with few side effects (Nathwani *et al.*, 2011).

A major advance in the field of gene therapy was the recent announcement from the European Committee for Medicinal Products for Human Use (CHMP), for the

recommended approval of the first registered gene therapy product in Europe, alipogene tiparvovec (also known as Glybera), which is based on an AAV-1 vector (Miller *et al.*, 2012, Burnett *et al.*, 2009). Amsterdam Molecular Therapeutics (AMT) developed Glybera for the correction of familial lipoprotein lipase deficiency, a rare disorder in which failure to metabolise chylomicrons leads to massive hyperlipidaemia and potentially life-threatening pancreatitis (Miller *et al.*, 2012, Burnett *et al.*, 2009). The approval of the first product in Europe represents a very exciting step forward in the development of future gene therapy.

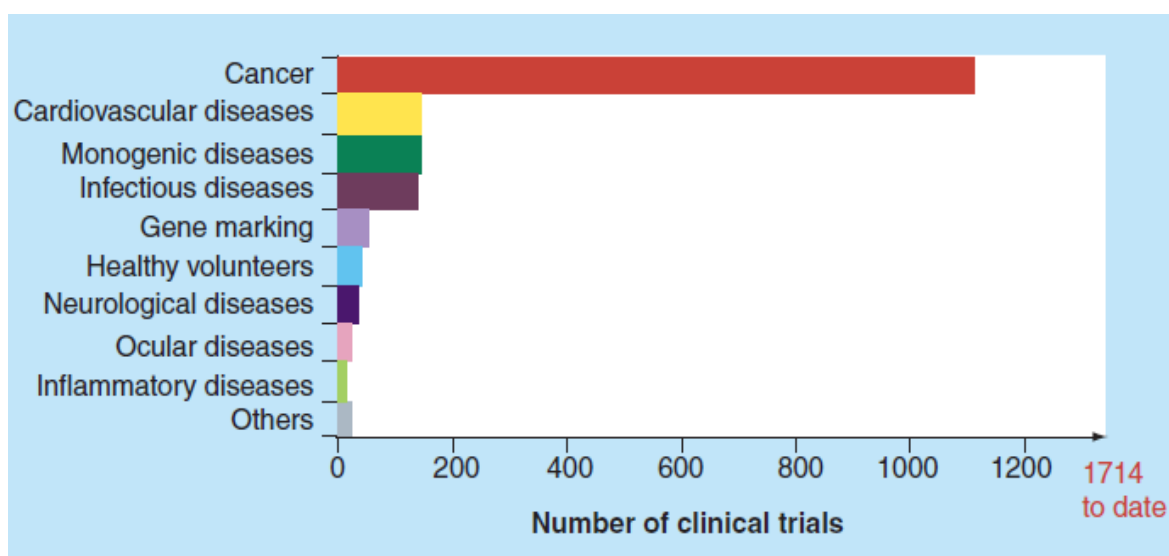


Figure 1.1. Gene therapy clinical trials summarised by indication.

Trials (n = 1714) grouped according to indication; cancer (n = 1107, 64.6%), cardiovascular diseases (n = 146, 8.5%), monogenic diseases (n = 143, 8.3%), infectious diseases (n = 183, 8.1%), gene marking (n = 50, 2.9%), healthy volunteers (n = 40, 2.3%), neurological diseases (n = 35, 2%), ocular diseases (n = 23, 1.3%) and other (n = 19, 1.1%). Data were obtained from the Journal of Gene Medicine (<http://www.wiley.com//legacy/wileychi/genmed/clinical/>).

While the principle goal of gene therapy, to safely achieve stable transgene expression refined to the desired tissue, has not changed throughout its history, the understanding of the underlying complexity of just how to achieve this has increased greatly. The desire to overcome the outstanding challenges, along with the explosion of interest in the biotechnology industry and some major discoveries in the field of virology, has resulted in considerable attention and resources being focused on the manipulation of viruses for medical treatments. From this, vectors based on adenoviruses (Ad) have emerged as promising tools for gene therapy applications (Figure 1.2).

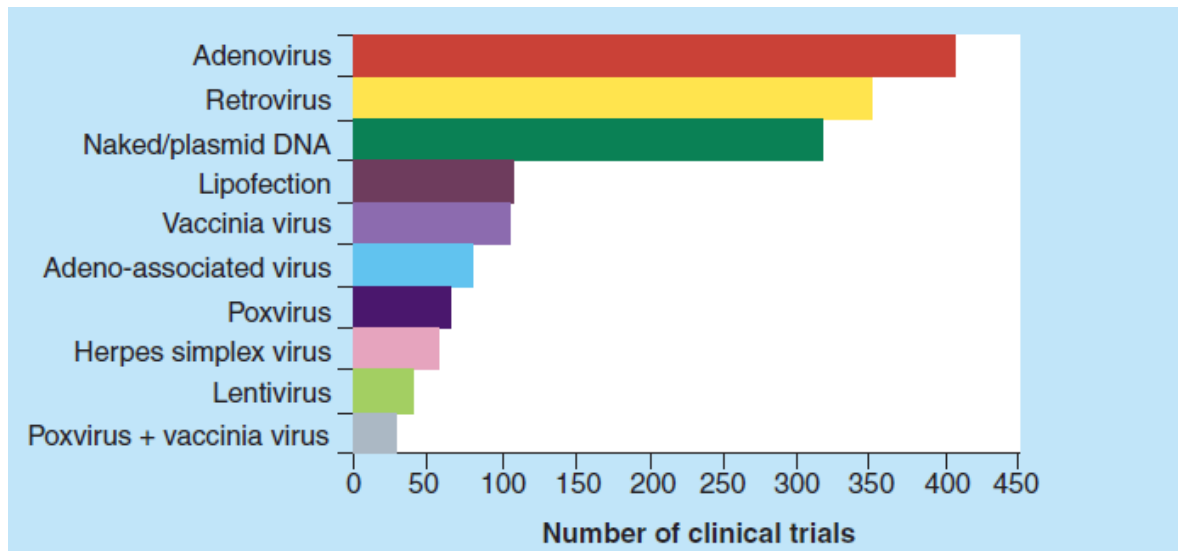


Figure 1.2. Gene therapy clinical trials summarised by vector.

Top ten most commonly used vectors for gene therapy clinical trials; adenovirus (n = 406, 23.7%), retrovirus (n = 352, 20.5%), naked/plasmid DNA (n = 318, 18.6%), lipofection (n = 109, 6.4%), vaccinia virus (n = 106, 6.2%), adeno-associated virus (n = 81, 4.7%), poxvirus (n = 66, 3.9%), herpes simplex virus (n = 57, 3.3%), lentivirus (n = 40, 2.3%) and poxvirus with vaccinia virus (n = 28, 1.6%). Data were obtained from the Journal of Gene Medicine (<http://www.wiley.com//legacy/wileychi/genmed/clinical/>).

1.2 Adenoviruses

Ads are non-enveloped, double-stranded DNA viruses, first isolated in 1953 from human adenoid tissue (Hilleman *et al.*, 1954; Rowe *et al.*, 1953). They belong to the *Adenoviridae* family, of which there are at least 57 different serotypes, subdivided into species A to G (Table 1.1). Ads are currently classified based on serologic profiles, DNA sequence similarity, receptor usage, capacity to agglutinate human, monkey and rat erythrocytes and oncogenicity in rodents (Catherine, 2002; Crawford-Miksza *et al.*, 1996). These common pathogens are associated with mostly self-limiting infection, causing acute respiratory, gastrointestinal and ocular infections. Since the early 1980s these viruses have been developed, engineered and partially optimised for use in gene therapy applications.

Table 1.1. Classification of Ad serotypes.

Ad serotypes are divided into species A to G. This classification is related to the Ad receptor usage.

Ad species	Ad serotype	Receptor usage
A	12, 18, 31	CAR
B	3, 7, 11, 14, 16, 21, 34, 35, 50, 55	CD46, HSPG, Desmoglein 2
C	1, 2, 5, 6	CAR, HSPG, Integrins
D	8, 9, 10, 13, 15, 17, 19, 20, 22, 23, 24, 25, 26, 27, 28, 29, 30, 32, 33, 36, 37, 38, 39, 42, 43, 44, 45, 46, 47, 48, 49, 51, 53, 54	CAR, Sialic acid, CD46
E	4	CAR
F	40, 41	CAR
G	52	Unknown

1.3 Adenoviral structure

The combined application of X-ray crystallography and electron microscopy has provided a wealth of information on the architecture of the Ad virion, now determined to a resolution of 3.5 angstroms (Liu *et al.*, 2010; Reddy *et al.*, 2010; Saban *et al.*, 2006). The Ad particle comprises two major structural elements; the outer capsid and the inner core.

1.3.1 Outer capsid

The icosahedral capsid of each Ad particle is approximately 70-90 nm in diameter and encloses the viral genome. It is composed of three principle proteins; the hexon, penton base and fiber (Figure 1.3). The major capsomer hexon is a pseudo-hexagonal trimer, the 240 copies of which are situated on the 20 faces of the icosahedron (Benson *et al.*, 1999). The homotrimers are composed of three-fold repetitions of two β -barrels at the base of each hexon molecule. The two eight stranded β -barrels with ‘jelly roll’ topology and one loop at the hexon base are responsible for interacting with adjacent capsomers and contribute to the proteins extensive stability (Russell, 2009). There are four different types of hexon; H1 (also called peripentonal hexons) which associates with each of the 12 pentons, while H2, H3 and H4 form the ‘groups of nine’ (GON) on each of the 20 facets of the capsid structure (Figure 1.4) (Burnett, 1985). Comparative sequence analysis of serotypes has revealed the presence of hypervariable regions (HVRs) within the surface exposed regions of the hexon protein (Crawford-Miksza *et al.*, 1996; Rux *et al.*, 2003).

These regions relate to serotype-specific antigen recognition (Roberts *et al.*, 2006). At the 12 capsid vertices, the pentameric penton base protein is located along with the protruding trimeric fiber (van Oostrum *et al.*, 1985). In most cases the penton base contains the exposed arginine-glycine-aspartic acid (RGD) motif within a flexible loop, which is involved in cell internalisation (Wickham *et al.*, 1993). The rigid fiber is composed of three distinct regions, the N-terminal tail non-covalently bound to the penton base, the intertwined repeating 15-20 amino acid sequences in the shaft and the C-terminal globular knob domain (Henry *et al.*, 1994; Zubieta *et al.*, 2005). The capsid also contains several minor structural proteins including IIIa (60 copies per virion) (Stewart *et al.*, 1993), VI (360 copies) (Stewart *et al.*, 1993), VIII (120 copies) (Fabry *et al.*, 2005) and IX (240 copies) (Furcinitti *et al.*, 1989), which are implicated in cementing the capsid structure (Figure 1.4) (Furcinitti *et al.*, 1989; Stewart *et al.*, 1991).

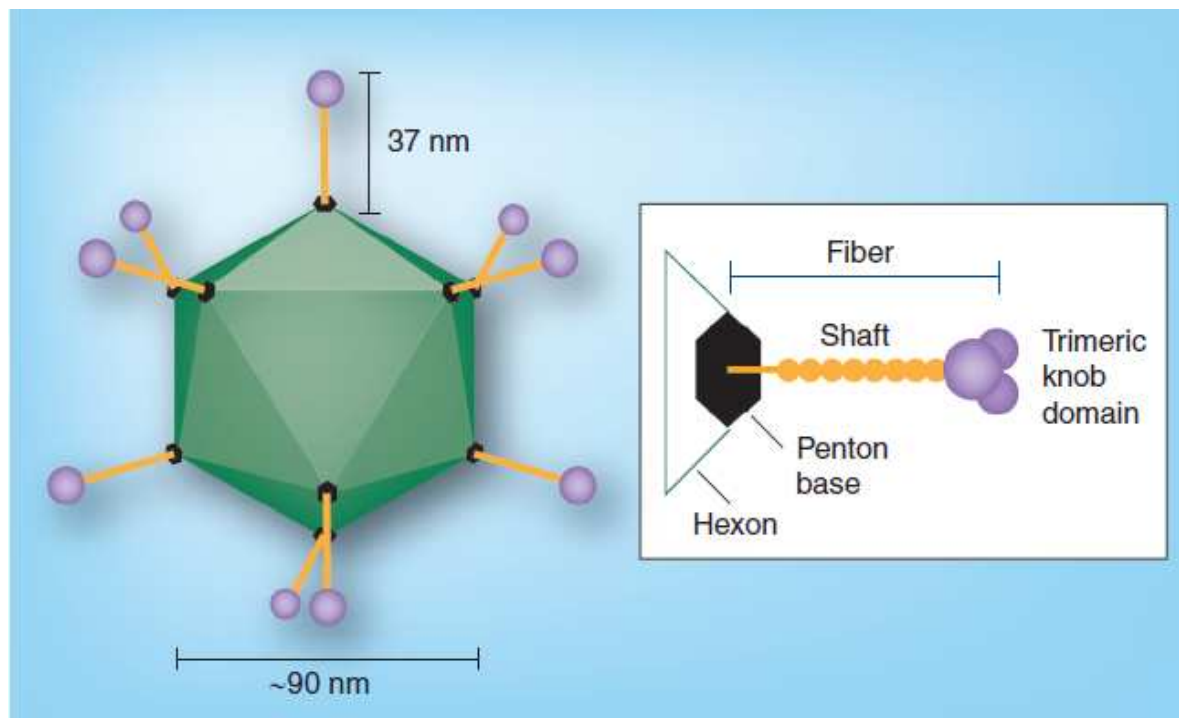


Figure 1.3. Ad capsid structure.

The icosahedral Ad capsid, with a core diameter of approximately 90 nm, is composed of three principal capsid proteins, the hexon, the penton base and the protruding flexible fiber. The Ad type 5 (Ad5) fiber is approximately 37 nm in length and consists of a trimeric knob domain, shaft and N-terminus tail attached to the penton base. In addition there are several minor capsid proteins, including pIIIa, pVI, pVIII and pIX, which stabilize the virus structure.

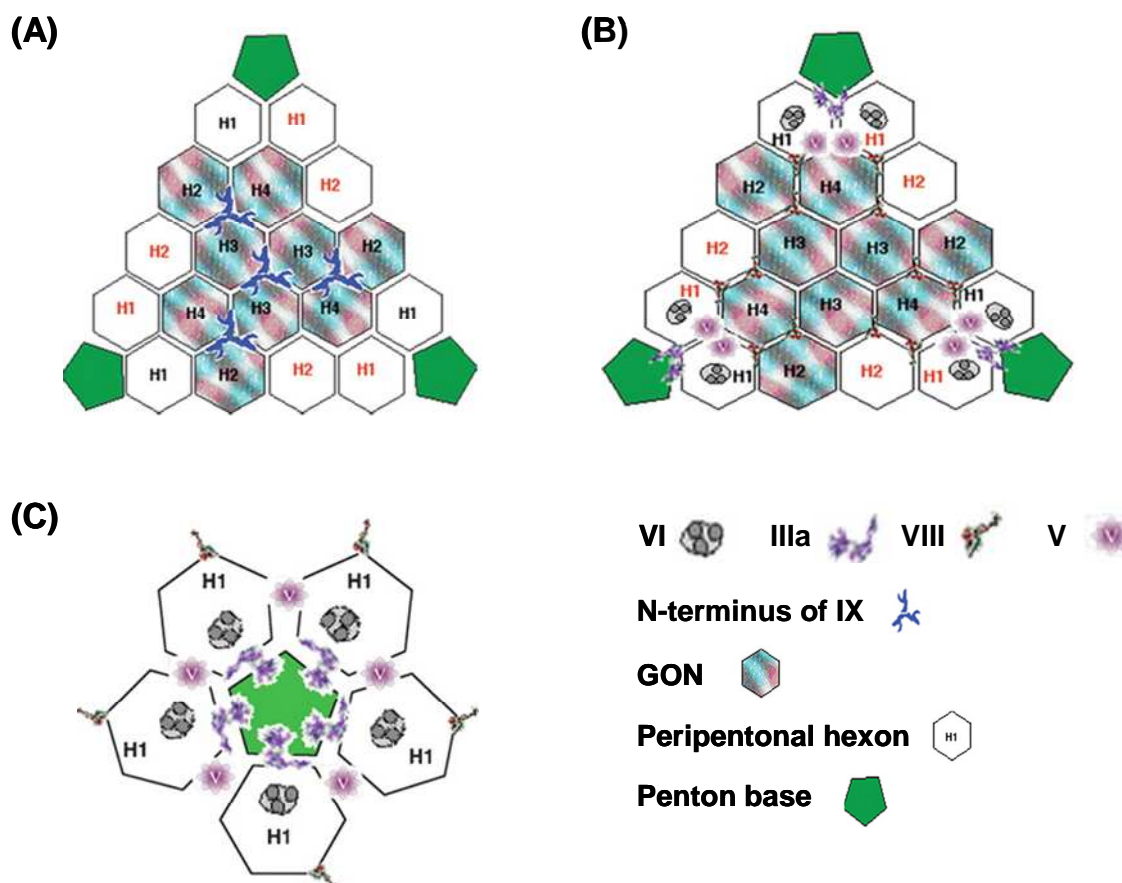


Figure 1.4. Facets of the Ad icosahedron capsid.

(A) External view - the GON hexons are multicoloured and the H1 peripentonal hexons are either lettered in black when they are on the same plane as the GONs or lettered in red where they are associated with GONs on a different facet. Similarly, the H2 hexons lettered in red are associated with GONs on a different facet. The symbol for protein IX is not to scale. (B) Internal view - hexons and associated minor capsid proteins. (C) Internal structure at the apex. This figure was taken from Russell (Russell, 2009).

1.3.2 Inner core

Protected within the outer Ad capsid is the linear double-stranded DNA, approximately 36 kb in length. The viral genome is condensed in association with the core proteins, namely histone-like protein VII (>800 copies), the capsid-to-core bridging protein V (160 copies), μ (100 copies), IVa2, terminal protein and the 23 K virion protease (10-70 copies), necessary for the production of the mature virus (Anderson *et al.*, 1989; Rekosh *et al.*, 1977; Robinson *et al.*, 1973; Russell, 2009; Webster *et al.*, 1989). Inverted terminal repeats (ITR) of 100-140 bp in size, flanking both ends of the viral DNA, act as origins of replication (Rekosh *et al.*, 1977). *Cis*-acting packaging elements in the left end of the DNA, are required for viral encapsidation (Gräble *et al.*, 1992). The Ad genome comprises two main transcription regions, termed the early and late. The early region consists of five transcription units (E1A, E1B, E2, E3, E4), two delayed early units (IX and IVa2), and the

late region is composed of five units (Figure 1.5) (L1-L5) (Mizuguchi *et al.*, 2001; Russell, 2000; Warnock *et al.*, 2011).

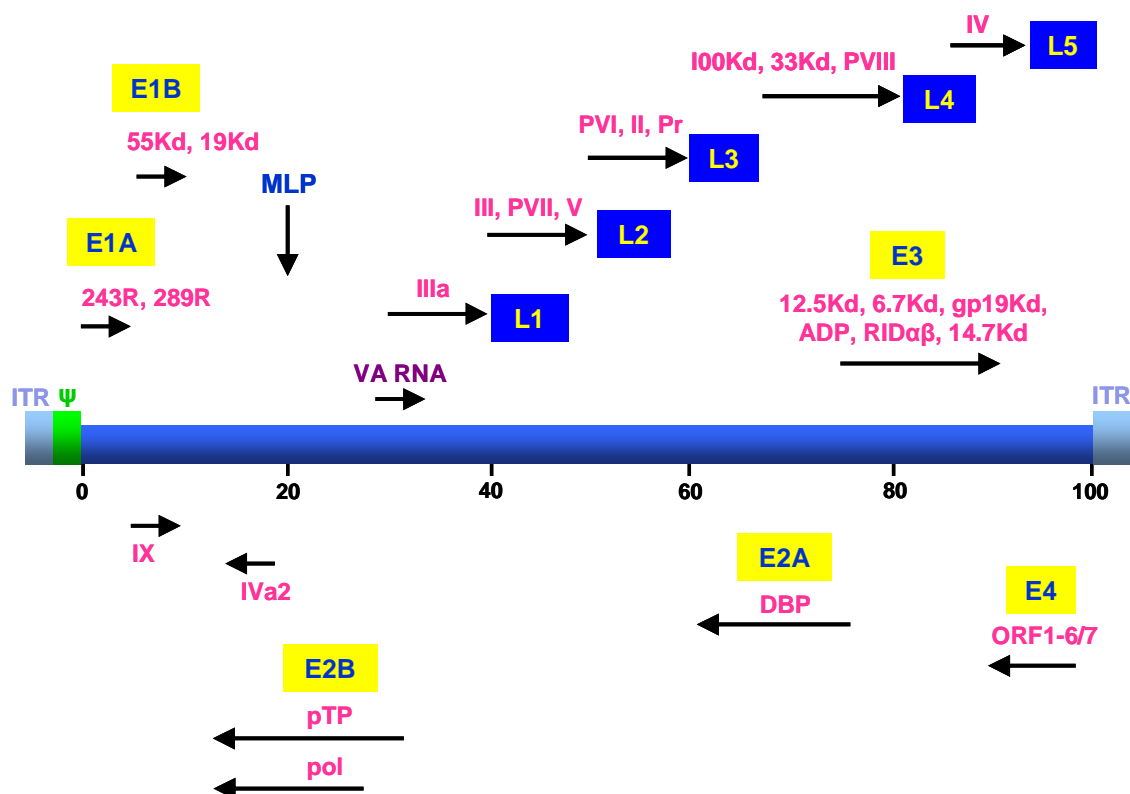


Figure 1.5. Transcription of the Ad genome.

The early transcripts are highlighted with yellow boxes, the late in blue and gene products are in pink. The arrows indicate the direction of transcription. The gene locations of the viral associated (VA) RNAs are denoted in purple. The genes have been mapped by superimposing an arbitrary scale of 100 map units. ITR = inverted terminal repeats, ψ = the packaging signal, MLP = Major late promoter, RID = Receptor internalisation and destruction, Pr = Protease, ADP = Adenovirus death protein, TP = Terminal protein, ORF = Open reading frame, DBP = DNA binding protein and Pol = Polymerase. This figure was adapted from Russell (Russell, 2000).

The E1 gene prepares the host cell for viral replication; the E1A region produces two transcripts 289R and 243R which promote cell cycle progression whilst synergistically the E1B unit prevents apoptosis (Chattopadhyay *et al.*, 2001; Debbas *et al.*, 1993). The adenoviral 289R and 243R E1A proteins can induce DNA synthesis and activate the S phase of the cell cycle in quiescent cells through the formation of complexes with two classes of cellular proteins, the retinoblastoma (Rb) family of growth suppressors and the transcriptional modulator p300 and related proteins (Eckner *et al.*, 1994; Howe *et al.*, 1990). The unscheduled induction of cell proliferation promoted by E1A triggers innate cellular tumour suppressor mechanisms (p53) by activating pro-apoptotic pathways

(Debbas *et al.*, 1993; Lowe *et al.*, 1993). The adenoviral E1B proteins, E1B-55kDa and E1B-19kDa, act to counteract the accumulation of pro-apoptotic p53. The E1B-55kDa protein, in conjunction with E4-open reading frame (ORF) 6 and cellular ubiquitination proteins, antagonises the ability of p53 to cause apoptosis by inducing its degradation (Harada *et al.*, 2002; Querido *et al.*, 1997; Querido *et al.*, 2001).

The E2 gene encodes the machinery to facilitate replication; DNA polymerase (pol), preterminal protein (pTP) and DNA binding protein (DBP) (Hay *et al.*, 1995). E3 codes for proteins that block natural cellular responses to viral infection, such as the adenovirus death protein (ADP) (Tollefson *et al.*, 1996) and E4 encodes ORF 1-6/7 that perform in mRNA transport and further promote replication (Goodrum *et al.*, 1999; Warnock *et al.*, 2011; Weigel *et al.*, 2000). Ads also transcribe a set of RNAs, termed the virus associated (VA) RNAs (I and II), and these play a role in combating cellular defence mechanisms, by preventing the interferon antiviral response. RNA-dependent protein kinase (PKR), an interferon-inducible serine-threonine protein kinase is activated in infected cells, by the presence of double-stranded RNA in the cytoplasm, leading to blockade of cellular mRNA translation (O'Malley *et al.*, 1989). VA RNAs can bind directly to and block the actions of PKR thereby overcoming this shutdown in protein synthesis (O'Malley *et al.*, 1986).

Following activation of early genes and viral replication, the major late promoter (MLP) (Shaw *et al.*, 1980) leads to the expression of late genes, involved in the expression of viral structural proteins required for packaging and maturation, and ultimately in the production of infectious viral particles.

1.4 Ads as gene delivery vectors

Several features make Ads attractive vectors for gene therapy. Ads are efficient in infecting a wide variety of both quiescent and proliferating cell types and exhibiting high level transgene expression in target cells. They remain episomal, therefore have minimal-to-no risk of insertational mutagenesis. As the vectors are non-integrating their genomes are lost in dividing cells and so transgene expression is transient, a factor which may be advantageous depending on the clinical applications. Ads have a large packaging capacity and can be produced at high titres (up to 10^{13} virus particles per ml) under Good Manufacturing Practice (GMP) conditions, an attribute key for successful development in the biotechnology industry.

Ads are easy to genetically manipulate to generate replication incompetent viruses or conditionally replicating Ads (CRAds). Replication deficient Ads can be classified into three categories; first, second and third generation vectors. The first generation vectors contain deletions in the early transcription E1 regions, essential for the initiation of viral replication, and often also the E3 region, dispensable for replication in cell culture, enabling the insertion of a transgene of approximately 8 kb. For vector production, the E1 functions have to be provided in trans by a complementing producer cell line. The development of the human embryonic kidney cell line 293, transfected with sheared Ad5 genomic DNA to stably express the E1 genes, has aided the efficient production of these replication deficient vectors (Graham *et al.*, 1977). A major limitation of first generation vectors is that in spite of the E1 deletion, viral genes can be expressed at low levels in cells due to transactivation by host transcription factors, causing short duration transgene expression and toxicity due to an adaptive cellular immune response against the transduced cells (Yang *et al.*, 1994a; Yang *et al.*, 1994b).

To increase the size of the genetic insert (up to 14 kb), second generation vectors were developed and are characterised by additional deletions in the E2 and E4 regions. These vectors were complemented by the development of more complex producer cell lines, stably co-expressing the E1 region, DNA polymerase, and preterminal proteins (Amalfitano *et al.*, 1997). Although some studies did report improved transgene persistence and decreased inflammatory responses using second generation vectors (Dedieu *et al.*, 1997; Wang *et al.*, 1997), their effects are controversial and may be related to tissue type (Lusky *et al.*, 1998; Lusky *et al.*, 1999). Lusky *et al.* generated Ad5 vectors with both single deletions (AdE1⁻) and double deletions (AdE1⁻E2A⁻ and AdE1⁻E4⁻), and compared the immunogenicity of these vectors *in vitro* and *in vivo* (Lusky *et al.*, 1998). AdE1⁻E2A⁻ demonstrated abolished expression of early and late viral genes, while deletion of E1 and E4 also impaired expression of viral genes, although at a lower level than the E1/E2A deletion. However, *in vivo* all vectors produced similar antibody responses and showed similar levels of viral genomes in the liver and lung 4 months post-administration (Lusky *et al.*, 1998). This study therefore indicates mouse cellular immunity to viral antigens plays a minor role in the persistence of the virus genome *in vivo* (Lusky *et al.*, 1998).

Third generation or helper-dependent vectors are devoid of all viral genes except essential ITRs and packaging sequences, and can accommodate inserts of 36-38 kb. At present, the lack of a suitable cell line to stably express all the viral helper functions make these vectors

more difficult to produce and scale-up for clinical applications is therefore a limiting factor. Nonetheless, helper-dependent Ads have great potential. Due to the lack of viral gene expression, they show promise for reduced immunogenicity and long term transgene expression (Brunetti-Pierri *et al.*, 2005; Kim *et al.*, 2001; Morsy *et al.*, 1998; Schiedner *et al.*, 1998). One early study reported the life long persistence of a helper-dependent Ad vector encoding the apolipoprotein (apo) E gene, which stably corrected hypercholesterolemia in apoE-deficient mice (Kim *et al.*, 2001).

In contrast to replication deficient Ads, conditionally replicating Ads (CRAds) or oncolytic Ads can selectively replicate in cancer cells, causing cell lysis and death of the infected cell along with the release of progeny virions, which in turn, can infect neighbouring tumour cells, thereby amplifying the effect. Oncolytic Ads exploit cancer-specific cellular changes, such as transcriptional dysregulation, for the purpose of viral replication. This can be achieved by genetic modification of the Ad genome, such as deletion of viral genes required for productive infection in normal cells but redundant in tumour cells or by the use of tumour specific promoters to drive viral replication (Chen *et al.*, 2011; Heise *et al.*, 2000; Öberg *et al.*, 2010; Radhakrishnan *et al.*, 2010). In 1996 Bischoff *et al.* developed the first CRAd, ONYX-015 (dl1520), which lacks the E1B-55kDa gene (Bischoff *et al.*, 1996). It was initially thought that ONYX-015 selectively replicates in tumour cells in which the p53 tumour suppressor pathway was dysfunctional (Bischoff *et al.*, 1996). However, it was later demonstrated that replication was not due to p53 deficiency and this property is now attributed to the unique ability of some tumour cells to compensate for the lack of E1B-55kDa-mediated late viral RNA export (O'Shea *et al.*, 2004). Subsequent strategies to generate oncolytic vectors included E1A mutant CRAds such as Ad Δ 24 (Ad5 containing a 24 base pair deletion within a conserved region (CR2) of E1A) which targeted the tumour suppressing Rb pathway defective in some cancer cells (Fueyo *et al.*, 2000).

1.5 Ad gene therapy – the highs and the lows

Of the Ads used in gene therapy, the human species C Ad type 5 (Ad5) is the most widely studied. However, despite extensive utilisation there are several pitfalls which need to be overcome in order to improve the viability of Ad5 as a therapeutic gene delivery vector in the broad sense. For many gene therapy targets such as disseminated metastatic tumours the optimal and arguably the only route suitable for targeting the multitude of micro-metastases is intravascular delivery. However, the safety and efficacy of Ad5 by intravascular delivery is hampered by the substantial propensity of the virus to transduce

the liver, as first documented by Huard *et al.* (Huard *et al.*, 1995). The resident liver macrophages, Kupffer cells (KC), sequester Ad5 and contribute to the host inflammatory response (Lieber *et al.*, 1997). Once the reticuloendothelial system is saturated, the virus is predominately taken up by hepatocytes (Vrancken Peeters *et al.*, 1996) (Figure 1.6). This inherent hepatic tropism greatly reduces the capability of specific targeting to disease sites. Increasing the vector dosage can result in toxic side effects (Lozier *et al.*, 2002). Most humans are exposed to Ad5 early in life, developing antibodies that efficiently neutralise vectorised forms of Ad5 (Sumida *et al.*, 2005). Furthermore, a general scepticism pervades the medical community ever since the death of Jesse Gelsinger in 1999, a participant in a phase I trial for ornithine transcarbamylase deficiency (Raper *et al.*, 2003; Raper *et al.*, 2002). Systemic inflammatory response syndrome, disseminated intravascular coagulation and multi-organ failure lead to his death 98 h following intravascular administration of 3.8×10^{13} virus particles. This tragedy highlighted the important deficits in knowledge of Ad:host interactions and emphasised the necessity for better understanding of these interactions to achieve optimal use of the vector.

Notwithstanding some of the set-backs in the gene therapy field, remarkable progress has been made in recent years with regards to understanding Ad biology. The ongoing advances at the lab bench translate into the latest successes observed in the clinic with a growing number of trials advancing to phases II and III. An integrated phase II/III, randomised and controlled study will commence shortly, investigating the safety and efficacy of a conditionally replicating oncolytic Ad (CG0070) expressing granulocyte macrophage colony-stimulating factor ((GM-CSF), a cytokine shown to be a potent inducer of specific, long-lasting anti-tumour immunity in animal models (Dranoff *et al.*, 1993; Ramesh *et al.*, 2006)). CG0070 will be tested in patients with non-muscle invasive bladder cancer who have failed current forms of treatments (Ramesh *et al.*, 2006). Also currently underway is a phase I/II study assessing the use of Ad5 encoding human adenylyl cyclase type 6 (functions in cardiac contractility) gene transfer via intracoronary delivery for congestive heart failure (Lai *et al.*, 2004). The first phase I/II trial in the UK not based on Ad serotype 5, is expected to commence later this year for the treatment of metastatic colorectal cancer (Kuhn *et al.*, 2008). This study will employ an oncolytic vector, termed ColoAd1, based on subgroup B Ad11p and Ad3 (Kuhn *et al.*, 2008; Kuhn *et al.*, 2005). In respect to cancer treatment the use of Ad5 for the delivery of the tumour suppressor gene p53 has been the focus of several studies (Bischoff *et al.*, 1996; Gabilovich, 2006; Heise *et al.*, 1997). Gendicine, a replication-deficient Ad5 expressing p53 vector, was the first

gene therapy product licensed, in China, for the treatment of head and neck cancers and also shows promise for use against other solid tumours (Peng, 2005).

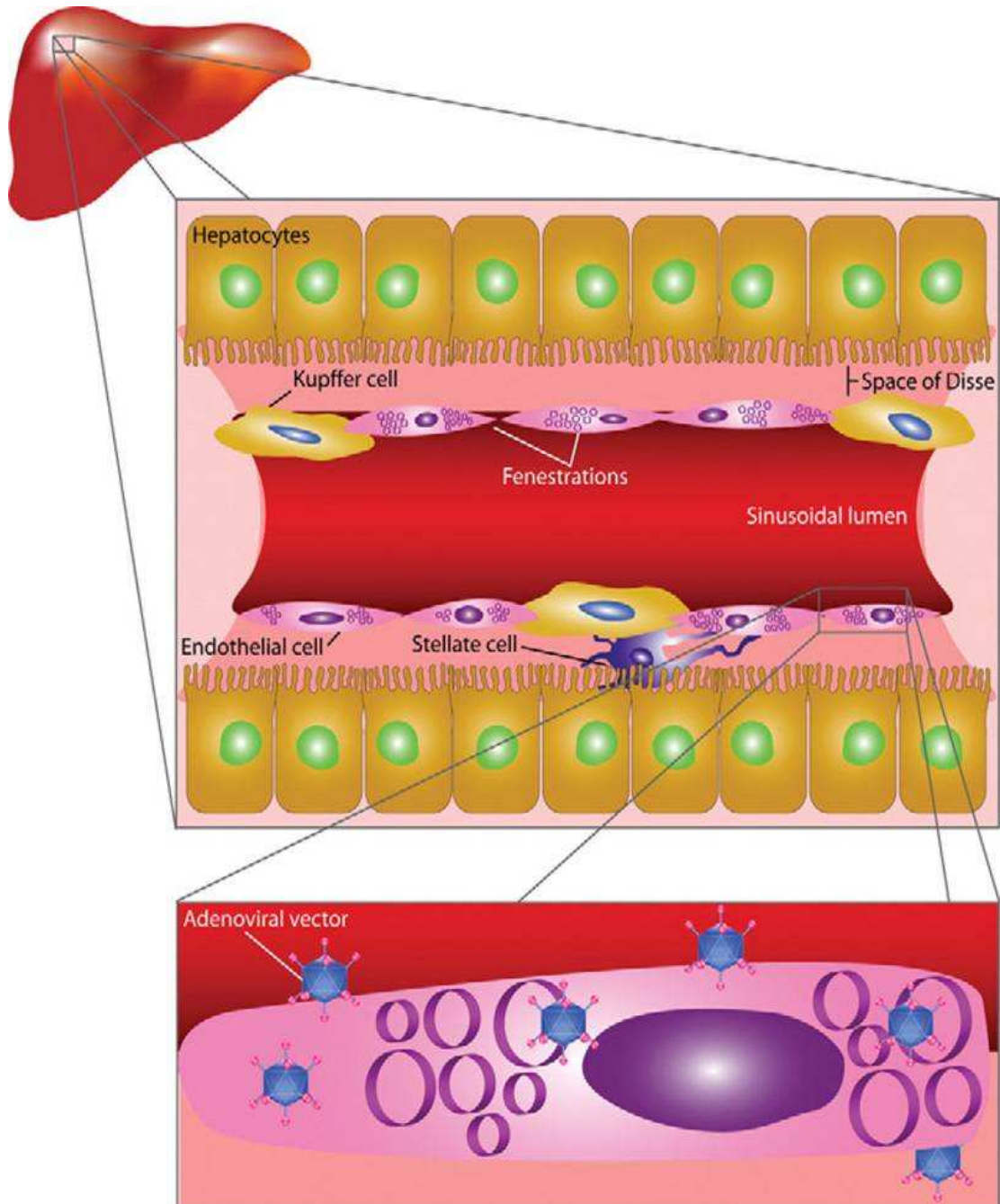


Figure 1.6. Liver cells and Ad5 hepatic uptake.

The liver sinusoidal wall is formed by liver sinusoidal endothelial cells and juxtaposed Kupfer cells. Whilst Kupfer cells and liver sinusoidal endothelial cells limit hepatocyte transduction by Ad5, the presence of fenestrae in liver sinusoidal endothelial cells provides a direct access to the space of Disse and the microvillous surface of hepatocytes. This figure was taken from Jacobs *et al.* (Jacobs *et al.*, 2010).

In addition to gene replacement and combinations of gene therapy with standard anti-tumour strategies, the concept of suicide gene therapy is another application under investigation (Barton *et al.*, 2011; Freytag *et al.*, 2007a). This refers to the viral delivery of enzymes that metabolise systemically administered non-toxic prodrugs into locally active anti-cancer agents. A randomised, controlled phase II/III study is currently underway to assess the efficacy of replication competent Ad-mediated suicide gene therapy in conjunction with radiation treatment for prostate cancer (Barton *et al.*, 2011; Freytag *et al.*, 2007a; Lu *et al.*, 2011). The virus used in the trial contains a bacterial cytosine deaminase (CD)/herpes simplex virus thymidine kinase (TK) fusion gene in the E1 region in place of the E1B-55kDa gene, and lacks the adenoviral genes of the E3 region. In addition to the oncolytic properties of the virus itself, expression of the CD/TK fusion gene renders tumour cells sensitive to 5-fluorocytosine (5-FC) and ganciclovir (GCV) prodrugs (Freytag *et al.*, 2007a; Freytag *et al.*, 2007b; Lu *et al.*, 2011). Another study using a similar approach has employed a replication deficient Ad vector encoding bacterial nitroreductase (NTR) in conjunction with the prodrug CB1954 (5-(aziridin-1-yl)-2,4-dinitrobenzamide), for the treatment of prostate cancer (Patel *et al.*, 2009). NTR converts the weak alkylating agent CB1954 to a highly potent alkylating agent, thereby producing cytotoxic effects (Friedlos *et al.*, 1992).

Whilst local delivery of Ads has proven to be very beneficial, design of a vector which can be delivered intravenously and specifically target the desired tissues, without causing an immune response (except for certain cancer treatments, in which this may be advantageous) remains a challenge for many applications. Future success of systemically delivered gene therapy will ultimately be determined by improved understanding and modulation of the complex viral interactions with host proteins leading to better prediction of *in vivo* efficacy, pharmacokinetics and toxicity and consequently the development of safer, targeted vectors, individualised for defined applications.

1.6 Ad interactions with host proteins

1.6.1 Coxsackie virus and adenovirus receptor

Ad receptor usage greatly influences viral tropism. The extensively studied Ad receptor, the 46 kDa coxsackie virus and adenovirus receptor (CAR), was initially identified over 30 years ago as an attachment receptor for coxsackie B viruses (Lonberg-Holm *et al.*, 1976), then later as for Ad2 and Ad5 (Bergelson *et al.*, 1997; Tomko *et al.*, 1997). CAR belongs

to the immunoglobulin (Ig) superfamily and is composed of two extracellular Ig-like domains (distal variable type - D1 and proximal C2 type - D2) and a single membrane-spanning sequence connected to the carboxy terminal cytoplasmic domain (Chrétien *et al.*, 1998; Wang *et al.*, 1999). The major function of CAR is as a cell-to-cell adhesion molecule in tight junctions of polarised epithelial cells. It also interacts with junctional adhesion molecule-like protein and has a role in T cell activation (Witherden *et al.*, 2010) and recruitment of phosphoinositide 3-kinase (PI3K) (Verdino *et al.*, 2010).

In vitro CAR is a primary cellular attachment receptor for Ads of species A, C, D, E and F, but not species B (Roelvink *et al.*, 1998). The CAR D1 domain binds to the side of each monomer of the trimeric fiber knob, an interaction which is conserved amongst the CAR binding Ads (Kirby *et al.*, 2000; Rolvink *et al.*, 1999). The CAR:knob interaction is responsible for the initial binding of the virus to the cell surface. The amino acid residues in the Ad fiber essential for CAR binding were identified through alignment of the knob domain sequences of those Ads known to interact with CAR (Rolvink *et al.*, 1999). Several mutations were found to affect the fiber knob:CAR interaction, including S408E/G, P409A, K417G/L (in the AB loop), K420A (B β -sheet), Y477A/T (DE loop), Y491A (FG loop), a four amino acid deletion of TAYT or replacement of EGTAY (FG loop) (Figure 1.7) (Rolvink *et al.*, 1999). Following cell attachment, subsequent virus internalisation is mediated by integrins (Wickham *et al.*, 1993). Integrins, cell surface adhesion molecules composed of α and β transmembrane subunits, interact with the RGD motif on the Ad5 penton base, primarily via the integrins $\alpha v\beta 3/\alpha v\beta 5$ (Wickham *et al.*, 1993). Integrins interact with a variety of signalling molecules and promote Ad internalisation, principally through clathrin-mediated endocytosis (Wang *et al.*, 1998). Once inside the cells and following release from the endosomes, the virus travels along microtubules toward the microtubule organising centre (MTOC), before binding to nuclear receptors and being imported into the nucleus (Greber *et al.*, 1997; Kelkar *et al.*, 2004; Suomalainen *et al.*, 1999). The intracellular trafficking of Ad from the cell surface to the nucleus and the viral uncoating process is described in further depth in Chapter 4.

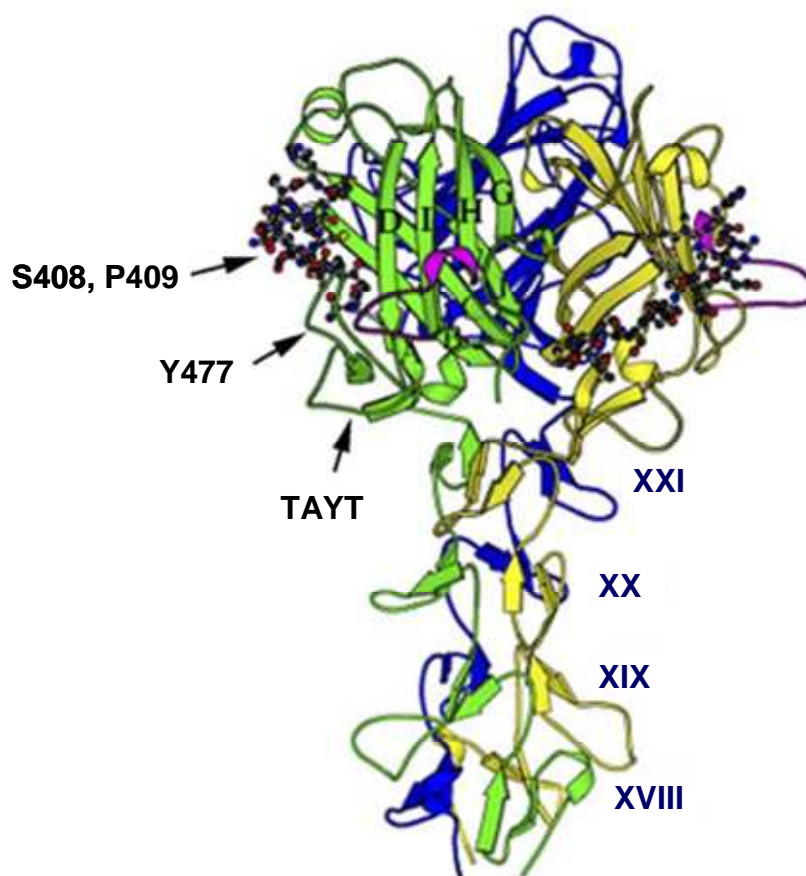


Figure 1.7. Critical features of the Ad fiber.

The strands of the fiber knob are lettered according to the nomenclature of Xia *et al.* (Xia *et al.*, 1994). The CAR binding site, which is made up mostly by the AB loop (ball and stick), lies along the side of the fiber knob trimer. Locations of some mutations that abolish CAR binding are indicated by arrows. The HI loop is shown in magenta. The final four-repeats of the fiber shaft (18–21) are shown with Roman numerals. This image was adapted from Nicklin *et al.* (Nicklin *et al.*, 2005).

Although this is a very well defined two step cell tethering and subsequent internalisation pathway, detailed by many *in vitro* studies, there is clear evidence to suggest CAR is not the primary attachment receptor *in vivo* following intravascular delivery of Ad5 vectors. Anatomically CAR is localised to tight junctions. Wild-type infection by Ad occurs primarily via airway epithelial cells, which release the replicating virus to basolateral and apical surfaces, allowing the Ad5 fiber to bind CAR and disrupt tight junction integrity, thus facilitating the spread of the virus (Walters *et al.*, 2002). However, tight junctions are not readily accessible for circulating Ad5 vectors. In addition, mRNA encoding CAR is expressed on a wide range of tissues; most highly in the pancreas, brain, heart, small intestine, testes, prostate and to a lesser extent in the liver and lung (Tomko *et al.*, 1997). This pattern of expression does not correlate to the pattern of Ad5 tropism *in vivo*, as following intravascular delivery the majority of the vectors are sequestered by the liver, as

discussed earlier (Huard *et al.*, 1995). Studies by Einfeld *et al.* and Koizuma *et al.* reported combined mutations in the fiber knob and the RGD motif of the penton base, to prevent CAR and integrin-mediated interactions, significantly reduced liver transduction following intravascular delivery (Einfeld *et al.*, 2001; Koizumi *et al.*, 2003). However, a vast number of studies employing Ad5 vectors with mutations that ablate CAR binding alone have demonstrated no difference in biodistribution, with similar levels of hepatocyte transduction to non-modified Ad5 vectors being observed in rodents and non-human primates (Alemany *et al.*, 2001; Martin *et al.*, 2003; Smith *et al.*, 2002). Recently, research focus has mainly been directed at uncovering alternate Ad pathways that define *in vivo* tropism.

1.6.2 The role of the immune system

A major obstacle to the use of Ad5 for gene therapy is the rapid induction of the innate and the adaptive immune response towards the vector, which can lead to rapid clearance of the virus and severely compromises the envisaged efficacy of the vector (Di Paolo *et al.*, 2009a; Sumida *et al.*, 2005; Varnavski *et al.*, 2005). The viral capsid proteins possess distinct antigenic determinants capable of eliciting cellular and humoral immune responses which can result in potent toxicity (Gahéry-Ségard *et al.*, 1997; Lieber *et al.*, 1997; Roberts *et al.*, 2006) (Figure 1.8).

1.6.2.1 Innate immunity

As previously mentioned, liver macrophages, KCs, can sequester up to 90% of virus particles within minutes of intravascular administration in mice (Lieber *et al.*, 1997; Worgall *et al.*, 1997). This triggers a rapid destruction of KCs as early as 10 min post-injection (Manickan *et al.*, 2006). In addition, the same study reported the translocation of Ad-positive KCs from the liver to the lungs by 30 min, suggesting KC displacement from the liver (Manickan *et al.*, 2006). The acute phase virus-induced KC response has been associated with the induction of proinflammatory cytokines and chemokines including interleukin (IL)-6, IL-10, IL-8, tumour necrosis factor alpha, gamma interferon and macrophage inflammatory proteins 1 and 2, thereby contributing to the extensive liver pathology caused by Ad5 (Lieber *et al.*, 1997; Muruve *et al.*, 1999).

There are several mechanisms involved in the uptake of Ads by KCs. Scavenger receptors recognise the negatively charged viral capsid and preinjecting mice with broad spectrum inhibitors of scavenger receptors such as dextran or polyinosinic acid (poly(I)) has been

shown to decrease Ad uptake by KCs and increase the circulating half-life of the virus *in vivo* (Haisma *et al.*, 2008; Xu *et al.*, 2008). A recent study by Khare *et al.* reported the involvement of HVR 1, 2, 5 and 7 in KC recognition by scavenger receptor SRA-II (Khare *et al.*, 2012). Antibody-deficient RAG-1 knockout mice exhibited significantly reduced levels of Ad particles within KCs, an effect which could be reversed by preinjection with serum from naïve C57BL/6 mice, thus demonstrating a requirement for natural antibodies (Xu *et al.*, 2008). Natural immunoglobulin M antibodies and complement proteins, in particular complement protein C3, opsonize the virus and are involved in KC uptake (Jiang *et al.*, 2004; Xu *et al.*, 2008). Pre-existing neutralising antibodies (NAb) of the adaptive immune system have also been reported to increase the targeting of Ad to macrophages (Zaiss *et al.*, 2009). *In vitro*, NAbs significantly increased FcR-dependent Ad internalisation of macrophages, while in pre-immunised mice, the innate response was enhanced, with significantly higher levels of inflammatory gene expression in the liver and IL-1 β levels in the serum compared to naïve animals (Zaiss *et al.*, 2009).

As well as cells such as macrophages and serum immune mediators, intra- and extra-cellular innate receptors, termed host pattern recognition receptors (PRR), can recognise the antigenic viral capsid, double-stranded genome or viral proteins (Zhu *et al.*, 2007). Activation of IL-1 α in splenic marginal zone macrophages in response to the Ad5 RGD motif binding to $\alpha v \beta_3$ integrins has also been elegantly shown (Di Paolo *et al.*, 2009a). Ad5 RGD activation of IL-1 α is required for the expression of IL1-RI dependent cytokines and chemokines including CXCL1 and CXCL2 and this occurs independently of genomic nucleic acid recognition by PRRs (Di Paolo *et al.*, 2009a).

Several successful strategies to deplete or inactivate KCs have been described including intravascular injection of gadolinium chloride (Lieber *et al.*, 1997), clodronate encapsulated liposomes (Van Rooijen *et al.*, 1996; Wolff *et al.*, 1997) or predosing animals with a null Ad vector (Tao *et al.*, 2001). Clodronate liposomes are ingested by the KCs, which are then killed following phospholipase-mediated disruption of the liposomal bilayers and release of the clodronate (van Rooijen *et al.*, 2003). Similarly, gadolinium chloride forms a colloidal precipitate in the bloodstream which is phagocytosed by the macrophages, resulting in cell destruction (Hardonk *et al.*, 1992). These methods provide a therapeutic window in which the vector can be delivered whilst bypassing clearance by KCs and decreasing liver damage. Whilst these methods are valuable for studying Ad host interactions in the laboratory setting, they are not likely to be of clinical relevance and the

multitude and complexity of the immune response to Ad5 remains a hurdle for clinical applications.

1.6.2.2 Adaptive immunity

An important consideration which must be taken into account is the lack of natural pre-existing neutralising antibodies in animals which may underestimate the importance of the human immune response. In the United States the seroprevalence to Ad5 is reported to be 50%, whilst in sub-Saharan Africa this number rises to 80% (Sumida *et al.*, 2005). The high seroprevalence of pre-existing NAb to the Ad5 capsid proteins, in particular the hexon, which has been shown by Sumida *et al.* to have NAb titers up to 10-fold higher than fiber-specific NAb titers, is a major hurdle for Ad5 gene therapy applications (Sumida *et al.*, 2005). A study by Roberts *et al.*, in which the seven HVRs of Ad5 were replaced with that of Ad48 (a so called “rare serotype”), demonstrated the vectors ability to largely evade Ad5 specific NAb in pre-immunised mice, therefore indicating a major role for the hexon HVRs in activating the adaptive immunity (Roberts *et al.*, 2006). Chimeric Ad5 vectors in which subsets of the HVRs were exchanged (Ad5HVR48(1-3), Ad5HVR48(4), and Ad5HVR48(5)) were generated to look more closely at the role of individual regions (Bradley *et al.*, 2012b). The Ad5HVR48(1-3) vector resulted in intermediate NAb titres compared to Ad5HVR48(1-7) and Ad5, and Ad5HVR48(4), and Ad5HVR48(5) were unable to bypass pre-existing Ad5 immunity in preimmunised mice, thereby indicating NAb target multiple HVRs (Bradley *et al.*, 2012b).

NAb responses have also been reported against the fiber protein (Bradley *et al.*, 2012a; Gahéry-Ségard *et al.*, 1998; Hong *et al.*, 2003; Parker *et al.*, 2009). Parker *et al.* pseudotyped the Ad5 fiber with a fiber from the less prevalent serotype Ad45 (Parker *et al.*, 2009). The Ad5f45 vector partially bypassed neutralisation *in vitro*, indicating a significant proportion of NAb identified by these assays are directed against the fiber (Parker *et al.*, 2009). In a separate study, the fiber knob of Ad5 and Ad5HVR48(1-7) were replaced with that of the chimpanzee adenovirus AdC68 (AdC68 rarely causes infection in humans) (Bradley *et al.*, 2012a; Xiang *et al.*, 2006). Ad5KC68 demonstrated lower NAb titres in pre-immunised mice (preimmunised with two injections of 10^{10} vp of Ad5 separated by 4 weeks) compared to Ad5, and Ad5HVR48(1-7)KC68 demonstrated a further decrease in Ad5-specific immunity compared to Ad5HVR48(1-7), thereby indicating the presence of antibodies directed against the fiber knob (Bradley *et al.*, 2012a). It has been suggested that Ad5-specific NAb are directed to different components of the

virion, depending on the route of infection (Cheng *et al.*, 2010). Following natural infection they were directed primarily against fiber, whereas Ad5-specific NAbs following Ad5 vector vaccination were directed primarily against hexon (Cheng *et al.*, 2010). Following natural Ad infection in airway epithelial cells, the fiber protein is produced in substantial excess to access CAR located in the tight junctions (Walters *et al.*, 2002), however this does not occur following intramuscular injection of Ad vectors and hence may explain the different anti-fiber (native) versus the anti-hexon (vaccine) host response. In summary, the use of rare Ad serotypes which are less seroprevalent (Abbink *et al.*, 2007) is an attractive prospect, however the caveat being they are less well studied and their tropism defining interactions are not always understood, necessitating further research.

1.6.3 Blood components

Efforts to elucidate the infectivity mechanisms of Ad5 vectors *in vivo* have lead researchers to evaluate the role of the blood in determining the Ad tropism. It is perhaps unsurprising that Ads have evolved a multitude of methods by which to harness host cells and proteins for their benefit, whilst in parallel the immune system exhibits a range of defense mechanisms upon contact with the virus. Following intravascular administration, Ads have been shown to interact directly with a variety of blood cells, plasma proteins and coagulation factors (summarised in Figure 1.8 (page 27)).

1.6.3.1 Erythrocytes

Following a 30 min incubation with blood *ex vivo*, 90% of Ad5 are bound to human erythrocytes, increasing to 98.8% after 1 h co-incubation (Cichon *et al.*, 2003; Lyons *et al.*, 2006). Ad5 interacts with and agglutinates human and rat erythrocytes, but not murine or rabbit (Carlisle *et al.*, 2009; Cichon *et al.*, 2003; Nicol *et al.*, 2004). Incubation of human erythrocytes with free RGD peptide did not prevent Ad5 binding, nor did Ad5 $_{\Delta}$ RGD (Ad5 vector in which the RGD motif is deleted) decrease binding compared to Ad5 (Lyons *et al.*, 2006). In the presence of human blood very low levels of virus transduction were observed in CAR positive cells *in vitro*, compared to Ad5 alone, indicating blood cells can prevent infection of epithelial cells (Lyons *et al.*, 2006). Furthermore when virus was allowed to bind to carcinoma cells for short incubation times (< 5 min), prior to washing with blood, Ad5 infection was significantly reduced demonstrating the ability of human blood cells to inhibit infection by viral particles prebound to epithelial cells, an important factor for Ad gene therapy applications (Lyons *et al.*, 2006). When the distribution of viral

genomes in blood samples from clinical trial patients injected intra-tumourally with 1×10^9 Ad5 particles were studied, 99% of viral DNA detected in the bloodstream was associated with blood cells. This is in contrast to the situation observed in mice following intravenous injection, in which 99% of Ad5 genomes remain free in plasma, highlighting the caution required when extrapolating data from animal studies for human trials (Lyons *et al.*, 2006).

More recently, two important studies demonstrated that human erythrocytes express CAR (Carlisle *et al.*, 2009; Seiradake *et al.*, 2009). Anti-CAR antibodies decrease the binding of Ad5 to human erythrocytes in plasma by less than 25%, indicating a dependency on CAR but also implicating additional mechanisms (Carlisle *et al.*, 2009). Furthermore, whilst the use of a CAR-binding ablated vector prevents binding to erythrocytes in phosphate buffered saline (PBS), it does not alter binding in human plasma (Carlisle *et al.*, 2009; Nicol *et al.*, 2004). Human erythrocytes also present complement receptor 1 (CR1), which binds Ad5 in the presence of antibodies and complement. The mechanism that the virus adopts to bind erythrocytes influences Ad5 circulation kinetics. Intravascular administration of Ad5 into CR1 transgenic mice resulted in a bloodstream half-life of less than 2 min, whilst injection into CAR transgenic mice resulted in up to 70% of Ad5 still detectable in the circulation at 6 h (Carlisle *et al.*, 2009). In a separate study, Ad5 was administered to GATA1-CAR (that express CAR on erythrocytes) and control C57BL/6 (CAR-negative erythrocytes) mice, resulting an 1000-fold higher viral load in the blood of GATA1-CAR versus control mice during the first 72 h post-injection (Seiradake *et al.*, 2009). Notably, viral genomes in the liver of GATA1-CAR mice were substantially lower compared to controls (Seiradake *et al.*, 2009). Although reducing liver transduction, sequestration of Ad by erythrocytes limits biodistribution and prevents specific targeting to desired tissues. Conversely, the study by Nicol *et al.*, showed no difference in liver transduction following intravascular delivery using Ad5 or non-CAR-binding Ad5 in rats, with erythrocytes expressing CAR (Nicol *et al.*, 2004). These data strongly support a role for erythrocytes in determining Ad tropism, however the effect of virus binding to erythrocytes on biodistribution and blood kinetics in non-transgenic animals warrants further detailed investigation.

Evidently, the complexity of Ad5 interactions with host factors is extensive but existing animal models may only provide limited information. The differences in the expression patterns of cellular receptors, such as the lack of CAR expression on mouse erythrocytes, may bypasses the very relevant sequestration mechanism observed in human blood. Another example is the expression of the Ad species B receptor, CD46, which is localised

to the testes in rodents, whereas it is widespread in humans. Whilst the use of transgenic models can help combat some of these problems, such as the recently reported desmoglein 2 transgenic mouse model for the study of species B Ads (Wang *et al.*, 2012), they will not aid the discovery of Ad:human host factor interactions which are currently undefined. A restraint to the successful development Ad gene therapy not to be underplayed is the species variation amongst the currently used animal models and humans.

1.6.3.2 Platelets

Ad5 can also bind to and activate circulating platelets (Othman *et al.*, 2007; Stone *et al.*, 2007). A study in which mice were administered via the tail vein with Ad5, demonstrated platelet counts were significantly reduced after 5 and 24 h (Othman *et al.*, 2007). The interaction between Ad and platelets initiates a cascade of events, as reported by Othman *et al.* Ad5 activates platelets and causes the rapid exposure of P-selectin, which is capable of binding to P-selectin glycoprotein ligand-1, detected on the majority of leukocytes and also present to a lesser extent on platelets, resulting in the formation of platelet-leukocyte aggregates (Othman *et al.*, 2007). This causes the release of platelet and leukocyte microparticles, which are cell vesicles with inflammatory and coagulatory potency (Othman *et al.*, 2007). P-selectin has been reported to mediate the tethering of leukocytes to endothelial cells (McEver, 1995). This study indicated that endothelial cells are activated after Ad5 administration (Othman *et al.*, 2007). Additionally, Ad5 injection into mice resulted in an acute, significant increase in plasma von Willebrand factor (vWF), which originated from the activated endothelial cells. vWF is reported to mediate the binding of platelets to the endothelium (Sadler, 1998). Furthermore, Ad administration in mice deficient in vWF did not result in thrombocytopenia by 24 h. Platelets exhibit significantly less P-selectin expression and platelet-leukocyte aggregate formation after 1 h, compared to vWF positive mice. Therefore these data indicate a role for P-selectin and vWF in mediating Ad induced thrombocytopenia. As 72% of human platelets are positive for CAR (Othman *et al.*, 2007), Ad5 may bind to platelets via this receptor, thereby acting as a 'sink' for systemically delivered Ads as well as causing endothelial activation, thrombocytopenia and leukocyte infiltration (Othman *et al.*, 2007; Stone *et al.*, 2007).

In a study by Stone *et al.*, immunohistochemistry performed on livers harvested at 5 min post-injection, indicated triple co-staining with hexon, macrophage and platelet markers (Stone *et al.*, 2007). Aggregates containing degranulated, virus-containing platelets were observed in the liver sinusoids, in the vicinity of KCs, implicating a role for platelets in

virus sequestration by KCs. Mice treated intravenously with an antibody against platelets, caused an approximate 66% reduction in platelet counts prior to Ad5 administration and viral genomes in the liver were significantly reduced at 5 min post-injection (Stone *et al.*, 2007). This suggests virus platelet aggregates may be rapidly captured in the hepatic reticuloendothelial system and degraded.

However, the role of platelets in reticuloendothelial system uptake remains controversial. A study by Xu *et al.* reported that platelets were not required for virus sequestration by KCs, as platelet depletion in mice did not result in any significant difference in Ad uptake by KCs at 10 min post-injection (Xu *et al.*, 2008). Therefore additional studies are required to confirm the importance of this interaction.

1.6.3.3 Lactoferrin

Lactoferrin, a multifunctional iron-binding glycoprotein produced at areas of inflammation and present at mucosal sites and in many bodily fluids (Masson *et al.*, 1966), has been shown to enhance Ad5 cell binding to corneal epithelial cells (Johansson *et al.*, 2007). Using monoclonal antibodies to block CAR caused no effect on human lactoferrin-mediated infection *in vitro*. Furthermore, human lactoferrin from tear fluid promoted Ad5 binding to CAR negative T cells more efficiently than T cells transfected to express CAR, thereby indicating cellular binding in a CAR-independent manner (Johansson *et al.*, 2007). Replacing the Ad5 fiber with that of Ad35 resulted in significantly lower levels of transgene expression compared to an Ad5 control vector, suggesting a role for the fiber in lactoferrin-mediated infection (Johansson *et al.*, 2007).

A study by Adams *et al.* reported the ability of human and bovine lactoferrin to enhance Ad5-mediated transduction of human primary antigen expressing cells, such as dendritic cells, in a dose-dependent manner independently of CAR (Adams *et al.*, 2009). The C-type lectin receptor dendritic cell-specific intercellular adhesion molecule-3-grabbing non-integrin (DC-SIGN) facilitated entry of Ad5 complexed with bovine lactoferrin in dendritic cells, however the receptor for human lactoferrin remains elusive (Adams *et al.*, 2009; Günther *et al.*, 2011).

1.6.3.4 Complement proteins

The human complement component C3, a central component of the complement pathway, has also been shown to bind to Ad5 (Jiang *et al.*, 2004). In complement C3 knockout mice,

administration of a relatively low dose Ad5 (2.3×10^9 vp) caused ~100-fold reduction in hepatocyte transduction after 3 days, in comparison to wild-type control mice (Zinn *et al.*, 2004). As the dose of Ad5 administered was increased (highest dose of 1.3×10^{10} vp) the difference between wild-type and C3^{-/-} mouse liver targeting was decreased, as shown by bioluminescence imaging over a 35 day period, independently of antibody responses against Ad (Zinn *et al.*, 2004). Preincubation of Ad5 with wild-type, C1q^{-/-}, or factor B (protein components of the alternative complement system) deficient mouse sera for 5 min significantly increased transduction of mouse liver hepatoma cells *in vitro*, as compared to preincubation with C3^{-/-} sera, indicating Ad-induced C3 activation is via a C1q or FB dependent mechanism (Zinn *et al.*, 2004). Tsai *et al.* demonstrated the ability of complement protein Cq1 to mediate Ad infection in a CAR-negative cell line (Tsai *et al.*, 2008). In a separate study, injection of high dose (1.5×10^{11} vp/mouse) Ad5 resulted in similar levels of hepatocyte transduction in wild-type and C3 knockout mice at 48 and 72 h. However thrombocytopenia and the acute inflammatory response was significantly reduced (Kiang *et al.*, 2006). Whilst these results indicate a dose-dependent role for C3 in determining liver gene transfer, they suggest it may have a pivotal role in determining the host immune response.

A study by Seregin *et al.* performed genetic engineering of Ad5 to ‘capsid display’ the human complement inhibitor decay-accelerating factor (DAF) following insertion into the C-terminus of Ad protein IX (Seregin *et al.*, 2010). The vector resulted in reduced complement activation *in vitro* and complement dependent immune responses *in vivo*, including decreased levels of pro-inflammatory cytokines, chemokine responses, thrombocytopenia and minimized endothelial cell activation compared to Ad5 (Seregin *et al.*, 2010). Ad5 capsid-displaying DAF vectors also reduced transgene and capsid specific adaptive immune responses, after intravascular and intramuscular delivery in Ad5-naïve and Ad5 immune mice (Seregin *et al.*, 2011).

1.6.3.5 Blood factors

In 2005, Shayakhmetov *et al.* were the first to describe a potential role of blood factors in determining Ad5 tropism (Shayakhmetov *et al.*, 2005). Using an *in situ* liver perfusion technique, they analysed gene delivery to the liver in the absence of blood. Hepatocyte transduction of Ad5 and the non-CAR binding vectors, Ad5 containing the Ad35 knob domain, and Ad5*F (which has a single point mutation at position Y477 in the fiber knob, ablating the CAR interaction) were assessed. In the absence of blood, hepatocyte

transduction by the non-CAR binding vectors was significantly decreased compared to Ad5, indicating the involvement of an alternative mechanism for Ad5 infection that are dependent on blood factors (Shayakhmetov *et al.*, 2005). To investigate the cellular receptor responsible for this novel pathway, mice were preinjected with competing ligands for hepatocellular receptors, including polymerised bovine serum albumin (saturates the scavenger receptor SR-BI), asialofetuin (saturates the asialoglycoprotein receptor), human low density lipoprotein (LDL) (saturates the LDL receptor) or lactoferrin (saturates low-density lipoprotein receptor-related protein (LRP) and heparan sulphate proteoglycans (HSPGs)). A 50-fold reduction of Ad5*F, a 600-fold reduction of Ad5/35 and an 8-fold reduction in Ad5 liver gene transfer in the presence of lactoferrin indicated cellular binding through LRP and HSPGs (Shayakhmetov *et al.*, 2005). Injection of heparinase I, resulting in enzymatic digestion of heparan sulphate side-chains, prior to vector administration resulted in significantly lower levels of liver transduction in wild-type mice, implicating HSPGs as the major cellular receptors (Shayakhmetov *et al.*, 2005). Consequently, tandem mass spectrometry and slot blot assays were used to identify blood factors capable of interacting with Ad. Coagulation factor IX and complement component C4-binding protein were shown to directly interact with the Ad fiber knob and mediate Ad infection *in vitro* (Shayakhmetov *et al.*, 2005). In addition, mouse livers perfused with saline containing FIX showed increased hepatocyte transduction of Ad5/35 and Ad5*F, reaching levels comparable to Ad5. However, injection of Ad5/35 and Ad5*F into FIX knockout mice resulted in no significant difference in liver gene transfer compared to wild-type mice (Shayakhmetov *et al.*, 2005). Whilst this data suggested a role of FIX and C4-binding protein in mediating Ad5 hepatic transduction, further studies supported the involvement of additional blood factors key to determining the Ad5 inherent liver tropism.

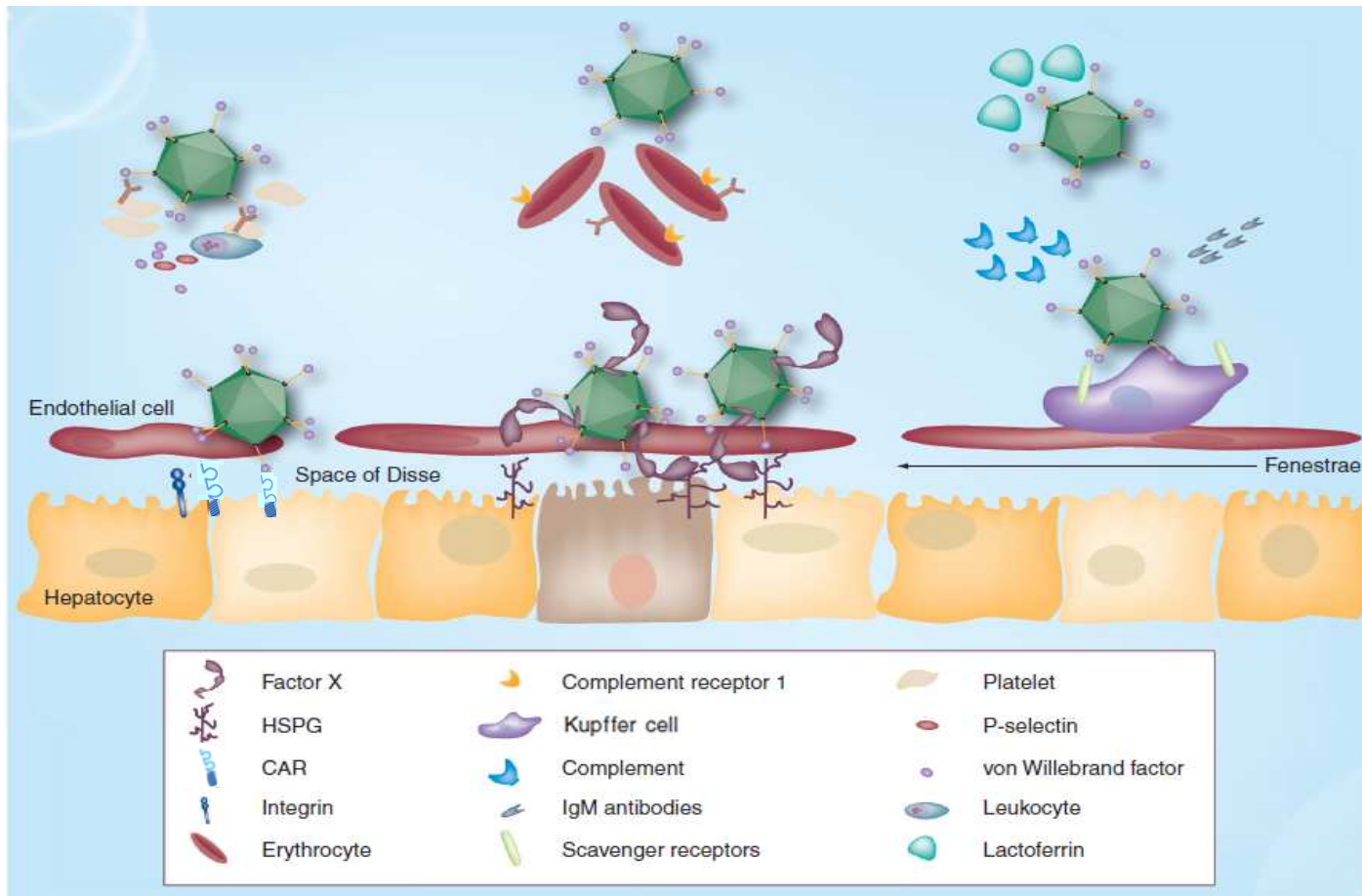


Figure 1.8. *In vivo* Ad5 interactions with host factors.

Ad5 binds to coagulation FX due to a high affinity interaction between the Ad5 hexon HVR domains and the FX Gla domain. FX subsequently bridges the complex to HSPGs on the surface of hepatocytes. Opsonisation by IgM antibodies, complement and scavenger receptors can promote Kupffer cell uptake. Ad5 fiber knob can bind to CAR-expressing erythrocytes or in the presence of complement and antibodies the virus binds to CR1 on the surface of erythrocytes. Ad5 can also interact with lactoferrin. Ad5 binding to platelets can induce the formation of platelet-leukocyte aggregates, a process dependent on von Willebrand factor and P-selectin.

1.7 A critical role for coagulation factor X in determining the Ad5 liver tropism

Several other vitamin-K dependent zymogens were subsequently found to enhance transduction of Ad5 in HepG2 cells (Parker *et al.*, 2006). These blood coagulation factors FVII, FIX, FX and protein C are zymogens of serine proteases. The vitamin-K dependent coagulation factors are structurally very similar and likely to be derived from a common ancestral gene via gene duplication and exon shuffling (Davidson *et al.*, 2003). They have a light chain consisting of a γ -carboxylated glutamic acid (Gla) rich domain and two epidermal growth factor-like domains which are disulfide linked to the serine protease (SP) heavy chain (Figure 1.9).

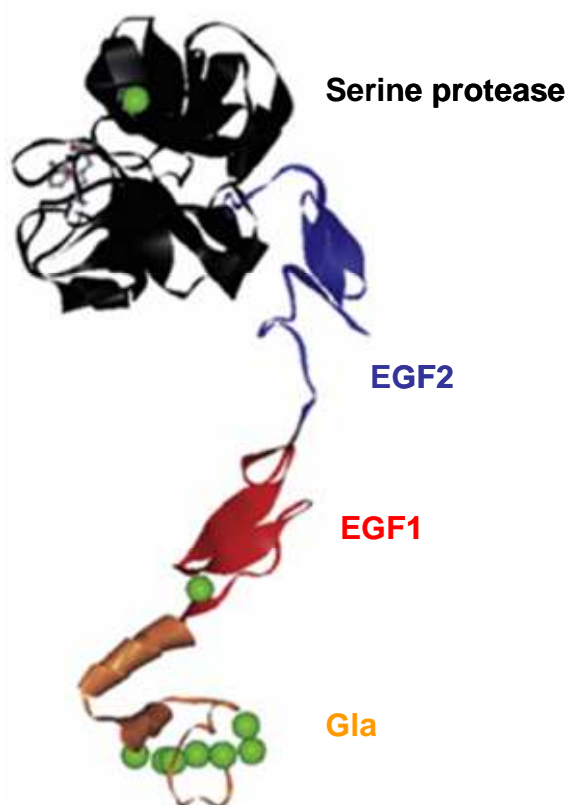


Figure 1.9. Coagulation factor X.

The domain structure of FX, highlighting the γ -carboxylated glutamic acid, the epidermal growth factor (EGF) 1-like, EGF2-like and serine protease domains. The green balls indicate calcium ions. This figure has been adapted from Venkateswarlu *et al.* (Venkateswarlu *et al.*, 2002).

To investigate whether zymogen activation was required to increase Ad infection, FX was incubated with recombinant tick anticoagulant protein (TAP), a highly specific direct FXa inhibitor, or fondaparinux, which inhibits FXa indirectly through antithrombin III. Neither

inhibitor had an effect on FX-mediated Ad transduction in HepG2 cells and pretreating mice with fondaparinux prior to injection of a CAR-binding ablated Ad5 vector (AdKO1) caused no effect on levels of liver transduction. Therefore, this demonstrated that zymogen activation was not necessary (Parker *et al.*, 2006). The authors went on to assess whether FX could interact with Ad5 and AdKO1 directly. Surface plasmon resonance (SPR) analysis revealed a strong association between each virus and FX in a dose-dependent manner, however upon the addition of ethylenediamine tetra-acetic acid (EDTA) the virus readily dissociated, indicating a dependency on calcium. In an attempt to investigate whether FX-mediated transduction was relevant *in vivo*, Parker *et al.*, first assessed the ability of FX to restore gene transfer of AdKO1 to levels of Ad5 in an *ex vivo* liver perfusion model. FX not only increased AdKO1 liver transduction to levels comparable to Ad5, but substantially increased hepatocyte transduction by both vectors, causing a 25-fold increase in Ad5 and an equivalent 250-fold increase in AdKO1 transgene expression (Parker *et al.*, 2006). Moreover, following intravascular delivery, Ad-mediated liver gene transfer was greatly reduced in warfarin pretreated mice demonstrating the requirement for vitamin-K dependent coagulation factors (Parker *et al.*, 2006; Waddington *et al.*, 2007). Warfarin inhibits the effective synthesis of vitamin K-dependent coagulation factors by preventing efficient γ -carboxylation of the Gla domain, thus reducing levels of functional circulating factors (Mosterd *et al.*, 1992; Stanton *et al.*, 1992). Despite FVII, FIX and protein C being effective enhancers of Ad5-mediated gene transfer *in vitro* only intravascular injection of physiological concentrations of FX, 30 min prior to AdKO1 or Ad5 administration, was reported to completely restore Ad hepatic transduction in warfarin-treated mice (Parker *et al.*, 2006; Waddington *et al.*, 2007). Another study investigated whether warfarin could block Ad liver sequestration by KCs, an effect which can occur within minutes after Ad administration (Waddington *et al.*, 2007). Warfarin treatment did not effect Ad5 virion levels in the liver and spleen at 1 h post-injection, however at 48 h virion accumulation was decreased, suggesting coagulation factors do not effect KC uptake but selectively influence hepatocyte transduction (Di Paolo *et al.*, 2009b; Waddington *et al.*, 2007). Together these data demonstrated a pivotal role for FX in determining the targeted liver gene transfer of Ad5 via a CAR-independent mechanism.

1.8 FX Gla domain mediates binding to Ad5

In order to identify the region of FX responsible for binding to Ad5, Waddington *et al.*, utilised SPR to demonstrate the ability of the monoclonal antibody HX-1, directed against the light chain (Gla-EGF1-EGF2) of FX, to block binding to Ad5 and inhibit AdKO1

transduction, in the presence of physiological levels of FX, in HepG2 cells (Waddington *et al.*, 2008). In addition, SPR analysis revealed that Ad5 failed to bind to Gla domainless FX (Kalyuzhniy *et al.*, 2008; Waddington *et al.*, 2008). *In vivo*, Gla domainless FX did not restore Ad5 liver gene transfer in warfarin-treated mice (Waddington *et al.*, 2008), thereby demonstrating the importance of the Gla domain in the Ad5:FX interaction. Factor X-binding protein (X-bp), an anticoagulant isolated from *Deinagkistrodon acutus* (the hundred pace snake), is a high affinity Gla domain binding protein (Atoda *et al.*, 1998). X-bp blocked Ad5 binding to FX as shown by SPR and preincubation of human FX with eqimolar concentrations of X-bp inhibited FX-mediated Ad5 infection in HepG2 cells (Waddington *et al.*, 2008). Preinjection of X-bp resulted in significantly lower levels of Ad5 liver transduction in mice. Moreover, preincubation of FX with X-bp prior to injection into warfarin-treated mice blocked the ability of FX to restore Ad5 hepatic gene transfer (Waddington *et al.*, 2008). These data demonstrate the FX Gla domain is critical for FX-mediated Ad5 liver transduction.

1.9 FX binds directly to the Ad5 hexon

Initially it was proposed that coagulation factor mediated hepatic gene transfer was as a result of FIX binding to the Ad5 fiber (Shayakhmetov *et al.*, 2005). A study using a panel of Ad5 vectors pseudotyped with fibers from species D, including f17, f24, f30, f33, f45 and f47, investigated the capacity of each vector to bind to coagulation factors (Parker *et al.*, 2007). SPR analysis indicated that all vectors directly bound to FX in a calcium-dependent manner, indicating bridging of FX to an alternative capsid protein or to a highly conserved region in the fiber. FX caused a significant increase in HepG2 cell binding and transgene expression for all vectors (Parker *et al.*, 2007). FX-mediated Ad infection was demonstrated to occur via HSPGs, as shown by the enhanced levels of transduction in Chinese hamster ovary (CHO) cells expressing HSPGs compared to the significantly reduced levels in genetically modified CHOpgsA745 cells, which have a defect in xylosyltransferase and do not produce glycosaminoglycans, therefore have no surface expression of the receptors (Parker *et al.*, 2007). Injection of Ad5/f47 into coagulation depleted mice significantly reduced levels of hepatic transduction (Waddington *et al.*, 2007), hence the effects of FX were relevant not only for Ad5 but also for Ad5 fiber pseudotyped vectors.

An unexpected finding was observed when SPR studies demonstrated that fully fiberless Ad5 virions bound to FX as efficiently as wild-type Ad5 (Waddington *et al.*, 2008).

Deletion of the Ad5 fiber had no effect on FX-mediated Ad5 cellular binding, thus confirming the binding of FX to an alternative capsid protein (Waddington *et al.*, 2008). Previously, hexon was thought to act principally as a structural protein. However, SPR analysis showed the FX Gla domain bound to the Ad5 hexon protein in a high affinity, calcium-dependent manner (Kalyuzhniy *et al.*, 2008; Waddington *et al.*, 2008). Both human and mouse FX bound to the Ad5 hexon with picomolar affinity (Kalyuzhniy *et al.*, 2008; Waddington *et al.*, 2008).

1.10 FX binds to hexon HVRs

Waddington *et al.* employed cryoelectron microscopy to generate a three-dimensional reconstruction of the Ad5:FX interaction (Figure 1.10). Cryoelectron microscopy revealed that the FX molecule binds within the central cavity formed by each hexon trimer, a region characterised by the presence of HVRs (Kalyuzhniy *et al.*, 2008; Waddington *et al.*, 2008). Ads have seven HVRs on the hexon which differ amongst Ad types. In addition to binding to the Ad5 HVRs, SPR studies demonstrated the ability of FX to bind Ads from species A, B, C, D, E and F with varying degrees, indicating that the Ad:FX interaction is highly conserved (Kalyuzhniy *et al.*, 2008; Waddington *et al.*, 2008).

Previously the hexon was thought not to be directly related to tropism determination. In 1999, a study by Vigne *et al.*, reported the inclusion of a RGD-containing peptide, targeted to αv integrins, in HVR5 of the hexon significantly increased transgene expression in human vascular smooth muscle cells, naturally refractory to Ad infection due to a lack of CAR expression (Pasqualini *et al.*, 1997; Vigne *et al.*, 1999). Vigne *et al.* demonstrated the ability of hexon HVR-modified capsids to be efficiently internalised by cells lacking the virus primary receptors and this was one of the earliest studies to imply a function of the HVRs in Ad cell entry (Vigne *et al.*, 1999). Intravenous delivery of the vector resulted in ~98% lower hepatic transgene expression after 48 h compared to control Ad5 and its counterpart containing the RGD peptide in the fiber (Vigant *et al.*, 2008). Vigant *et al.* also demonstrated substantially reduced liver transduction and hepatotoxicity using an Ad5 vector in which HVR5 was replaced by non-targeting peptides containing 8 or 24 glycine-alanine residues (Vigant *et al.*, 2008).

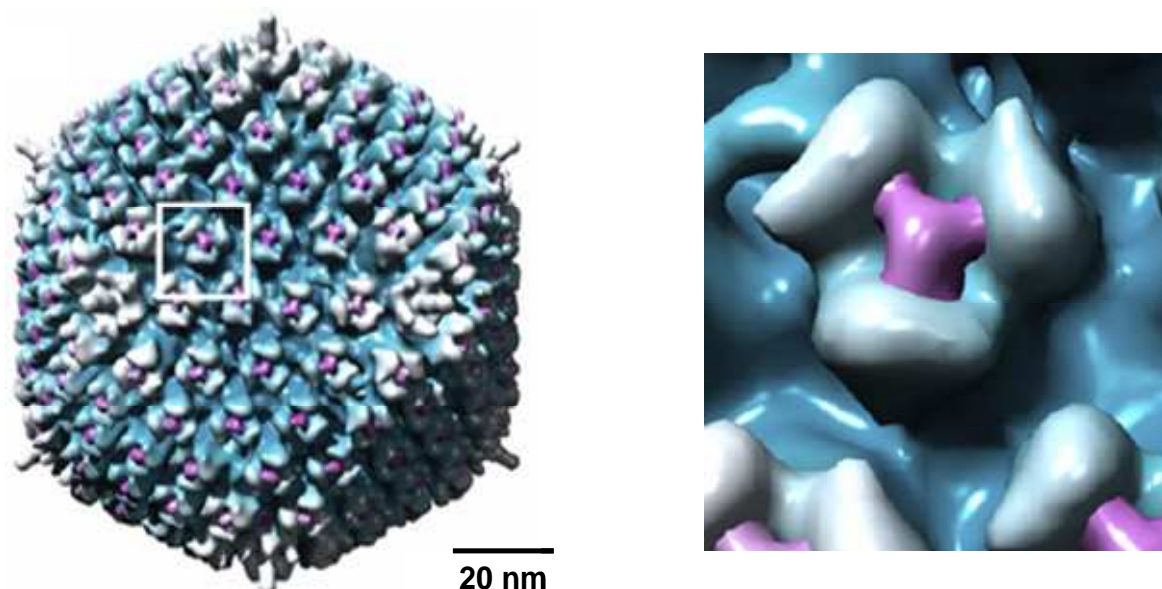


Figure 1.10. Analysis of Ad5 hexon binding to FX by cryoelectron microscopy.

The image on the left hand side is an overlay of three-dimensional cryoelectron microscopy reconstructions of uncomplexed Ad5 (blue) and the Ad5:FX complex (purple) and the image on the right hand side is a close-up view of FX-labelled hexon. This figure has been adapted from Waddington *et al.* (Waddington *et al.*, 2008).

A study using an engineered Ad5 vector, Ad5HVR48, in which all the amino acids of the HVRs in Ad5 were replaced with those of Ad48 (a species D Ad which does not bind FX), abolished FX binding (Waddington *et al.*, 2008). FX did not enhance Ad5HVR48 cellular binding or transduction *in vitro* and a 600-fold reduction of liver transgene expression compared to Ad5 was observed in mice depleted in KCs, due to preinjection with clodronate liposomes (Waddington *et al.*, 2008). In a separate study, FX binding was decreased using an Ad5 vector in which a 71 amino acid biotin acceptor peptide (BAP) was inserted into HVR5 (Kalyuzhniy *et al.*, 2008; Shashkova *et al.*, 2009). Incubation of coagulation factors with Ad5BAP did not enhance gene transfer *in vitro* and preinjection of FX failed to increase Ad5BAP liver transduction in warfarin-treated mice 48 h post-injection (Kalyuzhniy *et al.*, 2008), again confirming the importance of the HVRs for the Ad5:FX interaction.

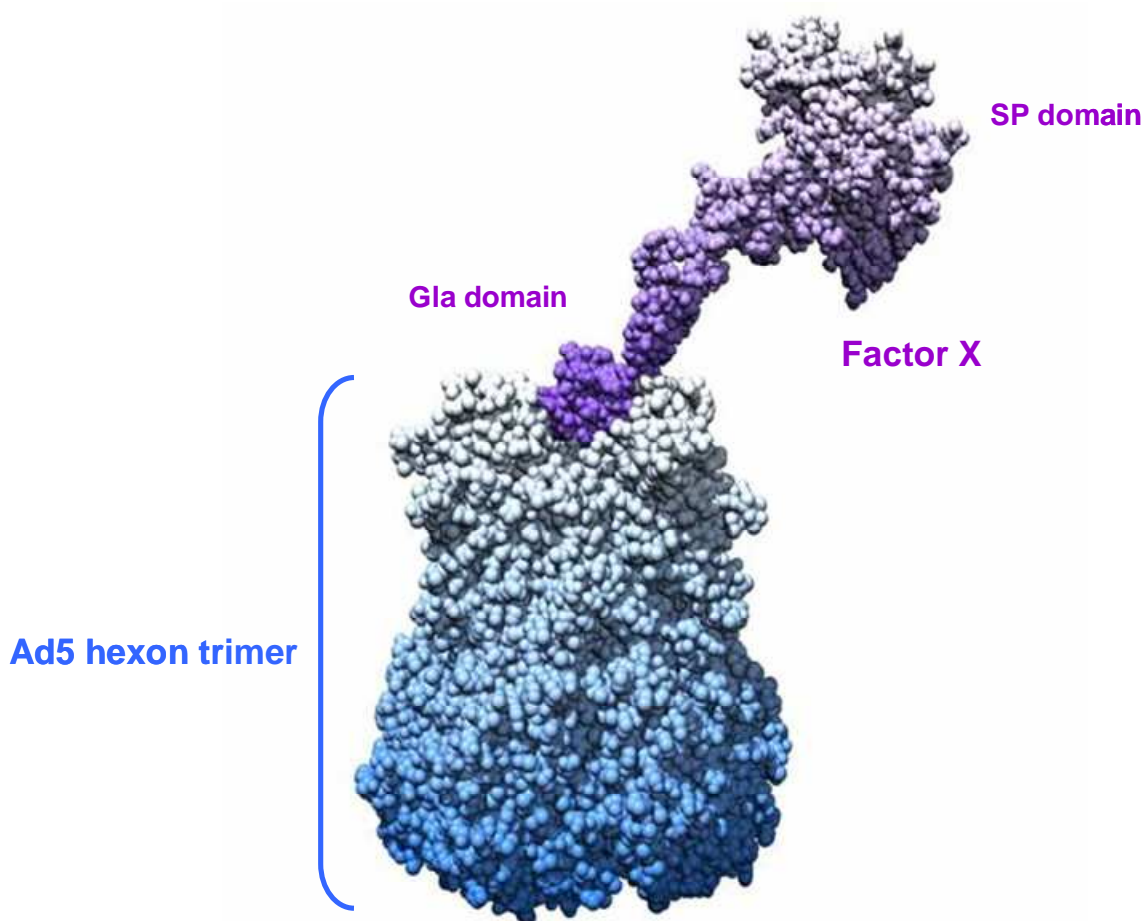


Figure 1.11. Model view of Ad5:FX interaction.

The Gla domain of one FX molecule bound within the cavity formed by the hexon trimer, whilst the FX SP domain is orientated outwards from the Ad5 capsid. This model was taken from Waddington *et al.* (Waddington *et al.*, 2008).

In order to dissect the hexon:FX interaction Alba *et al.* modelled it by fitting the published crystal structure of hexon (Rux *et al.*, 2003) and a molecular model of FX (Venkateswarlu *et al.*, 2002) to the cryoelectron microscopy model (Waddington *et al.*, 2008) in order to identify the relevant contact residues (Alba *et al.*, 2009). These were found to be HVR5 and HVR7 (Alba *et al.*, 2009). Phylogenetic analysis of HVR sequences of FX binding Ads, in comparison to those that do not bind FX, identified a glutamic acid residue at position 451 as common amongst FX binding Ads, which was replaced by a glutamine in non-binding Ads (Waddington *et al.*, 2008). Subsequently, the authors manipulated the viral capsid using point mutagenesis of two amino acids in HVR5 (T270P and E271G), four amino acids in HVR7 (I421G, T423N, E424S and L426Y) or a single mutation at position 451 in HVR7, swapping these residues with sequences of the species D, non-FX binding, Ad26. The mutations did not affect virus production. Ad5 with mutations in HVR5 resulted in decreased FX-mediated Ad5 cell binding and transduction *in vitro*, as

well as liver gene transfer in mice (Alba *et al.*, 2009). Ad vectors with HVR7 mutations showed profound inhibition of FX binding by SPR, ablated the enhancement in binding and transduction in cell lines and mouse hepatic transduction in the presence of FX. Furthermore, intravenous administration of the HVR5 (T270P and E271G) and HVR7 (I421G, T423N, E424S, L426Y and E451Q) mutated vector (Ad5-HVR5*7*E451Q) into non-human primates, *microcebus murinus*, substantially reduced hepatocyte transgene expression compared to control Ad5 (Alba *et al.*, 2012). Ad5 was also detected in the spleen, heart, lung, kidney, and to a lesser extent in the thymus, pancreas, intestines and lymph nodes. Whilst the FX-binding ablated vector genomes were found in the spleen, negligible amounts were detected in the other tissues (Alba *et al.*, 2012). This indicates a role for the FX pathway in mediating virus transduction and genome accumulation not only in the liver but also in several other organs. Heparin, which acts as a competitive inhibitor of HSPGs, blocked FX-mediated Ad5 binding to non-human primate livers *ex vivo*, showing a dependency on HSPGs and indicating conservation of this pathway across diverse species (Alba *et al.*, 2012). In addition to HVR5 and HVR7, Kalyuzhniy *et al.* used cryoelectron microscopy and sequencing alignment to implicate a site at the sequence TDT in HVR3 as a potential contact point between Ad and FX (Kalyuzhniy *et al.*, 2008), however the role of this motif is yet to be verified.

1.11 Ad:FX complex binding to hepatocytes

HSPGs are composed of a core protein to which one or more heparan sulphate (HS) glycosaminoglycan side-chains (linear polysaccharides composed of alternating N-acetylated or N-sulphated glucosamine units and uronic acids) are covalently linked (Esko *et al.*, 2001). Bradshaw *et al.* demonstrated the ability of heparinase III, a heparin lyase that specifically cleaves N-acetylated domains of HS, to inhibit Ad5 cellular binding and gene transfer *in vitro* in the presence of FX, hence indicating that the HS side-chains mediate attachment of Ad5:FX complexes to the cell surface (Bradshaw *et al.*, 2010). Experiments employing sodium chlorate, a selective inhibitor of sulfation (Safaiyan *et al.*, 1999), demonstrated that Ad5 uptake via the FX pathway is dependent on HS sulfation. The study showed inhibition of N-linked, and particularly inhibition of O-linked sulphate groups, which are highly expressed in the liver, attenuated FX-mediated Ad5 cell binding and transduction *in vitro*, in a dose-dependent manner (Bradshaw *et al.*, 2010). Attachment of fluorescently labelled Ad5 in the presence of FX to mouse liver sections *ex vivo* was significantly reduced in the presence of heparin, however neither de-O-sulphated heparin, which lacks O-sulphate groups, nor de-N-sulphated heparin, which lacks N-sulphated

groups had any effect on Ad5 attachment. Moreover, heparin substantially reduced FX-mediated Ad5 accumulation in the liver 1 h after intravascular administration in macrophage depleted mice, whilst no effect was observed with de-O-sulphated heparin and de-N-sulphated heparin (Bradshaw *et al.*, 2010).

1.12 Post-binding events via the FX infectivity pathway

Using non-CAR binding and/or αv integrin mutants Bradshaw *et al.* (Bradshaw *et al.*, 2010) showed a dependency on an intact penton base RGD motif for efficient post-attachment cell entry and intracellular transport via the FX pathway, thus indicating the interaction with cellular integrins as co-receptors for internalisation is retained. Whilst fluorescently-labelled Ad5 and AdKO1 resulted in similar levels of accumulation at the MTOC after 1 h in the presence of FX *in vitro*, accumulation of the penton base RGD mutant vectors were significantly delayed. In addition, using a short hairpin RNA approach to knockdown αv integrin expression in a CAR low expressing cell line, Ad5 trafficking to the perinuclear area was substantially reduced, thereby confirming the importance of integrin engagement for transport via the FX-mediated pathway.

After cell surface attachment via HSPGs, the fiber also plays a role in cell entry and subsequent intracellular trafficking. A study investigating the role of FX in Ad5, Ad35, Ad5/fiber 35 and Ad5/penton 35/fiber 35 chimeric vector gene transfer, used SPR to first show that all of the vectors could bind to the coagulation factor, with pseudotypes having FX-binding affinities similar to other vectors possessing the same serotype hexon (Greig *et al.*, 2009). In the absence of the native species B CD46 receptor, the vectors use FX to bridge the complex to HSPGs, thereby enhancing cell surface binding and internalisation, however in the presence of FX, transduction of all viruses capable of binding CD46 i.e. Ad5/f35, Ad5/p35/f35, and Ad35, was substantially reduced in CHO-BC1 cells, which express CD46 (Corjon *et al.*, 2011; Greig *et al.*, 2009). FX increased intracellular uptake of vectors in both CD46 and CD46 negative cells, indicating the decrease in gene transfer did not involve the endocytosis step of the infectivity pathway (Corjon *et al.*, 2011; Greig *et al.*, 2009). This suggests that FX limits post-internalisation mechanisms that lead to cellular transduction by viruses containing the Ad35 fiber. The negative effect of FX on Ad5/35 vector transduction *in vitro* was shown to be due to inefficient intracellular trafficking and accumulation of virus in the late endosomal compartment, resulting in a delayed release from vesicles and nuclear import (Corjon *et al.*, 2011; Greig *et al.*, 2009).

These studies, implying a functional role for the fiber protein, show some overlap with the well known classical CAR-mediated pathway, for which the fiber is critical.

Corjon *et al.* investigated whether or not FX was internalised with Ad5, using fluorescently labelled Alexa Fluor-555 FX and Alexa Fluor-488 Ad vectors (Corjon *et al.*, 2011). In HSPG expressing CHO cells, control FX alone was endocytosed, with signals observed intracellularly after 15 min. Following coincubation, fluorescent signals for both FX and Ad5 were detected colocalised within the cell at the same time point, as shown by confocal microscopy, thereby indicating co-endocytosis (Corjon *et al.*, 2011). By 1 h, Ad5 particles trafficked to the nucleus, resulting in reduced colocalisation with FX, which remained in the cell periphery. In the case of Ad5f35, at 3 h post-infection the FX:Ad5f35 complexes remained colocalised in the cytoplasm, again indicating inefficient intracellular trafficking compared to Ad5 (Corjon *et al.*, 2011).

1.13 Methods of manipulation of the Ad:FX interaction

In vivo kinetics and Ad biodistribution are defined by a range of host interactions. Many years of research have been focused on altering the tropism of Ad5, the majority of the early studies concentrating on targeting the vector to alternative receptors. A great deal of these efforts were not as successful as anticipated. In hindsight, this is perhaps unsurprising and can be explained by the recent discoveries regarding the role of blood coagulation FX in liver transduction and other tropism determining pathways of Ads (Nilsson *et al.*, 2011; Waddington *et al.*, 2008; Wang *et al.*, 2011), as well as having a more detailed knowledge of the Ad-induced immune response. Gaining a better understanding of Ad biology allows for a more informed progression and rationale design of optimised systems. Here a variety of methods to manipulate FX-mediated Ad gene transfer are discussed (Figure 1.12).

1.13.1 Genetic modification of the Ad hexon to prevent FX binding

Genetic manipulation of capsid proteins, designed to bypass host interactions and improve infectivity of desired tissues, is a frequently used targeting approach for Ad5. Mutagenesis strategies aimed at adapting viral tropism include pseudotyping with rare Ad types, non-human or those devoid of FX binding, hexon or fiber ‘swapping’ or incorporation of targeting moieties (reviewed extensively by Coughlan *et al.* (Coughlan *et al.*, 2010)). In the context of FX-mediated transduction, modification of the hexon protein is an attractive

strategy to prevent the virus interaction with FX following intravascular delivery, thereby reducing Ad hepatic gene transfer.

Several studies genetically modifying the HVR5 and HVR7 domains demonstrated significantly decreased hepatic transgene expression in both rodents and non-human primates (Adams *et al.*, 2009; Alba *et al.*, 2012; Kalyuzhniy *et al.*, 2008; Vigant *et al.*, 2008; Waddington *et al.*, 2008). As previously mentioned, a study by Alba *et al.* showed the levels of liver gene transfer were greatly reduced using FX-binding ablated vectors, point-mutated at HVR5 (T270P and E271G) and HVR7 (I421G, T423N, E424S, L426Y and E451Q), a so called Ad5HVR5*7*E451Q vector (Alba *et al.*, 2010; Alba *et al.*, 2011). This occurred regardless of macrophage depletion. At high viral doses (1×10^{11} vp/mouse or 4×10^{12} vp/kg), significantly higher quantities of Ad5HVR5*7*E451Q viral genomes were detected in the spleens of macrophage-depleted mice, compared with Ad5 (Alba *et al.*, 2010). This suggests that Ad clearance by macrophages significantly reduces splenic uptake independently of FX. At this high viral dose Ad5 and Ad5HVR5*7*E451Q caused an increase in several chemokines and cytokines including IL-12, monokine-induced by interferon γ and 10-kDa interferon γ -induced protein, all of which were elevated following FX-ablated vector administration compared to Ad5, whilst IL-6 was significantly decreased (Alba *et al.*, 2010). At such high doses (4×10^{12} vp/kg) it is difficult to predict whether such toxicities would be relevant in humans, as the dose administered in clinical trials is much lower (e.g. 2×10^{11} vp/person) (Au *et al.*, 2006; Hamid *et al.*, 2003; Small *et al.*, 2006). Attempts at retargeting the vector involved the generation of a non-FX binding Ad5 vector containing the Ad35 fiber (Ad5HVR5*7*E451/F35⁺⁺) (Alba *et al.*, 2010). This Ad35 fiber (Ad35⁺⁺) contains two amino acid changes, inducing a 60-fold higher affinity to the subgroup B receptor CD46 compared to native Ad35 (Wang *et al.*, 2008). Intravascular injection of Ad5HVR5*7*E451/F35⁺⁺ in macrophage-depleted CD46 transgenic mice showed increased gene transfer in the lung, coupled with reduced transduction in the liver and spleen (Alba *et al.*, 2010). In these animals the Ad5HVR5*7*E451/F35⁺⁺ lung/liver ratio was approximately 800:1, resulting in a 16,000-fold increase in lung transduction compared to Ad5HVR5*7*E451Q (Alba *et al.*, 2010).

A separate study by Short *et al.*, in which the Ad5 hexon was replaced with that of the species B Ad3 (Ad5H3), reduced vector binding to FX as demonstrated by SPR (Short *et al.*, 2010). Incubation with physiological levels of FX caused no enhancement of Ad5H3 infectivity *in vitro* and caused a 100-fold decrease in liver gene transfer. This was comparable to Ad5 in warfarin-treated mice. Substitution of the fiber knob domain with

that of CD46 binding Ad3 enhanced tumour transduction and anti-tumour efficacy by a conditionally replicating version of the vector (Short *et al.*, 2010).

Khare *et al.* adopted a different strategy to genetically manipulate the Ad:FX interaction (Khare *et al.*, 2011). As hexon is reported to be a major antigenic capsid protein (Sumida *et al.*, 2005), generating hexon-chimeric vectors utilising rare Ads may also be beneficial for overcoming pre-existing immunity (Roberts *et al.*, 2006; Youil *et al.*, 2002). Replacing the HVR domains of Ad5 with those of Ad6 (to create an Ad5/6 vector), another species C virus which is less seroprevalent and previously shown to evade KC uptake (Shashkova, May *et al.* 2009), this group achieved 10-fold higher transduction in the liver following intravenous delivery (Khare *et al.*, 2011). Both Ad5 and Ad6 retain the glutamic acid at position 451 in HVR7 that is conserved in all tested FX-binding Ads (Waddington *et al.*, 2008). Ad6 binds to FX *in vivo*, but in this instance the interaction was exploited in order to attain targeted hepatic delivery while escaping KC uptake. Liver transduction was significantly reduced for Ad5 and Ad5/6 in warfarin-treated animals indicating a sensitivity to vitamin K dependent coagulation factor depletion (Khare *et al.*, 2011). Ad5/6 is less efficiently phagocytosed by macrophages *in vitro*, and this is suggested to be due to the block of Ad5 HVR 1, 2, 5 and 7 binding to scavenger receptor SRA-II (Khare *et al.*, 2012). Therefore without induction of KC activation *in vivo* and subsequent virus sequestration, the vector can more efficiently target the liver, features desirable for liver gene therapy applications (Khare *et al.*, 2011; Khare *et al.*, 2012).

1.13.2 Polymer-conjugated Ad complexes shield the vector from FX

Chemical modification of Ads using polymers to 'shield' the hexon protein from FX is an alternative strategy. This has the additional advantage of also precluding other host interactions e.g. complement, neutralising antibodies. Polyethylene glycol (PEG) is an uncharged, hydrophilic, non-immunogenic polymer synthesised of repeating CH₂CH₂O subunits, with a molecular weight ranging from 200 to 40,000 Da. In general, chemical modifications based on monovalent PEG or also commonly used multivalent N-(2-hydroxypropyl methacrylamide) (HPMA) involves covalent attachment to the Ad surface by the use of activated tresyl-monomethoxy PEG (TMPEG), succinimidyl succinate-monomethoxy PEG (SSPEG) or monomethoxy PEG (MPEG) (Croyle *et al.*, 2000; O'Riordan *et al.*, 1999). The activated PEG reacts preferentially with the epsilon-amino groups of lysine residues, the most abundant functional group on the Ad capsid, present on the hexon, fiber and penton (O'Riordan *et al.*, 1999). Coating the Ad capsid in HPMA

molecules prevents virus binding to FX via the hexon (Subr *et al.*, 2009) and has been shown to improve pharmacological profiles by protecting from proteolytic degradation and extending plasma kinetics.

In the study by Subr *et al.* Ad5 was coated with HPMA modified to contain positively charged quaternary amine groups (N,N,N-trimethylammonium ethyl) (Subr *et al.*, 2009). As Ad5 possesses an overall negative charge, this improved the yield of the coating reaction by enhancing the electrostatic interaction of the positive coating polymer with negatively charged groups on the surface of the virus. Coincubation of the modified vectors with FX caused no increase in Ad transduction in a CAR^{low} expressing cell line *in vitro*, indicating that the FX-binding residues within the HVRs of the hexon are shielded by the polymer (Subr *et al.*, 2009).

Prill *et al.* combined genetic manipulation techniques, by mutagenesis of a single amino acid in HVR5 to introduce a surface accessible cysteine, with covalent chemical coupling to protein moieties at the site of genetic modification (Prill *et al.*, 2011). Coupling the vector to PEG molecules, ranging in sizes 750 to 5,000 Da, abolished transduction mediated by FX *in vitro*. Coupling to a 20,000 PEG moiety resulted in variability in its FX shielding efficiency due to only 50% coverage of the hexon. Intravenous administration of the 750, 2,000 or 20,000 Da PEGylated vectors resulted in significantly decreased liver transduction compared to Ad5, and to similar levels of Ad5 in warfarin-treated mice (Prill *et al.*, 2011).

Biodistribution characteristics of polymer coated Ad complexes are reported to be affected by the density of the PEG shield (Doronin *et al.*, 2009). Decreased liver transgene expression could be due to the size restrictions imposed by the liver sinusoid fenestrae and not solely due of the virus being masked from FX (Hofherr *et al.*, 2008). The presence of fenestrae allows the virus to navigate through the space of Disse and rapidly reach their receptors on the surface of hepatocytes. However, the size of fenestrae, varying significantly across species, ranging from 150-175 nm in rats (Wisse *et al.*, 1985) and ~140 nm in mice (Snoeys *et al.*, 2007), the two most commonly used animal models, whilst only ~107 nm in healthy human livers (Wisse *et al.*, 2008), may act as a sieve preventing entry depending on the dimensions of the vectors. This was highlighted when Hofherr *et al.* revealed Ad5 conjugated with 20 and 35 kDa PEG, but not 5 kDa markedly reduced liver transduction despite maintaining the ability to bind coagulation FX (Hofherr *et al.*, 2008). In the study by Prill *et al.* addition of 5 kDa PEG to the Ad vector resulted in an 11-fold

increase in hepatocyte transduction, an effect which was independent of FX and more likely due to vector shielding from KCs (Prill *et al.*, 2011). This may be a valuable approach for liver directed gene therapy. PEGylated Ad complexes are an attractive and viable targeted therapeutic gene therapy approach which will no doubt be improved by advances in polymer chemistry.

1.13.3 Adaptor molecules

Developing adaptor molecules, which consist of a capsid binding domain genetically or chemically fused to a specific cell targeting domain e.g. bispecific antibodies, single-chain antibody variable fragments (scFv) or growth factors, is another method which has been employed to manipulate the Ad5:FX interaction. Ad vectors conjugated to adaptor molecules serve a dual function; the antibody selectively retargets the Ad complex to the desired tissues whilst simultaneously blocking binding to the native receptors.

Chen *et al.* exploited the high affinity interaction between Ad5 and FX by generating FX fusion proteins (Chen *et al.*, 2010). As it is the Gla domain of FX which binds to the virus, plasmids were constructed that removed the FX SP domain and instead fused the Gla-EGF1 domain with scFv directed against the tumour markers Her2, EGFR or the stem cell marker ATP-binding cassette protein G2 (ABCG2) (Chen *et al.*, 2010). The Ad-scFv fusions caused increased targeting and cytotoxicity of cancer cells *in vitro* and *in vivo*. Although an effective method of targeting, levels of liver transduction were unaffected with Ad-scFv fusions suggesting Ad5 binding to Gla-scFv may not be stable *in vivo* and is displaced by the greater levels of FX in the bloodstream (Chen *et al.*, 2010).

1.13.4 Pharmacological agents to prevent Ad transduction

Recent advances in the understanding of the precise mechanisms involved in Ad5 binding to FX points to a target suitable for drug discovery. Ad5 in combination with pharmacological agents has already proven effective for mediating systemically delivered gene therapy in animal models. Factor X binding protein (X-bp), which binds with high affinity to the FX Gla domain preventing the Ad5:FX interaction (Waddington *et al.*, 2008), the use of warfarin to decrease circulating levels of functional blood factors (Parker *et al.*, 2006) or heparin to block HSPGs (Bradshaw *et al.*, 2010), have all reduced FX-mediated Ad5 liver transduction. These agents however are sub-optimal for administering to patients about to undergo a therapeutic gene therapy procedure due to anticoagulant properties (O'Donnell, 2012). The feasibility of viral/drug combination gene therapy

strategies to block redundant Ad infection whilst maintaining the integrity of the virus is yet to be fully realised.

The potential of novel pharmacological compounds to specifically block Ad interactions with their native receptors was elegantly illustrated by Spjut *et al.* (Spjut *et al.*, 2011). A recent study demonstrated that species D Ad37 infection causes epidemic keratoconjunctivitis by binding of the Ad fiber knob protein to glycoproteins containing two terminal sialic acid moieties on the surface of epithelial cells in the cornea or conjunctiva (Nilsson *et al.*, 2011). A combination of molecular modelling, nuclear magnetic resonance and X-ray crystallography dissected the interaction to reveal that the two sialic acids dock into two sialic acid binding sites in the trimeric Ad37 knob (Nilsson *et al.*, 2011). This finding led to Spjut *et al.* synthesizing tri- and tetravalent sialic acid compounds which effectively block Ad37 infection of human ocular cells. SPR and crystallography techniques demonstrated the trivalent sialic acid conjugate, ME0322, binds directly to the sialic acid-binding sites in the fiber knob, with similar affinity to GD1a hexasaccharide, and is a potent inhibitor of Ad37 infection (Spjut *et al.*, 2011). Although these studies are not directly focused on gene therapy applications, they underline the importance of a thorough understanding of virus interactions with the host and a subsequent development of chemical inhibitors. The detailed analysis of crystal structures of Ad capsid-host protein complexes allows the study of specific interactions at the atomic level and contributes immensely to rational drug design.

As well as taking advantage of the well defined Ad structure (Reddy *et al.*, 2010), known to near atomic resolution, along with the electron cryomicroscopy and the three-dimensional reconstructions of the Ad5:FX complex, an array of diverse *in vitro* assays exist to study Ads and manipulate their interactions for drug development. Many of these are cell-based including cytopathic effect or plaque formation assay, cell viability, haemagglutination, FX-mediated cell binding, gene transfer or intracellular transport assays etc. These assays can be time consuming but are flexible and could be adapted to investigate Ad5 infectivity in the presence of FX in a high throughput manner. High throughput screening of pharmacologically favourable small molecules in search of safe inhibitors of the Ad5 interaction with FX or FX-mediated gene transfer is an attractive prospect. This technique is commonly used in the anti-viral drug field (Campagnola *et al.*, 2011; Hoffmann *et al.*, 2011; Jegede *et al.*, 2011), emphasising the plausibility of this approach for enhancing the efficacy of therapeutic gene adenoviral delivery.

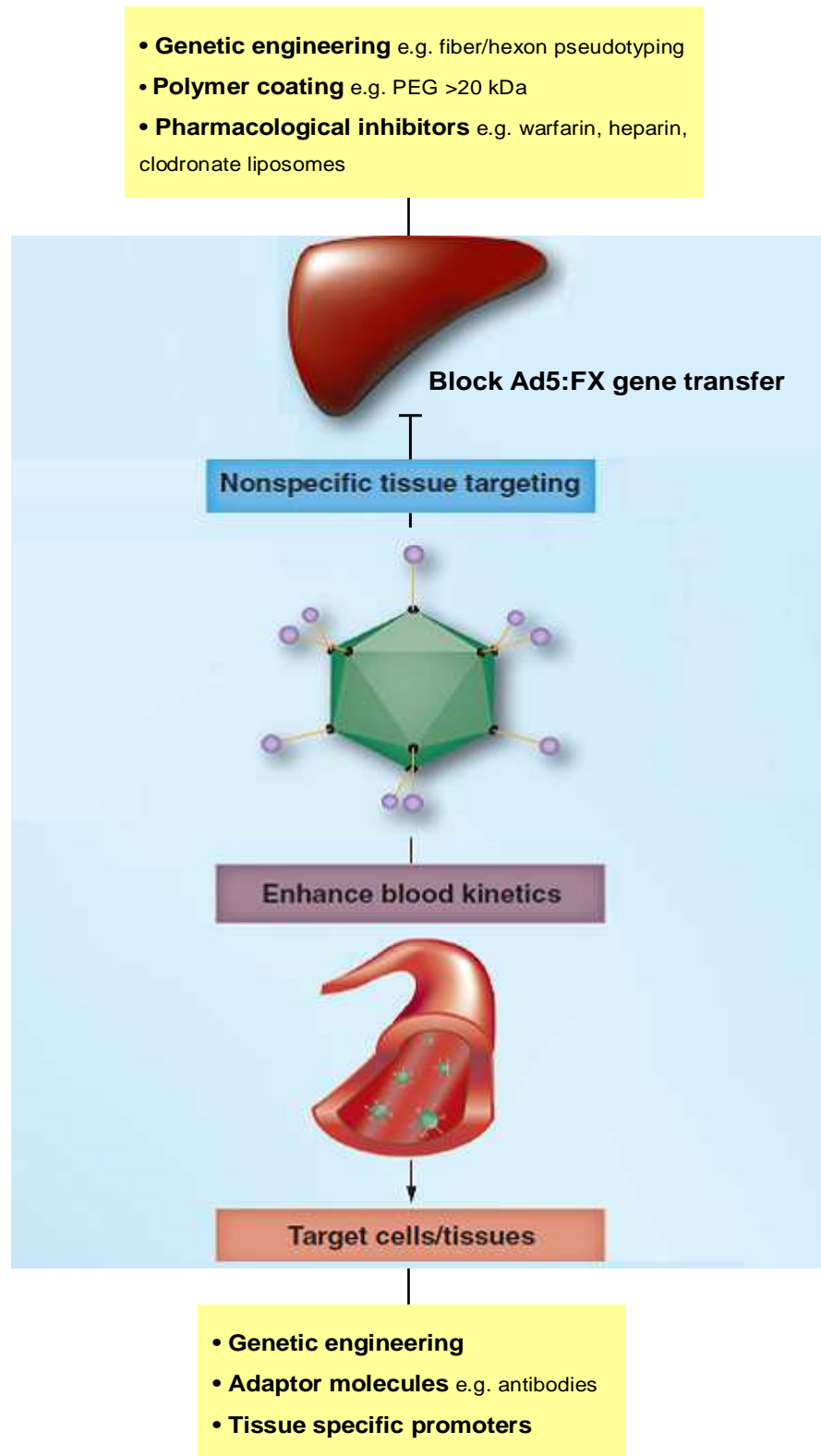


Figure 1.12. Tropism modifying strategies.

A range of potential strategies have been employed to block FX-mediated Ad5 gene transfer and detarget the virus from its inherent liver tropism. Bypassing such host interactions would result in increased Ad circulation times and allows for specific vector targeting to the desired cells or tissues.

1.14 Future of Ad-based gene therapy

The transition from relevant Ad *in vitro* pathways to key *in vivo* mechanisms has taken three decades of study and will no doubt continue for many more years. Better understanding the intricacies of Ad pathways through the use of shrewd *in vitro* or cell-based assays, along with the correlation of these results in relevant *in vivo* models, has had major implications for Ad based gene therapy. Discovering the role of FX in determining the substantial hepatic transduction of Ad5 upon contact with the blood was a major advance toward achieving the long desired goal of effective liver detargeting for systemic gene therapy applications. In many ways, this finding has redefined several tropism modifying strategies, and changed the focus of those previously concentrated on bypassing Ad binding to CAR. Building on this result and gaining a greater depth of knowledge of the FX-mediated infectivity pathway will help piece together the precise sequence of complex events which define the Ad5 tropism *in vivo* and aid in the design of pioneering strategies to manipulate FX-mediated Ad5 gene transfer. This will no doubt ultimately contribute to the development of more efficient vectors targeting defined tissues with reduced toxicity, and holds great promise for improving the therapeutic viability of Ads for targeted delivery following intravascular administration. The promise of pre-clinical results will hopefully soon be converted into triumphs in the clinical setting and the true appeal of Ad based gene therapy will begin to be fulfilled in the coming years.

1.15 Aims of this thesis

The principle aims of this thesis were to gain a greater understanding of FX-mediated Ad5 infection and to use several strategies to manipulate Ad5:FX gene transfer. To this end, three approaches were employed. These focused on different aspects of the FX-mediated Ad5 pathway, from the initial stages to cellular binding, intracellular transport to preventing effective Ad transgene expression. This thesis is divided into three studies, each with an individual aim.

- **Investigation of the mechanism by which Ad5:FX complexes bind to the cell surface.**

This was performed using mutagenesis techniques to genetically modify amino acid residues within the FX SP domain and subsequent examination of the effects of the mutations using *in vitro* and *ex vivo* assays.

- **Investigation of cellular and signalling events occurring during Ad5 transduction in the presence of FX.**

This involved the use of pharmacological agents to interfere with efficient virus cell binding, internalisation, trafficking and transduction.

- **Identification of a small molecule inhibitor of FX-mediated Ad5 gene transfer.**

This was carried out using a high throughput approach to screen a library of over 10,000 compounds in search of one which prevented virus transduction.

Chapter 2

Materials and Methods

Materials

2.1 Chemicals

The Pharmacological Diversity Drug-like Set compound library was purchased from Enamine (Kiev, Ukraine). Analogue compounds of the hits from the high throughput screen were also purchased from Enamine. The Tocris Kinase Inhibitor Toolbox, a kind gift from Dr. Jo Mountford (University of Glasgow, Glasgow, UK), was originally obtained from Tocris Bioscience (Bristol, UK). Oligonucleotides were obtained from MWG-Biotech (Edersberg, Germany). All other chemicals unless otherwise indicated were obtained from Sigma-Aldrich (Poole, UK).

2.2 Proteins

Purified human plasma derived (pd) blood coagulation FX and activated FX were purchased from Haematologic Technologies (Vermont, USA).

2.3 Plasmid DNA constructs

The wild-type FX cDNA cloned into the mammalian expression pCMV4 vector (human prothrombin signal sequence and propeptide followed by the sequence for the FX derivative - pCMV4-ss-pro-II-FX) was a kind gift from Prof. John McVey (Thrombosis Research Institute, London, UK). The pMK-RQ_FX SP mutant plasmid was purchased from GeneArt (Invitrogen, Paisley, UK).

2.4 Antibodies

Primary rabbit polyclonal antibodies raised against pericentrin and ezrin, and rabbit monoclonal antibodies against radixin and moesin were obtained from Abcam (Cambridge, UK). The mouse monoclonal antibody raised against intact heparan sulphate (clone 10E4) was obtained from AMS Biotechnology (Oxford, UK). The monoclonal mouse antibody raised against spleen tyrosine kinase (Syk) was obtained from Antibodies-online GmbH (Aachen, Germany). IgGs and secondary antibodies were obtained from Invitrogen (Paisley, UK) unless otherwise stated. The mouse monoclonal antibody against human FX (clone HX-1) was obtained from Sigma-Aldrich. The hybridoma expressing the monoclonal anti-human FX antibody 4G3 was a kind gift of Dr R. Camire (Children's

Hospital of Philadelphia, USA). The 4G3 antibody was purified by protein G affinity chromatography by Prof. John McVey (Thrombosis Research Institute, London, UK).

2.5 Cell culture materials

All tissue culture reagents were purchased from Invitrogen (Paisley, UK) unless otherwise stated.

Methods

2.6 Tissue culture

Tissue culture was performed under sterile conditions using biological safety class II vertical laminar flow cabinets. Cells were grown as a monolayer in 150 cm² tissue culture flasks in 37°C, 5% CO₂ and 95% air incubators. Tissue culture experiments involving Ad vectors were performed in a dedicated tissue culture laboratory and maintained in separate incubators.

2.7 Maintenance of established cell lines

Cells were routinely passaged at approximately 80% confluence to prevent overgrowth and loss of surface contact in culture flasks. The cells and media used are described in Table 2.1. To passage, cells were washed twice in Dulbecco's calcium and magnesium free PBS and incubated with 3 ml trypsin-ethylenediamine tetra-acetic acid (trypsin-EDTA) (Invitrogen) at 37°C for approximately 5 min. Once detached, cells were collected in 5 ml complete media (media supplemented with 10% (v/v) fetal calf serum (FCS), 1% (v/v) penicillin, 100 µg/ml streptomycin and 2 mM L-glutamine) which inactivates the trypsin. Cells were centrifuged at 480 g for 5 min. Media and trypsin-EDTA were poured off and the cell pellet resuspended in complete media for passaging or plating. To accurately seed cell culture dishes or plates with a known number of cells, cells were counted using a haemocytometer (Hausser Scientific, PA, USA).

2.8 Cryopreservation

For cryopreservation cells were collected as described in section 2.7. Cells from a 80% confluent 150 cm² tissue culture flask were resuspended in 2 ml complete media supplemented with 10% dimethyl sulphoxide (DMSO) and aliquoted into cryo-

preservation vials. Vials were cooled at a constant $-1^{\circ}\text{C}/\text{min}$ to -80°C using isopropanol. Cells were transferred for long term storage in liquid nitrogen. When recovering cells from liquid nitrogen, vials were thawed at 37°C and then the cell suspension was carefully added dropwise to 10 ml complete media in a universal container. Cells were pelleted by centrifugation at 480 g for 5 min. The cell pellet was resuspended in complete media, transferred to a 150 cm^2 tissue culture flask and incubated in a 37°C , 5% CO_2 and 95% air incubator.

Table 2.1. Cell lines and media used.

Cell type	Description	Cell culture medium
SKOV3	Human ovary adenocarcinoma cell line	RPMI 1640 media supplemented with 10% (v/v) FCS, 1% (v/v) penicillin, 100 $\mu\text{g}/\text{ml}$ streptomycin and 2 mM L-glutamine.
A549	Human lung adenocarcinoma epithelial cell line	RPMI 1640 media supplemented with 10% (v/v) FCS, 1% (v/v) penicillin, 100 $\mu\text{g}/\text{ml}$ streptomycin and 2 mM L-glutamine.
HepG2	Human hepatocellular carcinoma cell line	Dulbecco's Modified Eagle's Medium (DMEM) supplemented with 10 % FCS, 1% (v/v) penicillin, 100 $\mu\text{g}/\text{ml}$ streptomycin and 2 mM L-glutamine.
SW 620	Human colon cancer cell line	RPMI 1640 media supplemented with 10% (v/v) FCS, 1% (v/v) penicillin, 100 $\mu\text{g}/\text{ml}$ streptomycin and 2 mM L-glutamine.
293	Human embryonic kidney cell line	DMEM supplemented with 10% FCS, 1% (v/v) penicillin, 100 $\mu\text{g}/\text{ml}$ streptomycin and 2 mM L-glutamine.
293T	Transformed human embryonic kidney cell line	DMEM supplemented with 10% FCS, 1% (v/v) penicillin, 100 $\mu\text{g}/\text{ml}$ streptomycin and 2 mM L-glutamine.

2.9 Cloning procedures

2.9.1 Plasmid preparation

Bacterial stock culture containing plasmid DNA from a glycerol stock was spread on to an ampicillin (100 $\mu\text{g}/\text{ml}$) containing agar plate and incubated at 37°C overnight to allow the bacteria to grow. Single bacterial colonies were then picked from the agar plate and used to

inoculate a starter culture of 5 ml (for small scale preparation of plasmid DNA) or 10 ml Luria-Broth (LB) containing ampicillin. This was incubated at 37°C for 8 h whilst shaking. For large scale preparation of plasmid DNA the starter culture was transferred to 500 ml of LB in a 2 L flask and incubated at 37°C overnight whilst shaking.

2.9.2 Small scale preparation of plasmid DNA

Plasmid DNA was extracted from bacteria on a small scale using the QIAprep Spin Miniprep Kit (QIAGEN, Crawley, UK) according to the manufacturer's instructions. Briefly, bacterial cells were harvested by centrifugation for 5 min at 16,000 g. The pellet was resuspended in 250 µl of Buffer P1 (50 mM tris(hydroxymethyl)aminomethane (Tris)-HCl, pH 8, 10 mM EDTA, 100 µg/ml RNase A). The EDTA in this buffer chelates divalent metals (primarily magnesium and calcium). Removal of these cations destabilises the cell membrane, resulting in the lysis of the bacterial cells. The RNase A is a ribonuclease which degrades RNA. 250 µl of Buffer P2 (200 mM NaOH, 1% sodium dodecyl sulphate (SDS)) was added and the sample was mixed thoroughly. The NaOH in this buffer denatures chromosomal DNA and the SDS disrupts the cell membranes. The lysis step was neutralised by 350 µl Buffer N3 (4.2 M guanidinium chloride, 0.9 M potassium acetate, pH 4.8), which causes the precipitation of genomic DNA, proteins, cell debris and SDS. The precipitated samples were centrifuged at 16,000 g for 10 min. The supernatant was transferred to an equilibrated QIAGEN-tip 20 column, which contains a silica membrane to which the plasmid DNA binds, and centrifuged for 1 min. The DNA bound to the column was washed with 500 µl Buffer PB (5 M guanidinium chloride, 30% (v/v) isopropanol) to remove endonucleases and the column centrifuged for 1 min. 750 µl Buffer PE (10 mM Tris-HCl pH 7.5, 80% (v/v) ethanol) was added to further wash and remove salts and the column centrifuged for 1 min. DNA was eluted from the column by adding 50 µl dH₂O, allowed to stand for 1 min and then centrifuged for 1 min. The amount of DNA in each sample was quantified by measuring absorbance at 260 nm (NanoDrop, ND-1000 spectrophotometer (Labtech International, Ringmer, UK)).

2.9.3 Large scale preparation of plasmid DNA

Plasmid DNA was extracted from bacteria on a large scale using the Plasmid Maxi Kit (QIAGEN) according to the manufacturer's instructions. Briefly, bacterial cells were harvested by centrifugation at 6000 g for 15 min at 4°C. The pellet was resuspended in 10 ml of Buffer P1. 10 ml of Buffer P2 was added, the sample was mixed thoroughly and

incubated at room temperature for 5 min. The lysis step was neutralised by 10 ml Buffer P3 (3 M potassium acetate, pH 5.5). The potassium acetate in this buffer allows for the precipitation of genomic DNA, proteins, cell debris and potassium dodecyl sulphate. The samples were centrifuged at 20,000 g for 30 min at 4°C. The supernatant containing the plasmid DNA was collected and transferred to an equilibrated QIAGEN-tip 500 column. The sample was allowed to pass through the resin of the anion-exchange column by gravity flow. During this step the plasmid DNA selectively binds to the resin. The QIAGEN-tip 500 was washed with 30 ml Buffer QC (1 M NaCl, 50 mM 3-(N-morpholino)propanesulfonic acid pH 7, 15% (v/v) isopropanol) twice. This is a medium-salt wash to remove RNA, proteins, metabolites and other low-molecular-weight impurities. The plasmid DNA was eluted from the column by the addition of 15 ml Buffer QF (1.25 M NaCl, 50 mM Tris pH 8.5, 15% (v/v) isopropanol). The plasmid DNA was concentrated and desalted by precipitation with 10.5 ml isopropanol and centrifuged immediately at 15000 g for 30 min at 4°C. 5 ml 70% (v/v) ethanol was added to wash the DNA pellet, which was then centrifuged again at 15,000 g for 10 min. The supernatant was removed and the DNA pellet left to air dry for 20 min prior to resuspension in 200 µl dH₂O. The concentration of DNA in each sample was quantified by measuring absorbance at 260 nm (NanoDrop, ND-1000 spectrophotometer).

2.9.4 Generation of glycerol stocks

Plasmid DNA glycerol stocks were generated for long term storage. 200 µl of sterile glycerol was added to 800 µl of bacterial culture containing the plasmid DNA in a 1.5 ml Eppendorf. Stocks were stored at -80°C.

2.9.5 Site-directed polymerase chain reaction mutagenesis

Polymerase chain reaction (PCR) is a technique used to amplify a specific DNA sequence. Single (R125A)) or double (R93A_K96A, R165A_K169A or K236A_R240A) amino acid residues mutations in the WT FX (pCMV4-ss-pro-II-FX) plasmid were generated by substituting basic residues with alanine using site-directed PCR mutagenesis (amino acids are numbered from the amino terminal residue of the mature FX). For this the QuikChange Site-Directed Mutagenesis Kit (Agilent Technologies, Edinburgh, UK) was used as per manufacturer's instructions (for overview of the method see Figure 2.1). The procedure utilised the WT FX plasmid and two synthetic mutagenic oligonucleotide primers (forward and reverse) containing the desired mutation. For primer design see section 2.9.6.

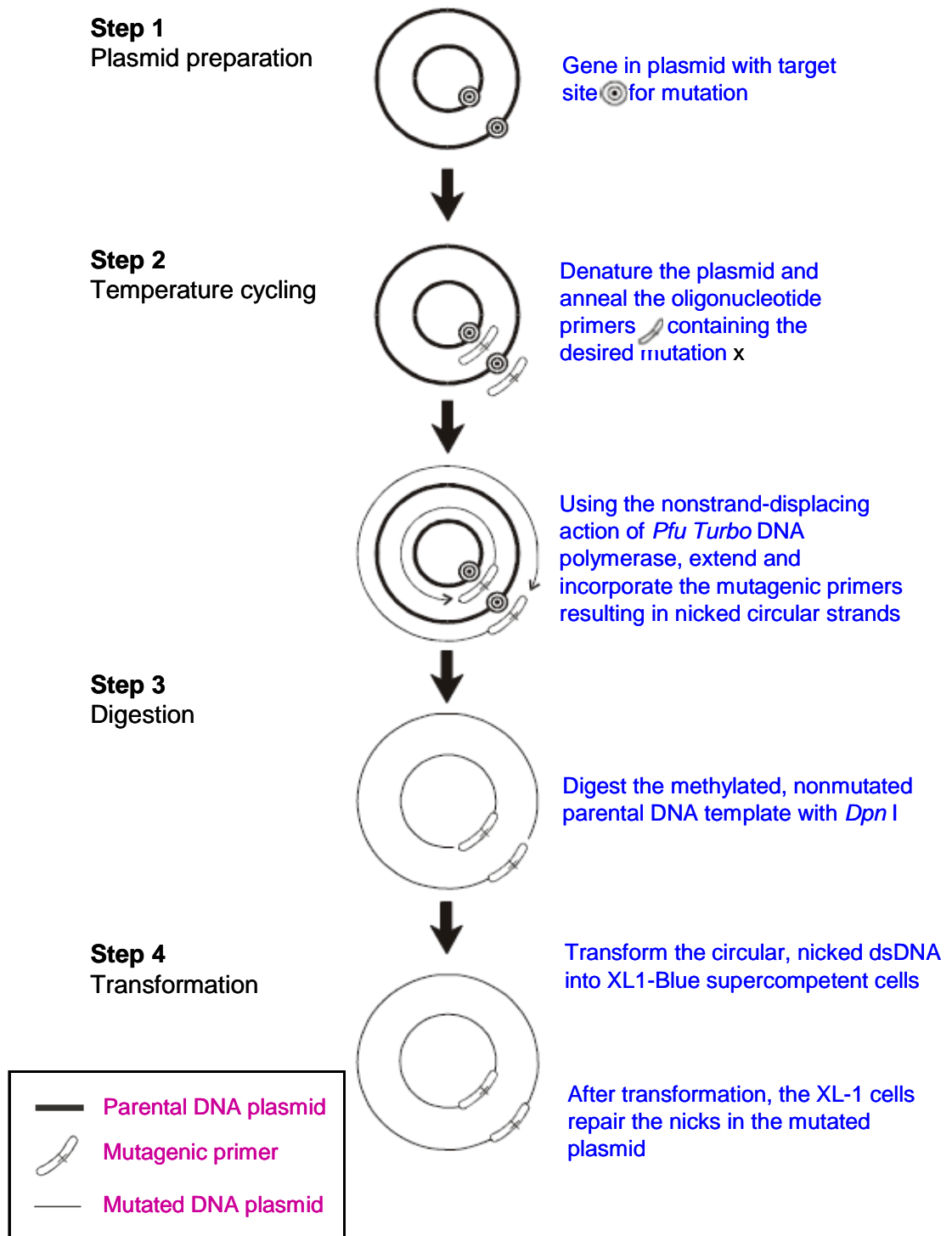


Figure 2.1. Overview of the QuikChange site-directed mutagenesis method.

This figure was adapted for the Stratagene QuikChange Site-Directed Mutagenesis instruction manual.

2.9.5.1 Step 1: Plasmid preparation

In order to test the mutagenesis efficiency of the mutant plasmid generation, a pWhitescript 4.5 kb control plasmid was used. The control reaction was prepared as follows, 5 μ l of 10 x reaction buffer (100 mM KCl, 100 mM $(\text{NH}_4)_2\text{SO}_4$, 200 mM Tris-HCl (pH 8.8), 20 mM MgSO_4 , 1% Triton X-100, 1 mg/ml nuclease-free bovine serum albumin (BSA)), 2 μ l (10 ng) of pWhitescript 4.5 kb control plasmid, 1.25 μ l (125 ng) of oligonucleotide control forward primer #1, 1.25 μ l (125 ng) of oligonucleotide control reverse primer #2, 1 μ l dNTP mix and 39.5 μ l of double distilled water (ddH_2O) to a final volume of 50 μ l. Then 1 μ l of *PfuTurbo* DNA polymerase was added. The forward and reverse primers contain the desired mutations and are complementary to opposite strands of the vector and each other. The primers are extended during the temperature cycling step by using *PfuTurbo* DNA polymerase. *PfuTurbo* DNA polymerase replicates both plasmid strands with high fidelity and without displacing the mutant oligonucleotide primers. Incorporation of the oligonucleotide primers generates a mutated plasmid with staggered nicks. The sample reaction was prepared as follows, 5 μ l of 10 x reaction buffer, 2.5 μ l (25 ng) of WT FX plasmid, 1.25 μ l (125 ng) of the forward mutagenic oligonucleotide primer, 1.25 μ l (125 ng) of the corresponding reverse mutagenic oligonucleotide primer #2, 1 μ l dNTP mix and 39 μ l of ddH_2O to a final volume of 50 μ l. Then 1 μ l of *PfuTurbo* DNA polymerase was added.

2.9.5.2 Step 2: Temperature cycling

The temperature cycling used for synthesis and amplification was in accordance with the type of mutation desired. In the first step, the plasmid gets denatured. Following denaturation, the oligonucleotide primers containing the desired mutation(s) anneal to the vector and are then incorporated to the synthesised strand of DNA, resulting in two nicked circular DNA strands. The first segment is one cycle at 95°C for 30 sec, the second segment is 16 (for single amino acid change of residue R125A of FX) or 18 cycles (for double amino acid changes of R93A_K96A, R165A_K169A or K236A_R240A) of 95°C for 30 sec, 55°C for 1 min and 68°C for 6 min (1 min/kb of plasmid length, WT FX is 6405 base pairs). The control reaction was run under the same conditions. Following temperature cycling the reaction was placed on ice for 2 min.

2.9.5.3 Step 3: Digestion

The next step was to digest the amplification products. 1 μl of the *Dpn* I restriction enzyme (10 U/ μl) was added directly to each amplification reaction. *Dpn* I is an enzyme specific for methylated and hemimethylated DNA and is used to digest the parental DNA template and select for the mutation-containing synthesised DNA. DNA isolated from *E.coli* is dam methylated and therefore susceptible to *Dpn* I digestion. The samples were incubated at 37°C for 1 h to digest the parental (i.e. non-mutated) supercoiled dsDNA.

2.9.5.4 Step 4: Transformation

The final step was the transformation of Epicurian Coli® XL1-Blue Supercompetent Cells. 1 μl of the DpnI treated DNA (circular nicked vector DNA containing the desired mutations) from each sample reaction was added to 50 μl of the cells in separate polypropylene tubes and incubated on ice for 30 min. The transformations were heat shocked for 45 sec at 42°C and then placed on ice for 2 min. 500 μl of LB broth was added and the mix incubated at 37°C for 1 h with shaking. 250 μl of each transformation reaction was spread on to LB ampicillin agar plates and incubated overnight at 37°C. The pWhitescript 4.5 kb control plasmid contains a stop codon (TAA) at the position where a glutamine (CAA) would normally appear in the β -galactosidase gene. XL1-Blue cells transformed with this control plasmid appear white in ampicillin agar plates containing IPTG (isopropyl-beta-thio galactopyranoside, a lactose analog which binds and inhibits the *lac* repressor and thereby strongly induces β -galactosidase production) and X-gal (5-bromo-4-chloro-indoly- β -D-galactoside, stain used in the detection of β -galactosidase) since β -galactosidase activity is removed. The oligonucleotide control primers mutate the T residue in the stop codon to a C residue, changing the stop codon to a glutamine codon found in the WT sequence thus restoring β -galactosidase activity and forming blue colonies on the ampicillin agar plates, thereby testing the mutagenesis efficiency of this protocol.

2.9.6 Design of mutagenic oligonucleotide primers

Mutagenic oligonucleotide primers with either single (for mutagenesis of amino acid residue R125) or double (for mutagenesis of amino acid residues R93 and K96, R165 and K169 or K236 and R240) amino acid changes were designed. Both the mutagenic primers (forward and reverse) for each set of mutations contain the desired mutation(s) and anneal to the same sequence on the opposite strands of the plasmid. All primers were between 28

and 49 bases in length and had a melting temperature below 78°C. The desired mutation(s) were located near the middle of each primer with approximately 8-15 bases of correct sequence on both sides. All primers terminate in G or C bases. See Table 2.2 for primer sequences.

Table 2.2. Mutagenic oligonucleotide primers.

Primer	Sequence
R93A_K96A	Forward 5'-GGTGGTCATCAAGCACAAACGCGTTCACAGCGGAGACCTATGACTTCGAC-3' Reverse 5'-GTCGAAGTCATAGGTCTCCGCTGTGAACGCGTTGTGCTTGATGACCACC-3'
R125A	Forward 5'-CTGCCTCCCCGAGGCTGACTGGGCCGAG-3' Reverse 5'-CTCGGCCAGTCAGCCTCGGGGAGGCAG-3'
R165A_K169A	Forward 5'-CCCTACGTGGACGCCAACAGCTGCGCGCTGTCCAGCAG-3' Reverse 5'-CTGCTGGACAGCGCGCAGCTGTTGGCGTCCACGTAGGG-3'
K236A_R240A	Forward 5'-GTCACCGCCTTCCTCGCGTGGATCGACGCGTCCATGAAAACCAGG-3' Reverse 5'-CCTGGTTTTTCATGGACGCGTCGATCCACGCGAGGAAGGCGGTGAC-3'

2.9.7 Cloning FX SP mutant cDNA into pcDNA3.1+zeocin

The FX SP mutant cDNA coding sequence within the pMK-RQ_FX SP mutant plasmid (Invitrogen) was firstly cloned into a pSCb plasmid and then into a pcDNA3.1+zeocin plasmid (Figure 2.2). Cloning into the pSCb plasmid allows the FX SP mutant to be sequence verified, as well as providing a plasmid to easily transform and make large scale preparations of the DNA.

2.9.7.1 Step 1: Excision of FX SP mutant cDNA from the pMK-RQ_FX SP mutant plasmid

Oligonucleotides were designed to amplify the FX SP mutant cDNA from the pMK-RQ plasmid, adding an *Afl*III site at the 5' end and amplifying through *Hind*III at the 3' end. *Afl*III-FX SP mutant-*Hind*III was amplified by polymerase chain reaction (PCR) using the two oligonucleotides (MWG-Biotech) described in Table 2.3 and Herculase II proof reading polymerase. To 25 ng of pMK-RQ_FX SP mutant plasmid DNA, 1 µl Herculase II fusion DNA polymerase (Agilent Technologies), 10 µl 5x Herculase II reaction buffer (Agilent Technologies), 0.5 µl dNTP mix (Agilent Technologies), 10 µM of forward and reverse primers were added and made up to a final volume of 50 µl with dH₂O. Thermal cycling steps were as follows; 1 cycle at 95°C for 2 min, 30 cycles at 95°C for 20 sec, 50°C for 20 sec and 72°C for 45 sec, followed by 1 cycle at 72°C for 3 min.

Table 2.3. Primer design.

FX SP mutant forward (containing *Afl*III sequences (highlighted in blue)), reverse and sequencing primers were designed and commercially synthesised.

Primer	Sequence
pMK-RQ_FX SP mut_ <i>Afl</i> III	Forward 5'-GAATCTTAAGAGGAAGGCCGTCA-3'
pMK-RQ_FX SP mut_rv	Reverse 5'-GGCCCATGAGGCCAGG-3'
FX SP mutant #1	5'-CCATGGCCCACGTGCG-3'
FX SP mutant #2	5'-GCCTGCATCCCTACCG-3'
FX SP mutant #3	5'-ACTGCGACCAGTTCTGCCA-3'
FX SP mutant #4	5'-TGGTCATCAAGCACAACGC-3'

The PCR products were electrophoresed on a 1% agarose gel in 1x Tris/Borate/EDTA (TBE) (10 mM Tris, 10 mM boric acid, 10 mM EDTA, pH 8.3) and ethidium bromide (10 ng/ml). Gels were electrophoresed at a constant voltage of 100 V with TBE as running

buffer. Bands were visualised and photographed on a molecular imager ChemiDoc™ XRS+ Imaging System (Bio-Rad Laboratories, Hemel Hempstead, UK).

The band for FX SP mutant was gel extracted and placed in a microcentrifuge tube. Gel extraction of DNA was used to excise DNA fragments following restriction endonuclease digestion to eliminate excess primers, nucleotides or enzyme reaction reagents. The Wizard SV Gel and PCR Clean-Up System (Promega, South Hampton, UK) was used to extract plasmid DNA according to the manufacturer's instructions. Briefly, 10 µl of membrane binding solution (4.5 M guanidine isothiocyanate, 0.5 M potassium acetate, pH 5) was added per 10 µg DNA. The sample was vortexed and incubated at 50-65°C for 10 min, when the band was fully dissolved. The sample was transferred to a SV Minicolumn and centrifuged at 16,000 g for 1 min at 4°C. The SV Minicolumn was washed twice with 700 µl and 500 µl Membrane Wash Solution (10 mM potassium acetate pH 5, 16.7 mM EDTA pH 8, 80% (v/v) ethanol). After each wash samples were subjected to centrifugation at 16,000 g for 1 min and 5 min at 4°C. Gel purified DNA was eluted with 40 µl dH₂O and centrifuged at 16,000 g for 1 min. DNA was stored at -20°C.

2.9.7.2 Step 2: Ligation of the FX SP mutant cDNA into the pSCb plasmid

The purified FX SP mutant PCR product was ligated into a pSCb plasmid using the StrataClone Blunt PCR Cloning Kit (Agilent Technologies) as per manufacturer's instructions. Briefly, the ligation reaction mixture was produced by adding (in order) 3 µl StrataClone Blunt Cloning Buffer, 2 µl (32 ng) FX SP mutant PCR product and 1 µl StrataClone Blunt Vector Mix ampicillin. The mixture was incubated at room temperature for 5 min, then placed on ice. 1 µl of the mixture was added to a tube of thawed StrataClone SoloPack Competent Cells and mixed gently. The transformation mixture was incubated on ice for 20 min and then heat-shocked at 42°C for 45 sec, followed by incubation on ice for 2 min. 250 µl of prewarmed LB was added and the cells were allowed to recover at 37°C for 2 h with gentle shaking. Either 5 µl or 100 µl of the transformation mixture was plated on agar plates and incubated at 37°C overnight. The next day, colonies were picked and small scale preparation of DNA performed as described in section 2.9.1. The samples were sequenced as described in section 2.10 and using the sample with the correct DNA sequence, large scale preparation of DNA was performed as described in section 2.9.3. Sequencing primers are described in section Table 2.3.

2.9.7.3 Step 3: Excision of the FX SP mutant cDNA from the pSCb plasmid and ligation into pcDNA3.1+zeocin

Restriction endonuclease digestion is a procedure to cut double-stranded DNA using a restriction endonuclease. 20 µg pSCb_FX SP mutant or pcDNA3.1+zeocin plasmid was digested overnight at 37°C with 5 µl enzyme *EcoRI* (Promega) and 5 µl enzyme *EcoRI* buffer (Promega), made up to a final volume of 50 µl with dH₂O. The pSCb_FX SP mutant and pcDNA3.1+zeocin restriction endonuclease digests were electrophoresed on a 1% agarose gel. Bands for FX SP mutant and pcDNA3.1+zeocin were gel extracted. To prevent recircularisation of the digested pcDNA3.1+zeocin DNA in the ligation reaction, the 5' phosphates from digested DNA were removed using 5 U shrimp alkaline phosphatase (SAP) (Promega) by incubation at 37°C for 15 min. SAP was inactivated by incubation at 65°C for 15 min. Dephosphorylated pcDNA3.1+zeocin and FX SP mutant DNA were ligated using T4 DNA ligase (Promega). Ligation reactions were performed at a 1:3 molar ratio (pcDNA3.1+zeocin_FX SP mutant). The DNA, 1 µl T4 DNA ligase and 1 µl T4 DNA ligase buffer were made up to a final volume of 10 µl with dH₂O and incubated at 4°C for 2 h. The mixture was then transformed into competent *E.coli* JM109 (Promega) and the transformation mixture streaked on to agar plates. The next day, colonies were picked and small scale preparation of DNA was performed as described in section 2.9.1.

2.9.7.4 Step 4: Investigating the efficiency of FX SP mutant cDNA ligation into pcDNA3.1+zeocin

In order to ensure the FX SP mutant DNA was successfully ligated a diagnostic digest was performed. To 5 µl (500 ng DNA) of the miniprep sample, 2 µl enzyme *BglII*, 1 µl *BglII* buffer, 0.2 µl 10x BSA were added and made up to a final volume of 20 µl with dH₂O. Samples were incubated at 37°C for 3 h before being electrophoresed on a 1% agarose gel as previously described in Step 1. The samples showing the band for FX SP mutant were sequenced and, using the sample with the correct DNA sequence, large scale preparation of DNA was performed as described in section 2.9.3. Sequencing primers are described in section Table 2.3.

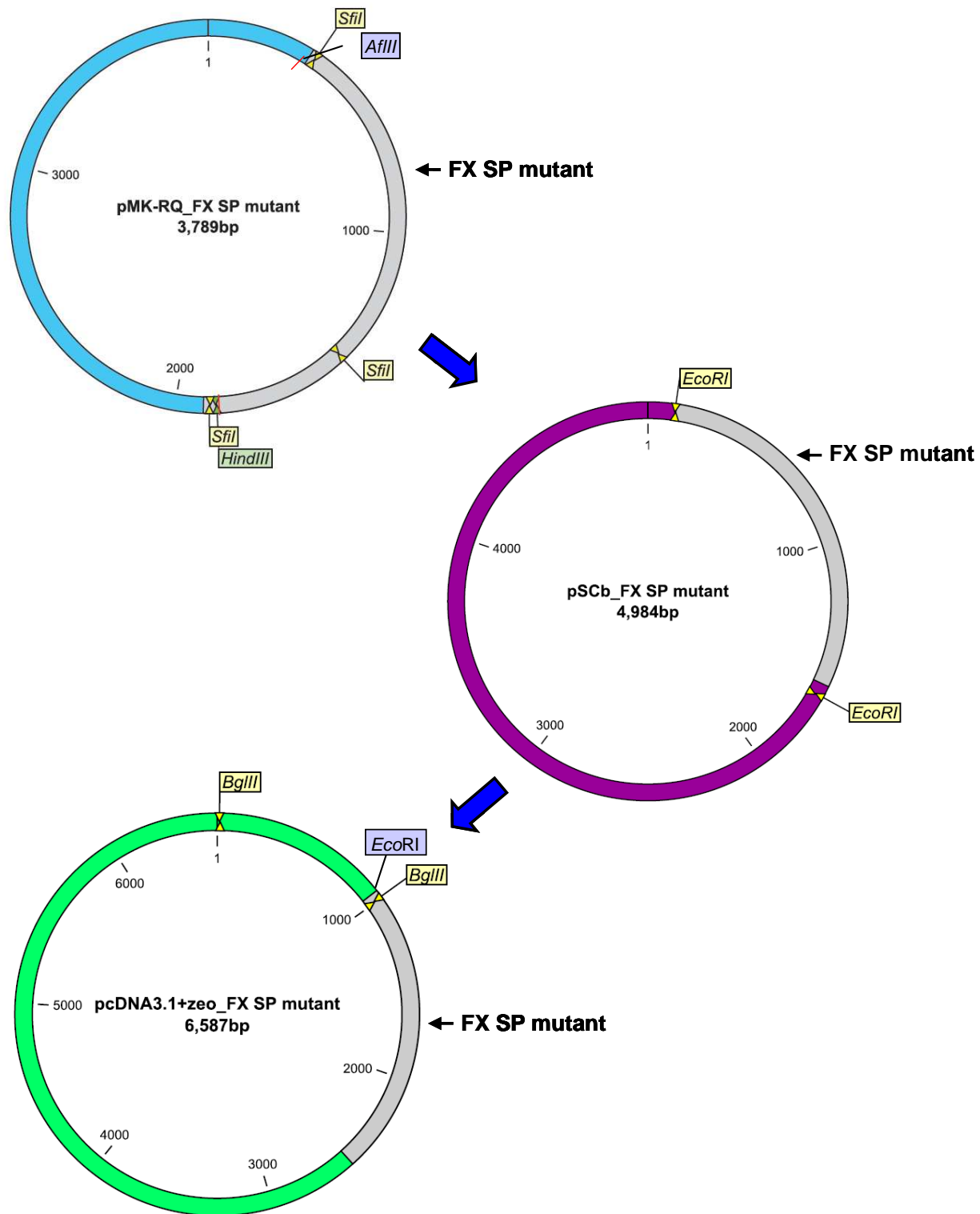


Figure 2.2. Strategy for cloning FX SP mutant into pcDNA3.1+zeocin.

Firstly the SP mutant fragment was amplified from the pMK-RQ construct by adding an *AflIII* site at the 5' end and amplifying through the *HindIII* site on the 3' end. The purified PCR product was ligated into a pSCb construct. The pSCb_FX SP mutant and the pcDNA3.1+zeocin plasmid were digested with *EcoRI*. The FX SP mutant fragment was ligated into pcDNA3.1+zeocin. A diagnostic digestion was performed cutting at *BglII* sites, one present in the pcDNA3.1+zeocin backbone and one in the FX SP mutant insert, to ensure the insert was present.

2.10 DNA sequencing

To confirm the sequence of plasmid DNA generated from small or large scale preparations dideoxy sequencing was performed. This process takes advantage of the ability of DNA polymerase to incorporate 2', 3'-dideoxynucleotides, nucleotide base analogs that lack the 3'-hydroxyl group essential in phosphodiester bond formation. It requires a DNA template, a sequencing primer, a thermal stable DNA polymerase, nucleotides (dNTPs), dideoxynucleotides (ddNTPs) (provided in the Ready Reaction mix (Applied Biosystems) see below), and buffer. DeVised from Sanger sequencing, the Applied Biosystems fluorescence-based cycle sequencing system used here employs fluorescent dyes to label the extension products and the components are combined in a reaction that is subjected to cycles of annealing, extension, and denaturation in a thermal cycler. Thermal cycling the sequencing reactions creates and amplifies extension products that are terminated by one of the four dideoxynucleotides, resulting in the formation of extension products of various lengths. The sequencing products are then separated based on size by capillary electrophoresis.

2.10.1 Sequencing PCR

300 ng DNA was used as a template for sequencing using specific forward and reverse primers. Each sequencing reaction contained 1.6 nM primer (forward or reverse), 0.5 μ l v3.1 Ready Reaction mix (Applied Biosystems), 4 μ l v3.1 sequencing buffer (Applied Biosystems, MA, USA) made up to a final volume of 20 μ l with dH₂O. The cycle conditions were 25 cycles to denature at 96°C for 50 sec, anneal at 50°C for 20 sec and extend the DNA fragment at 60°C for 3 min.

2.10.2 Sequencing reaction purification

Sequencing reactions were purified to remove reaction constituents and unincorporated nucleotides and primers using CleanSEQ (Agencourt Bioscience Corporation, MA, USA) according to the manufacturer's instructions. Briefly, 10 μ l of CleanSEQ reagent was added to each sequencing reaction, followed by 62 μ l of 85% ethanol. Plates were vortexed briefly and centrifuged for 30 sec to collect the liquid in the bottom of the wells. Plates were placed on a SPRIplate (Beckman Coulter, UK) for 2 min. The plate was turned upside down to empty the liquid from it. Wells were washed in 150 μ l of 85% ethanol and plates were vortexed briefly and placed on a SPRIplate for 2 min. Wells were emptied as much as possible by centrifugation of inverted plates for 1 sec. Plates were removed from

the SPRIPlate and air dried for 10 min. 40 μ l of dH₂O was added to each well and the plate returned on to the SPRIPlate for 2 min. 20 μ l of sequencing products were loaded into optically clear barcoded 96 well plates and plates were sealed to prevent evaporation. DNA sequencing was performed using a 96-capillary ABI 3730 automated sequencer (Applied Biosystems). The sequences were analysed using Applied Biosystems SeqScape software version 2.

2.11 Recombinant FX production

2.11.1 Differential pH transient transfections

293T cells were seeded in 10 cm² culture dishes and incubated at 37°C overnight to reach approximately 70% confluence. Cells were gently washed once in PBS. 4.5 ml media A (DMEM, high glucose, GlutaMAX (Invitrogen), 10% (v/v) FCS, 2 mM L-glutamine, 1% (v/v) penicillin-streptomycin, 25 mM HEPES, pH 7.9) was added to each dish. 100 mM CaCl₂ and 21 μ g plasmid DNA were added to 960 μ l media B (DMEM, high glucose, GlutaMAX (Invitrogen), 2 mM L-glutamine, 1% (v/v) penicillin-streptomycin, 25 mM HEPES, pH 7.1) in a universal tube. 1 ml of this mixture was added per dish, volumes were scaled up for multiple transfections. The mixture was added on to the cells in a drop-wise fashion, whilst the dishes were gently shaken. The cells were incubated at 37°C overnight. The next day cells were washed once in PBS and 15 ml fresh media was added per dish.

2.11.2 Determining optimal concentration of zeocin

To determine the optimal concentration of zeocin for use in the generation of stable cell lines i.e. the minimum concentration of zeocin required to kill the untransfected host cell line, cells were firstly seeded in 24-well plates at 1×10^5 cell/well and incubated at 37°C overnight. 100, 200, 300, 400 or 500 μ g/ml of zeocin in 10% media was added to the cells. Cells were incubated at 37°C. Zeocin containing media was replenished every 2 days. Cell death was visually assessed after 7 days.

2.11.3 Generation of FX stable cell lines

Stable cell lines were generated based on zeocin resistance. 293T cells were seeded in 10 cm² culture dishes and incubated at 37°C overnight to reach approximately 70% confluence. Cells were transfected using the differential pH transfection method as

described in section 2.11.1 with either the pcDNA3.1+zeocin/FX SP mutant plasmid, cotransfected with the plasmid encoding WT FX and the pcDNA3.1+zeocin or cotransfected with the control green fluorescent protein (GFP) and the pcDNA3.1+zeocin plasmid. Cotransfection was performed at a 1:10 molar ratio (pcDNA3.1 zeocin:WT FX or GFP). Cells were incubated at 37°C for 24 h then the media was replaced with 10% media supplemented with 5 µg/ml vitamin K and 200 µg/ml zeocin. Cell growth was observed every 2 to 3 days and the media was replenished every 3 to 4 days, taking care not to pipette directly on to the cells. After 2 weeks there was mass cell death, leaving stable cell colonies behind. To pick colonies, 24-well plates with 1 ml 10% media supplemented with 5 µg/ml vitamin K and 200 µg/ml zeocin in each well were prepared. The 10 cm² dishes were washed once with PBS to remove any cell debris. Using a 1 ml wide bore pipette tip, the tip was lowered to the surface of the colony of interest and media was added gently through the tip secured over the colony. The colony was transferred to a well of a 24-well plate. This was repeated with other colonies. Cells were grown until 90% confluent in the presence of 200 µg/ml zeocin. Conditioned media was collected from individual wells and FX enzyme-linked immunosorbent assay (ELISA) (Affinity Biologicals, Canada) was performed to identify the highest producing cells. The high producing cells were grown and expanded into 6-well plates, 25 cm², 75 cm² and finally 150 cm² tissue culture flasks.

2.12 Human FX ELISA

Protein was quantified using a matched-pair antibody set for ELISA of human FX antigen (Affinity Biologicals, Canada). The affinity purified polyclonal antibody to FX was diluted 1/100 in coating buffer (50 mM Carbonate, 15 mM Na₂CO₃ and 35 mM NaHCO₃ in 1 L dH₂O, pH 9.6) and 100 µl was added to each well of a 96-well plate. The plate was incubated at 4°C overnight. The contents of the plate were emptied and 150 µl of blocking buffer (2.5 g BSA in 200 ml PBS, pH 7.4) was added to each well. The plate was incubated at room temperature for 60 min. The plates were washed three times with 0.1% Tween. The commercially bought pd FX was diluted in sample diluent (5.95 g HEPES, 1.46 g NaCl, 2.5 g BSA, 0.25 ml Tween-20 in 250 ml dH₂O, pH 7.2). The pd FX dilutions (20, 10, 5, 2.5, 1.25, 0.625, 0.3125, 0.1516, 0.078, 0.039, 0.0195 and 0.00976 µg/ml) were used as controls in this experiment. Conditioned media from cells stably or transiently transfected with FX plasmids were added neat or diluted 1/10 or 1/50 in the sample diluent. 100 µl of control or samples were added to the plate and incubated at room temperature for 90 min. The antibody coated on the plate captured any FX in the samples. The plates were washed three times with 0.1% Tween-20 to remove any unbound material. A peroxidase

conjugated polyclonal FX antibody was diluted 1/100 in sample diluted and 100 μ l added to each well. The plate was incubated at room temperature for 90 min. The plates were washed three times with 0.1% Tween-20 to remove any unbound conjugated antibody. The peroxidase activity is expressed by adding 100 μ l o-phenylenediamine (OPD) substrate (5 mg OPD in 12 ml substrate buffer (2.6 g citric acid and 6.9 g Na_2HPO_4 in 500 ml dH_2O) and 12 μ l 30% H_2O_2) to each well. After 15 min incubation at room temperature the reaction was quenched with the addition of 50 μ l/well of 2.5 M H_2SO_4 . The colour produced was measured using a Wallac VICTOR² plate reader (Wallac) at a wavelength of 490 nm.

2.13 rFX purification

rFX was affinity purified from conditioned serum free cell culture media using a chromatographic approach employing the AKTAexploror chromatography system (GE Healthcare) and the 4G3 mouse monoclonal antibody coupled to sepharose as previously described (Kim *et al.*, 1994). Briefly, the conditioned media was dialysed in 4 L of buffer HBS- Ca^{2+} (10 mM HEPES, pH 7, 150 mM NaCl, 5 mM CaCl_2) twice, for 12 h each. The buffered cell culture media was applied to the 4G3 sepharose column and the column was extensively washed in buffer HBS- Ca^{2+} . Bound proteins were eluted by applying a linear gradient of buffer HBS-E (10 mM HEPES, pH 7, 150 mM NaCl and 10 mM EDTA) to the column. The bound fractions were collected and further analysed or stored at -20°C .

2.14 Activation of rFX

The amidolytic activity of samples was measured in a two stage process. Firstly, the FX was activated to factor Xa (FXa) in the presence of tissue factor, factor VIIa and calcium. In the second stage, the generated FXa hydrolyses the chromogenic substrate Z-D-Arg-Gly-Arg-pNA (S-2765 (Quadrantech, Surrey, UK)), thus liberating the chromophoric group pNA (p-nitroaniline). rFX, commercially bought pd FX and FXa (Haematologic Technologies) were diluted in TBSA (50 mM Tris-HCl, 150 mM NaCl, 1 mg/ml albumin, pH 7.4). rFX and pd FX were used at 10, 5 and 1 μ g/ml. The FXa dilutions (0.5, 0.2, 0.1, 0.05, 0.02 and 0.01 μ g/ml) were used as controls in this experiment. 40 μ l of each sample or standard was added to each well of a 96-well plate, followed by 160 μ l of the mastermix containing 1 mM chromogenic substrate S-2765 (Quadrantech), 100 nM tissue factor, 100 nM factor VIIa (Novo Nordisk Ltd., Crawley, UK) and 6 mM CaCl_2 . Samples were incubated at room temperature for 15 min. The colour produced was measured using a

Wallac VICTOR² plate reader (Wallac) at a wavelength of 405 nm. The generated FXa (and thus the intensity of colour) is directly proportional to the FX activity of the sample.

2.15 Surface plasmon resonance analysis

SPR was performed using a Biacore T100 (GE Healthcare, London, UK).

2.15.1 Analysis of purified FX fractions

Briefly, the monoclonal anti-human FX 4G3 antibody was covalently immobilised on to the flowcell of a CM5 biosensor chip by amine coupling according to the manufacturer's instructions. Sensorgrams were generated at a flow rate of 30 μ l/min using 10 mM HEPES pH 7.4, 150 mM NaCl, 5 mM CaCl₂, 0.05% Tween-20 as running buffer and regeneration between injections with HEPES pH 7.4, 150 mM NaCl, 3 mM EDTA, 0.05% Tween-20. Injections of WT rFX or SP mutant rFX fractions eluted from the 4G3 affinity column diluted in running buffer were passed over the chip. This was followed by regeneration of the sensorchip surface. Subtracted sensorgrams were generated by subtracting the signal from a surface subjected to a blank amine immobilisation. Data was analysed using Biacore T100 Evaluation software.

2.15.2 Analysis of rFX binding to Ad5 hexon

Briefly, virus was biotinylated using sulfo-NHS-LC-biotin (Pierce, Rockford IL, USA). Ad5 hexon was covalently immobilised on to the flowcell of a CM5 biosensor chip by amine coupling according to the manufacturer's instructions. The immobilisation density of the Ad5 hexon was 1036 response units. Sensorgrams were generated at a flow rate of 30 μ l/min using 10 mM HEPES pH 7.4, 150 mM NaCl, 5 mM CaCl₂, 0.05% Tween-20 as running buffer and regeneration between injections with HEPES pH 7.4, 150 mM NaCl, 3 mM EDTA, 0.05% Tween-20. Injections of pd FX, WT rFX or SP mutant rFX conditioned media diluted in running buffer were immediately followed by injections of the monoclonal anti-FX antibodies HX-1 and 4G3 prior to regeneration of the biosensor chip surface. Subtracted sensorgrams were generated by subtracting the signal from a surface subjected to a blank amine immobilisation.

2.15.3 Analysis of pharmacological compounds binding to FX and Ad5 binding to FX in the presence of compounds

Briefly, human FX was covalently immobilised on to the flowcell of a CM5 biosensor chip by amine coupling according to the manufacturer's instructions. Sensorgrams were generated at a flow rate of 30 μ l/min using 10 mM HEPES pH 7.4, 150 mM NaCl, 5 mM CaCl₂, 0.05% Tween-20 as running buffer and regeneration between injections with HEPES pH 7.4, 150 mM NaCl, 3 mM EDTA, 0.05% Tween-20. Injections of 10 μ M compound T5550585, T5424837, T5660138, T5677956, T5660136 or T5572402 from the Pharmacological Diversity Drug-like Set (Enamine, Ukraine) or an equivalent volume of DMSO in the absence and presence of Ad5 diluted in running buffer were passed over the chip. This was followed by regeneration of the biosensor chip surface. DMSO subtracted sensorgrams were generated and data analysed using Biacore T100 Evaluation software.

2.16 Protein extraction

Protein was extracted from SKOV3, A549 and SW620 cells in 6-well plates by first adding lysis buffer (20 mM Tris pH 7.5, 150 mM NaCl, 2.5 mM sodium pyrophosphate, 1 mM β -glycerophosphate, 1 mM sodium orthovanadate (Na₃VO₄), 1 mM ethylenediaminetetraacetic acid (EDTA), 1 mM ethylene glycol tetraacetic acid (EGTA), 1% (v/v) Triton X, 1 μ g/ml leupeptin and 1 mM phenylmethylsulfonyl fluoride (PMSF)). Each well was scraped, the lysed cells collected in 1.5 ml Eppendorfs and centrifuged to pellet the cells. The supernatant was discarded.

2.17 Determination of protein concentration in cells

The concentration of protein in cell lysates was determined using the bicinchoninic acid assay (BCA) Protein Assay Kit (Pierce), a colorimetric detection and quantification protocol, as per manufacturer's instructions. A protein standard curve was generated using BSA at concentrations of 2000, 1500, 1000, 750, 500, 250, 125 and 25 μ g/ml. 200 μ l of BCA working reagent was added to 25 μ l of cell lysate or standard, in duplicate in a 96-well plate. PBS was used as the blank control. The plate was incubated at 37°C for 1 h in the dark. The absorbance was measured at 570 nm on the Wallac Victor² plate reader (Wallac).

2.18 Electrophoresis

2.18.1 SDS-PAGE

Sodium dodecyl sulphate polyacrylamide gel electrophoresis (SDS-PAGE), Coomassie blue staining and western immunoblotting were used to detect specific proteins. Protein concentration in the samples were quantified as described in section 2.17 and samples prepared with equal concentrations in 5x loading buffer (10% (v/v) Tris-HCl pH 6.8, 10% (w/v) SDS, 30% (v/v) glycerol, 0.1% (w/v) bromophenol blue and 2% (v/v) β -mercaptoethanol). In order to denature the protein, samples were heated at 95°C for 5 min prior to loading on to the gel. 40 μ l rainbow ladder (Amersham Bioscience UK Ltd, Buckingham, UK) was also added to the gel as a marker of protein size. The polyacrylamide gel consisted of a 4% stacking gel containing 13.3% (v/v) polyacrylamide 30%, 12.5 mM Tris pH 6.8, 0.1% (v/v) SDS, 1% ammonium persulphate (APS) and 0.1% N,N,N',N'- Tetramethylethylenediamine (TEMED) and a 10% polyacrylamide gel, consisting of 33.3% (v/v) polyacrylamide 30%, 37.5 mM Tris pH 8.8, 0.1% (v/v) SDS, 1% APS and 0.1% TEMED. Samples were electrophoresed at 200 V in running buffer (0.025 M Tris-HCl, 0.2 M glycine, 0.001 M SDS) for approximately 5 h. The gel was then either subjected to Coomassie blue staining (section 2.18.2) or to further processing and western immunoblotting (section 2.18.3).

2.18.2 Coomassie blue staining

The SDS-PAGE gel was washed in dH₂O three times, for 5 min each. The gel was then stained in Coomassie Simply Blue Safe Stain (Invitrogen, Paisley, UK) at room temperature with gentle shaking for 1 h. The stain was discarded and the gel washed in dH₂O twice, for 1 h each, with gentle shaking. The stained gel was visualised using an Odyssey infra-red imaging system (LI-COR, Nebraska, USA).

2.18.3 Western immunoblotting

The proteins from the SDS-PAGE (section 2.18.1) were transferred to Hybond-P membrane (Amersham Bioscience UK Ltd, Buckingham, UK) using 80 mV in transfer buffer (0.2 M glycine, 0.025 M Tris, 20% (v/v) methanol, 0.1 M SDS) overnight at 4°C. After transferring, the membrane was blocked in TBS-T (150 mM NaCl, 50 mM Tris, 0.1% (v/v) Tween-20) and 10% (w/v) fat free milk powder (blocking buffer) for 3 h at room temperature. The membrane was either incubated with primary antibody for 1 h at

room temperature (for the monoclonal human anti-FX clone HX1 antibody (1:1000 dilution in blocking buffer)) or overnight at 4°C (for the rabbit polyclonal antibody anti-ezrin (1:750 dilution), the rabbit monoclonal anti-radixin (1:1000 dilution), rabbit monoclonal anti-moesin (1:2500 dilution) or the mouse monoclonal anti-Syk (1:500) antibodies) whilst shaking. The membrane was washed twice in blocking buffer, for 5 min and incubated with the appropriate secondary antibody; goat anti-mouse IR dye 800CW labelled secondary antibody (1:1000 dilution) (LI-COR, Nebraska USA), rabbit anti-mouse HRP (1:1000 dilution) or swine anti-rabbit HRP (1:1000 dilution) (Neomarkers, Fremont, CA, USA), for 1 h at room temperature, whilst shaking. The membrane was washed six times for 15 min each at room temperature whilst shaking, four times with blocking buffer and twice in TBS-T. The blot was visualised using either an Odyssey infra-red imaging system (LI-COR) or Enhanced Chemiluminescent (ECL) Detection System (Amersham Biosciences UK Limited) following the manufacturer's instructions. Briefly, equal quantities of the two solutions from the ECL kit were mixed and poured on to the membrane. After 1 min, the excess ECL was drained off and films were exposed for various lengths of time ranging from 30 sec to overnight.

2.19 Adenovirus production

2.19.1 Recombinant Ad5 production

High titre stocks of recombinant E1/E3-deleted Ad5 were produced by large-scale expansion of a plaque pure stock of Ad5 in 293 cells. AdKO1 was previously generated in house as described by Bradshaw *et al.* (Bradshaw *et al.*, 2010). Ad5KO1 is based on the Ad5 vector and contains a two-amino acid substitution in the fiber knob domain (S408E, P409A) that ablates CAR binding. For recombinant Ad5 production, cells were grown to approximately 80% confluence and infected with virus with a multiplicity of infection of 1 plaque forming unit (pfu) per cell. After 3 to 4 days the cytopathic effect (CPE) of the virus caused the cells to detach from the base of the tissue culture flask. The media containing the cells was collected and the cells were harvested by centrifugation at 850 g for 10 min. The supernatant was removed and the cells were resuspended in 8 ml PBS. Next, 8 ml Arklone P (trichlorotrifluoroethane) was added to the cells and the mixture gently shaken and inverted several times. The mixture was centrifuged at 1900 g for 15 min. The top aqueous layer containing the virus was removed and stored at -80°C.

2.19.2 Ad5 purification using caesium chloride (CsCl) gradient

Clear ultracentrifuge tubes (Beckman Coulter, London, UK) were sterilised with 70% ethanol and sterile H₂O. A CsCl gradient was produced by adding, in order, 2.5 ml of CsCl with a density of 1.4 g/ml and 2.5 ml of CsCl with a density of 1.25 g/ml to an ultracentrifuge tube. The crude Ad5 stock was gently poured on top and the remaining volume in the tube was filled with PBS. The tube was placed in a Sorvall Discovery 90 rotor container (Sorvall Centrifuges, Connecticut, USA) and subjected to ultracentrifugation at 90,000 g for 1.5 h at 4°C with maximum acceleration and zero deceleration. On completion of this step a distinct, opalescent band containing the virus was observed between the CsCl 1.4 g/ml and CsCl 1.25 g/ml density layers in the tube (Figure 2.3). The virus band was removed by piercing the tube below the band using a 21 gauge needle and removing the band in the minimal volume possible whilst taking care not to disrupt the other bands. The extracted virus was gently added to a fresh ultracentrifuge tube containing 5 ml of CsCl with a density of 1.34 g/ml and the remaining volume in the tube was filled with PBS. The tube was placed in a Sorvall Discovery 90 rotor container and subjected to ultracentrifugation at 90,000 g for 18 h at 4°C with maximum acceleration and zero deceleration. The distinct, opalescent band containing the virus visible above the CsCl 1.34 g/ml density layer was removed as before (Figure 2.3). The virus was transferred to a SlideA-Lyzer Dialysis Cassette (molecular weight cut-off of 10,000 Da) (Perbio Science, Cramlington, UK) for dialysis after hydration of the cassette for 1 min in dialysis solution. The virus was dialysed in 2 L 0.01 M Tris pH 8 and 0.001 M EDTA twice, first for 2 h then overnight in fresh buffer, and for a further 2 h in fresh buffer supplemented with 10% (v/v) glycerol. The virus was extracted from the cassette and stored at -80°C.

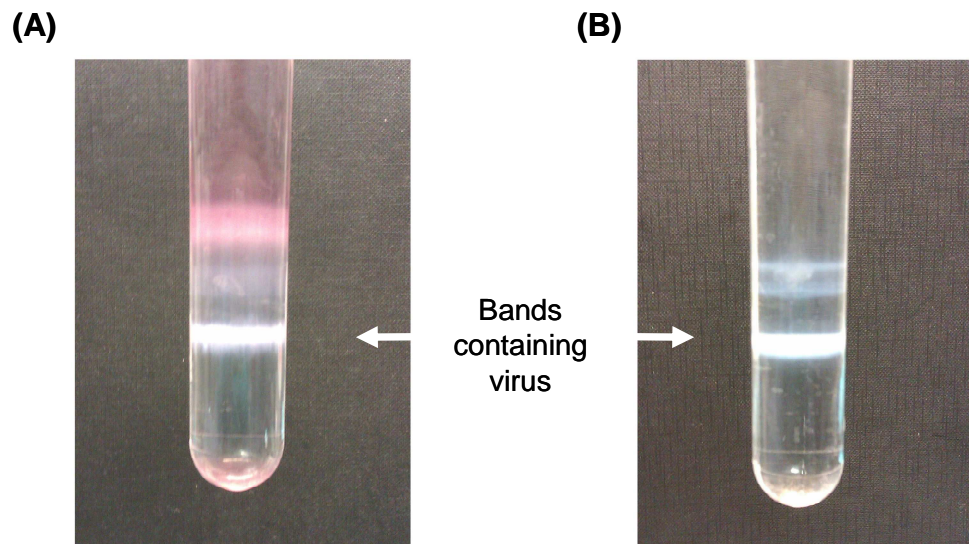


Figure 2.3. Purification of Ad5 by CsCl gradient.

(A) After the first ultracentrifugation step a distinct, opalescent band containing the virus forms between the CsCl 1.4 g/ml and CsCl 1.25 g/ml density layers (B) After the second ultracentrifugation step a band containing virus is visible above the CsCl 1.34 g/ml density layer in the tube.

2.20 Virus titration by end-point dilution assay

Ten-fold serial dilutions of viral stocks were titrated on 293 cells (~60% confluent), seeded in a 96-well plate with ten replicates of each titration on the plate. The next day the media was replaced with 200 μ l complete media. Media was replenished every 2-3 days. Infection was detected by induction of CPE. Once the CPE was apparent in a well, that well was marked and the media no longer replaced. The cells were incubated at 37°C for 8 days, at which point the number of wells containing plaques were counted and results fitted into the following equations in order to obtain the titre of the adenoviral stocks in pfu/ml. The proportionate distance = (% positive above 50% - 50%) / (% positive above 50% - % positive below 50%). The log ID₅₀ (infectivity dose) = (log dilution above 50% + (proportionate distance x -1) x dilution factor). Viral tissue culture ID₅₀ (TCID₅₀) values were then adjusted (1 x TCID₅₀ = 0.7 pfu) to enable viral titres to be expressed as pfu/ml.

2.21 Quantification of virus particles

Virus particle titre was determined based on the protein content of the virus stock using a Micro BCA Protein Assay Kit (Pierce) according to the manufacturer's instructions. Briefly, BSA standards at concentrations of 200, 40, 20, 10, 5, 2.5, 1 and 0.5 μ g/ml were prepared in PBS and 150 μ l of each were pipetted in duplicate into a 96-well plate. 150 μ l

PBS was used as a blank control. 1, 3 and 5 μl of the virus stock were added in duplicate and each well was made up to 150 μl with PBS. 150 μl working reagent (made up of 25:24:1 part Reagent A, B, C supplied with the kit) was added to each well. The plate was incubated at 37°C for 2 h. The absorbance was measured at 570 nm using a Wallac VICTOR 2 plate reader (Wallac). Background or the blank control absorbance was subtracted from all samples and standards. The amount of protein present in each virus was determined from the standard curve. The virus particle titre was calculated using the established formula, 1 μg protein = 1×10^9 viral particles (Von Seggern *et al.*, 1998).

2.22 Adenovirus infection

2.22.1 Virus cell binding

Cells were seeded in 24-well plates at a density of 2×10^5 cells/well and incubated overnight at 37°C. Cells were washed in ice cold PBS and incubated with 1000 vp/cell of Ad5 in serum free media for 1 h on ice in the absence or presence of 1 $\mu\text{g}/\text{ml}$ pd FX, WT or SP mutant rFX. Cells were then washed three times in PBS before cells were mechanically dislodged into 500 μl PBS. The cell suspension was collected in a 1.5 ml Eppendorf. The cells were pelleted by centrifugation at 16000 g for 3 min at room temperature. The supernatant was removed and the cell pellet was resuspended in 200 μl PBS.

2.22.2 DNA extractions

Viral and genomic DNA was extracted from samples using the QIAamp DNA mini kit (QIAGEN) according to the manufacturer's instructions. Briefly, to the cell pellet resuspended in 200 μl PBS, 20 μl proteinase K and 200 μl buffer AL were added and the mixture was vortexed. Samples were incubated for 10 min at 56°C. Next, 200 μl 100% ethanol was added to the samples, mixed and the complete sample was loaded on to a QIAamp Spin Column. Samples were centrifuged at 6000 g for 1 min at room temperature to allow the DNA to adsorb on to the silica-gel membrane of the spin column. The spin column was then washed with 500 μl buffer AW1 and centrifuged at 6000 g for 1 min at room temperature, followed by a second wash step with 500 μl buffer AW2 and centrifuged at 16000 g for 3 min at room temperature. Finally the DNA was eluted in 50 μl dH₂O by centrifugation at 6000 g for 1 min. The amount of DNA in each sample was quantified by measuring absorbance at 260 nm (NanoDrop, ND-1000 spectrophotometer).

2.22.3 Quantitative PCR for quantifying Ad genomes

Virus particles remaining bound to cells from the virus cell binding experiment were quantified by quantitative polymerase chain reaction (qPCR). This quantitative measurement is based on the detection of a fluorescent signal produced proportionally during the amplification of a PCR product. The amount of fluorescence released during the amplification cycle is proportional to the amount of product generated in each cycle and can be measured directly. Acquisition of data occurs when PCR amplification is in the exponential phase. The Power SYBR Green detection system (Applied Biosystems, Warrington, UK) was used. Power SYBR Green PCR master mix with 0.2 μ M hexon primers, forward (5'-CGCGGTGCGGCTGGTG-3') and reverse (5'-TGGCGCATCCCATTCTCC-3') were used to amplify the DNA. A standard curve was produced from serial dilutions of Ad5 (10^2 - 10^7 vp). For each reaction 125 ng of total DNA was used. The following conditions were used; 95°C for 10 min for denaturation, 95°C for 15 sec for amplification, 60°C for 1 min (repeated for 50 cycles) for annealing, 95°C for 15 sec, 60°C for 15 sec and 95°C for 15 sec for dissociation. Total adenoviral genomes were calculated using the SDS 2.3 software.

2.22.4 Fluorescence activated cell sorting (FACS) analysis of virus:cell binding

SKOV3 cells were detached from culture vessels using a 1 x citric saline solution and seeded at a density of 2×10^5 cell/tube in 50 μ l of ice cold serum free media. Cells were incubated with 50 μ l ice cold serum free media containing 5000 vp/cell of Alexa Fluor-488 fluorescently-labelled Ad5 in the absence or presence of FX plus 10 μ M compound T5550585, T5424837, T5660138, T5677956, T5660136 or T5572402 from the Pharmacological Diversity Drug-like Set or ER-27319 (Tocris Bioscience). The cells:virus mixes were incubated at 4°C for 1 h, in the dark, whilst shaking. Samples were washed twice in serum free media, undergoing centrifugation at 498 g for 3 min each time and resuspended in a final volume of 150 μ l ice cold serum free media. Alexa Fluor-488 fluorescently-labelled virus bound to the cells was detected on FACS Canto II flow cytometer (Beckton Dickinson, Oxford, UK) using FACS DIVA software. Viable cells were gated on the basis of forward and side light scatter profiles, with a minimum of 5000 gated events analysed per sample. Results are expressed as geometric mean x percentage positive cells per condition.

2.22.5 Virus cell transduction in the presence of rFX

Cells were seeded in 96-well plates at a density of 2×10^4 cells/well and incubated overnight at 37°C. Cells were washed with PBS and incubated with 1000 vp/cell Ad5 in serum free media in the absence or presence of 1 µg/ml FX, WT, SP mutant rFX and 100 µg/ml soluble heparin or for transduction experiments involving the single and double mutants of rFX in the absence or presence of 10 ng/ml FX, WT, SP mutant rFX, or rFX with mutations R93A_K96A, R125A, R165A_K169A, K236A_R240A for 3 h at 37°C. Cells were then washed once in serum free media and 200 µl complete media added. Cells were incubated at 37°C for a further 45 h.

2.22.6 Virus cell transduction in the presence of pharmacological agents

Cells were seeded in 96-well plates at a density of 2×10^4 cells/well and incubated overnight at 37°C. Cells were washed with PBS and for experiments involving the kinase inhibitors, were preincubated with 20 µM compound at 37°C for 30 min. Cells were incubated with 1000 vp/cell Ad5 in serum free media in the absence or presence of 10 µg/ml FX with or without kinase inhibitors or compounds from the Pharmacological Diversity Drug-like Set for 3 h at 37°C. 100 µl of complete media containing 20% serum was added to cells and they were incubated at 37°C for a further 45 h.

2.22.7 β-galactosidase transgene quantification

Expression of β-galactosidase was quantified using Tropix Galacto-Light Plus (Applied Biosystems). Briefly, cells were washed in PBS and 70 µl 1 x Reporter Lysis Buffer (5 x Reporter Lysis Buffer stock (Promega) diluted in PBS) was added. The plate was freeze thawed to ensure complete lysis of cells. 10 µl of each sample was transferred to a black 96-well plate and 70 µl of Tropix Galacton Plus:β-gal diluent mix (1:100 dilution of Tropix Galacton Plus in 100 mM NaH₂PO₄ and 1mM MgCl₂, pH 8) was added. Cells were covered in tinfoil to protect from light and incubated at room temperature for 1 h. 100 µl of Tropix Accelerator II was added to each well and incubated for 2 min. Luminescence was measured using a Wallac VICTOR² plate reader (Wallac). β-Galactosidase activity was then normalised to total protein content of the samples, measured by BCA assay (section 2.17) producing relative light units per milligram protein (RLU/mg protein).

2.22.8 GFP transgene quantification

Cells were washed in PBS and 50 μ l 1 x Reporter Lysis Buffer was added. Cells were placed on ice and mechanically dislodged from each well of the plate. A standard curve of recombinant GFP ranging from 0.01 to 1 μ g/ml was produced and 100 μ l of each dilution was added in duplicate to the plate. 100 μ l of PBS was added in duplicate as a blank control. 20 μ l of each sample was transferred to the plate and 80 μ l 1 x Reporter Lysis Buffer was added. The plate was incubated at room temperature for 10 min. Luminescence was measured using a Wallac VICTOR² plate reader (Wallac). GFP activity was then normalised to total protein content of the samples, measured by BCA assay (section 2.17) producing relative light units per milligram protein (RLU/mg protein).

2.22.9 Luciferase transgene quantification

Expression of luciferase transgene was quantified using Luciferase Assay System (Promega, Madison, WI, USA) and recombinant luciferase protein (Promega, Madison, WI, USA) was used as the standard. Briefly, cells were washed with PBS and 50 μ l 1 x Reporter Lysis Buffer was added. The plate was freeze/thawed to ensure complete lysis of the cells. 10 μ l of each sample was transferred to a white 96-well plate and 90 μ l 1 x Reporter Lysis Buffer was added to each well. Standard curves of recombinant luciferase ranging from 0-100 pg/ml and 0-1 pg/ml were produced and 100 μ l of each dilution was added in duplicate. Luciferase Assay Buffer was added to Luciferase Assay substrate and 100 μ l was then added to each well. Luminescence was measured using a Wallac VICTOR² plate reader (Wallac). Luciferase activity was then normalised to total protein content of the samples, measured by BCA assay (section 2.17) producing relative light units per milligram protein (RLU/mg protein).

2.23 Investigating intracellular Ad5 transport

2.23.1 Fluorescently labelling vectors

Ad5 was fluorescently labelled using an Alexa Fluor-488 Protein Labeling Kit (Invitrogen, Paisley, UK) according to the manufacturer's instructions. This kit can be used to label 100 μ g of protein per reaction and as 1 μ g = 4 x 10⁹ vp, using the established formula (Von Seggern *et al.*, 1998), 4 x 10¹¹ vp were used per labelling reaction. The vector was transferred to a SlideA-Lyzer Dialysis Cassette (molecular weight cut-off of 10000 Da) (Perbio Science) for dialysis after hydration of the cassette for 1 min in dialysis solution.

The vector was dialysed twice in 2 L of PBS, for 3 h each. The dialysis removes any glycerol which the vector was stored in, as this may interfere with labelling efficiency. The vector was removed from the cassette and added to the reaction tube (Component C) supplied by the kit. A 1 M sodium bicarbonate solution (pH ~8.3) was prepared by adding 1 ml dH₂O to the vial of sodium bicarbonate (Component B) supplied by the kit. A 1/10 volume of 1 M sodium bicarbonate was added to the reaction tube (Component C) and the sample was mixed. 10 µl dH₂O was added to one vial of Alexa Fluor® 488 TFP ester (Component A) and mixed to ensure the contents of the vial were completely dissolved. 10 µl of the reactive dye solution was added to the reaction tube and mixed thoroughly. A 3:1 ratio for dye:virus was used. The reaction mixture was incubated at room temperature in the dark for 15 min. The reaction mixture was transferred to a SlideA-Lyzer Dialysis Cassette for dialysis after hydration of the cassette for 1 min in dialysis solution. The labelled vector was dialysed in 2 L of 0.01 M Tris pH 8 and 0.001 M EDTA for 3 h in the dark. The buffer was then replaced with 2 L of 0.01 M Tris pH 8, 0.001 M EDTA and 10% (v/v) glycerol and the vector dialysed overnight in the dark. Labelled vectors were removed from the cassette, aliquoted and viral titre was reassessed as in section 2.21. Infectivity of labelled adenoviruses was verified by *in vitro* gene transfer assay as described in section 2.23.2. Labelled vectors were stored in the dark at -80°C.

2.23.2 Cell trafficking of fluorescently-labelled vectors

Cells were seeded in 8-well chamber slides at 4×10^4 cells/well and incubated at 37°C overnight. Cells were washed with PBS and for experiments involving the kinase inhibitors, were preincubated with 20 µM compound at 37°C for 30 min. Cells were then washed and incubated with 1×10^4 vp/cell of fluorescently-labelled Ad5 in 150 µl serum free media for 1 h on ice in the absence or presence of 1 µg/ml pd FX, WT or SP mutant rFX or in the presence of 10 µg/ml pd FX with or without pharmacological compound. Cells were either immediately washed in PBS and fixed in 4% paraformaldehyde (PFA) for 15 min at room temperature or incubated at 37°C for 15, 60 or 180 min prior to fixation. Prolong Gold Antifade Reagent with DAPI (Invitrogen) was added to counterstain the nuclei or cells were subjected to immunocytochemistry (section 2.24). Coverslips were added. The mounting agent was allowed to set overnight before viewing on the Zeiss confocal imaging system LSM 500 (Carl Zeiss Ltd., Germany).

2.24 Immunocytochemistry

Cells were treated as described in section 2.23.2. After fixation, cells were washed twice in PBS and permeabilised with 0.1% (v/v) Triton X for 10 min at room temperature. Cells were washed three times in PBS and incubated in 10% (v/v) goat serum (Vector Laboratories Inc., Burlingame, CA) for 30 min. Cells were washed in 0.1% (v/v) Triton X and incubated overnight at 4°C with the primary antibody or relevant IgG negative control (diluted in PBS and 10% (v/v) goat serum, for concentrations see Table 2.4). The primary antibody was removed and cells washed three times in PBS for 5 min each. Next cells were incubated with a secondary fluorescein isothiocyanate (FITC)- or tetramethyl rhodamine isothiocyanate (TRITC)-labelled antibody for 1 h in the dark. Cells were washed three times in PBS for 5 min each to remove the secondary antibody. Prolong Gold Antifade Reagent with DAPI (Invitrogen) was added to counterstain the nuclei. Coverslips were added. Images were taken using the Zeiss confocal imaging system LSM 500 (Carl Zeiss Ltd.).

Table 2.4. Antibodies used in experimental procedures.

Antibody	Species raised in	Cross reactivity	Clone	Final concentration
Mouse IgG (isotype matched)	Mouse	Human, rat, rabbit	N/A	Equivalent to primary antibody
Rabbit IgG (isotype matched)	Rabbit	Human, mouse, rat,	N/A	Equivalent to primary antibody
Goat-anti-rabbit	Goat	Rabbit	N/A	4 µg/ml
Goat-anti-mouse	Goat	Mouse	N/A	4 µg/ml
Pericentrin	Rabbit	Human, mouse, rat, rabbit	Polyclonal	5 µg/ml
Radixin	Rabbit	Human, mouse, rat	Monoclonal - # EP1862Y	0.34 µg/ml
Moesin	Rabbit	Human, mouse, rat	Monoclonal - # EP1863Y	1.15 µg/ml
Ezrin	Rabbit	Human, mouse, rat	Polyclonal	5 µg/ml
Pan-heparan sulphate	Mouse	Human	Monoclonal - # 10E4	5 µg/ml

2.25 Quantification of Ad5 colocalisation with the MTOC

Cells from virus trafficking assays were fixed and stained using the rabbit polyclonal pericentrin antibody as described in section 2.24. The pericentrin antibody stains the MTOC of cells. Colocalisation of fluorescently-labelled Ad5 with the MTOC was quantified by counting the number of cells with fluorescently-labelled virus and pericentrin co-staining using the Zeiss confocal imaging system LSM 500 (Carl Zeiss Ltd.). Data were averaged from five 40 x microscope fields per experimental condition.

2.26 Analysis of Ad5 attachment *ex vivo*

Liver sections from MF-1 mice were embedded in Tissue-Tek Optimum Cutting Temperature (OCT) compound (Sakura Finetek, The Netherlands) in intermediate Tissue-Tek cryomolds (Sakura Finetek) on dry ice. Cryostat sections 4 μm thick were cut and mounted on Tissue Tek AutoWrite StarFrost Adhesion Microscope Slides with Cut Edges (Sakura Finetek). Slides were stored at $-80\text{ }^{\circ}\text{C}$ until required. Liver sections were air dried at room temperature for 20 min and fixed in 4% PFA. The sections were incubated with 2×10^9 vp of Alexa Fluor-488 fluorescently-labelled Ad5 in serum free media in the presence of 7 $\mu\text{g}/\text{ml}$ WT or SP mutant rFX for 1 h on ice followed by 1 h at 37°C . Sections were washed twice in PBS, fixed and the nuclei stained using Prolong Gold Antifade Reagent with DAPI. Sections were imaged using an Olympus Cell M imaging system. To quantify adherent Alexa Fluor-488 fluorescently-labelled Ad5 particles, 40x images were captured using an Olympus Cell M imaging system and processed using Image J counting software. At least six captured images were analysed per experimental condition.

2.27 MTT assay

Cells were plated at a seeding density of 2×10^4 in 96-well plates and incubated at 37°C overnight. Cells were transduced with virus in the presence of pharmacological compounds as described in section 2.22.6. 48 h post-infection, media on the cells was replaced with 100 μl complete media and 15 μl of dye solution containing terazolium. MTT (3-(4,5-dimethylthiazol-2-yl)-2,5-diphenyltetrazolium bromide) is a pale yellow substrate that produces a dark blue formazan product when incubated with live cells and is commonly used to measure cell death (Tim, 1983). Cells were incubated for 4 h at 37°C . Next, 100 μl of Solubilization Solution/Stop Mix was added to each well to solubilise the formazan product. Cells were incubated for a further 1 h at 37°C . The colour produced was measured

using a Wallac VICTOR² plate reader (Wallac) at a wavelength of 570 nm and was directly proportional to the amount of live cells in the sample.

2.28 RNA extractions

A549, SKOV3 or SW620 were plated at 4×10^5 cells/well in 6-well plates and incubated at 37°C overnight. Total RNA was extracted from cells using the RNeasy Mini Kit (Qiagen). Briefly, cells were lysed, collected in a 1.5 ml Eppendorf and centrifuged at 16,000 g for 5 min to pellet the cells. 600 µl RLT buffer was added to the cell pellet and the mixture was vortexed. RLT buffer contains denaturing guanidine isothiocyanate. This immediately inactivates RNases and ensures extraction of intact RNA. In order to facilitate binding to the spin column, 600 µl 70% ethanol was added and the sample was then loaded on to the spin column. This was subjected to centrifugation at 8,000 g for 15 sec to allow the RNA to bind to the silica-gel membrane of the spin column. To wash the spin column 700 µl buffer RWT was added and the spin column was centrifuged at 8,000 g for 15 sec. This was followed by two further wash steps with 500 µl RPE buffer, the first wash centrifuged at 8,000 g for 15 sec and the second wash centrifuged at 8,000 g for 2 min. This eliminates contaminants. To elute the purified RNA, 30 µl RNase-free water was added and the spin column centrifuged at 8,000 g for 1 min.

2.29 DNase treatment of RNA

DNase treatment of RNA samples was performed using the TURBO DNA-free kit (Applied Biosystems) according to the manufacturer's instructions. This removes contaminating DNA from RNA extractions. Briefly, to 40 µl of the RNA sample, 0.5 µl 10x TURBO buffer and 1 µl TURBO DNase were added and the mixture was incubated at 37°C for 30 min. DNase inactivation reagent (0.1% v/v) was added and the mixture was incubated at room temperature for 2 min. This was followed by centrifugation at 10,000 g for 1.5 min. The supernatant was kept as a DNA-free RNA sample. RNA was quantified by measuring absorbance at 260 nm (NanoDrop, ND-1000 spectrophotometer). The samples were stored at -80°C.

2.30 cDNA synthesis

The Reverse Transcription Kit (Applied Biosystems, Warrington, UK) was used to convert mRNA into complementary DNA (cDNA) as per the manufacturer's instructions. To 1 µg RNA, 2 µl RT buffer, 5.5 mM MgCl₂, 4 µl deoxyribonucleotide triphosphates (dNTPs)

mix, 1 μ l random hexamers, 1 μ l RNase inhibitor and 0.5 μ l Multiscribe Reverse Transcriptase were added in a final volume of 20 μ l. The samples were incubated at 25°C for 10 min for preannealing, at 48°C for 30 min to allow reverse transcription to occur and at 95°C for 5 min for reverse transcription inactivation. The samples were stored at -20°C.

2.30.1 QPCR for quantification of cellular genes

QPCR (as described in section 2.22.3) was used to detect expression of Syk, ezrin, moesin and radixin in SKOV3, A549 and SW620 cells. The Power SYBR Green detection system (Applied Biosystems, Warrington, UK) was used with the QuantiTect Primer Assay kit containing forward and reverse primers (QIAGEN, UK) for human Syk (Hs_SYK_2_SG, catalogue QT01886521), ezrin (Hs_EZR_1_SG, catalogue number QT00078127), moesin (Hs_MSN_1_SG, catalogue number QT00015169) or radixin (Hs_RDX_1_SG, catalogue number QT00047397) to amplify the cDNA. To 2.5 μ l of the cDNA, 6.25 μ l SYBR Green master mix, 1.25 μ l primer mix and 2.5 μ l dH₂O were added. The following thermal cycling conditions were used; 95°C for 10 min for denaturation, 95°C for 15 sec for amplification, 60°C for 1 min for annealing (repeated for 50 cycles), followed by 95°C for 15 sec, 60°C for 15 sec and 95°C for 15 sec for dissociation.

2.31 High throughput screening

2.31.1 Compound library

The Pharmacological Diversity Drug-like Set (Enamine, Kiev, Ukraine) library consisted of 10,240 compounds preplated in columns 3 to 22 of 32 Matrix 384-well, clear, V-bottom, polypropylene plates (catalogue number 4312, Thermo Scientific, Surrey, UK) as single compounds at a concentration of 10 mM in 100% DMSO. Each plate had an individual barcode and sample ID for tracking purposes. Plates were sealed and compounds stored under nitrogen (BOC, Glasgow, UK) using the Platesealer SILVERseal, aluminium (Greiner Bio One, Gloucestershire, UK). Compounds were stored at -80°C. Information about the library including compound I.D., molecular weight and structure can be found on the [Enamine website](http://www.enamine.net), following the link www.enamine.net/index.php?option=com_content&task=view&id=83. All compounds were assured by the vendor (Enamine, Kiev, Ukraine) to be at least 90% pure as assessed by liquid chromatography-mass spectrometry and proton nuclear magnetic resonance spectrometry.

2.31.2 Production of compound library dilution plates

Three individual replicate plates of each compound library plate were generated, each with a barcode and sample ID related to the parent plate. Using the Biomek FX^P 96 multichannel pipetting head (Beckman Coulter) 3 µl from each well of the compound library plate was directly dispensed into a 384 deep well, small volume, polypropylene plate (catalogue number 784201, Greiner Bio One, Gloucestershire, UK) previously loaded with 27 µl of DMSO using the Multidrop Combi (Thermo Scientific). This was performed in triplicate. These plates, in which compounds were at a concentration of 1 mM, were named mother plates. All robotics protocol designing and scheduling was performed using Biomek Software (Beckman Coulter) and SAMI Workstation EX Software (Beckman Coulter) (Figure 2.4). Plates were sealed, compounds stored under nitrogen using the Platesealer SILVERseal, aluminium (Greiner Bio One) and stored at -80°C.

2.31.3 Seeding cells

Following optimisation, SKOV3 cells were seeded at a density of 1500 cells per well in 50 µl complete media in 384 µ-clear flat bottom, black, cell culture microplates (catalogue number 781091, Greiner Bio One, Gloucestershire, UK) using the Multidrop Combi (Thermo Scientific). These plates were termed assay plates. Each plate had an individual barcode and sample ID for tracking purposes. Cells were tested prior to use to ensure they were mycoplasma free. Cells were incubated in 37°C, 5% CO₂ and 95% air incubators overnight. All tissue culture procedures for robotic screening experiments was performed under sterile conditions using biological safety class II vertical laminar flow robotics enclosure cabinets (Bigneat Containment Technology, Bigneat Ltd, Waterlooville, UK).

2.31.4 Screening the compound library

Plates were loaded on to the Cytomat Hotel (Thermo Scientific), a microplate stacking and handling system integrated with the liquid handling robotics. As plates were imported from the hotel, the barcodes were scanned and sample IDs read, this was to ensure all liquid aspirations from one plate were dispensed in the corresponding daughter or assay plate. Using the Biomek FX^P 96 multichannel pipetting head 2 µl of each well in columns 3 to 22 of the mother plate was directly dispensed into a 384 deep well, small volume, polypropylene plates (Greiner Bio One) in which all wells were previously loaded with 8 µl of serum free media using the Multidrop Combi (Thermo Scientific). Using the Span-8 (Beckman Coulter) 2 µl of DMSO was added into every second well of column 2 (starting

with 2A) and 23 (starting with 23B) as vehicle controls. The Span-8 configuration allows for independent well access. 1000 vp/cell of Ad5GFP was added to columns 2 to 23 in a final volume of 20 μl using the Multidrop Combi. Compounds were at a concentration of 100 μM . This plate was referred to as the daughter plate. Cells in the assay plate were washed once in 50 μl of serum free media using the Biomek FX^P 96 multichannel pipetting head. 22.5 μl of serum free media was added to each well in columns 1, 2, 23 and 24 and 22.5 μl of serum free media containing FX was added to each well in columns 3 to 22 using the Multidrop Combi.

Controls: Each compound was tested in triplicate, with each replicate on a separate plate. This allowed for interplate and intraplate controls. Columns 1 and 24 contained the untreated control samples. To each well in columns 1 and 24, 2.5 μl of serum free media was added using the Span-8 (Beckman Coulter). Columns 2 and 23 contained the positive and negative control samples. Into every second well of column 2 (starting with 2A) and 23 (starting with 23B) 2.5 μl of serum free media containing FX was added (+FX negative controls (final concentration of 10 $\mu\text{g}/\text{ml}$ FX and 1% (v/v) DMSO vehicle) and into every other well of those columns, 2.5 μl of serum free media was dispensed (-FX positive controls) using the Span-8.

From each well in columns 2 to 23 of the working plate, 2.5 μl of virus and compound mixture was added to the cells in the corresponding wells in columns 2 to 23 of the assay plate. All wells in columns 3 to 22 had a concentration of 10 μM compound, 10 $\mu\text{g}/\text{ml}$ FX and 1% (v/v) DMSO. Daughter and assay plates were returned to the Cytomat Hotel. Daughter plates were disposed of and assay plates were incubated in 37°C, 5% CO₂ and 95% air for 3 h. After this incubation, 25 μl of complete media containing 20% (v/v) FCS, 1% (v/v) penicillin, 100 $\mu\text{g}/\text{ml}$ streptomycin and 2 mM L-glutamine was added to all wells using the Multidrop Combi. Assay plates were further incubated in 37°C, 5% CO₂ and 95% air for 45 h.

2.31.5 Fixing cells from the HTS screen

Assay plates were loaded on to the Cytomat Hotel. Cells were washed once in 50 μl PBS and 50 μl 4% PFA was added to each well using the Plate Washer (Beckman Coulter). Cells were incubated at room temperature for 15 min and washed in 50 μl PBS using the Plate Washer. The Biomek FX^P 96 multichannel pipetting head was employed to dispense 10 $\mu\text{g}/\text{ml}$ Hoechst 33342 (Sigma Aldrich) and 10 $\mu\text{g}/\text{ml}$ propidium iodide (Sigma Aldrich)

on to cells in a final volume of 25 μ l. Cells were incubated at room temperature for 20 min and washed in 50 μ l PBS twice using the Plate Washer (Beckman Coulter). Assay plates were either analysed immediately or stored at 4°C in the dark.

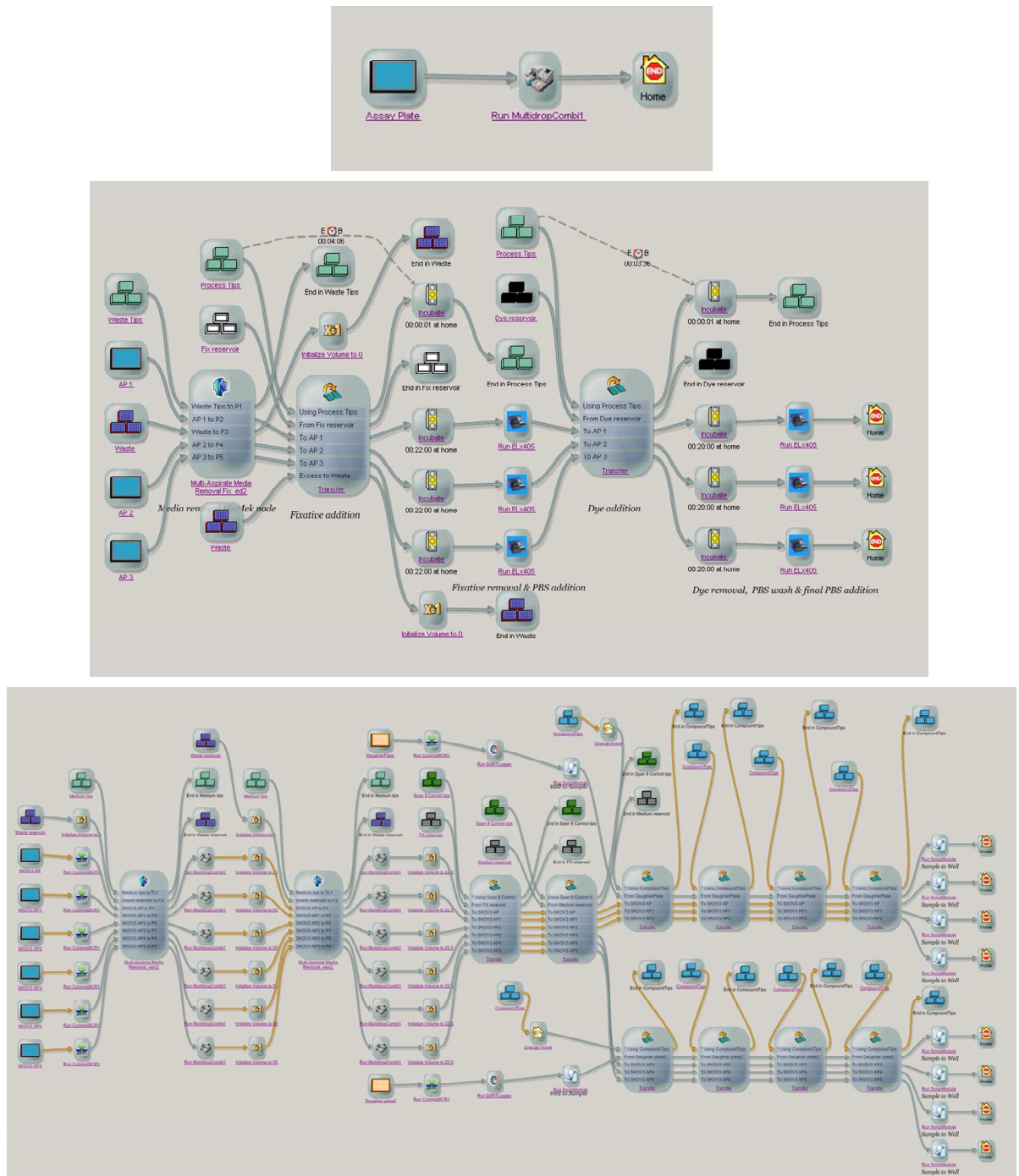


Figure 2.4. SAMI Workstation EX Software screening protocols.

Screen shot from the SAMI Workstation EX Software, in which liquid handling assay protocols were designed, from simple media additions (top panel), to more complex protocols with multiple steps such as those designed for cell fixation (middle panel) and compound additions (bottom panel).

2.31.6 Using the IN Cell Analyser 2000 to capture screen images

Assay plates were imaged using the IN Cell Analyser 2000 (GE Healthcare). A single image of the central field of view in each well was captured using the Nikon 10x objective (Figure 2.5). Preview scans of 5 random wells were performed prior to starting the acquisition run (Figure 2.6). Imaging conditions were as follows, filter sets were matched to each fluorophore; $350_{\text{excitation (ex)}}$ and $455_{\text{emission (em)}}$ for Hoechst 33342 nuclear staining and an exposure time of 40 millisecc (ms), 490_{ex} and 525_{em} for GFP expression and an exposure time of 60 ms; 579_{ex} and 624_{em} for propidium iodide non-viable nuclear staining and an exposure time of 45 ms. The short exposure times contributed to the speed of acquisition. Hardware and laser autofocus options were chosen to optimise the quality of the images.

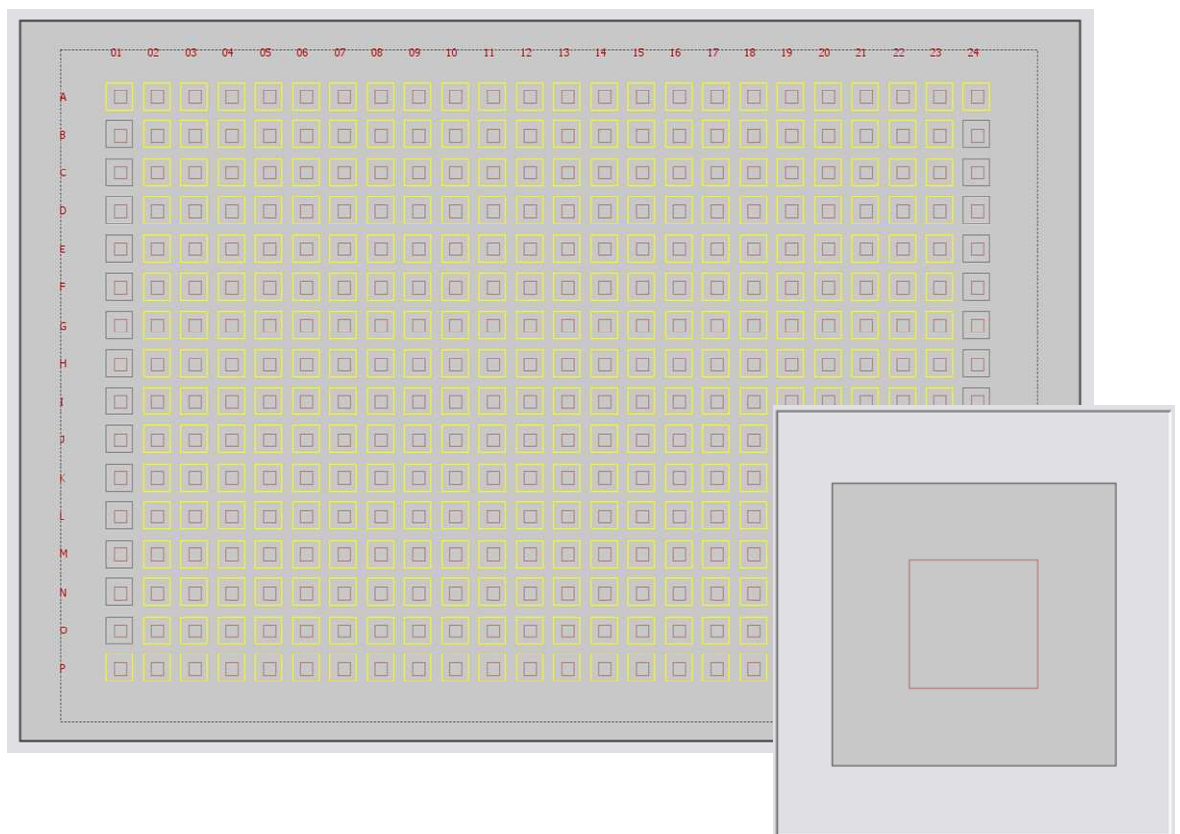


Figure 2.5. Determining the field of view using the IN Cell Analyser 2000.

A single image of the central field of view in each well of a 384-well plate was captured using a 10x objective.

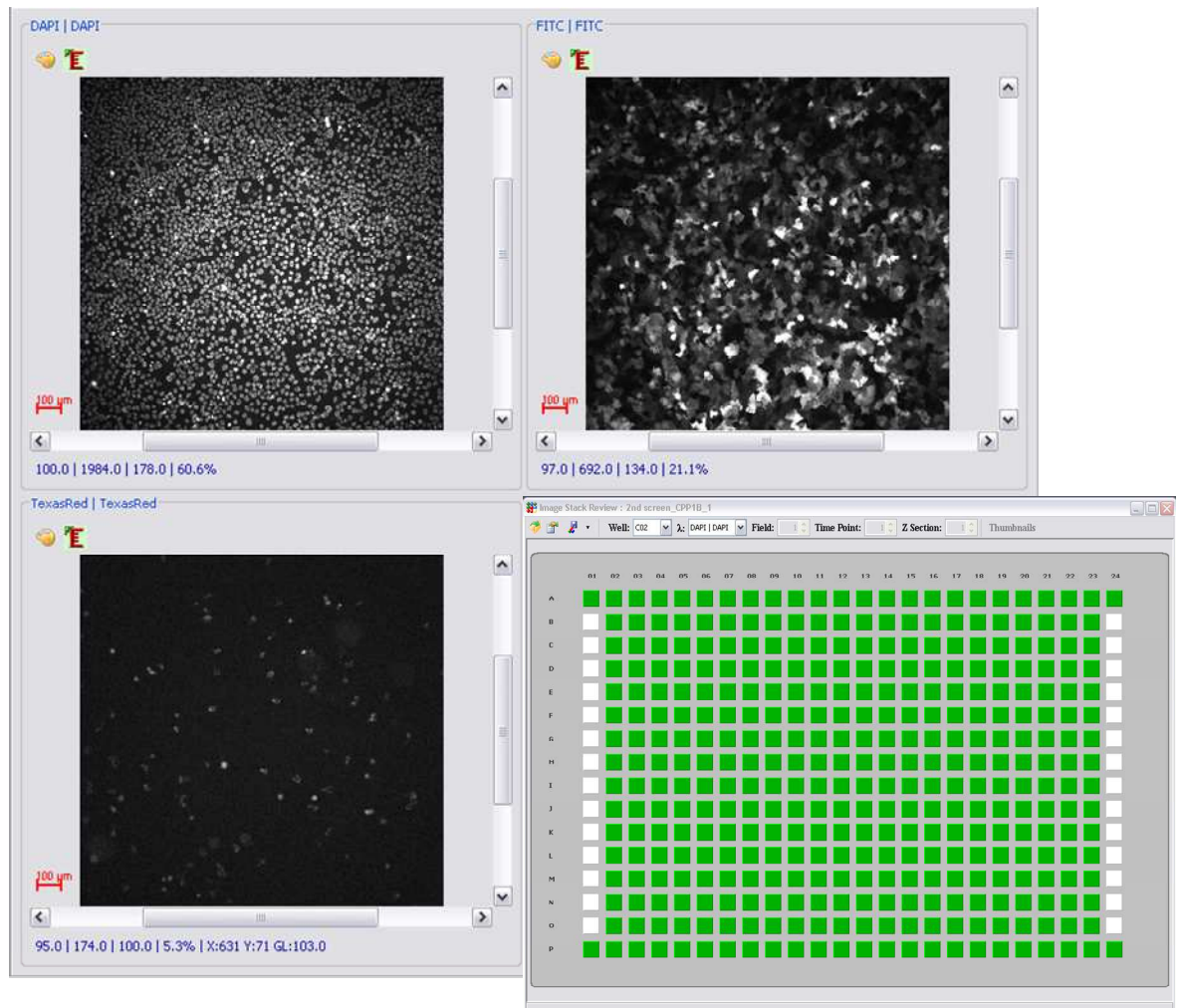


Figure 2.6. IN Cell Analyser 2000 preview scan.

Screen shot from the IN Cell Analyser 2000 software program. A random well from the 384-well plate was chosen and a preview scan was performed to ensure imaging conditions were correct prior to starting the acquisition run.

2.31.7 Analysing the screen images and acquiring screen data

To quantify the amount of GFP expression per viable cell per field of view the images were analysed using IN Cell Developer Toolbox V1.6 software (GE Healthcare). The screen images were of high quality and provided sufficient resolution for effective segmentation of cellular components and GFP expression. Nuclei were segmented based on Hoeschst 33342 staining and shape, GFP expression was outlined based on its intensity and cell shape was estimated based on previous measurements outlined from brightfield images. Non-viable cell segmentation was related to propidium iodide staining. Nuclei, GFP expression and cells were termed targets and the targets were linked. An algorithm was designed to measure the total number of cells per field of view, to quantify all viable

cells per field of view, to quantify all GFP expression per field of view and then to measure the amount of GFP expression per viable cell per field of view;

$$\frac{[\text{DxA} < \text{Sum} : / \text{Cell Nuc GFP} / \text{GFP}]}{[\text{Count} < \text{Sum} : / \text{Cell_Nuc} / \text{Cell}]}$$

or

$$\frac{[\text{Intensity of total GFP per field of view}]}{[\text{Total number of viable cells per field of view}]}$$

This resulted in a numerical output enabling the calculation of results. All untreated control values were zero. All data were normalised to intraplate positive (Ad5-FX (low level Ad5 transduction)) and negative (Ad5+FX and vehicle (high levels of Ad5 transduction mediated by FX)) controls and expressed as percentage inhibition of FX-mediated Ad5GFP expression.

$$\% \text{ Inhibition} = (\text{Negative control} - \text{compound}) / (\text{Negative control} - \text{Positive control})$$

Data were pooled for each compound from the three replicate plates. Any compounds causing greater than 75% inhibition of FX-mediated Ad5GFP expression were selected for second round screening analysis. Preliminary candidate compounds from the library were selected manually and directly dispensed into columns 3 to 22 of a 384 deep well, small volume, polypropylene plates. Compounds were retested as described in section 2.31.4 to 2.31.7.

2.32 Animals

All animals were housed under controlled environmental conditions. Temperature was maintained at ambient temperature with 12 h light/dark cycles. Mice were fed standard chow and water was provided *ad libitum*. All animal experiments were approved by the University of Glasgow Animal Procedures and Ethics Committee and performed under UK Home Office licence (PPL 60/3752) in strict accordance with UK Home Office guidelines.

2.32.1 *In vivo* administration of Ad5

In vivo Ad5 administration was performed in 8 week old, male, MF1 mice. Mice were injected via lateral tail vein injection with PBS or 1×10^{11} vp/mouse of Ad5 expressing a luciferase transgene in the absence or presence of 0.1% DMSO, 10 μ M compound

T5550585, T5424837, T5660138, T5677956, T5660136 or T5572402 from the Pharmacological Diversity Drug-like Set.

2.32.2 Quantification of adenoviral transgene expression

Mice were injected subcutaneously with 300 µl of XenoLight D-Luciferin (Caliper, Life Sciences, Hopkinton, MA, USA) 48 h post-administration of Ad5. Luciferin becomes oxidised under the catalytic effects of luciferase and ATP, and a bluish-green light is produced. This was measured using the IVIS Imaging System (IVIS Spectrum, Caliper). Mice were subject to whole body bioluminescence quantification (IVIS Spectrum, Caliper Life Sciences). 48 h post-Ad5 injection mice were sacrificed for tissue analysis. Tissue homogenates were produced from 25 mg liver tissue using TissueLyser II (QIAGEN, Crawley, UK). DNA was isolated from tissue homogenates using QIAamp DNA mini kit (QIAGEN, Crawley, UK). 50 ng of total DNA was subject to qPCR analysis as described in section 2.22.3.

2.33 Statistical analysis

Results presented are representative data from a minimum of three separate experiments with at least three experimental replicates per group, unless otherwise stated. High throughput screening of the complete Pharmacological Diversity Drug-like Set compound library was performed once. Statistical analysis was performed in Prism version 4.0 (Graph Pad Software, San Diego, CA, USA). Data are shown as mean \pm standard error of the mean. Comparisons were made using one way ANOVA or paired Student's t-test. $p < 0.05$ after Dunnett's or Bonferroni's post-analysis were considered statistically significant.

Chapter 3

Identification of a cluster of basic amino acids involved in Ad5:FX complex binding to the cell surface

3.1 Introduction

Hepatic transduction of Ad5 following intravascular administration is due to a high affinity interaction between the Ad5 hexon and coagulation FX (Kalyuzhnyi *et al.*, 2008; Vigant *et al.*, 2008; Waddington *et al.*, 2008). FX is synthesised in the liver and circulates in the blood at a concentration of 8-10 $\mu\text{g/ml}$, as a two chain glycoprotein, with a molecular weight of 59,000 Da. The light chain consists of the Gla rich domain with 11 Gla residues, which are important for calcium-dependent binding, and two EGF-like domains, with an additional calcium binding site in EGF-1 (Nelsestuen *et al.*, 1976). The light chain is linked to the heavy chain by a disulphide bond. The heavy chain contains the SP domain which features the active site of the catalytic triad; histidine 57, aspartic acid 102 and serine 195. Whilst the Gla domain of FX binds with high affinity within the cup formed by each hexon trimer (Waddington *et al.*, 2008), the SP domain has been reported to be responsible for mediating the Ad5:FX complex interaction with HSPGs (Bradshaw *et al.*, 2010; Parker *et al.*, 2006; Waddington *et al.*, 2008). However the exact mechanism by which the FX SP domain binds to HSPGs has not been fully elucidated.

The physiological function of FX is as a plasma zymogen, central to the blood coagulation cascade, a complex, multi-step process leading to the initiation of blood clotting, localisation at the injured vasculature, fibrin clot formation and generation of the platelet plug (Figure 3.1). During the clotting process FX is converted to its active enzyme, FXa, via cleavage of an arginine-isoleucine (Arg51-Ile52) peptide bond in the heavy chain, releasing a 52 amino acid activation peptide fragment (Fujikawa *et al.*, 1974; Furie *et al.*, 1988). This process occurs at the point of convergence of the intrinsic and extrinsic pathways, either via FIXa and FVIIIa or tissue factor and FVIIa complexes, which assemble on phospholipid membranes, in the presence of calcium (Bom *et al.*, 1990). FXa then participates with FVa to activate prothrombin to thrombin, which in turn converts fibrinogen to fibrin (Figure 3.1) (Davie *et al.*, 1964; Macfarlane, 1964; Osterud *et al.*, 1977).

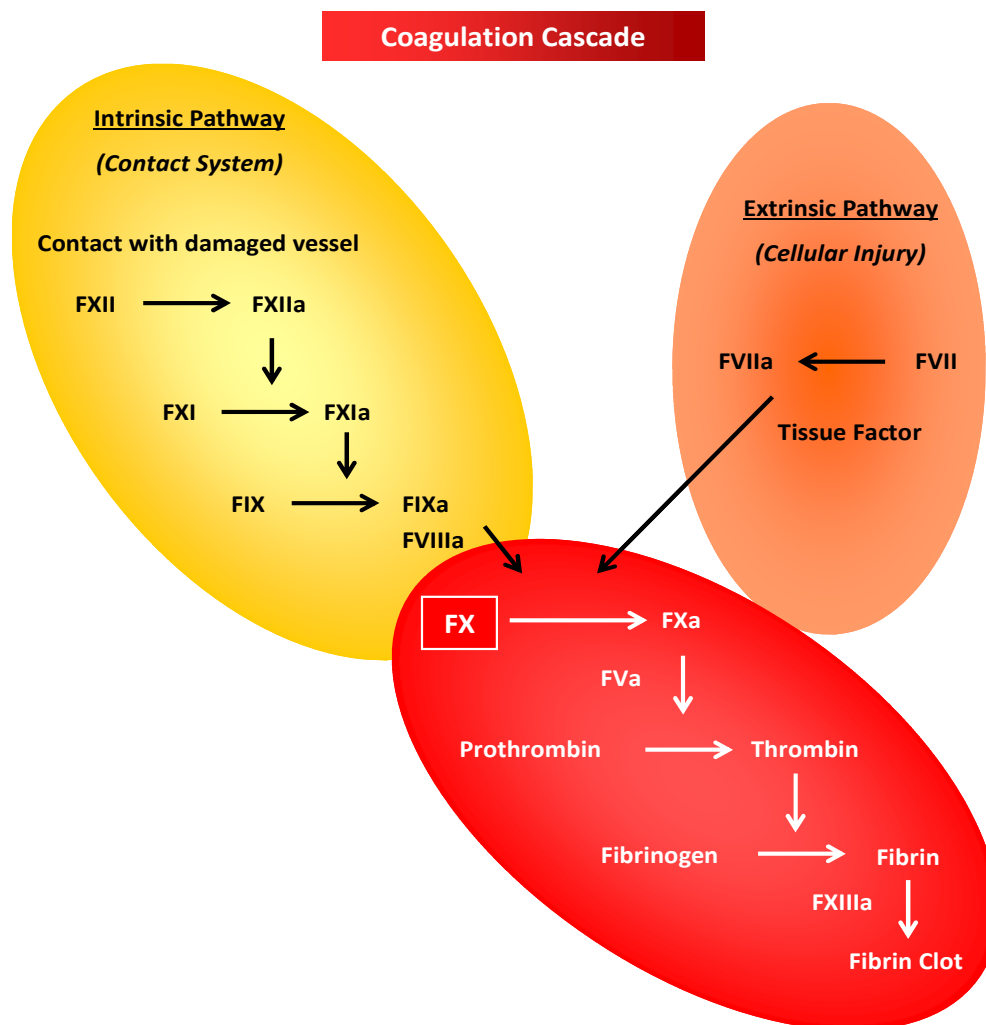


Figure 3.1. Coagulation cascade.

Summary of the blood coagulation cascade, showing the intrinsic pathway (yellow), the extrinsic pathway (orange) and the common pathway (red).

Despite the great homology between the serine proteases in the blood coagulation cascade, they exhibit narrow and distinctive specificity to their own protein substrates. Substrate recognition by several surface exposed residues in the catalytic domain, in addition to those surrounding the active site exist. Studies have shown that the basic residues Arg-93, Lys-96, Arg-125, Arg-165, Lys-169, Lys-236 and Arg-240 constitute an exosite in the SP domain of FXa which can bind to heparin, a highly sulphated glycosaminoglycan which serves as an anticoagulant (Figure 3.2) (Hirsh *et al.*, 2001; Rezaie, 2000). Mutagenesis studies, in which each of these amino acids were substituted with a neutral alanine in separate Gla domainless FXa (GDFXa) constructs, investigated the contribution of individual residues for binding heparin (Rezaie, 2000). Elution with NaCl of each of the seven mutants from a heparin-sepharose column was assessed. As FXa binds to heparin via ionic forces, elution was accomplished by a stepwise gradient of increasing ionic strength

i.e. the higher the concentration of NaCl required to elute the protein, the stronger the binding and the lesser the effect of the mutation. The relative decrease in concentration of NaCl for elution was reported for GDFXa and R125A (0.4 M NaCl), R93A and K96A (0.38 M), R165A and K169A (0.35 M), K236A (0.28 M) and R240A (0.24 M) (Rezaie, 2000). In addition, the effects of antithrombin on FXa inactivation were analysed. Antithrombin acts as an inhibitor of FXa and thrombin, an effect which is accelerated in the presence of heparin-like glycosaminoglycans (Figure 3.2) (Evans *et al.*, 1992; Olson *et al.*, 1992). When the mutants were incubated with antithrombin, GDFXa and FXa derivatives were inactivated with similar order association rate constants (k_2). However in the presence of antithrombin and heparin, mutant FXa inactivation was impaired to varying degrees compared to GDFXa. This effect was minimal for R93A and R125A, whilst a significant decrease in k_2 values was observed with all other mutants, ranging from a 4-fold decrease for K96A to a 25-fold decrease for R240A (Rezaie, 2000). These data suggests the order of importance of these FXa residues for binding heparin is Arg-240 > Lys-236 > Lys-169 > Arg-165 > Lys-96 > Arg-93 > Arg-125.

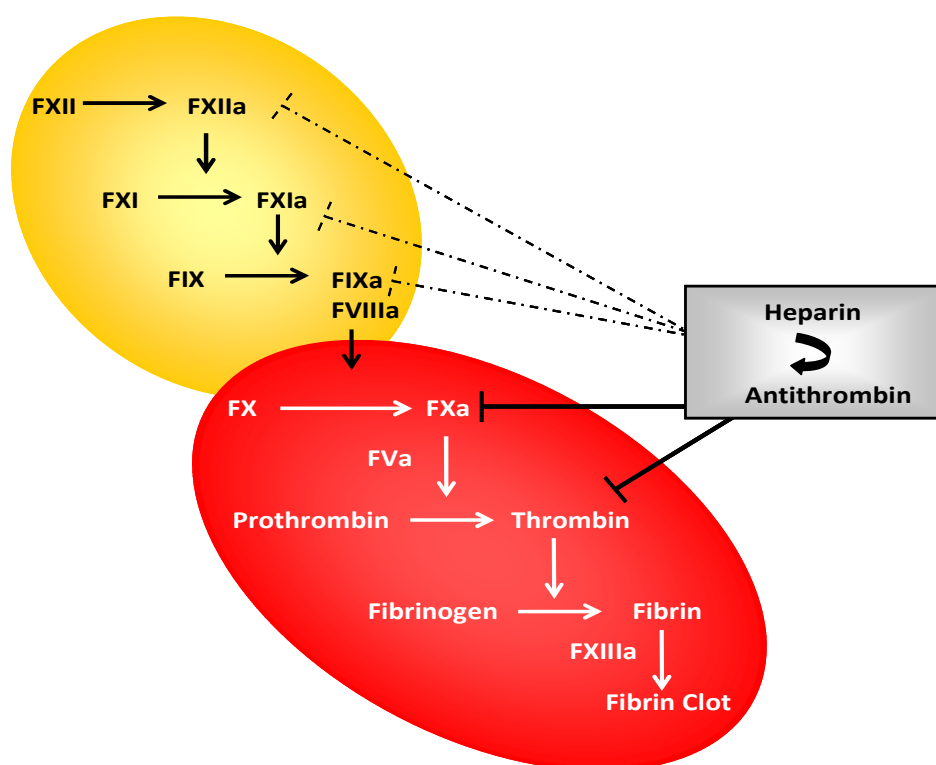


Figure 3.2. Mechanism of action of heparin.

Heparin produces its major anticoagulant effect by inactivating thrombin and FXa through an antithrombin-dependent mechanism. The heparin:antithrombin complex can inactivate FXIIa, FXIa, FIXa, FXa and thrombin, with the later two being most sensitive.

In contrast to FXa, FX exhibits a very weak affinity for heparin (Nogami *et al.*, 2004). A study by Nogami *et al.*, investigated the mechanism of interaction of FX and FXa with FVIIIa. FVIIIa bound to FXa via its heparin binding exosite (HBE), an interaction which was abolished in the presence of heparin (Nogami *et al.*, 2004). However the effect of heparin on FX binding to FVIIIa was marginal. The affinities of FXa and FX for heparin were assessed using a heparin-sepharose column. In this study FXa was eluted at a NaCl concentration of 0.22 M, whilst FX failed to bind the column at 0.1 M and was instead detected in the column flow through fractions. This study suggests heparin binding to FXa is via the HBE, whilst this exosite is not as readily accessible in the zymogen (Nogami *et al.*, 2004).

In an attempt to investigate the role of the SP domain of FX in Ad5:FX binding to the cell surface, Waddington *et al.* employed the anticoagulants Ixolaris and nematode anticoagulant peptide 2 (NAPc2) to pharmacologically block the FX SP domain (Waddington *et al.*, 2008). Ixolaris is isolated from the salivary gland of the tick *Ixodes scapularis* (Francischetti *et al.*, 2002). It consists of 140 amino acids containing 10 cysteines and 2 Kunitz-like domains and binds to FX or FXa, inhibiting tissue factor/FVIIa activation (Francischetti *et al.*, 2002). NAPc2 is an 85 amino acid anticoagulant protein, isolated from the hematophagous hookworm *Ancylostoma caninum* (Cappello *et al.*, 1995; Stassens *et al.*, 1996). It is a potent inhibitor of FX activation mediated by tissue factor and FVIIa. SPR analysis revealed a high affinity interaction between human FX and NAPc2 (dissociation rate constant (K_D) = 7.28×10^{-11} M) or Ixolaris (K_D = 1.30×10^{-9} M) (Waddington *et al.*, 2008). This binding had no effect on Ad5 binding to FX (Waddington *et al.*, 2008). Either anticoagulant alone was capable of decreasing the FX-mediated AdKO1 cell binding and transduction in HepG2 cells. Moreover, preinjection of FX in the presence of a three molar excess of either NAPc2 or Ixolaris, 30 min prior to administration of AdKO1 in warfarin-treated mice, significantly decreased hepatic gene transfer (Waddington *et al.*, 2008).

Ixolaris acts by binding to the HBE of FXa and mutagenesis studies indicate the order of importance of residues involved in this interaction is Arg-93 > Arg-165 > Lys-169 > Lys-236 > Lys-96 > Arg-240 > Arg-125 (Monteiro *et al.*, 2005). When the role of the amino acids in FX were analysed, the order of importance for Ixolaris complex formation was Arg-93 > Arg-165 > Lys-169 > Lys-236 > Arg-125 (Monteiro *et al.*, 2008). Ixolaris binding to FX strongly decreases FX activation by the intrinsic FIXa/FVIIIa complex (Monteiro *et al.*, 2008). This study suggests Ixolaris binds to residues within a heparin

binding proexosite (HBPE) in FX, a region which is not readily exposed to heparin or is in a distinct conformation in the zymogen form (Monteiro *et al.*, 2008; Nogami *et al.*, 2004).

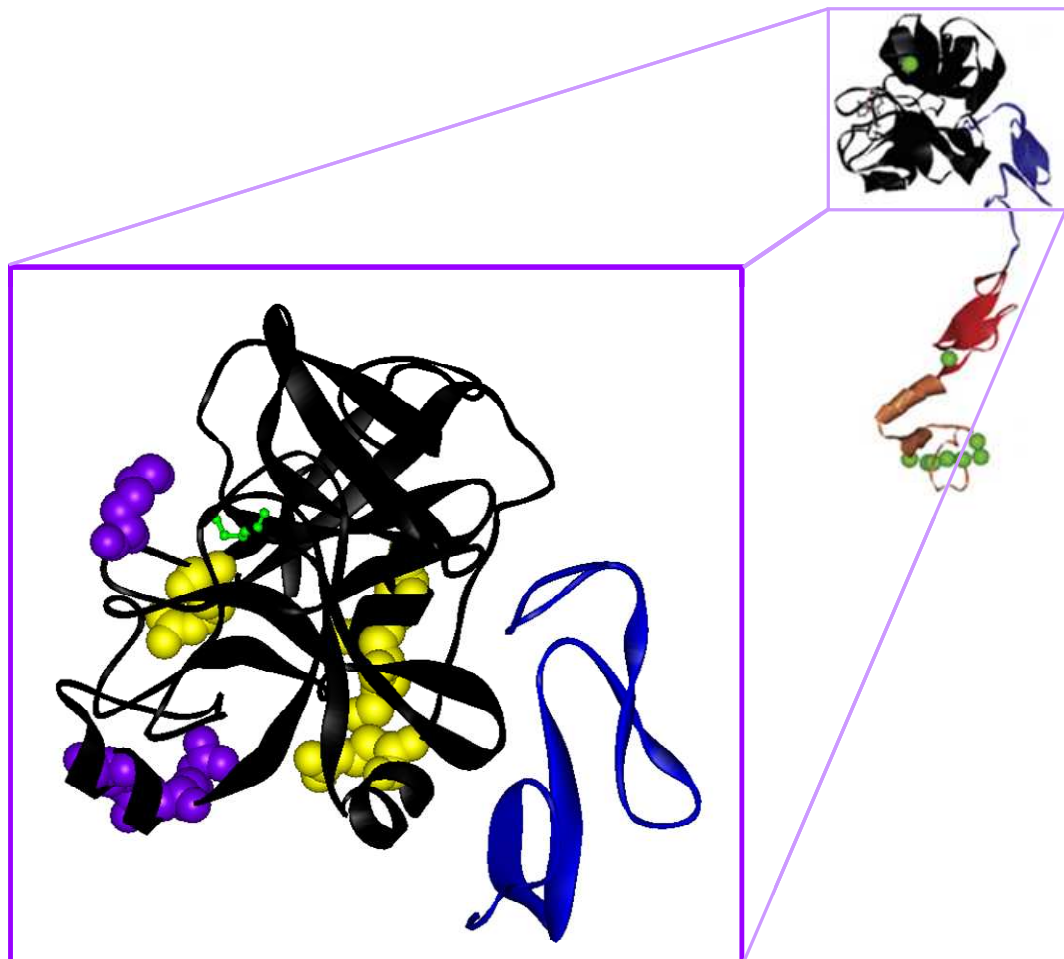
NAPc2 can bind with high affinity ($K_D \sim 1$ nM) to both FX and FXa (Buddai *et al.*, 2002). This reaction occurs independently of calcium and does not require zymogen activation or a fully functional active site (Buddai *et al.*, 2002). A weaker interaction between NAPc2 and bovine FX or FXa has been reported (Buddai *et al.*, 2002). This may be due to sequence differences in the protease domains following residue 240, as in the presence of recombinant bovine FX, containing 25 residues from the COOH terminus of human FX, the high affinity interaction with NAPc2 was restored (Buddai *et al.*, 2002; Murakami *et al.*, 2007). The crystal structure of Gla domainless FXa and NAPc2, determined to 2.2 Å, indicates binding to amino acid residues at positions 60-62, 88-93, 125, 178, 235-237, 240 and 243 of FXa (Murakami *et al.*, 2007). Table 3.1 and Figure 3.3 summarises the residues in FX or FXa to which Ixolaris and/or NAPc2 bind.

Table 3.1. Amino acid residues of FX and FXa to which NAPc2 or Ixolaris bind.

A list of the residues in the SP domain of FX or FXa to which Ixolaris or NAPc2 bind.

FX/FXa amino acid	Anticoagulant
93R	Ixolaris/NAPc2
96K	Ixolaris
125R	Ixolaris/NAPc2
165R	Ixolaris
169K	Ixolaris
236K	Ixolaris/NAPc2
240R	Ixolaris/NAPc2

Although the study by Waddington *et al.* implicated a role for the FX SP domain in Ad5 transduction (Waddington *et al.*, 2008), the precise mechanism and amino acid residues responsible for FX-mediated Ad5 attachment to HSPGs have not been reported. Understanding the exact infectivity pathways of Ad5 is important to its optimisation and successful development as a gene therapy vector. Here, we investigate the role of the seven basic amino acid residues in the FX HBPE in Ad5:FX complex binding to HSPGs.



- = residues interacting with Ixolaris only
- = residues interacting with NAPc2 and Ixolaris

Figure 3.3. Residues to which NAPc2 and Ixolaris bind.

Ribbon diagram of the human FX SP-EGF-2 domains (1HCG; Accelrys ViewerLite software (Padmanabhan *et al.*, 1993)) highlighting amino acids residues to which Ixolaris alone (purple) or both Ixolaris and NAPc2 (yellow) bind.

3.2 Results

3.2.1 Generation of FX plasmid constructs

To assess the role of the SP domain of FX in Ad5:FX complex binding to HSPGs a FX plasmid construct was designed, in which the seven basic residues previously shown to constitute the HBPE were chosen for mutation (Monteiro *et al.*, 2008; Nogami *et al.*, 2004; Rezaie, 2000). The residues were Arg-93, Lys-96, Arg-125, Arg-165, Lys-169, Lys-236 and Arg-240. First, human wild-type FX (WT FX) cDNA including the human prothrombin signal sequence and propeptide was cloned into the mammalian expression pCMV4 vector (human prothrombin signal sequence and propeptide followed by the sequence for the FX derivative - pCMV4-ss-pro-II-FX (Camire *et al.*, 2000)). Efficient γ -carboxylation is a critical post-translational modification of FX. FX is synthesised in its precursor form, which is translocated to the endoplasmic reticulum where glutamic acid residues in the Gla domain undergo γ -carboxylation. This depends on membrane bound γ -carboxylase and vitamin K, as well as the propeptide acting as a substrate for the enzyme (Suttie *et al.*, 1987). Previous studies have shown that exchanging the FX propeptide with one that binds γ -carboxylase with a reduced affinity, such as prothrombin, results in an increase in γ -carboxylase activity by allowing greater substrate turnover thus improving protein production by increasing the yields of the functional γ -carboxylated protein (Camire *et al.*, 2000; Stanley *et al.*, 1999). This WT FX plasmid was a kind gift from Prof. John McVey (Thrombosis Research Institute, London, UK). Seven codons encoding the basic amino acid residues R93, K96, R125, R165, K169, K236 and R240 in the WT FX cDNA sequence were substituted with alanine, as performed by GeneArt (Paisley, UK). This was called “SP mutant”. In addition, site-directed polymerase chain reaction mutagenesis to convert the basic residues arginine or lysine to alanine was used to create four FX mutant constructs in house; R93A_K96A, R125A, R165A_K169A and K236A_R240A. DNA sequencing analysis confirmed the mutations in the WT FX at the desired amino acid residues.

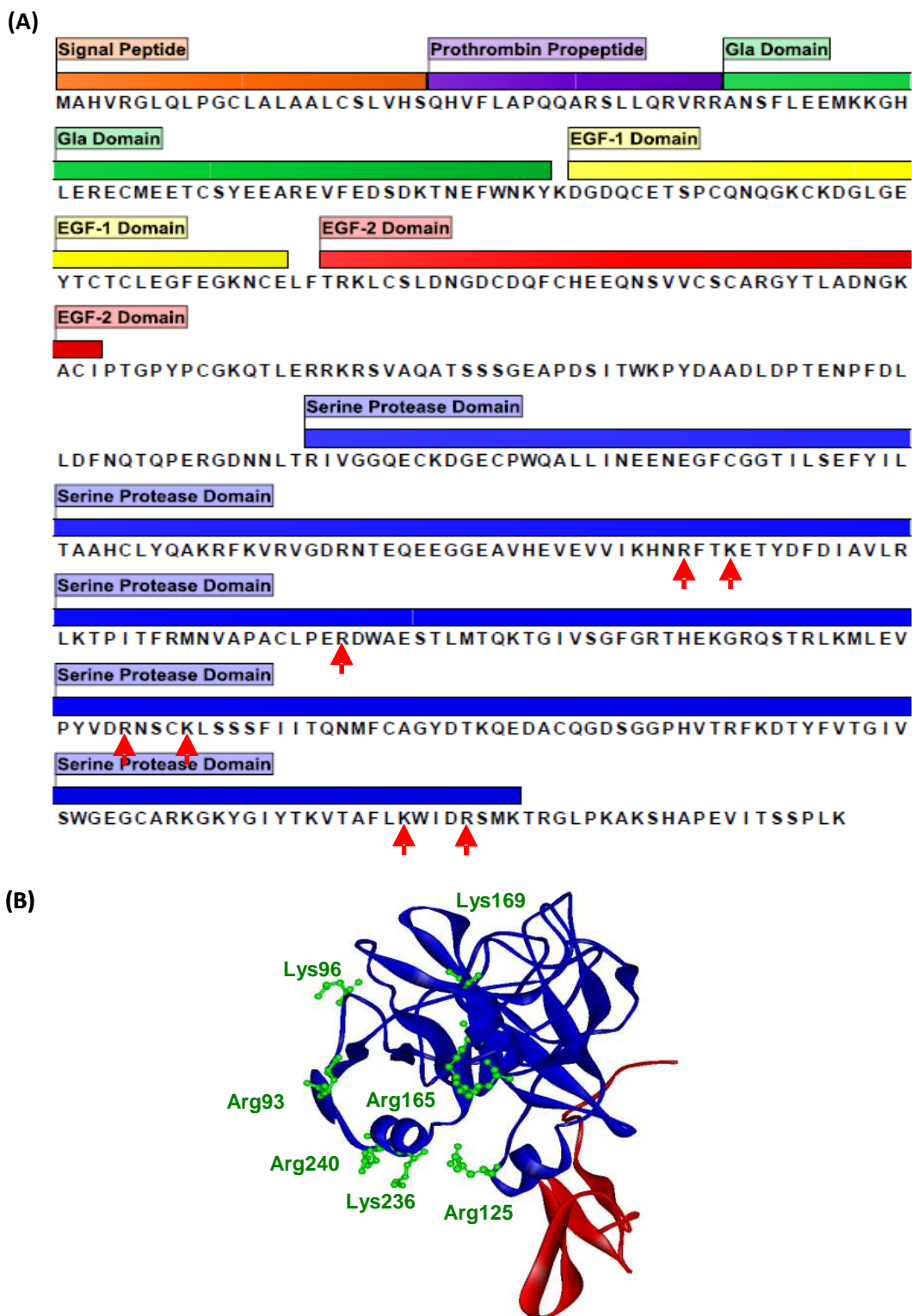


Figure 3.4. Amino acids residues for mutagenesis studies.

(A) Amino acid sequence of human FX including the human prothrombin signal sequence and propeptide (obtained for the Swiss-Prot database and annotated using CLC Protein Workbench 5). Red arrows indicate the seven amino acid residues targeted for mutagenesis studies. (B) Ribbon diagram of the human FX SP-EGF-2 domains (1HCG; Accelrys ViewerLite software (Padmanabhan *et al.*, 1993)), SP is in blue and EGF-2 is in red. The diagram highlights the amino acids residues (green) chosen for mutagenesis.

3.2.2 Cloning FX SP mutant into pcDNA3.1+zeocin

The SP mutant cDNA was cloned into a pMK-RQ plasmid using *Sfi*I cloning sites. pMK-RQ was not a viable expression cassette for use in order to produce rFX protein via transfection into a mammalian cell line as this plasmid construct did not possess a suitable promoter. Therefore a cloning strategy was designed in which the SP mutant fragment was firstly inserted into a pSCb plasmid and then finally into a pcDNA3.1+zeocin plasmid (Figure 3.5). Primers were designed to amplify the FX SP mutant from the pMK-RQ plasmid, adding an *Afl*III site at the 5' end and amplifying through *Hind*III at the 3' end. *Afl*III-FX SP mutant-*Hind*III was amplified by PCR using two commercially synthesised primers and Herculase II proofreading polymerase (Table 3.2). The FX SP mutant PCR products were electrophoresed on a 1% agarose gel. Bands of 1.5 kb were isolated from the gel (Figure 3.5). Bands were gel extracted and the purified PCR product was ligated into the pSCb plasmid. pSCb_FX SP mutant was digested with *Eco*RI. At this point, pcDNA3.1+zeocin was dephosphorylated by digestion with *Eco*RI. The digests were electrophoresed on a 1% agarose gel. Bands of 1.5 kb for FX SP mutant and 5 kb for pcDNA3.1+zeocin were isolated from the gel (Figure 3.5). The FX SP mutant insert was ligated into the pcDNA3.1+zeocin plasmid according to the T4 ligase ligation protocol (3:1 insert:vector ratio). After 1 h ligation at room temperature the ligation product was transformed into competent cells and spread on ampicillin resistant agar plates. The colonies were picked and small scale preparations of the DNA were performed. A diagnostic digest using *Bgl*III enzyme (two *Bgl*III sites present, one in the backbone and one in the SP mutant insert) was electrophoresed on a 1% agarose gel to ensure the insert was present. There were two fragments on the gel, a 5609 bp fragment for pcDNA3.1+zeocin_FX SP mutant backbone and a 978 bp fragment for the *Bgl*III digestion product (Figure 3.5). The sequence was confirmed by DNA sequencing.

Table 3.2. Primer design.

FX SP mutant forward (containing *Afl*III sequence highlighted in blue) and reverse primers were designed and commercially synthesised.

Primer		Sequence		T _m
FX SPmutant – forward	5'	GAATCTTAAAGGAAGGCCGTCA	3'	60.6
FX SPmutant – reverse	5'	GGCCCATGAGGCCAGG	3'	62

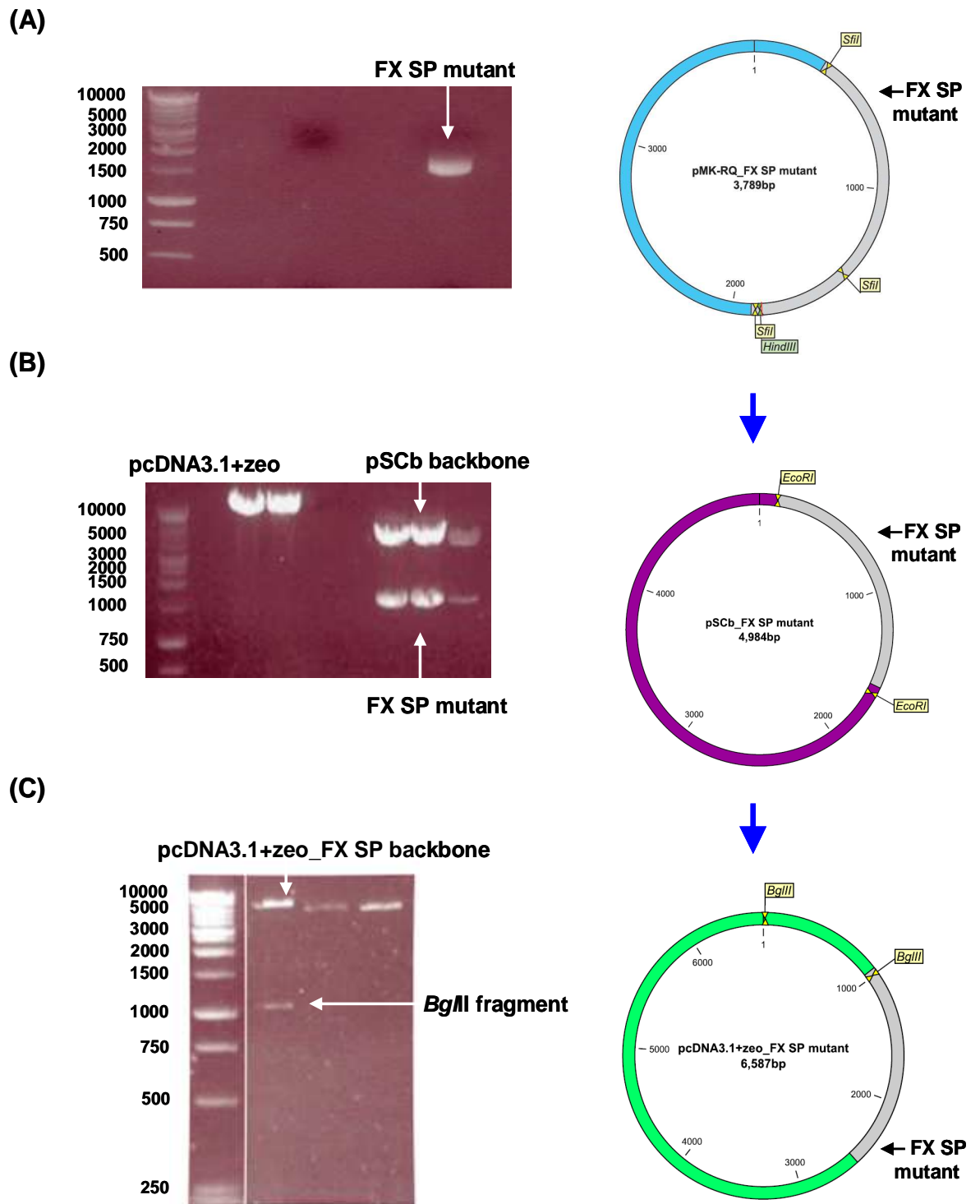


Figure 3.5. Cloning of the FX SP mutant sequence into pcDNA3.1+zeocin.

Gel electrophoresis was performed on (A) The FX SP mutant fragment which was amplified from the pMK-RQ construct, producing a band of 1.5 kb. (B) The pcDNA3.1+zeocin was digested, producing a band of 5 kb and the FX SP mutant fragment (band of 1.5 kb) was cut from the pSCb construct. (C) The pcDNA3.1+zeo_FX SP mutant vector was digested using *Bgl*II enzyme producing a fragment of 978 bp and a band of 5609 bp for the pcDNA3.1+zeo_FX SP mutant backbone.

3.2.3 Producing recombinant FX protein

The WT and SP mutant FX constructs were transiently transfected into 293T cells in the presence of 5 $\mu\text{g/ml}$ vitamin K. Recombinant FX (rFX) in the conditioned media was quantified by human FX ELISA and found to be at concentrations ranging from 0.1 $\mu\text{g/ml}$ to 0.4 $\mu\text{g/ml}$ after 5 days. To increase the yield of the protein produced, stable cell lines were generated based on zeocin resistance. Zeocin belongs to the family of antibiotics isolated from *Streptomyces*. It shows strong toxicity against mammalian cell lines and is commonly used as a selection tool. To generate a stable cell line that expresses a protein from an expression construct, the minimum concentration of zeocin required to kill the untransfected host cell line has to be determined. Therefore doses ranging from 100 $\mu\text{g/ml}$ to 500 $\mu\text{g/ml}$ of zeocin were tested on the ability to kill 293T cells after seven days. Cells sensitive to zeocin show morphological changes upon exposure to the antibiotic. The cells become an abnormal shape and long appendages appear as the plasma membrane breaks down (Figure 3.6). Eventually, the cells completely break down and only cellular debris remains in the media. A concentration of 200 $\mu\text{g/ml}$ zeocin was chosen as the optimum dose for generating stable cell lines (Figure 3.6).

Next stable cell lines to constitutively produce the WT and SP mutant rFX were generated. Firstly, 293T cells were transfected with the pcDNA3.1+zeocin_FX SP mutant plasmid, co-transfected with a plasmid encoding the WT FX and the pcDNA3.1+zeocin or co-transfected with a control GFP plasmid and the pcDNA3.1+zeocin. Transfection efficiency was ~70% at 48 h post-transfection as assessed by GFP control cells under a fluorescent microscope (Figure 3.6). Media in the cell culture dishes was replaced with 10% complete media supplemented with 5 $\mu\text{g/ml}$ vitamin K and 200 $\mu\text{g/ml}$ zeocin. After 2-3 weeks mock transfected cells were dead and colonies had formed with cells transfected with pcDNA3.1+zeocin_FX SP mutant plasmid, co-transfected with WT FX and pcDNA3.1+zeocin or co-transfected with a control GFP and pcDNA3.1+zeocin (Figure 3.6). Colonies were picked and grown until 90% confluent. Conditioned media was collected from individual wells and a FX ELISA was performed to identify the highest producing cells. These cells were then grown up in larger culture flasks.

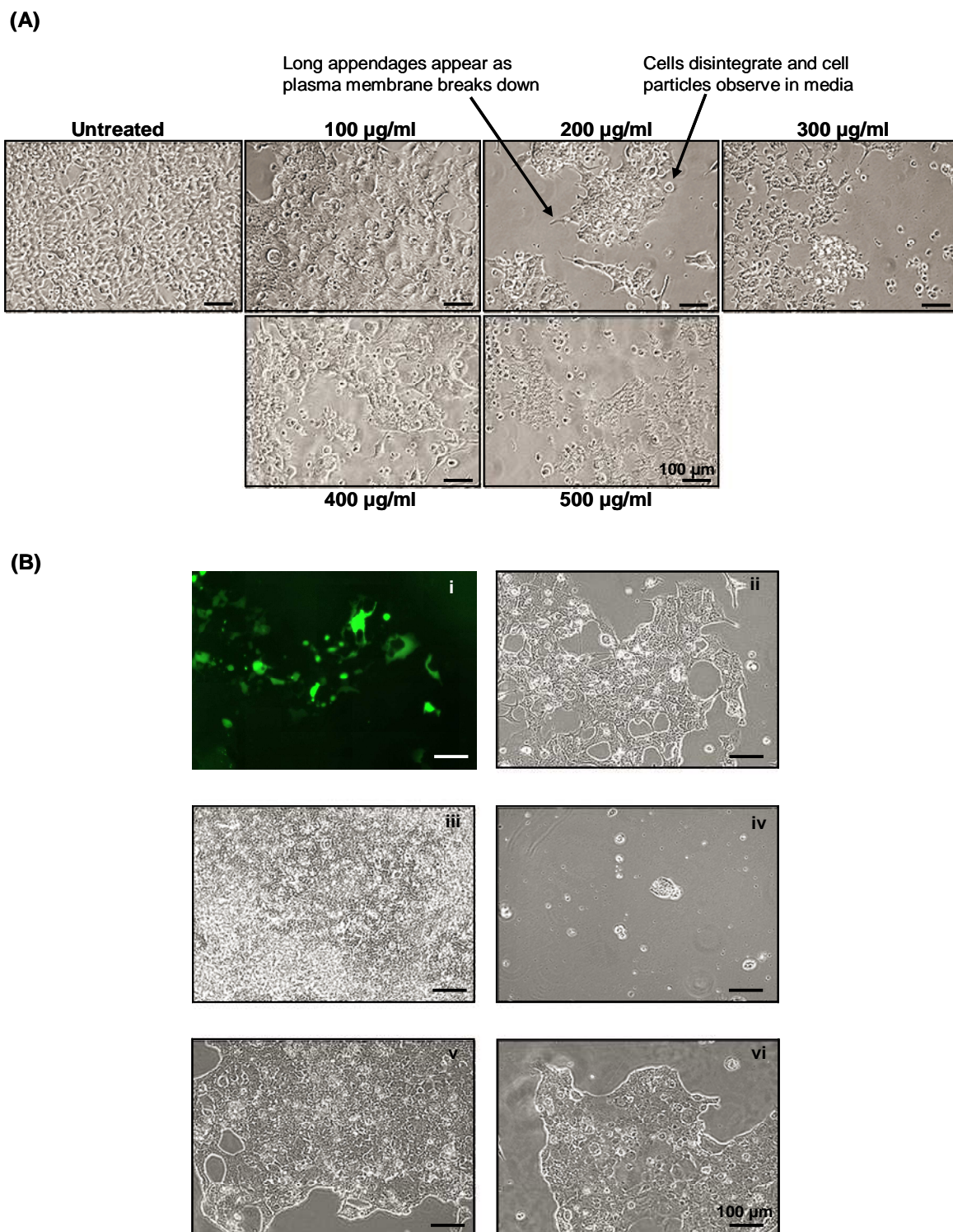


Figure 3.6. Generating stable cell lines.

Determining optimal concentration of zeocin (100-500 $\mu\text{g/ml}$) required to kill mock transfected 293T cells after seven days incubation. (B) Cells 15 days post-transfection (i) GFP transfected cells. (ii) Bright-field view of GFP transfected cells in the presence of 200 $\mu\text{g/ml}$ zeocin. (iii) Mock transfected cells in the absence of zeocin. (iv) Mock transfected cells, (v) SP mutant FX transfected cells and (vi) WT FX transfected cells in the presence of 200 $\mu\text{g/ml}$ zeocin. Images captured at 40x magnification and scale bar = 100 μm , applicable to all panels.

3.2.4 Purification and validation of rFX protein

Conditioned media from cells cultured in serum free media supplemented with 5 µg/ml vitamin K was collected, dialysed and immunoaffinity purified using the calcium-dependent 4G3 mouse monoclonal antibody coupled to a sepharose column. The conditioned media was applied to the monoclonal human FX immunoaffinity column and any FX in the media bound to the column. Bound proteins were eluted with the addition of EDTA (Figure 3.7). Fractions eluted from the column were analysed by SPR to assess binding to the 4G3 mouse monoclonal antibody. The 4G3 antibody was covalently immobilised on a biosensor chip and the individual fractions eluted from the column were injected over the chip at a flow rate of 30 µl/min. Eluted fractions 1, 2, 3 and 4 from the media from WT rFX cells and eluted fractions 2, 3 and 4 from the media from SP mutant rFX cells bound to the chip (Figure 3.7), indicating the presence of FX. These results correlate to the elution profiles obtained whilst passing the media through the 4G3 sepharose column. In order to further confirm this, the load (the media prior to passing through the column), the flow through and the purified rFX was subjected to SDS-PAGE. Coomassie staining showed a number of different bands for the load and the flow through, however for each of the eluted fractions a single band was observed of 59 kDa, similar to the positive control purified plasma derived (pd) FX (HTI Technologies Ltd) (Figure 3.8). Furthermore, each rFX protein migrated as a single band with an apparent molecular mass of 59 kDa similar to the positive control FX as assessed by Western blot analysis using a primary monoclonal human anti-FX clone HX1 antibody (Figure 3.8). The purified rFX was quantified by both microBCA and ELISA for human FX. The WT rFX was ~57 µg/ml and the SP mutant rFX was ~9 µg/ml.

3.2.5 Assessment of the biological activity of rFX

The biological activity of the purified rFX was assessed. A chromogenic assay was used to monitor the conversion of FX to its active state (FXa), measured in the presence of tissue factor and FVIIa. Positive control FX, WT and SP mutant rFX proteins were converted to their active forms (FXa) in the presence of tissue factor and FVIIa, thus confirming their biological activity (Figure 3.9). This data demonstrates the mutations within the HBPE of the SP domain of FX did not affect the catalytic activity of FX or hinder activation by tissue factor and FVIIa complexes.

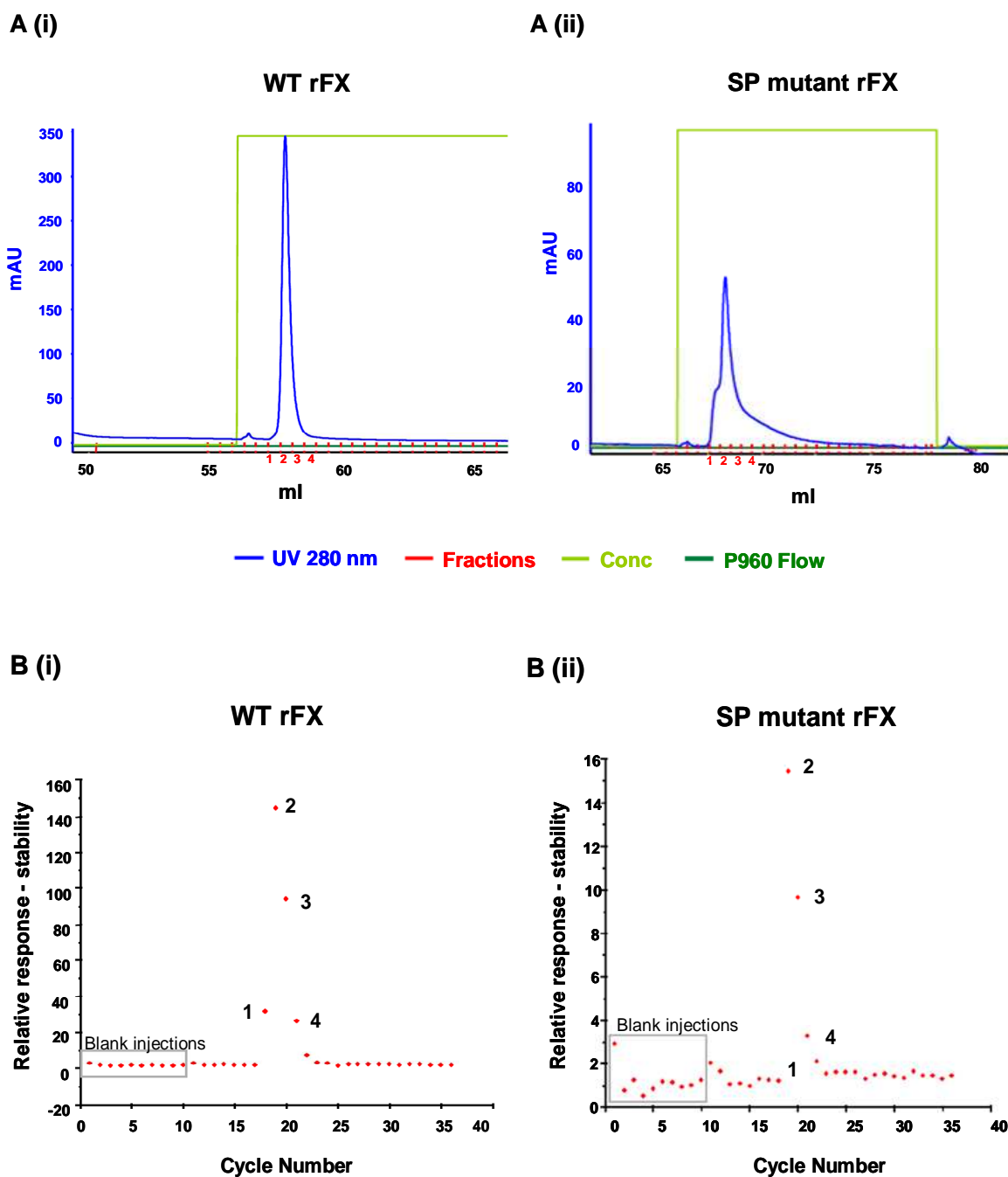


Figure 3.7. Purification and validation of rFX.

(A) Immunoaffinity elution profiles of (i) WT and (ii) SP mutant rFX. Elution is monitored by absorbance at 280 nm. WT rFX and SP mutant rFX are recovered as single peaks when eluted from the calcium-dependent anti-FX 4G3 antibody affinity column with the addition of EDTA. (B) SPR analysis of (i) WT and (ii) SP mutant rFX fractions eluted from the 4G3 antibody affinity column binding to the 4G3 antibody immobilised on a biacore sensor chip.

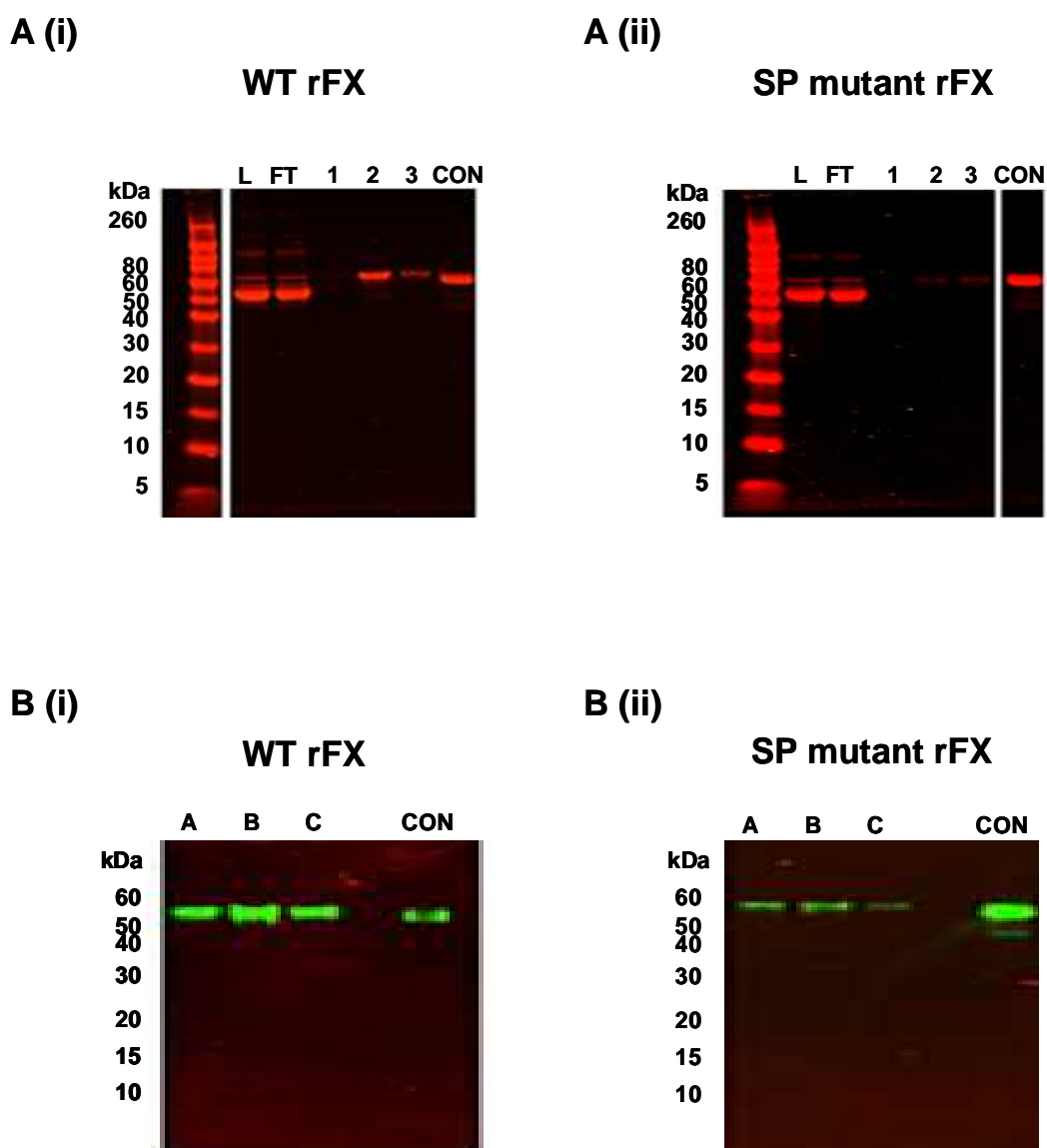


Figure 3.8. Validation of purified rFX.

(A) Coomassie staining of SDS-PAGE for (i) WT and (ii) SP mutant rFX. Lanes (L) represent load prior to passing through the column, (FT) represents unbound material that flowed through the column, (1, 2, 3) represents fractions eluted from the column, (CON) represents plasma derived human FX positive control. (B) Western blot analysis of rFX was performed. rFX was probed with a primary monoclonal human anti-FX clone HX1 antibody (1:1,000 dilution) and a goat anti-mouse infrared dye (800CW)-labelled secondary antibody (LI-COR). (i) Lanes A, B, C, represent WT rFX purified by 4G3 column; lane CON represents plasma derived human FX positive control (ii) lanes A, B, C, represent SP mutant rFX purified by 4G3 column.

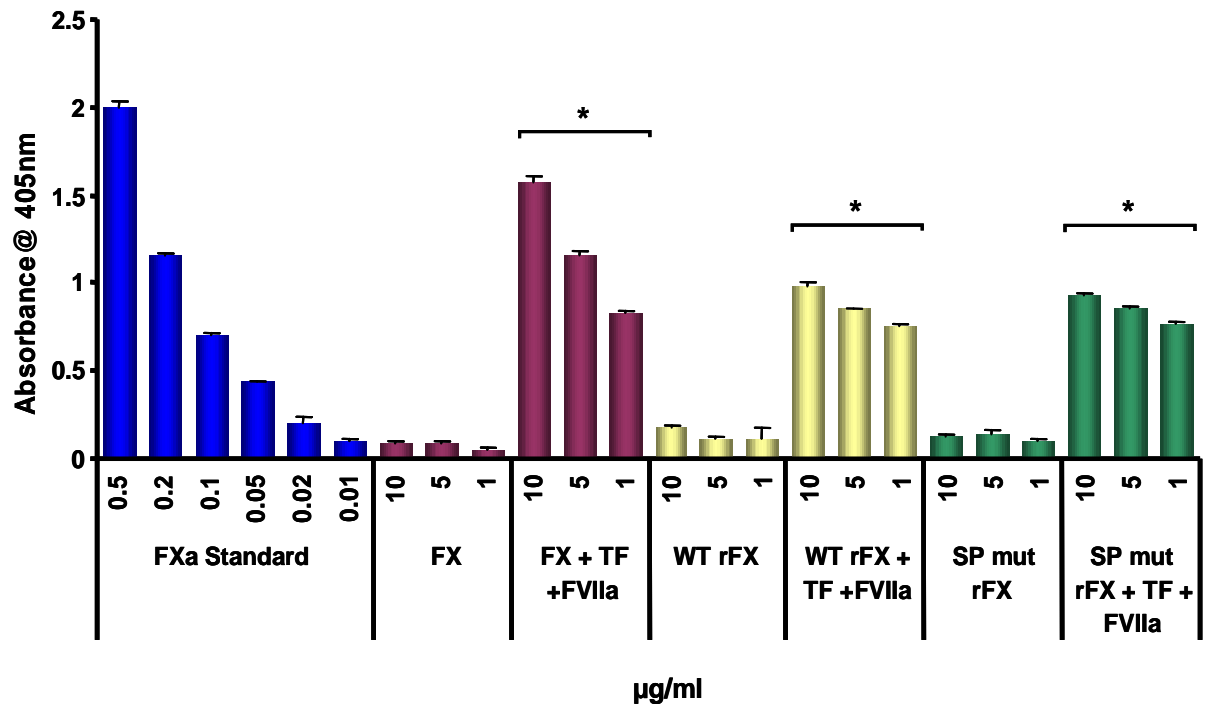


Figure 3.9. Activation of rFX.

Activation of positive control FX, WT rFX and SP mutant rFX. The amidolytic activity of FXa was measured using 1 mM chromogenic substrate S-2765 (Quadrachem, Surrey, UK) in the presence of 100 nM tissue factor, 100 nM factor VIIa and 6 mM CaCl₂. All measurements were determined kinetically at 405 nm. * $p < 0.05$ as compared to the corresponding positive control FX, WT or SP mutant conditions, as determined by one-way ANOVA and Dunnett's multiple comparison post-test. Error bars represent SEM ($n = 3/\text{group}$).

3.2.6 Mutating residues in the FX HBPE has no effect on FX binding to Ad5 hexon

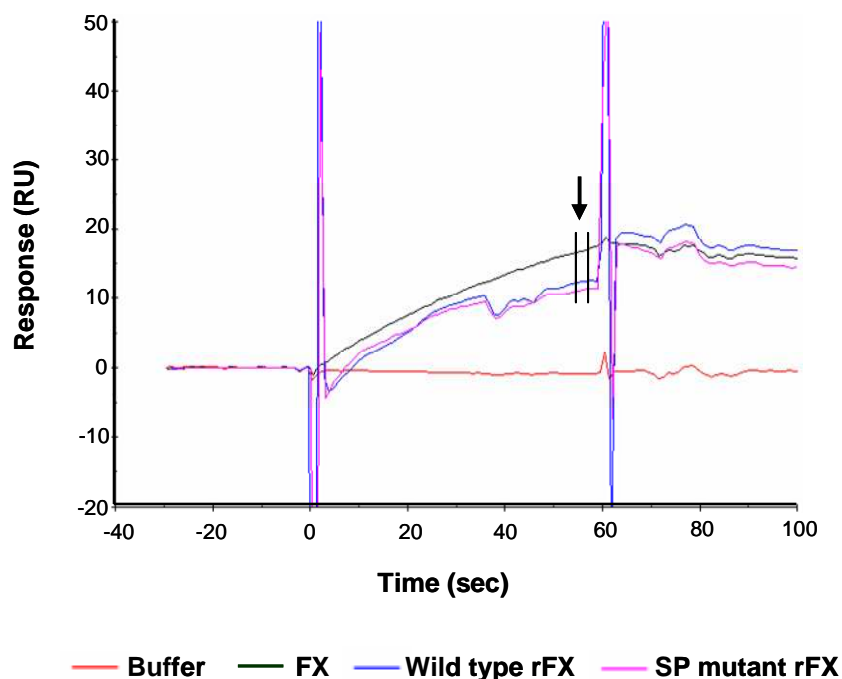
To ensure the mutations in the FX SP domain had no effect on FX binding to Ad5 both WT and SP mutant rFX binding to Ad5 hexon was analysed using SPR (performed by Prof. John McVey (Thrombosis Research Institute, London, UK)). Ad5 hexon was covalently immobilised on a biosensor chip and running buffer, positive control FX, WT or SP mutant rFX was injected over the chip at a flow rate of 30 $\mu\text{l}/\text{min}$. Directly after injection of running buffer, positive control FX, WT or SP mutant rFX, either the FX monoclonal antibody HX-1 or the monoclonal antibody 4G3, were passed over the chip at a flow rate of 30 $\mu\text{l}/\text{min}$. Protein binding to the Ad5 hexon and binding of the antibodies to the material bound to the chip was detected as a change in response units. Data was analysed using Biacore T100 Evaluation software.

SPR analysis indicated that the positive control FX, conditioned media of cells transfected with either WT or SP mutant FX bound to hexon. The positive control FX or rFX dissociated from the chip upon the addition of EDTA indicating that the reaction occurs in a calcium-dependent manner (Figure 3.10). There was no significant difference in response units for binding to hexon for the WT and SP mutant rFX (Figure 3.10). The conditioned media of cells transfected with either WT or SP mutant FX bound to the chip was subsequently confirmed to be FX by binding of the two monoclonal antibodies against human FX (HX-1 and 4G3) (Figure 3.11). Therefore the seven mutated residues in the HBPE of FX have no effect on FX binding to Ad5 hexon.

3.2.7 FX dose response

Previous studies have shown FX at concentrations below physiological levels (< 8-10 $\mu\text{g}/\text{ml}$) to be effective in increasing Ad5 gene transfer (Parker *et al.*, 2006; Zaiss *et al.*, 2011). Here, the effects of lower concentrations of FX than previously described were assessed for their ability to increase Ad5 transduction. SKOV3 cells were incubated with Ad5 in the absence or presence of 10 ng/ml, 100 ng/ml, 1 $\mu\text{g}/\text{ml}$ or 10 $\mu\text{g}/\text{ml}$ pd FX for 3 h at 37°C. Cells were washed once, complete media added and incubated at 37°C for a further 45 h when transgene expression was analysed. All four doses of FX tested caused a significant increase in Ad5 gene transfer as shown by β -galactosidase transgene expression (Figure 3.12). The ability of FX to be effective at concentrations as low as 10 ng/ml highlights the high affinity interaction between Ad5 hexon and FX.

(A)



(B)

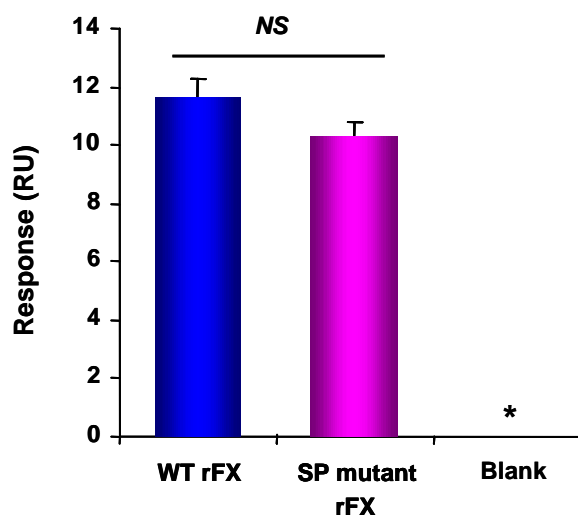


Figure 3.10. HBPE mutations have no effect on rFX binding to Ad5 hexon.

(A) Representative subtracted sensorgrams of positive control FX, WT rFX and SP mutant rFX binding hexon, injected at time 0 for 60 sec at a flow rate of 30 $\mu\text{l}/\text{min}$ (B) Quantification of relative binding of running buffer, WT rFX or SP mutant rFX to hexon at the end of the injection as indicated by the arrow. * $p < 0.05$ as compared to WT rFX conditions as determined by one-way ANOVA and Dunnett's multiple comparison post-test. NS = non-significant, $p > 0.05$. Error bars represent SEM ($n = 5/\text{group}$).

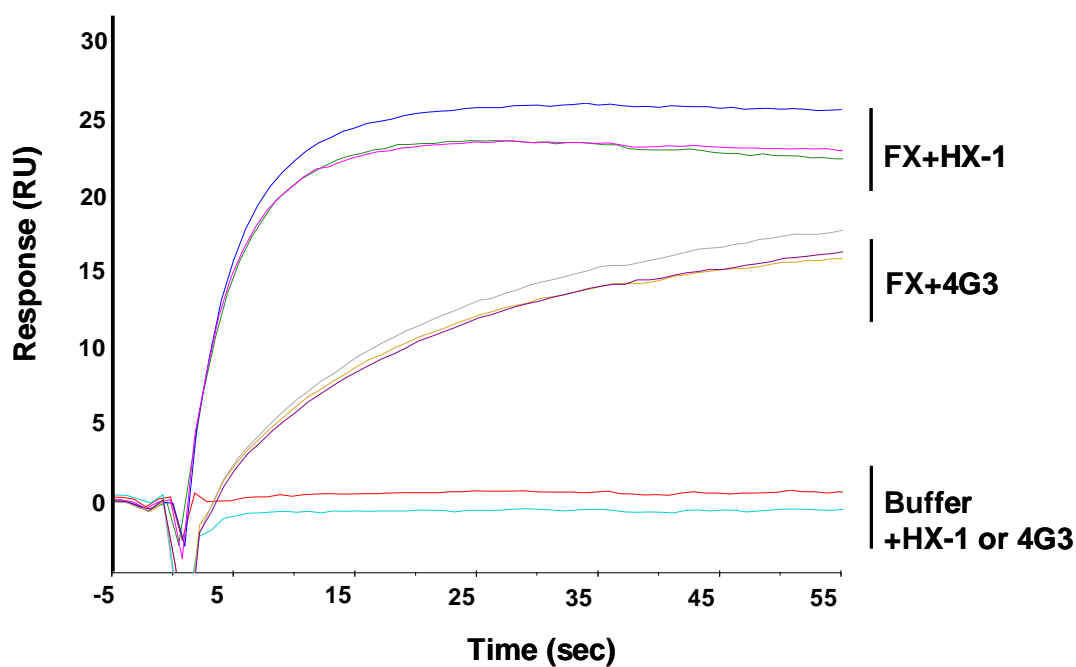


Figure 3.11. Anti-FX antibody binding to rFX bound to Ad5 hexon.

Representative subtracted sensorgrams of binding of anti-FX antibodies 4G3 or HX-1 to the chip following injection of running buffer, positive control FX (green and yellow lines), WT (blue and grey lines) or SP mutant rFX (pink and purple lines), injected at time 0 for 60 sec at a flow rate of 30 $\mu\text{l}/\text{min}$.

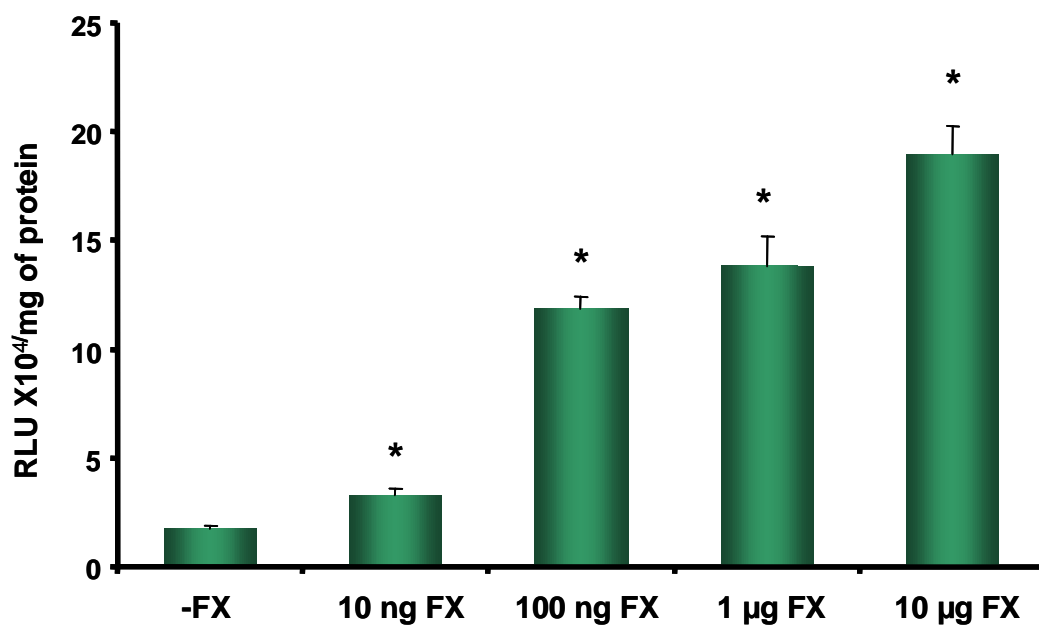


Figure 3.12. Ad5 transduction in the presence of increasing concentrations of FX.

SKOV3 cells were infected with 1000 vp/cell of Ad5 in the absence or presence of increasing concentrations (10 ng/ml, 100 ng/ml, 1 µg/ml or 10 µg/ml) of positive control pd FX. Ad5 transgene expression was measured 48 h post-infection. * $p < 0.05$ as compared to non-FX conditions as determined by one-way ANOVA and Dunnett's multiple comparison post-test. Error bars represent SEM (n = 4/group).

3.2.8 Effect of the FX SP domain mutations on Ad5:FX binding to HSPGs

As cell surface binding of Ad5:FX complexes is mediated by HSPGs (Bradshaw *et al.*, 2010), confocal microscopy was used to evaluate the interaction of fluorescently-labelled Ad5 with cell surface HSPGs when complexed with WT or the SP mutant rFX. This was assessed by infection of SKOV3 cells (which have low levels of CAR expression, therefore allows us to look more specifically at Ad5 binding and transduction mediated by FX) with Alexa Fluor-488 fluorescently-labelled Ad5 in the presence of WT or SP mutant rFX for 1 h at 4°C. Incubation with Ad5 at 4°C allows binding to the cell surface but not internalisation, which is energy dependent and hence occurs at 37°C. After washing with PBS to remove unbound virus, the cells were fixed in 4% PFA. Immunocytochemistry was carried out using the pan-heparan sulphate antibody (clone 10E4) to stain for cellular HSPGs. Following pretreatment with WT rFX, Ad5 complexes were clearly visible on the cell surface and colocalised with HSPGs as shown by confocal microscopy (Figure 3.13). In contrast, in the absence of FX or when Ad5 was pretreated with equivalent concentrations of SP mutant rFX there were few virus particles bound to the cell surface and no observed colocalisation with HSPGs (Figure 3.13). This qualitative data indicates that the FX HBPE is required for efficient binding of Ad5:FX to HSPGs on the cell surface.

3.2.9 The FX SP domain mutations decrease FX-mediated Ad5 cell binding

To quantitatively assess the effects of the HBPE mutations on Ad5:FX-mediated cell binding, SKOV3 and HepG2 cells were used as they can be readily transduced via the FX pathway (Bradshaw *et al.*, 2010). For experiments involving SKOV3 cells, a CAR_{low} cell line (Kim *et al.*, 2002), a β -galactosidase expressing Ad5 was utilised and for experiments involving HepG2 cells which have higher CAR expression Ad5KO1 was utilised. Vectors were incubated with SKOV3 or HepG2 cells in the absence or presence of positive control FX, WT or the SP mutant rFX for 1 h at 4°C. After washing with PBS to remove unbound virus, cells were collected, total DNA was isolated and qPCR for Ad5 hexon was performed. Quantification of Ad5 cell surface binding by qPCR revealed that positive control FX and WT rFX caused a significant increase in binding of Ad5 to SKOV3 cells and Ad5KO1 to HepG2 cells compared to cells not treated with FX (Figure 3.14). WT rFX caused a significant ~14 fold increase compared to cells not treated with FX, whereas no significant increase was observed when SP mutant rFX was used at an equivalent concentration to WT rFX (Figure 3.14) Therefore, these results demonstrate that the

residues within the FX HBPE are required for FX-mediated Ad5 binding to the cell surface.

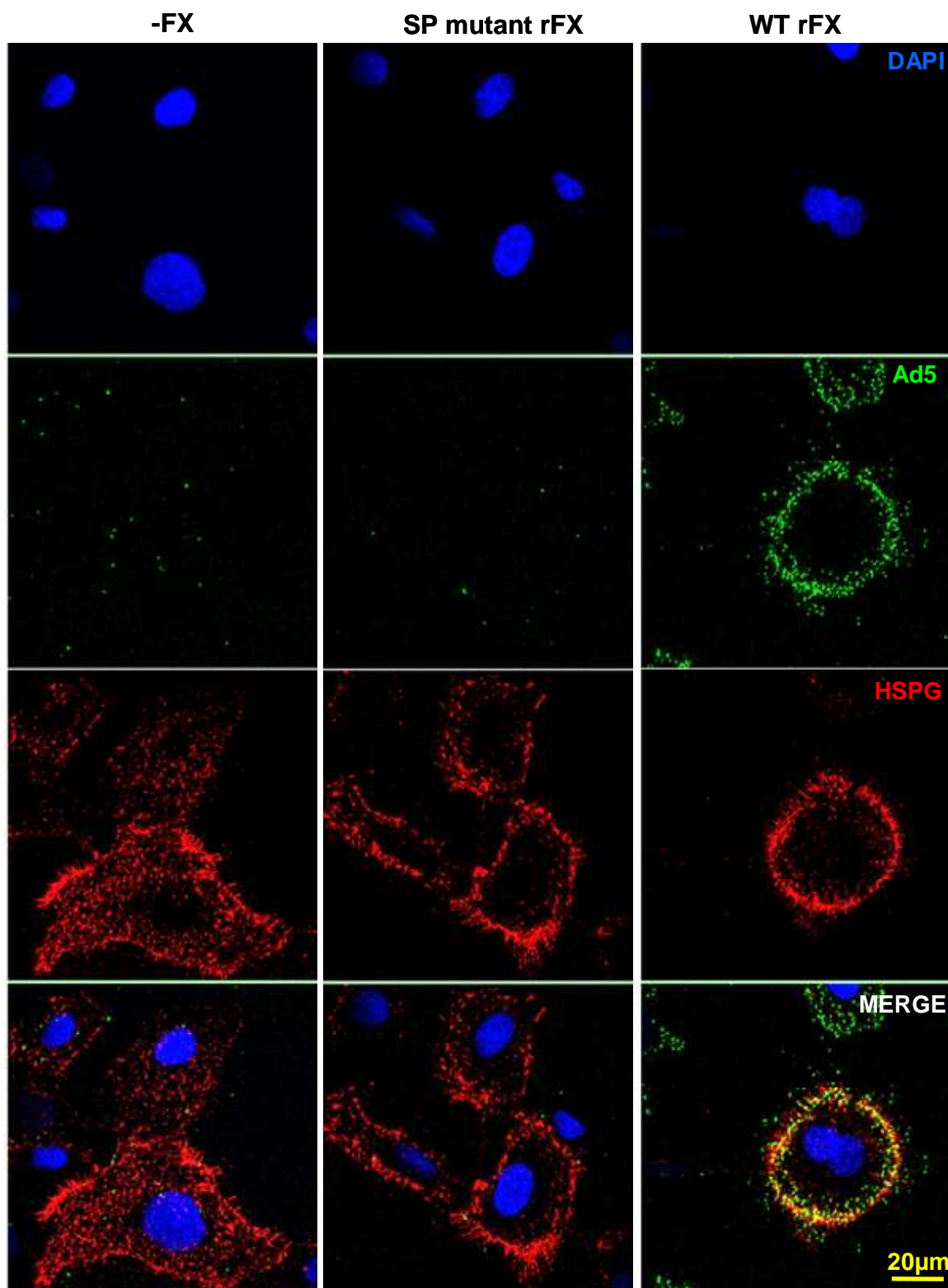


Figure 3.13. Role of the HBPE in the FX SP domain in Ad5 binding to HSPGs.

10,000 vp/cell of Alexa Fluor-488 fluorescently-labelled Ad5 (green) were allowed to bind SKOV3 cells for 1 h at 4°C in the absence or presence of WT rFX or SP mutant rFX. Cells were then stained with a pan-heparan sulphate antibody (clone 10E4) (red). Nuclei were counterstained using DAPI. Images were captured on a confocal microscope using a 63x objective, scale bar = 20 µm, applicable to all panels.

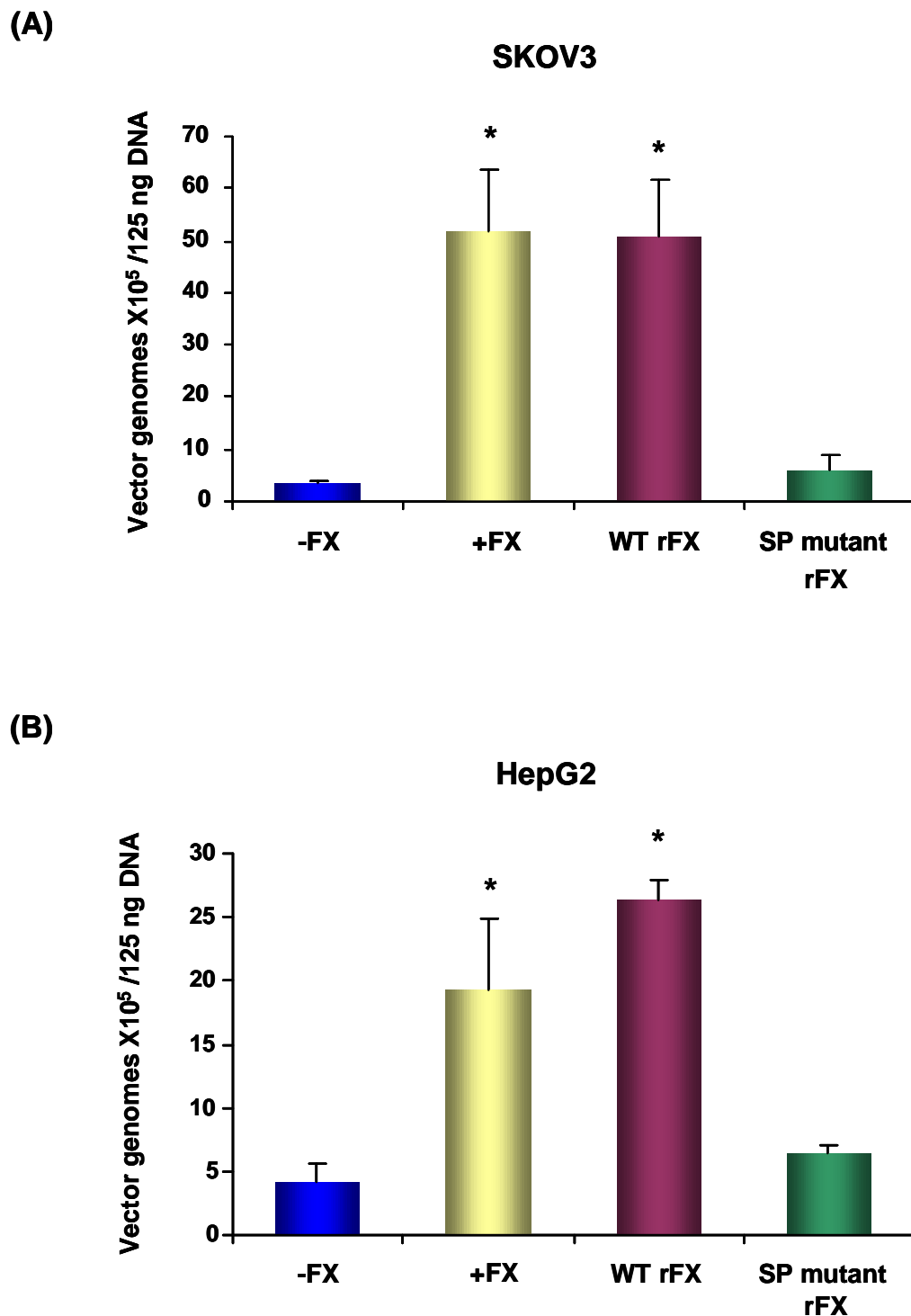


Figure 3.14. Role of the FX SP domain in Ad5 cell binding.

(A) Binding of 1000 vp/cell Ad5 to SKOV3 or (B) 1000 vp/cell Ad5KO1 to HepG2 cells for 1 h at 4°C in the absence or presence of positive control FX, WT rFX or SP mutant rFX was analysed. Vector genomes were detected by quantitative SYBR green PCR. * $p < 0.05$ as compared to non-FX conditions as determined by one-way ANOVA and Dunnett's multiple comparison post-test. Error bars represent SEM ($n = 4/\text{group}$).

3.2.10 The FX SP domain mutations inhibit FX-mediated Ad5 cell binding, internalisation and cytosolic transport

To analyse the effects of FX mutagenesis on Ad5 cell binding, internalisation and cytosolic transport, cell trafficking assays using Alexa Fluor-488 fluorescently-labelled Ad5 were performed in SKOV3 cells. Cells were exposed to Ad5 in the absence or presence of positive control FX, WT or SP mutant rFX for 1 h at 4°C to allow binding to occur. The cells were then either immediately washed in PBS and fixed in 4% PFA or fixed after 1 h at 37°C to allow Ad5 internalisation and trafficking. Immunocytochemistry was carried out using a pericentrin antibody to stain the MTOC. Cells were counterstained using DAPI nuclear stain. Images were captured using a confocal microscope.

In the presence of positive control FX or WT rFX, Ad5 bound the cell surface after 1 h at 4°C and after 1 h incubation at 37°C efficiently trafficked toward the nucleus where it colocalised with the MTOC (Figure 3.15). However, when the same experiment was performed using the SP mutant rFX, Ad5 cell surface binding and trafficking to the perinuclear region was significantly decreased (Figure 3.15). Colocalisation of Ad5 with the MTOC was quantified visually by assessing the percentage of cells with Alexa Fluor-488 fluorescently-labelled Ad5 and pericentrin co-staining. The percentage of cells with Ad5:MTOC colocalisation in the presence of SP mutant rFX conditions was significantly reduced compared to positive control FX and WT rFX. Ad5:MTOC colocalisation under SP mutant conditions closely resembled conditions in the absence of FX. These data demonstrate that mutating the seven amino acids in the FX SP domain inhibits FX-mediated Ad5 cell binding, subsequent internalisation and cytosolic transport.

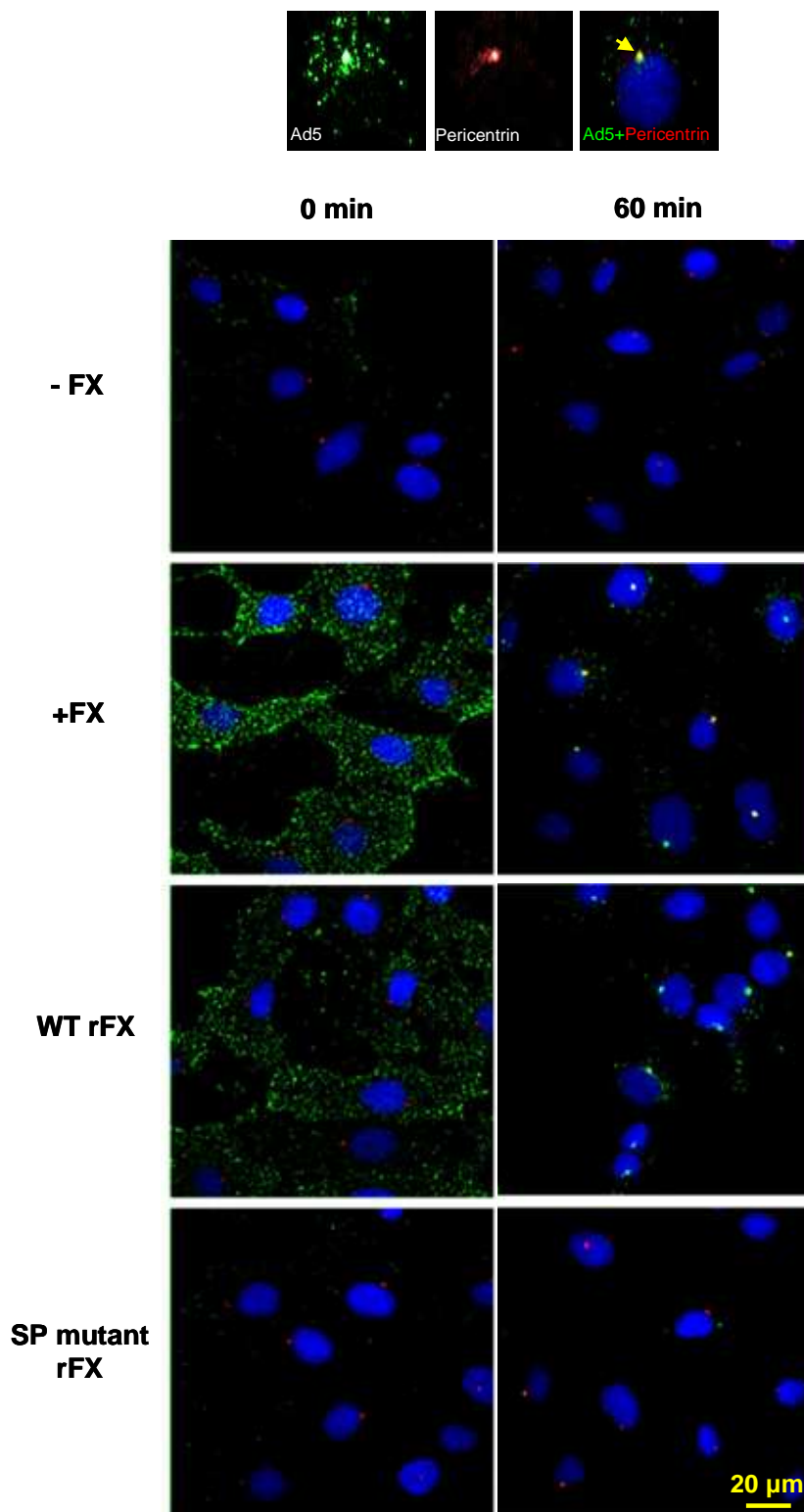


Figure 3.15. Role of the FX HBPE in Ad5 cellular trafficking.

10,000 vp/cell of Alexa Fluor-488 fluorescently-labelled Ad5 (green) were allowed to bind SKOV3 cells for 1 h at 4°C in the absence or presence of positive control FX, WT rFX or SP mutant rFX. Cells were then incubated at 37°C for 0 or 60 min prior to fixation and staining for the MTOC marker pericentrin (red). Nuclei were counterstained using DAPI. Upper panel - colocalisation of fluorescently-labelled Ad5 particles with pericentrin is indicated by the yellow arrow. Images were captured on a confocal microscope using a 63x objective, scale bar = 20 μm, applicable to all panels.

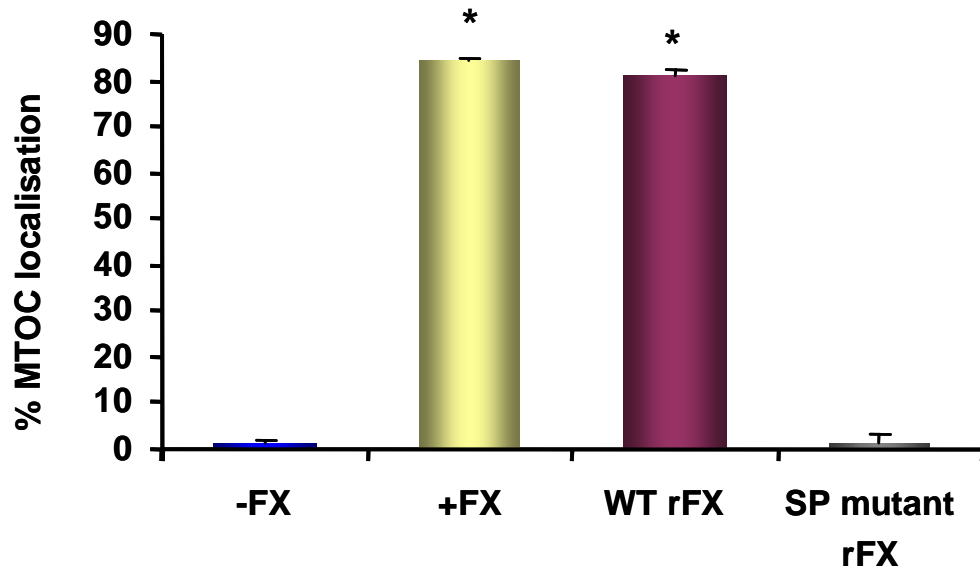


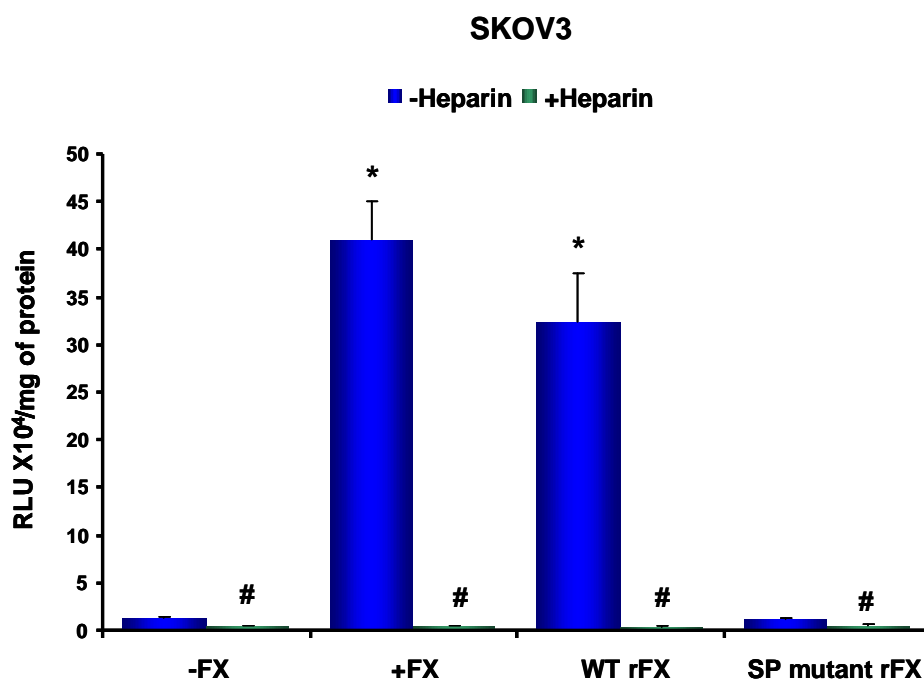
Figure 3.16. Role of the FX HBPE in Ad5 accumulation at the MTOC.

Percentage of cells with colocalisation of fluorescently-labelled Ad5 with the MTOC marker pericentrin was calculated by analysing at least 5 separate 40x microscope fields per experimental condition. * $p < 0.05$ as compared to non-FX conditions as determined by one-way ANOVA and Dunnett's multiple comparison post-test. Error bars represent SEM ($n = 5/\text{group}$).

3.2.11 The FX SP domain mutations decrease FX-mediated Ad5 transduction compared to WT rFX

The mutations in the FX HBPE inhibit FX-mediated Ad5 cell binding to HSPGs, subsequent internalisation and cytosolic transport to the nucleus. These data were further confirmed by analysing expression of the β -galactosidase transgene following transduction of β -galactosidase-expressing Ad5 in SKOV3 cells or Ad5KO1 in HepG2 cells, either in the absence and presence of heparin. Cells were incubated with the vector in the absence or presence of positive control FX, WT, SP mutant rFX and 100 μ g/ml soluble heparin for 3 h at 37°C. Cells were then washed once, complete media added and incubated at 37°C for a further 45 h when transgene expression was analysed. Both WT rFX and positive control FX mediated a significant increase in Ad transgene expression in the absence of heparin in both cell types, whereas the SP mutant rFX resulted in no significant change in transgene expression compared to non-FX conditions in SKOV3 or HepG2 cells (Figure 3.17). In the presence of heparin, positive control FX-mediated and WT rFX-mediated Ad5 transduction was ablated, thereby confirming the requirement for HSPGs in this infectivity pathway. There was also a significant decrease in Ad5 transduction under non-FX and SP mutant conditions in the presence of heparin compared to in its absence, in both cell types (Figure 3.17). These data indicates the critical importance of the HBPE in FX-mediated Ad5 gene transfer, an effect mediated via HSPGs.

(A)



(B)

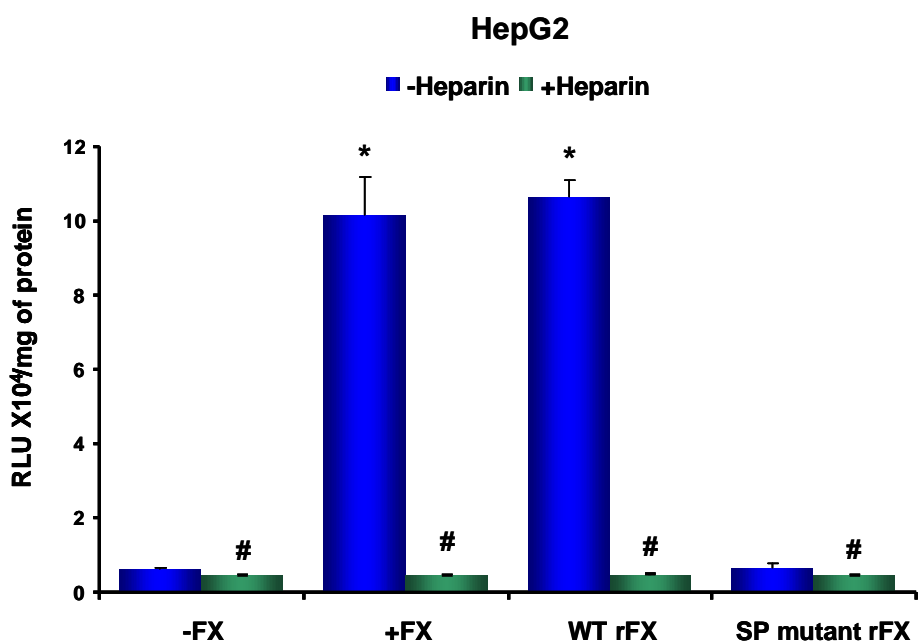


Figure 3.17. Role of the FX HBPE in Ad5 gene transfer.

(A) SKOV3 were infected with 1000 vp/cell of Ad5 and (B) HepG2 cell were infected with 1000 vp/cell of Ad5KO1 in the absence or presence of positive control FX, WT rFX or SP mutant rFX with or without 100 μ g/ml soluble heparin. Ad5 transgene expression was measured 48 h post-infection. * $p < 0.05$ as compared to non-FX conditions, # $p < 0.05$ as compared to matched treatments (-FX, +FX, WT or SP mutant rFX) in the absence of heparin, as determined by one-way ANOVA and Dunnett's multiple comparison post-test. Error bars represent SEM ($n = 4$ /group).

3.2.12 Effects of single and double amino acid mutations in the SP domain on FX-mediated Ad5 gene transfer

The importance of individual basic residues in the FX SP domain was dissected by generating single and double mutations in the HBPE. The double mutations were chosen based on their proximity to one another in the SP domain (Figure 3.18).

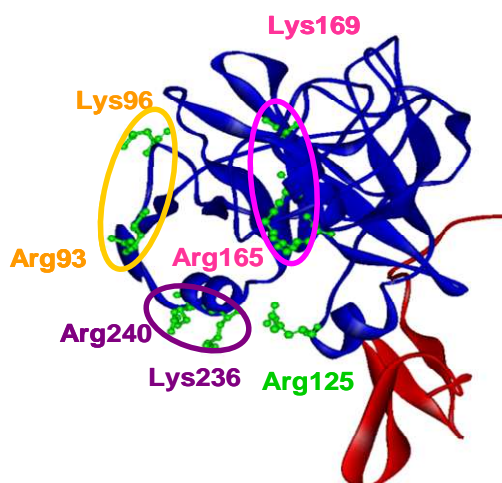


Figure 3.18. Ribbon diagram of the FX SP and EGF-2 domain.

Ribbon diagram of the FX SP domain (blue) and EGF-2 domain (red) highlighting the single and double amino acids chosen for mutagenesis studies (1HCG; Accelrys ViewerLite software (Padmanabhan *et al.*, 1993)).

The single (R125A) and double mutant (R93A_K96A, R165A_K169A and K236A_R240A) FX plasmids were transiently transfected into 293T cells in the presence of 5 $\mu\text{g/ml}$ vitamin K. rFX was expressed into serum free media supplemented with 5 $\mu\text{g/ml}$ vitamin K and conditioned media was concentrated using centricon centrifugal filter devices. The yield of rFX protein gained from the transient transfection of the single and double mutant FX encoding cDNAs was lower than the rFX protein purified from the WT or SP mutant stable cell lines (Table 3.3). Therefore experiments involving single and double FX mutants were carried out at a concentration of 10 ng/ml. Ad5 gene transfer in the absence or presence of 10 ng/ml positive control FX, WT rFX, SP mutant rFX, or rFX with mutations R93A_K96A, R125A, R165A_K169A, K236A_R240A in SKOV3 cells was assessed. β -galactosidase transgene expression was quantified 48 h post-infection. WT rFX mediated a significant increase in Ad5 gene expression in SKOV3 cells compared to Ad5 in the absence of FX (data normalised to non-FX conditions) (Figure 3.19). In contrast the SP mutant rFX resulted in no significant change in β -galactosidase expression compared to non-FX conditions. Analysis of Ad5 gene transfer in the presence of single or

double FX point mutants revealed that mutations at R93A_K96A, R125A, K236A_R240A but not R165A_K169A caused a significant reduction in Ad5 transduction compared to WT rFX (Figure 3.19). These results suggest that amino acids residues within the HBPE exhibit different levels of contribution in Ad5:FX complex binding to HSPGs.

Table 3.3. Concentration of rFX protein.

The average concentrations of rFX containing single and double point mutations produced by transient transfection in 293T cells.

FX mutant	µg/ml
R93A_K96A	0.25
R125A	0.18
K236A_R240A	0.39
R165A_K169A	0.27

3.2.13 Role of HBPE on FX-mediated cell binding *ex vivo*

To confirm the importance of the HBPE we characterised the effect of the SP mutations *ex vivo* by examining fluorescently-labelled Ad5 attachment to mouse liver sections. 4 µm liver sections from MF-1 mice were incubated with Alexa Fluor-488 fluorescently-labelled Ad5 in the absence or presence of WT or SP mutant rFX for 1 h on ice followed by 1 h at 37°C. Sections were washed to remove unbound virus, fixed and the nuclei stained using DAPI. Sections were imaged using an Olympus Cell M imaging system. To quantify adherent Alexa Fluor-488 fluorescently-labelled Ad5 particles, 40x magnification images were captured and processed using ImageJ counting software. In the presence of WT rFX there is a significant increase in the number of Ad5 virus particles associated with the mouse liver slices (Figure 3.20). However, under SP mutant rFX conditions there was ~5-fold less adherent Ad5 particles compared to WT rFX conditions (Figure 3.21). Ad5 binding to liver sections in the absence of FX closely resembled the levels of binding in the presence of SP mutant rFX. These results indicate that the residues in the HBPE of FX are responsible for FX-mediated Ad5 binding to liver sections *ex vivo*.

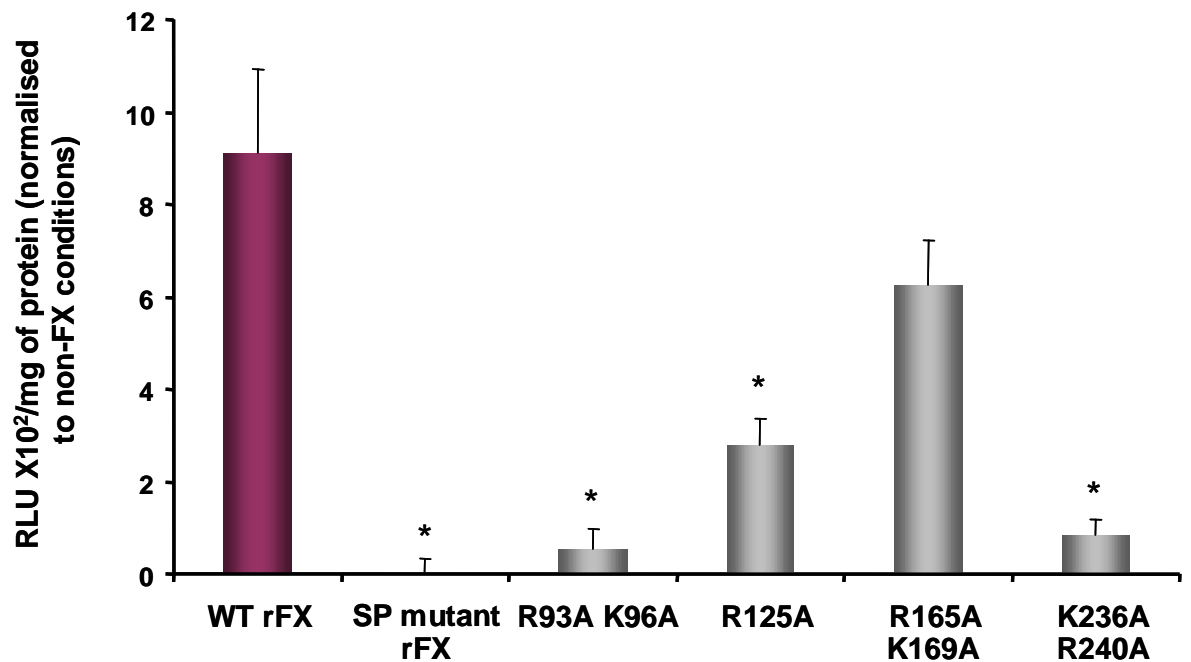


Figure 3.19. Effect of single and double point HBPE mutations on Ad5 gene transfer. SKOV3 cells were exposed to Ad5 alone or in the presence of 10 ng/ml WT rFX, SP mutant rFX, rFX with mutations at R93A_K96A, R125A, R165A_K169A, or K236A_R240A for 3 h and transgene expression was measured 48 h post-infection. * $p < 0.05$ as compared to WT rFX as determined by one-way ANOVA and Dunnett's multiple comparison post-test. Error bars represent SEM ($n = 4$ /group).

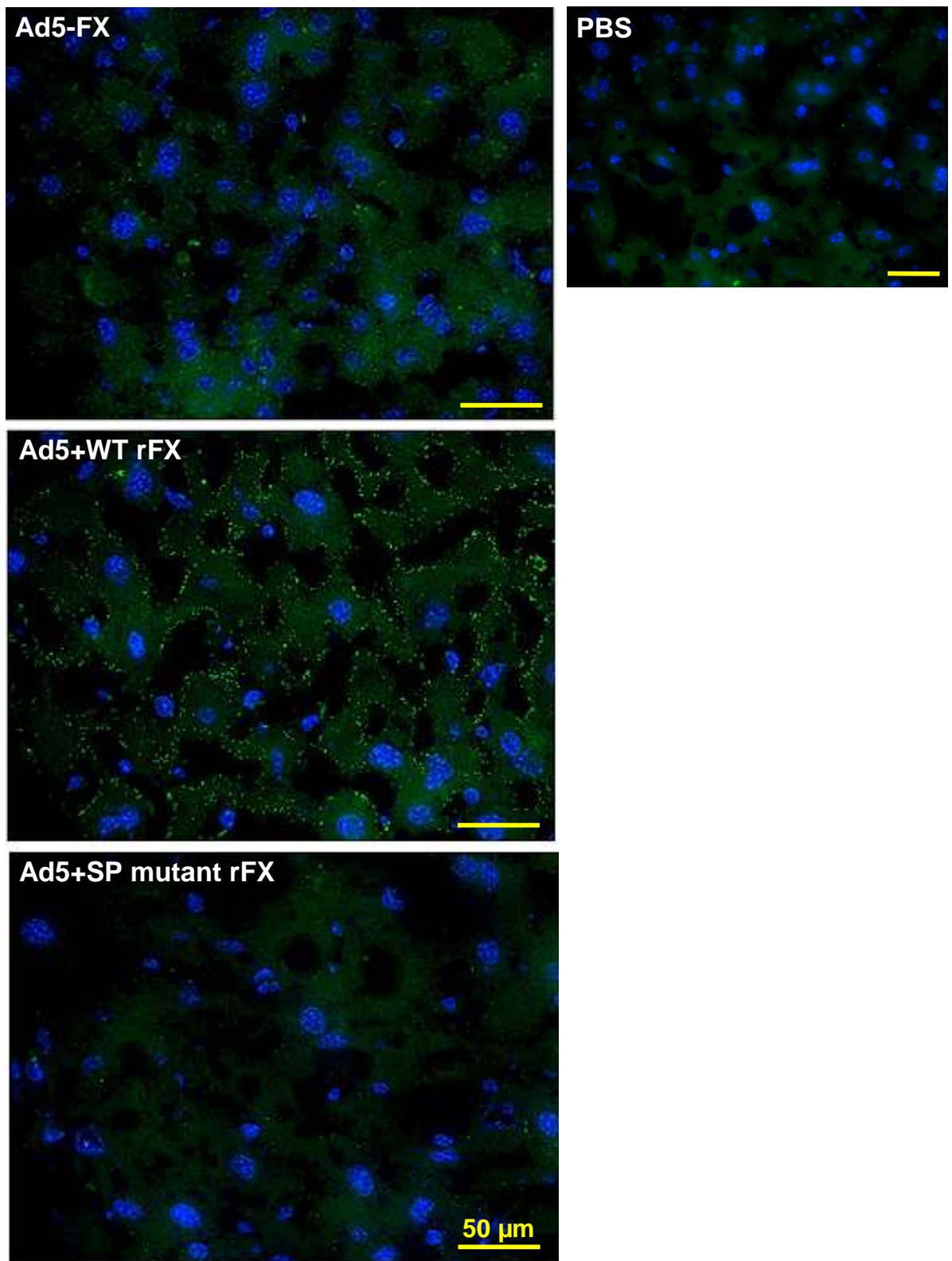


Figure 3.20. Effect of mutations on Ad5 binding to liver sections *ex vivo*.

Liver slices from MF-1 mice were incubated with PBS (negative control) or 2×10^9 vp of Alexa Fluor-488 fluorescently-labelled Ad5 in the absence or presence of WT or SP mutant rFX. Images captured at 40x magnification, scale bar = 50 μ m, applicable to all panels.

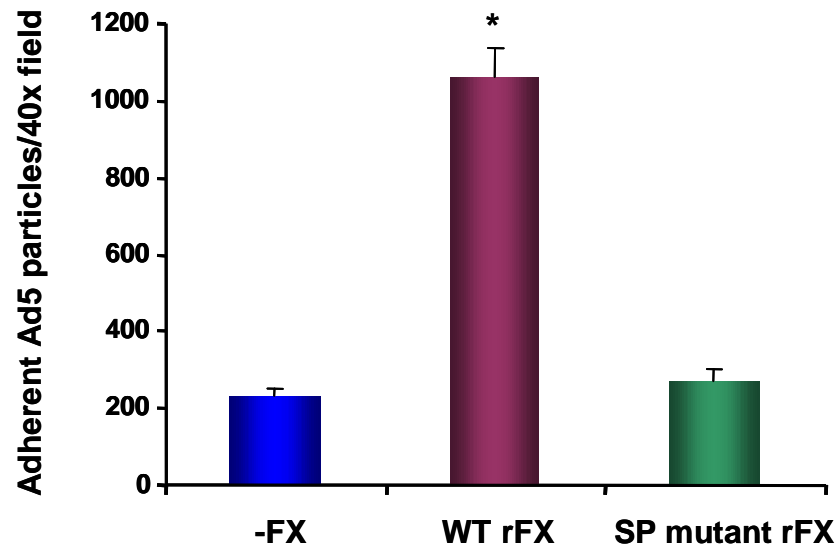


Figure 3.21. Quantification of Ad5 binding to liver sections *ex vivo*

Attachment of Ad5 particles to liver slices were quantified using ImageJ counting software. Data represents the average number of particles by analysing at least six separate 40x microscope fields per experimental condition. * $p < 0.05$ as compared to non-FX conditions as determined by one-way ANOVA and Dunnett's multiple comparison post-test. Error bars represent SEM ($n = 6/\text{group}$).

3.3 Discussion

This study investigated the precise mechanism by which the Ad5:FX complex interacts with HSPGs by identifying the critical receptor interacting residues in the FX SP domain. Site-directed mutagenesis of residues Arg-93, Lys-96, Arg-125, Arg-165, Lys-169, Lys-236 and Arg-240 was carried out in order to assess the contribution of these residues in Ad5:FX binding to the cell surface. Previous studies have employed similar mutagenesis techniques to investigate the involvement of these seven basic residues of FX for binding specific ligands (Monteiro *et al.*, 2008; Monteiro *et al.*, 2005; Rezaie, 2000). It was determined that unlike FXa in which the same residues are readily accessible by heparin, these amino acids in FX consist of a HBPE (Monteiro *et al.*, 2008; Monteiro *et al.*, 2005; Nogami *et al.*, 2004). To note, this is similar to that reported for the heparin binding site (also known as thrombin-anion binding exosite 2) in thrombin and the partially exposed thrombin-anion binding exosite 1 in prothrombin, again suggesting a precursor state in the zymogen (Liu *et al.*, 1991; Sheehan *et al.*, 1994).

In order to test the effects of the mutated HBPE, firstly the recombinant protein was produced by WT or SP mutant FX plasmid transfection into HEK 293T cells. Prior to purification the rFX protein was at concentrations ranging from 0.1 µg/ml to 0.4 µg/ml after 4-5 days. These yields are relatively low compared to other studies in which concentrations of up to 5 µg/ml after 24 h were achieved (Camire *et al.*, 2000; Rudolph *et al.*, 1997). The biosynthesis of FX is a complex process, involving extensive co- and post-translational modifications including glycosylation, γ -carboxylation and β -hydroxylation. These involve the removal of the signal sequence, the propeptide and the internal tripeptide and the addition of N- and O- linked oligosaccharides to the heavy chain. The 11 glutamic acid residues in the Gla domain undergo γ -carboxylation by the vitamin-K dependent γ -glutamyl carboxylase located in the endoplasmic reticulum, a process directed by the propeptide. In addition, the EGF-1 domain contains an aspartic acid (Asp63) which is post-translationally modified to β -hydroxyaspartic acid (McMullen *et al.*, 1983).

Next, the rFX protein was purified and validated. The protein was immunoaffinity purified using the calcium-dependent 4G3 mouse monoclonal antibody coupled to a sepharose column. SPR, Coomassie gel and western blot analysis confirmed the generation of purified rFX protein of the correct molecular weight (59 kDa), similar to the FX positive control (Furie *et al.*, 1988). Production of FX in HEK cells and purification using a calcium-dependent monoclonal antibody has previously been shown to have functional

properties almost indistinguishable to plasma purified FX (Rudolph *et al.*, 1997). Therefore, this expression system is useful for producing FX variants to correlate structure and function. In order to test the functionality of the rFX, amidolytic activity assays were carried out. There was no difference in the amidolytic activity of the SP mutant relative to WT rFX. This suggests the mutagenesis of the HBPE residues did not alter tissue factor and FVIIa activation and therefore did not effect the catalytic pocket of FXa, as is in concordance with previous studies (Rezaie, 2000). In relation to this, Parker *et al.* demonstrated that zymogen activation to FXa is not required for the FX-mediated increase in Ad5 gene transfer (Parker *et al.*, 2006).

It was necessary to ascertain whether the mutations in the FX SP domain caused any effect on the FX Gla domain binding to the Ad5 hexon. SPR analysis indicated that the WT or SP mutant rFX bound to hexon in a calcium-dependent manner, suggesting the mutations did not hinder the direct interaction with the virus. Human FX has previously been reported to bind to Ad5 in the presence of calcium and readily dissociate upon the addition of EDTA (Parker *et al.*, 2006; Waddington *et al.*, 2008). As both WT and SP mutant rFX bound to the hexon and there was no significant difference in the binding response units, these data also indirectly suggest the glutamic acid residues of the Gla domain were efficiently γ -carboxylated, a process necessary for calcium-dependent binding.

In recent years the Ad5:FX pathway has been the focus of several studies, accumulating data on the effects of FX on Ad5 binding and gene transfer (Kalyuzhniy *et al.*, 2008; Parker *et al.*, 2006; Waddington *et al.*, 2008). It has been well documented that Ad5:FX complex binding to the cell surface of hepatocytes is mediated by HSPGs (Bradshaw *et al.*, 2010; Parker *et al.*, 2006; Waddington *et al.*, 2008). In addition, several other pathogens also exploit HSPGs as primary attachment receptors for infection *in vivo*, including human papilloma virus (Johnson *et al.*, 2009), herpes simplex virus (Shukla *et al.*, 1999), human immunodeficiency virus-1 (Endress *et al.*, 2008) and adeno-associated virus (Summerford *et al.*, 1998). Moreover, FIX but not FX has been demonstrated to efficiently mediate binding of Ad18 and Ad31, to HSPGs (Jonsson *et al.*, 2009; Lenman *et al.*, 2011). FIX binds to the hexon protein of species A Ad18 and Ad31 but not Ad12 to enhance cell surface binding and gene transfer (Lenman *et al.*, 2011). Therefore, using confocal microscopy the interaction of fluorescently-labelled Ad5 with HSPGs when complexed with WT or the SP mutant rFX was assessed. As expected in the presence of WT rFX there were an abundance of viral particles at the cell surface which colocalised with HSPGs (Bradshaw *et al.*, 2010; Parker *et al.*, 2006), whilst in the presence of SP mutant rFX there

was no colocalisation, closely resembling conditions in the absence of FX. This qualitative report was further confirmed by qPCR, showing a significant decrease in Ad5 cellular binding in the presence of SP mutant compared to WT rFX. These data support the previously demonstrated function of HSPGs in Ad infection, and indicates the inability of SP mutant rFX to mediate binding to these cellular receptors, thereby supporting a role for the HBPE in bridging the Ad5:FX interaction to the cell surface.

Subsequently, the effects of FX mutagenesis on Ad5 cell binding, internalisation and cytosolic transport in cell trafficking assays were analysed. In the presence of human FX, Ad5 has been shown to bind to the cell surface, internalise and efficiently traffic toward the nucleus, reaching the MTOC by as early as 15 min and by 1 h approximately 90% of cells had viral particles colocalised with the MTOC (Bradshaw *et al.*, 2010). In this study, fluorescently-labelled Ad5 in the presence of positive control FX or WT rFX efficiently trafficked toward the nucleus, with > 80% Ad5:MTOC colocalisation by 1 h, whereas in the absence of FX or the presence of the SP mutant rFX surface binding and cytosolic trafficking was abolished.

Several studies have employed heparin to demonstrate the role of HSPGs as primary attachment receptors, which is structurally very similar to heparin sulphate (HS) side chains but displays higher general sulfation and therefore acts as a competitive inhibitor (Bradshaw *et al.*, 2010; Lenman *et al.*, 2011). In addition, heparinase which cleaves HS side chains has been used to inhibit HS-mediated viral attachment (Boyle *et al.*, 2006; Bradshaw *et al.*, 2010; Lenman *et al.*, 2011; O'Donnell *et al.*, 2009). In the present study the ability of the rFX proteins to enhance Ad5 gene transfer in the absence and presence of soluble heparin was investigated. In agreement with previous data, Ad5 transduction was enhanced in the presence of control FX in SKOV3 and HepG2 cells (Alba *et al.*, 2009; Parker *et al.*, 2006; Waddington *et al.*, 2008). In contrast, the SP mutant rFX caused no significant increase in gene transfer compared to conditions in the absence of FX. FX-mediated Ad5 gene transfer was ablated in the presence of soluble heparin, as in agreement with previous work (Bradshaw *et al.*, 2010). There was also a significant decrease in gene transfer under non-FX and SP mutant conditions, in the presence of heparin versus in its absence. Earlier work by Dechecchi *et al.* has demonstrated a role for HSPGs for Ad5 and Ad2 in non-FX-mediated cellular binding (Dechecchi *et al.*, 2001; Dechecchi *et al.*, 2000). This was initially thought to be due to an interaction with a ${}_{91}\text{KKTK}_{94}$ motif in the Ad fiber shaft, but later found that mutation of this motif instead hinders efficient intracellular trafficking (Kritz *et al.*, 2007).

It should be pointed out that whilst previous studies have demonstrated a very low affinity for FX to interact with heparin due to the precursor state of heparin binding residues, heparin efficiently blocked Ad5:FX mediated transduction (Bradshaw *et al.*, 2010; Nogami *et al.*, 2004). This may simply be due to the inaccessibility of the HSPGs in the presence of heparin. However, heparin possesses a very similar structure to HSPGs, the attachment receptors for Ad5:FX complexes, thus perhaps indicating a conformational change in the catalytic domain of FX upon binding to Ad5 which exposes the HBPE. Currently this is solely a hypothesis but may warrant additional investigation.

In order to further dissect the interaction, the effects of single and double point mutations in the FX HBPE on Ad5 transduction *in vitro* were assessed. The double point mutations R93A_K96A, R125A, R165A_K169A and K236A_R240A were chosen due to their relative positions in the FX construct and orientation in the 3D model of the human FX SP domain. As mentioned previously rFX yields were low following plasmid transfections. Due to time restraints, stable cell lines producing these rFX derivatives were not generated. The ability of FX to enhance Ad5 gene transfer at concentrations below physiological levels was shown in this study as well as others (Parker *et al.*, 2006; Zaiss *et al.*, 2011). Therefore, we tested the effects of the four rFX mutants R93A_K96A, R125A, R165A_K169A and K236A_R240A at a concentration of 10 ng/ml for effects on Ad5 gene transfer in SKOV3 cells. As before, the SP mutant rFX showed significantly lowered levels of Ad5 gene transfer compared to WT rFX. rFX with mutations at positions 93 and 93 as well as positions 125, 236 and 240 showed a significant decrease in Ad5 transduction compared to WT rFX. This indicates that the residues Arg-93, Lys-96, Arg-125, Lys-236 and Arg-240 but not Arg-165 and Lys-169 play a fundamental role in Ad5:FX binding to the cell surface. Of interest, four of these residues Arg-93, Arg-125, Lys-236 and Arg-240 were bound by both NAPc2 and Ixolaris, which effectively blocked Ad5 binding and transduction *in vitro* and *in vivo* (Monteiro *et al.*, 2008; Monteiro *et al.*, 2005; Murakami *et al.*, 2007; Waddington *et al.*, 2008). In addition future studies investigating the roles of Arg-93, Lys-96, Arg-125, Lys-236 and Arg-240 using individually mutated FX constructs could further evaluate the contribution of each of these amino acid residues in this interaction.

To investigate whether the role of the HBPE in FX-mediated Ad5 infection translates to a more physiological setting, a previously established *ex vivo* liver model was used (Bradshaw *et al.*, 2010). Attachment of fluorescently-labelled Ad5 particles to mouse liver sections was significantly increased in the presence of WT rFX. This result is in agreement

with previously published data (Bradshaw *et al.*, 2010). However in the presence of SP mutant rFX, Ad5 binding to mouse livers was not enhanced, thereby indicating that residues in this HBPE have a critical role in FX-mediated Ad5 cellular binding *ex vivo*. Due to time constraints and the low yields of FX produced, *in vivo* analysis of the involvement of the FX HBPE in Ad5 hepatic gene transfer was not performed. Ideally, if sufficient quantities were available, 10 µg/ml of the WT or mutated rFX proteins would be injected into warfarin-treated mice 30 min prior to the injection of Ad5. At 48 h post-administration the levels of Ad5 gene transfer would be assessed to investigate if the HBPE mutations in FX abrogated FX-mediated liver transduction *in vivo*.

A number of studies suggesting methods to improve rFX production involve cotransfection of certain intracellular processing enzymes required for efficient biosynthesis (Camire *et al.*, 2000; Drews *et al.*, 1995; Preininger *et al.*, 1999). FX requires efficient post-translational endoproteolytic processing for production of the mature FX protein. One such approach aimed at achieving full propeptide cleavage from recombinant vWF involves co-expression of the endoprotease furin with vWF in Chinese hamster ovarian cells (Drews *et al.*, 1995; Plaimauer *et al.*, 2001; Preininger *et al.*, 1999). This may be another viable approach to enhancing rFX protein production.

Previous studies have shown the ability of physiological concentrations of FIX, FVII and protein C to enhance Ad5 transduction *in vitro*, however only FX was demonstrated to fully restore Ad hepatic gene transfer in warfarin-treated mice (Parker *et al.*, 2006; Waddington *et al.*, 2008). Sequence comparisons revealed that the seven residues within the HBPE of FX were not conserved across the other vitamin K-dependent coagulation factors (Figure 3.22). When FX is compared to FVII, FIX or protein C six of the seven residues in the serine proteases differ. This may imply differences in binding to HSPGs *in vivo* could be due to the lack of a conserved HBPE. In addition, human FX demonstrated a greater ability to mediate Ad5 hepatic gene transfer in mice compared to murine FX (Zaiss *et al.*, 2011). The sequence alignment of human and murine FX demonstrates the four residues in the HBPE, R165, K169, K236 and R240, are conserved (Figure 3.23). The remaining three residues are charge conserved (i.e. Arg-Lys or Lys-Arg) thus maintaining positive charge. Analysis of heparin-sepharose binding of Ad5 suggested that human FX complexed with Ad5 has a greater affinity for HSPGs than Ad5: murine FX, which may contribute in differences in their ability to enhance Ad5 transduction both *in vitro* and *in vivo* (Zaiss *et al.*, 2011).

Understanding the precise infectivity pathways of Ad5 is important to its successful development and optimisation as a clinical gene therapy vector. This study has concentrated on gaining a greater knowledge of the mechanism of Ad5:FX complex engagement with the cell surface. In this study, FX HBPE mutant constructs were generated and functional rFX produced in order to study the importance of the seven proexosite residues for Ad5:FX binding to HSPGs. SPR analysis of recombinant protein demonstrated that the SP mutations had no effect on FX-specific binding to the Ad5 hexon, however FX-mediated binding and transduction was ablated both *in vitro* and *ex vivo*. Taken together, this study uncovers the HBPE to have a fundamental involvement in FX-mediated Ad5 complex engagement with HSPGs at the surface of target cells and broadens the knowledge of a key *in vivo* tropism determining pathway.

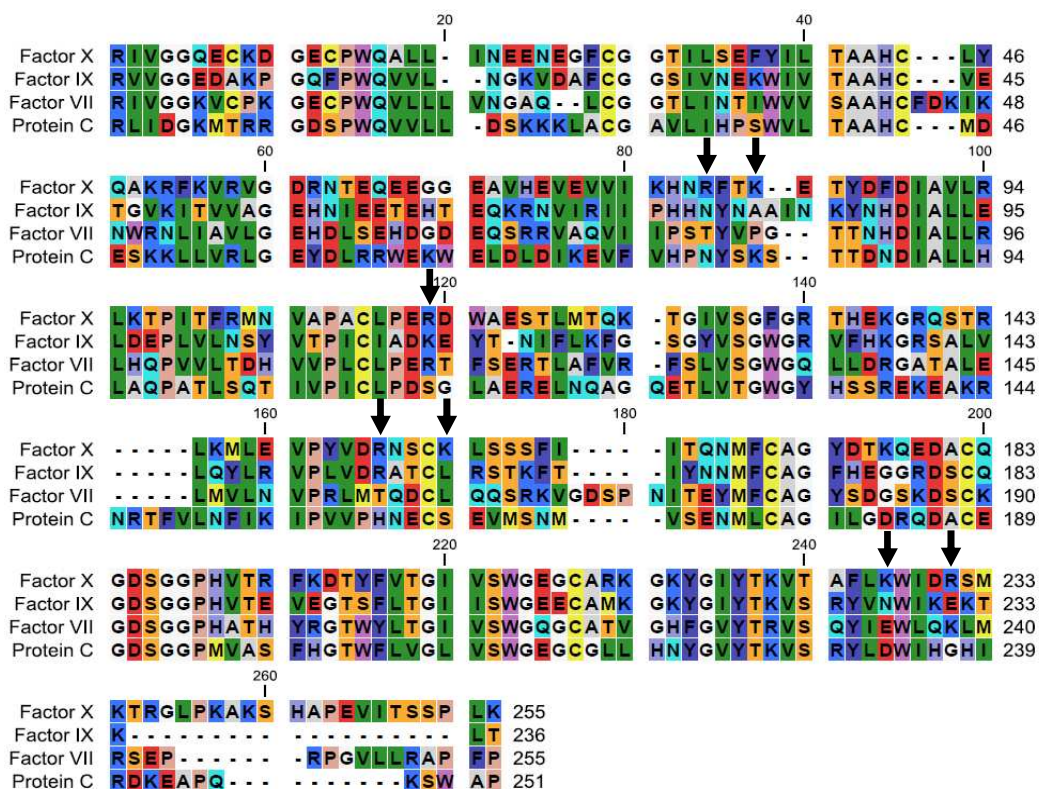


Figure 3.22. Sequence alignments of human FX, FVII, FIX and protein C.

Sequences for the SP domains of human FX, FVII, FIX and protein C were obtained for the Swiss-Prot database. Arrows point to the residues within the HBPE of human FX.

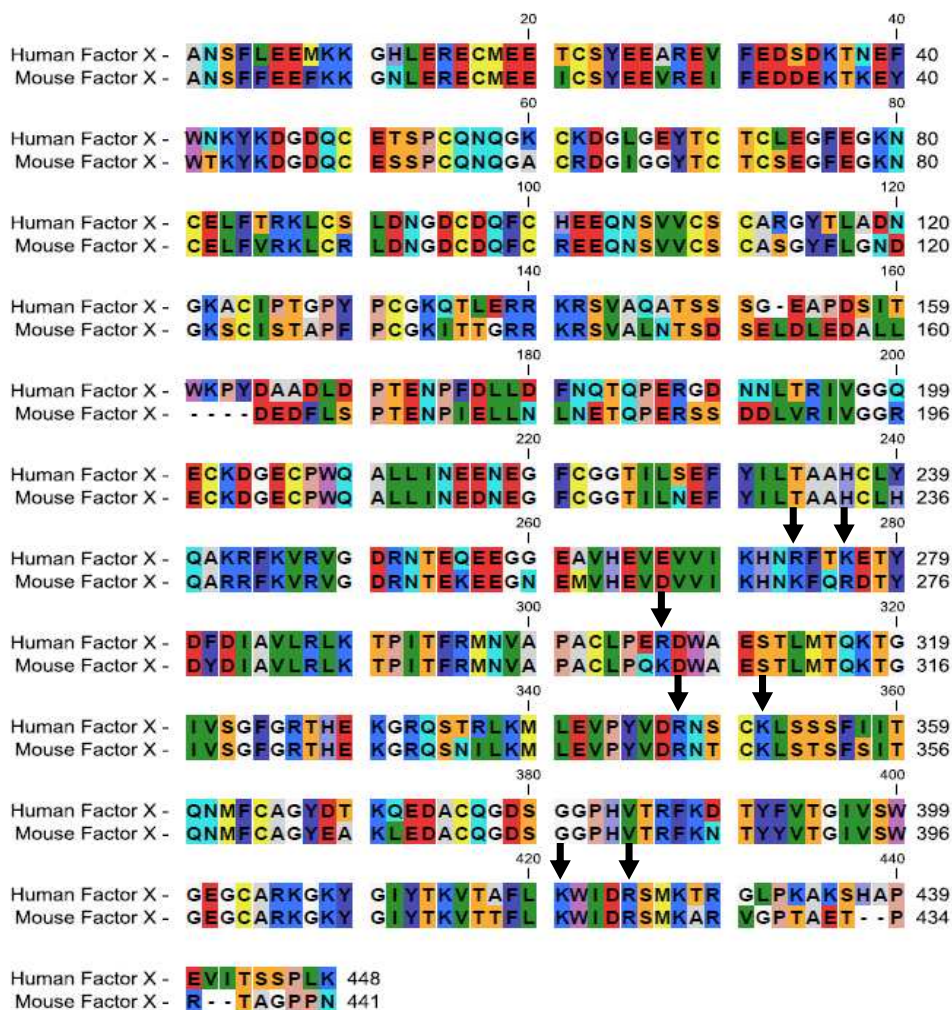


Figure 3.23. Sequence alignments of human FX and murine FX.

Human and murine FX sequences were obtained for the Swiss-Prot database and annotated using CLC Protein Workbench 5. Arrows point to the amino acid residues within the HBPE of human FX.

Chapter 4

Assessing the effects of a panel of small molecule inhibitors of cellular kinases on FX-mediated Ad5 transduction

4.1 Introduction

A great deal of research has been devoted to investigating the early stages of Ad5 cell entry and infection, the majority of which is based around the uptake of Ad5 via the classical *in vitro* pathway, initiated by the virus docking to CAR (Bergelson *et al.*, 1997). The activation of surface receptors initiates multiple virus-induced cell signaling pathways, host cell responses to incoming virus particles and viral uncoating events (Burckhardt *et al.*, 2011; Farmer *et al.*, 2009; Greber *et al.*, 1993; Li *et al.*, 1998a; Nakano *et al.*, 2000). Whilst CAR-mediated Ad5 infectivity has been extensively studied, the post-binding events governing FX-mediated Ad5 intracellular transport and gene expression have not been fully characterised.

In vitro, following engagement of the Ad5 fiber knob with CAR, the cytoplasmic domain of CAR activates p44/42 MAPK, which in turn promotes CAR clustering at the plasma membrane (Farmer *et al.*, 2009). When cells were preincubated with a MEK 1/2 inhibitor, integrin activation and CAR-induced cell adhesion to $\alpha v\beta 3$ ligands were prevented, indicating a secondary role for p44/42 MAPK in integrin localisation (Farmer *et al.*, 2009). Binding of the pentameric penton base to integrin receptors also promotes integrin clustering which in turn initiates signalling cascades involving kinases such as PI3K and protein kinase A (PKA) (Li *et al.*, 1998b; Suomalainen *et al.*, 2001). Pharmacological inhibition of PI3K, using the compounds wortmannin or LY293002 inhibit Ad5 internalisation and gene transfer, indicating its requirement for efficient Ad5 infection (Li *et al.*, 1998b). Recent work also demonstrates the ability of CAR to mediate clustering of JAML and recruit PI3K (Verdino *et al.*, 2010). A further study utilised pharmacological agents to inhibit PKA activity or the p38MAPK inhibitor SB203580, which disrupted cytoplasmic motility and prevented effective nuclear targeting of incoming Ad5 (Suomalainen *et al.*, 2001). Inhibition of protein kinase C has also been shown to affect membrane trafficking of Ad5 by preventing viral escape from endosomes (Nakano *et al.*, 2000). It is clear that intracellular signalling molecules play an important role in virus internalisation, actin cytoskeleton polymerisation and microtubule-dependent motility during Ad5 infectivity and thereby act as important regulators of early virus-host interactions (Li *et al.*, 1998b; Nakano *et al.*, 2000; Suomalainen *et al.*, 2001).

Initial engagement of Ad5 particles to cellular receptors elicits viral motion along the plasma membrane, three types of which exist; diffusive motions, drifting motions, and confinement (Burckhardt *et al.*, 2011). Studies by Wodrich *et al.* and Burckhardt *et al.*

demonstrated that viral uncoating is initiated at the cell surface, caused by the drifting motions mediated by CAR combined with the immobile integrins confining such movement (Burckhardt *et al.*, 2011; Wodrich *et al.*, 2010). This dual action results in the shedding of viral fibers as well as exposing protein VI, an internal Ad capsid protein that possesses membrane lytic activity (Burckhardt *et al.*, 2011). A study by Bradshaw *et al.* demonstrated a requirement for an intact penton base RGD motif for optimal post-attachment cell entry via the FX pathway, thus indicating the interaction with cellular integrins as co-receptors for internalisation is retained (Bradshaw *et al.*, 2010). However, the involvement of integrins in Ad capsid disassembly and signalling in the FX pathway requires further investigation.

Following CAR and integrin receptor engagement and the initial stages of viral uncoating, virus endocytosis takes place, primarily via the formation of clathrin coated vesicles regulated by adaptor protein complex 2 and the GTPase dynamin (Figure 4.1) (Boucrot *et al.*, 2010; Varga *et al.*, 1991; Wang *et al.*, 1998). Subsequently, the low pH of the endosomes acts as a trigger for further viral disassembly and membrane penetration (Greber *et al.*, 1993), contributed to by the activation of PKC and the viral protease (Medina-Kauwe, 2003). In the endosomes the lytic factor, protein VI, remains partially associated with the viral capsid as Ad travels towards the nucleus (Wodrich *et al.*, 2010). Rab5 is a regulator of clathrin-mediated endocytosis of Ad5 and vesicle fusion with early endosomes (Rauma *et al.*, 1999). Bradshaw *et al.* demonstrated colocalisation of Ad5 particles with the early endosomal markers Rab5 and the Rab5 effector protein early endosome antigen 1 (EEA1) 15 min post-infection following incubation with FX in SKOV3 cells (Bradshaw *et al.*, 2010), indicative of a correlation between the CAR and FX-mediated intracellular pathways. Lysis of the endosomes leads to viral escape and the cytosolic Ad5 is then engaged in bidirectional microtubule-based transport (Suomalainen *et al.*, 1999). The minus ends of microtubules are located in the perinuclear area, while plus ends extend toward the cell periphery. Ad5 is transported along the microtubule cytoskeleton in a minus-ended directed movement towards the MTOC, as a result of Ad5 hexon directly binding to dynein intermediate and light chains (Bremner *et al.*, 2009; Kelkar *et al.*, 2004; Suomalainen *et al.*, 1999). FX-mediated Ad5 cell transport also appears to follow a similar pattern of trafficking, with accumulation of viral particles at the MTOC by 60 min post-infection (Bradshaw *et al.*, 2010). When the virus disassembles from the microtubules it reaches the nuclear pore complex (NPC) (Greber *et al.*, 1997). At this point the Ad genome disengages from the capsid, through attachment to nuclear histone 1

binds to the CAN/Nup214 receptor, and the viral DNA is imported into the nucleus (Trotman *et al.*, 2001) (Figure 4.1).

Understanding the precise mechanism of viral MTOC release and transport to the nuclear pores has been at the centre of several investigations. It has been suggested that this process may occur due to a switch in motor proteins, from dynein- to kinesin-mediated transport (Henaff *et al.*, 2011). A recent study by Strunze *et al.* demonstrated that kinesin-1, which directs viral particles towards the plus end of microtubules disrupted Ad capsids bound to the NPC and the NPC itself, thereby releasing capsid fragments in the cytoplasm and increasing nuclear envelope permeability, thus facilitating nuclear import of viral DNA (Strunze *et al.*, 2011). Other studies have implicated a critical role for protein VI in efficient nuclear targeting. Protein VI encodes a proline rich PPxY motif (where x can be any amino acid) which recruits ubiquitin ligases, Nedd4.1 and Nedd4.2, and mutation of this motif does not affect capsid morphology, membrane penetration and endosomal escape but the virus particles are defective in microtubule-dependent trafficking and genome delivery to the nucleus (Wodrich *et al.*, 2010). As with several steps of early Ad infection these processes may not be mutually exclusive but act in cohort to result in efficient gene transfer.

It is evident that over the years an abundance of data has accumulated based on CAR-mediated Ad5 cell entry, signalling and intracellular transport. Whilst recent studies have shown similarities in intracellular trafficking following engagement of Ad5:FX to cellular HSPGs, whether there is general overlap between Ad5 capsid uncoating, intracellular transport and signalling via both pathways requires further elucidation. Thus, gaining a greater understanding of the early stages of Ad5 infection via FX bridging the virus to HSPGs is an important step in improving the knowledge of this pathway. The present study employs a series of pharmacological interventions *in vitro* to investigate cellular and signalling events occurring during FX-mediated Ad5 infection.

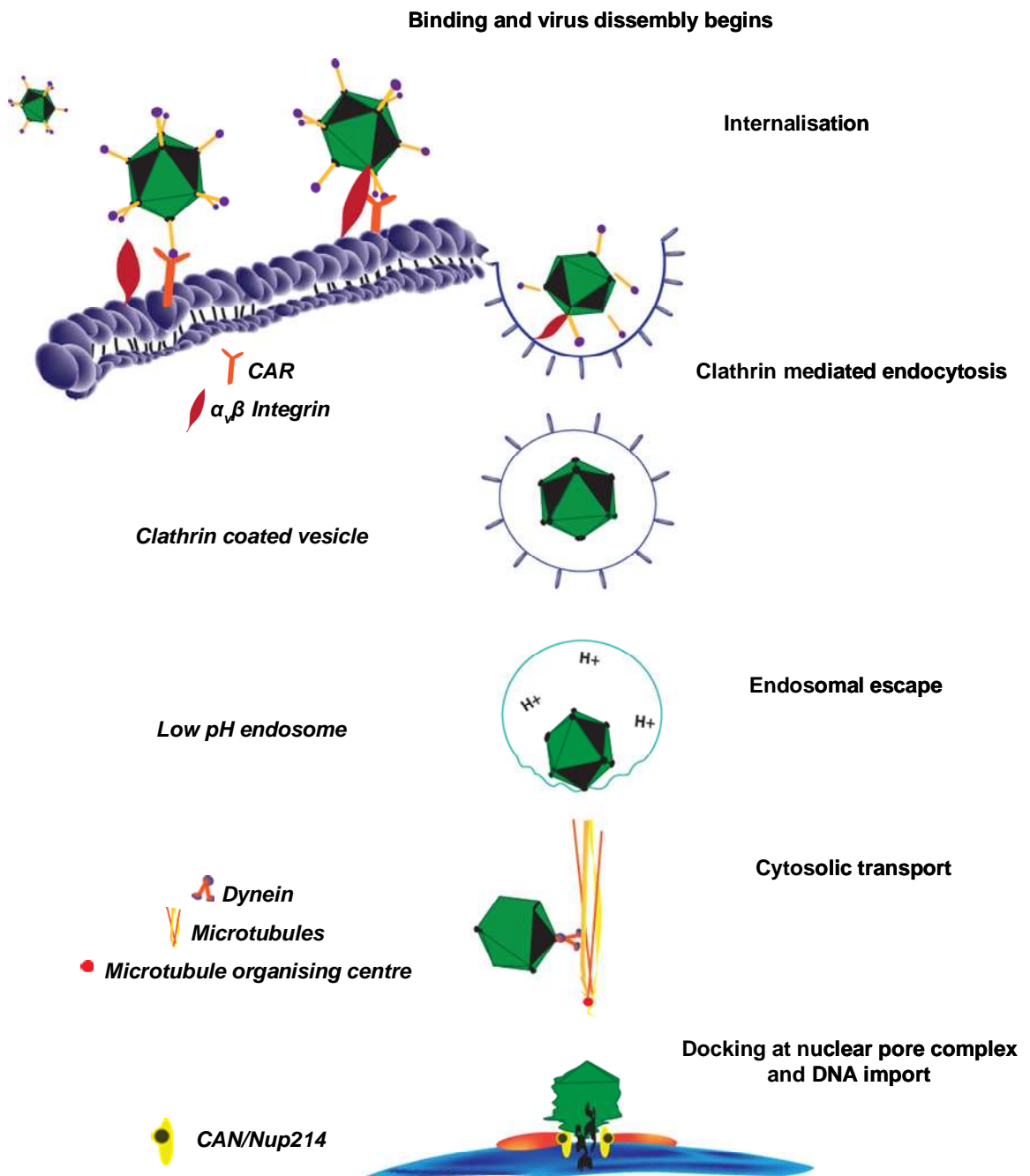


Figure 4.1. Ad5 infectivity pathway.

In vitro Ad5 uses CAR as its primary attachment receptor, this promotes binding of the penton base RGD motif to $\alpha\beta$ integrins. This then triggers clathrin-mediated endocytosis and partial virus disassembly. Ad5 enters the low pH endosomes, pVI is released and the endosomes are lysed. Cytosolic Ad5 binds dynein and is transported along microtubules towards the MTOC. The virus docks to the nuclear pore complex receptor CAN/Nup214 and the viral DNA is imported into the nucleus for subsequent transcription and replication.

4.2 Results

4.2.1 Role for PKA, PI3K and p38MAPK in FX-mediated Ad5 intracellular transport

The effect of kinase inhibitors that have previously been reported to affect cell entry and intracellular transport of Ad via the CAR pathway were analysed for effects on FX-mediated Ad5 cellular trafficking (Li *et al.*, 1998b; Suomalainen *et al.*, 2001). Human adenocarcinomic alveolar basal epithelial A549 cells were preincubated with the PKA inhibitor H89 dihydrochloride (40 μ M), the PI3K inhibitor LY 294002 hydrochloride (100 μ M) or the p38 MAPK inhibitor SB 203580 (10 μ M). Cells were then exposed to Ad5 in the presence of FX and the kinase inhibitors for 1 h at 4°C to allow for cellular binding, followed by 3 h at 37°C, providing sufficient time for virus internalisation and transport to the MTOC. Using confocal microscopy the effects of each of the kinase inhibitors on FX-mediated Ad5 cytosolic transport was visually assessed. By 180 min Ad5 trafficking to the MTOC was disrupted in the presence of all inhibitors. Unlike the control conditions, in the presence of the compounds the virus did not colocalise in a punctuate spot at the MTOC, but instead formed a diffuse pattern around the perinuclear region. When colocalisation of Ad5 with the MTOC was quantified it was found to be significantly reduced in the presence of FX by coincubation with PKA, PI3K or p38 MAPK inhibitors (Figure 4.2). This suggests a requirement for these kinases for efficient Ad5 intracellular trafficking via FX-mediated Ad5 infection.

4.2.2 Screening a library of kinase inhibitors for effects on FX-mediated Ad5 gene transfer

A collection of 80 different kinase inhibitors were investigated for their effects on FX-mediated Ad5 transduction in SKOV3 cells (Table 4.1). The Tocris Kinase Inhibitor Toolbox library was a kind gift from Dr. Jo Mountford (University of Glasgow) who obtained the set from Tocris Bioscience. The library was designed to selectively target a diverse range of cellular kinases. SKOV3 cells express very low levels of CAR (Kim *et al.*, 2002) and therefore allow for a more specific investigation of the Ad5:FX pathway. All kinase inhibitors were screened at the same dose of 20 μ M for the first 3 h, followed by 10 μ M for the remainder of the assay. This shift in concentrations was primarily to accommodate experimental design. Of the 80 kinase inhibitors tested, 23 caused a significant reduction in FX-mediated Ad5 transduction and exhibited no significant difference compared to levels of Ad5 transduction in non-FX control conditions, as

assessed by β -galactosidase expression at 48 h post-infection and subsequent statistical analysis (Figure 4.3). These consisted of a wide range of divergent kinase inhibitors including; I κ B kinases, protein kinase C, TGF- β type I receptor activin receptor-like kinases, epidermal growth factor receptor, rho-kinase, spleen tyrosine kinase, checkpoint kinases, cyclin-dependent kinases, met kinase, mitogen activated protein kinase, Akt kinase, glycogen synthase kinase 3 and c-Jun N-terminal kinases. However, as the same dose of each inhibitor was applied to the cells, many of the described inhibitors were found to cause substantial cytotoxicity as visually assessed, therefore were excluded from additional analysis. ER-27319 is an inhibitor of spleen tyrosine kinase (Syk) (Moriya *et al.*, 1997). This compound significantly reduced FX-mediated Ad5 transduction (Figure 4.3). When quantified, this inhibitor caused approximately 35% decrease in cell viability compared to untreated control conditions after coincubation with cells for 48 h (Figure 4.4). Syk has not previously been described in relation to Ad5 infection, therefore this inhibitor was chosen for further studies as it blocked Ad5:FX gene transfer with a minimally toxic effect.

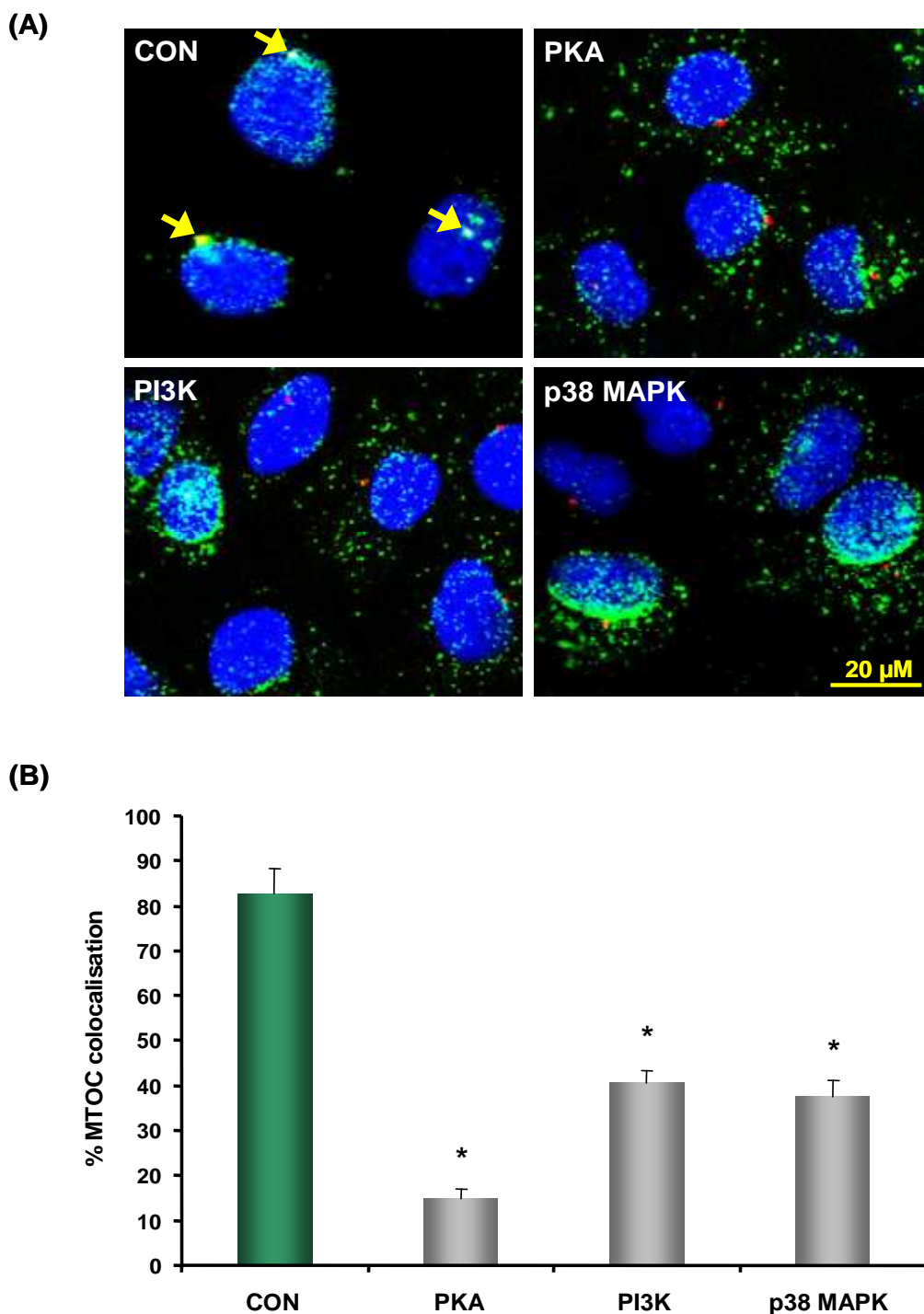


Figure 4.2. Ad5 transport in the presence of PKA, PI3K and p38MAPK inhibitors.

(A) A549 cells were incubated with PKA, PI3K or p38MAPK inhibitors for 30 min at 37°C then 10,000 vp/cell of Alexa Fluor-488-labelled Ad5 (green) in the presence of FX and the different kinase inhibitors were allowed to bind cells for 1 h at 4°C, followed by incubation at 37°C for 3 h prior to fixation and staining for pericentrin (red). Examples of colocalisation of Ad5 with pericentrin are indicated by the yellow arrows. Scale bar = 20 µm, applicable to all images. (B) % cells with colocalisation of Ad5 with the MTOC marker pericentrin was calculated by analysing at least 5 separate 40x microscope fields per condition. * $p < 0.05$ as compared to control conditions as determined by one-way ANOVA and Dunnett's multiple comparison post-test. Error bars represent SEM ($n = 5/\text{group}$).

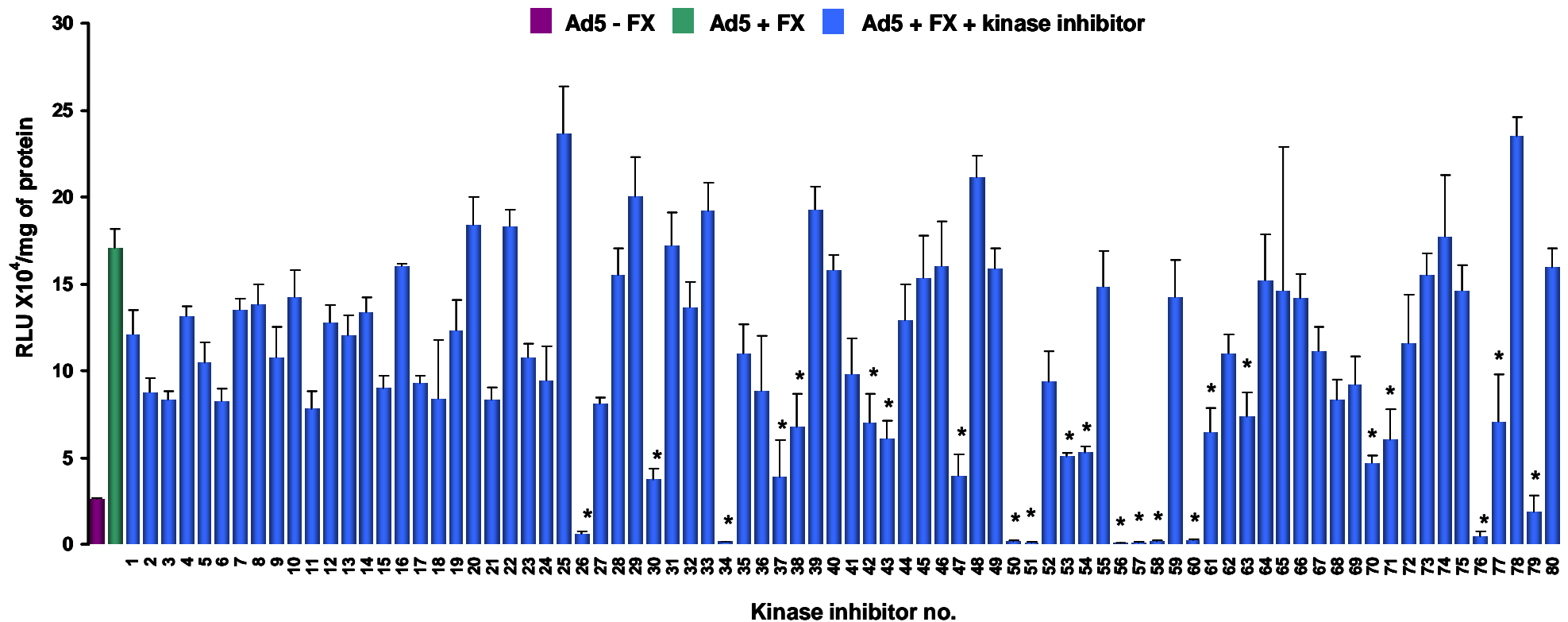


Figure 4.3. Effect of kinase inhibitors on FX-mediated Ad5 gene transfer.

SKOV3 cells were incubated with 20 μ M of each kinase inhibitor for 30 min at 37°C, washed, then incubated with 100 μ l serum free media with 1000 vp/cell Ad5 in the absence or presence of FX and 20 μ M kinase inhibitor for 3 h at 37°C, followed by the addition of 100 μ l media containing 20% serum and further incubation at 37°C. Ad5 transgene expression was quantified 48 h post-infection. Kinase inhibitors are listed in Table 4.1 *p<0.05 as compared to plus FX conditions and not significantly greater than minus FX conditions, as determined by one-way ANOVA and Bonferroni's multiple comparison post-test. Error bars represent SEM (n = 4/group).

Table 4.1. Kinase inhibitor library.

List of the 80 kinase inhibitors from the Tocriscreen™ Kinase Inhibitor Toolbox'.

No.	Compound Name	Main target
1	AG 490	EGFR
2	ML 9 hydrochloride	MLCK
3	AG 213	EGFR and PDGFR
4	Fasudil hydrochloride	CDK and ROCK
5	GF 109203X	PKC
6	Genistein	EGFR
7	LY 294002 hydrochloride	PI3K
8	U0126	MEK
9	PD 98059	MEK
10	Y-27632 dihydrochloride	p160ROCK
11	SB 202190	p38 MAPK
12	Olomoucine	CDK
13	LFM-A13	BTK
14	ZM 336372	c-Raf
15	ZM 449829	JAK3
16	ZM 39923 hydrochloride	JAK3
17	GW 5074	c-Raf1
18	PP 1	Src
19	SB 203580 hydrochloride	p38MAPK
20	(-)- Terreic acid	BTK
21	PP 2	Src
22	SU 4312	VEGFR
23	SP 600125	JNK
24	Purvalanol A	CDK
25	Purvalanol B	CDK
26	Rottlerin	PKC
27	SB 431542	TGF-βRI ALK5
28	SB 216763	GSK-3
29	SB 415286	GSK-3
30	Arctigenin	IκBα
31	NSC 693868	CDK, GSK-3
32	SB 239063	p38 MAPK
33	SL 327	MEK1 and MEK2
34	Ro 31-8220 mesylate	Broad spectrum
35	Aminopurvalanol A	CDK
36	API-2	Akt
37	GW 441756	NGF receptor tyrosine kinase A (TrkA)
38	GW 583340 dihydrochloride	EGFR
39	Ro 08-2750	NGF
40	TBB	CK2
41	1,2,3,4,5,6-Hexabromocyclohexane	JAK2

42	HA 1100 hydrochloride	ROCK
43	BIBX 1382 dihydrochloride	EGFR
44	CGP 53353	PKC
45	Arcyriaflavin A	CDK4/cyclin D1
46	ZM 447439	Aurora B
47	ER-27319	Syk
48	ZM 323881 hydrochloride	VEGFR-2/KDR
49	ZM 306416 hydrochloride	VEGFR
50	IKK 16	IKK
51	Ki 8751	VEGFR
52	10-DEBC hydrochloride	Akt/PKB
53	TPCA-1	IKK
54	SB 218078	ChK1
55	TCS 359	FLT3R
56	PD 198306	MEK
57	Ryuvidine	CDK 4
58	IMD 0354	IKK
59	CGK 733	ATR, ATM
60	PHA 665752	cMET
61	PD 407824	ChK1, Wee1
62	LY 364947	TGF- β RI
63	CGP 57380	MAPK
64	PQ 401	IGF1R
65	PI 828	PI3K
66	NU 7026	DNA-PK
67	D 4476	CK1 and TGF- β RI ALK5
68	EO 1428	p38MAPK
69	H 89 dihydrochloride	PKA
70	FPA 124	Akt
71	GW 843682X	PLK
72	Iressa	EGFR
73	SU 5416	VEGFR
74	1-Naphthyl PP1	Src
75	Dorsomorphin dihydrochloride	AMPK
76	BIO	GSK-3
77	SD 208	TGF- β RI
78	Compound 401	DNA-PK
79	BI 78D3	cJNK
80	SC 514	IKK

Abbreviations: epidermal growth factor receptor (EGFR), myosin light chain kinase (MLCK), platelet-derived growth factor receptor (PDGFR), cyclic nucleotide-dependent protein kinase (CDK), rho-associated protein kinase (ROCK), protein kinase C (PKC), mitogen-activated protein kinase kinase (MAPK), mitogen-activated protein kinase/extracellular signal-regulated kinase kinase (MEK), rho-associated kinase (ROCK), Bruton's tyrosine kinase (BTK), Janus tyrosine kinase 3 (JAK3), c-Jun N-terminal kinase (JNK), transforming growth factor- β type I receptor (TGF β R1) activin

receptor-like kinase (ALK), glycogen synthase kinase-3 (GSK-3), nerve growth factor (NGF), casein kinase-2 (CK2), I κ B kinase (IKK), checkpoint kinase 1 (ChK1), polo-like kinase (PLK), vascular endothelial growth factor (VEGF), FMS-like tyrosine kinase 3 receptor (FLT3), insulin-like growth factor receptor (IGF1R), DNA-dependent protein kinase (DNA-PK).

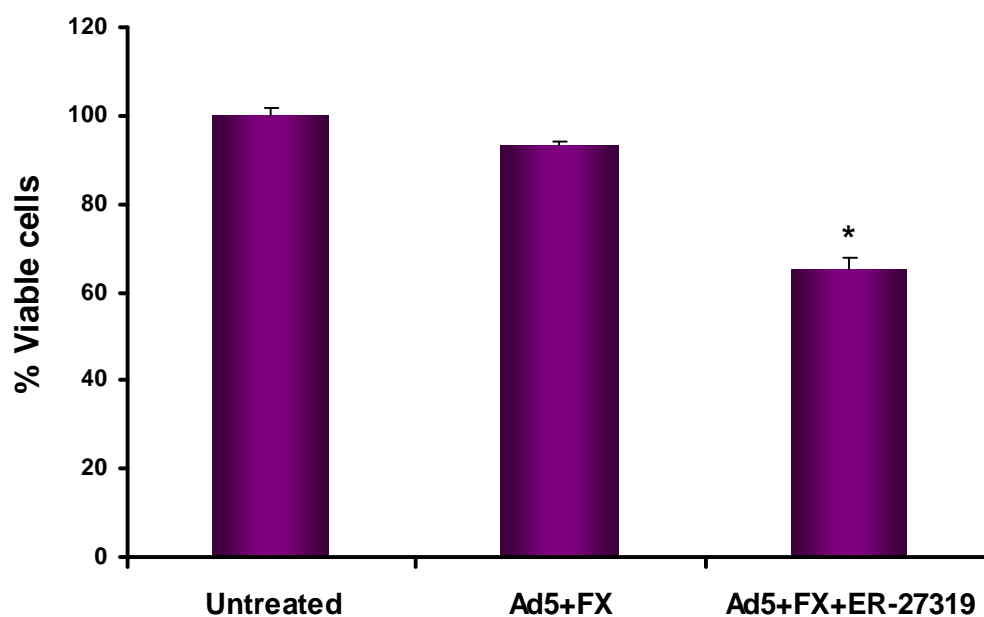


Figure 4.4. Effect of ER-27319 on cell viability after 48 h.

SKOV3 cells were infected with 1000 vp/cell of Ad5 in the presence of FX and 20 μ M ER-27319 for 3 h, followed by 10 μ M ER-27319 for a further 45 h, when a MTT assay was performed. * $p < 0.05$ as compared to Ad5+FX treated cells as determined by one-way ANOVA and Dunnett's multiple comparison post-test. Error bars represent SEM ($n = 4$ /group).

4.2.3 Effect of ER-27319 on FX-mediated Ad5 cell attachment and intracellular transport

The effect of ER-27319 on FX-mediated Ad5 cell attachment and intracellular trafficking was investigated. Firstly, Ad5 binding to SKOV3 cells was assessed. The compound resulted in no significant difference in cellular binding compared to control conditions in the absence or presence of FX indicating it acts at a post-entry level (Figure 4.5). Next, A549 and SKOV3 cells were incubated with 20, 50 or 100 μ M ER-27319 and fluorescently labelled-Ad5 in the presence of FX for 1 h at 4°C and then fixed after 15 min, 60 min or 180 min at 37°C. In both A549 and SKOV3 cells, virus binding to the cell surface and subsequent internalisation were not decreased in the presence of ER-27319, as assessed visually (Figure 4.6 and Figure 4.7). In the presence of FX control conditions, Ad5 trafficked efficiently toward the nucleus. By 60 min Ad5 was found to be colocalised with the MTOC, as stained for using the pericentrin marker. This is in contrast to cells incubated with ER-27319, in which Ad5 trafficking was observed to be substantially disrupted (Figure 4.6 and Figure 4.7). This was evident at all doses of ER-27319 but the effect was made more prominent as the dose was increased. In the presence of the kinase inhibitor the virus did travel toward the nucleus, however it accumulated within the perinuclear region and did not form punctuate colocalised spots with the MTOC staining but more diffusely around the nucleus. At 180 min, the pattern of Ad5 in the presence of ER-27319 remained dissimilar to control conditions, with the virus inhibited from fully colocalising with the MTOC and preventing efficient trafficking. The percentage of cells where complete MTOC:virus colocalisation did occur were quantified and the number of cells was found to be significantly decreased in the presence of ER-27319 demonstrating the ability of this compound to disrupt Ad5 intracellular transport compared to controls (Figure 4.8). Coincubation of cells with ER-27319 resulted in no displacement or abnormal staining of the MTOC as shown by immunocytochemistry experiments staining with an antibody against pericentrin. Concentrations of up to 100 μ M ER-27319 have been used *in vitro* in previous publications (Moriya *et al.*, 1997). However, to ensure the effects on intracellular transport observed in this assay were not as a result of ER-27319 induced toxicity, we assessed the effects of such concentrations on cell viability at the 180 min time point. ER-27319 did have a negligible effect on cell viability at the higher concentration, however this did not reach statistical significance (Figure 4.9).

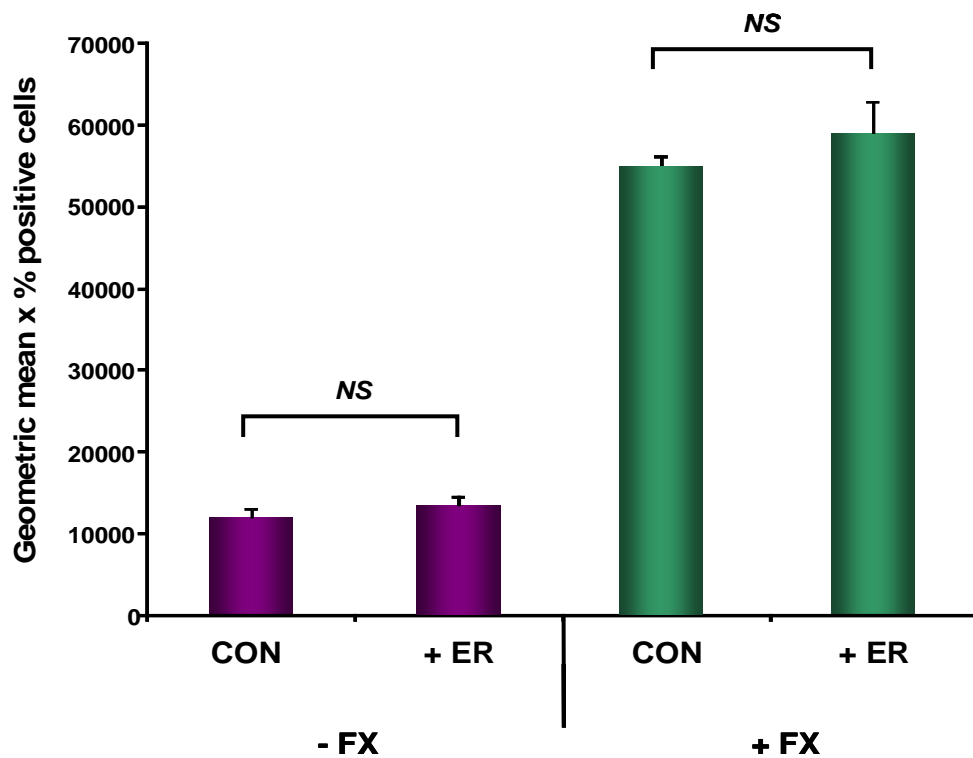


Figure 4.5. Effect of ER-27319 on Ad5 binding to SKOV3 cells.

SKOV3 cells were preincubated with 20 μ M ER-27319 for 30 min prior to the addition of 5000 vp/cell of Alexa488-labelled Ad5 in the absence or presence of FX. Fluorescently labelled Ad5 binding to cells was quantified by FACS analysis. *NS* = non significant, $p > 0.05$ as compared to matched control conditions as determined by one-way ANOVA and Dunnett's multiple comparison post-test. Error bars represent SEM ($n = 4$).

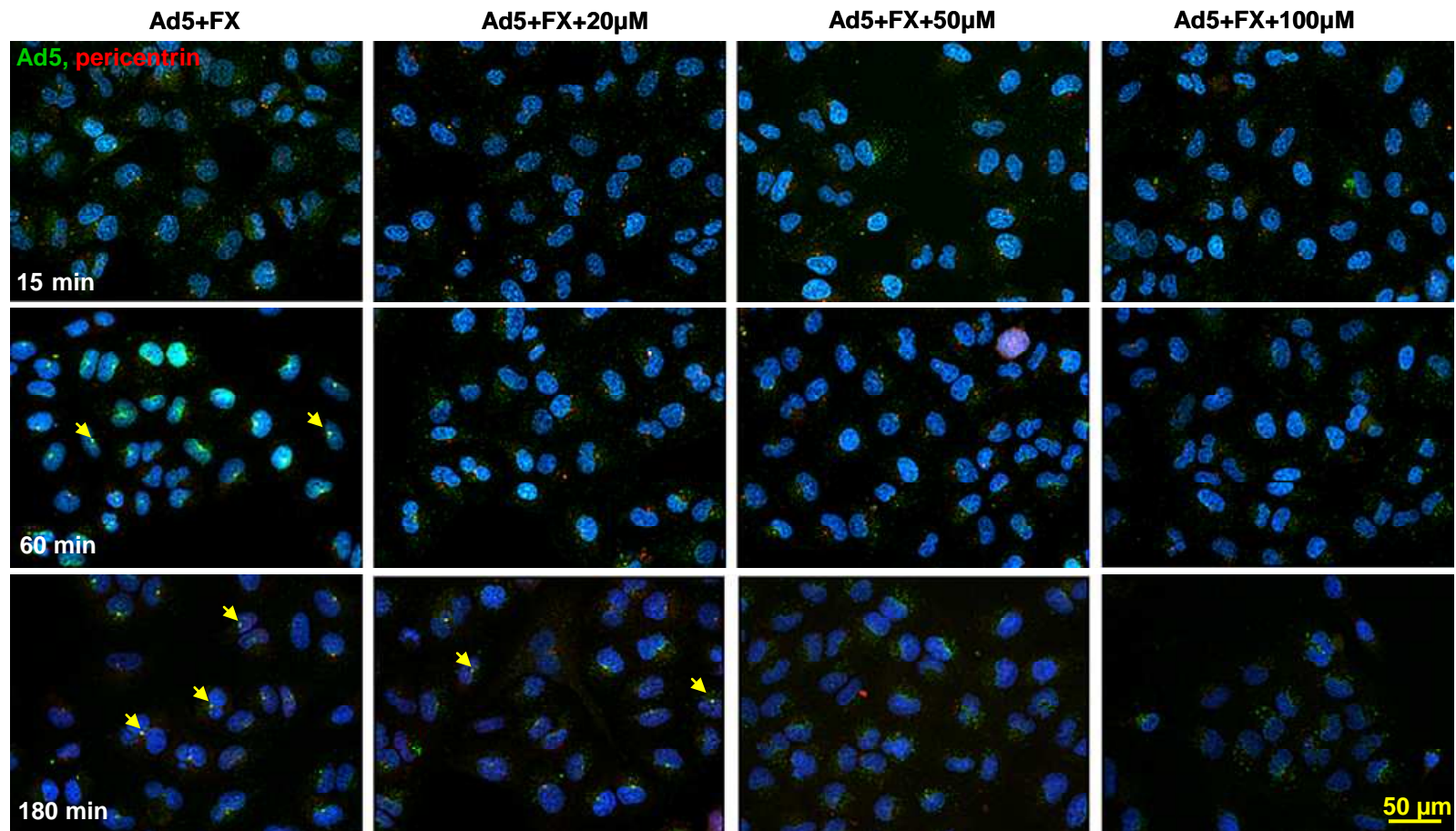


Figure 4.6. Effect of ER-27319 on FX-mediated Ad5 trafficking in A549 cells.

Cells were incubated with ER-27319 for 30 min at 37°C then 10,000 vp/cell of Alexa488-labelled Ad5 (green) in the presence of FX and ER-27319 were added for 1 h at 4°C, followed by incubation at 37°C for 1 h or 3 h prior to staining for pericentrin (red). Examples of fluorescently-labelled Ad5 colocalisation with pericentrin are indicated by yellow arrows. 63x magnification, scale bar = 20 µm, applicable to all images.

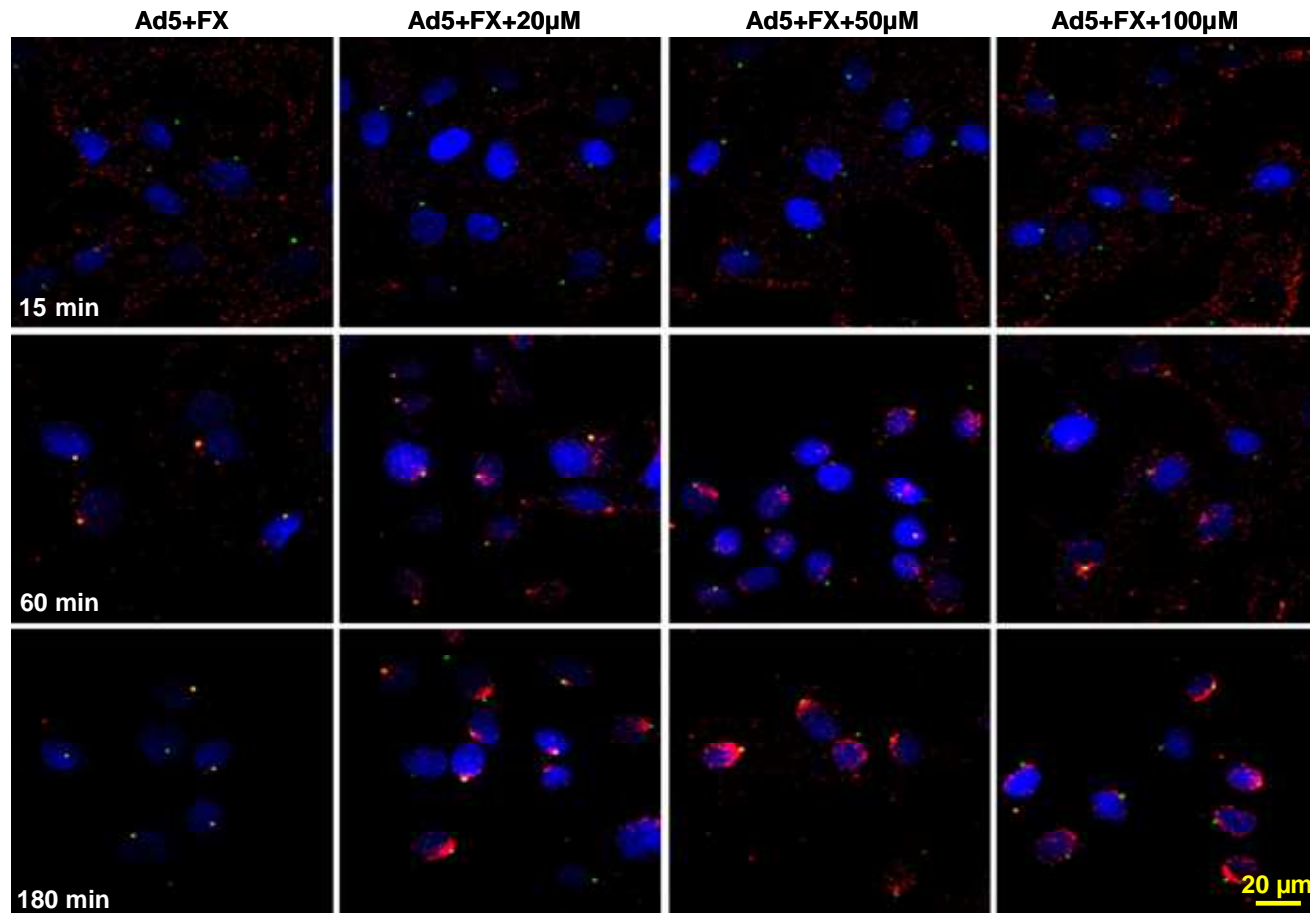


Figure 4.7. Effect of ER-27319 on FX-mediated Ad5 trafficking in SKOV3 cells.

Cells were incubated with ER-27319 for 30 min at 37°C then 10,000 vp/cell of Alexa555-labelled Ad5 (green) in the presence of FX and ER-27319 were added for 1 h at 4°C, followed by incubation at 37°C for 1 h or 3 h prior to staining for pericentrin (red). 63x magnification, scale bar = 20 µm, applicable to all images.

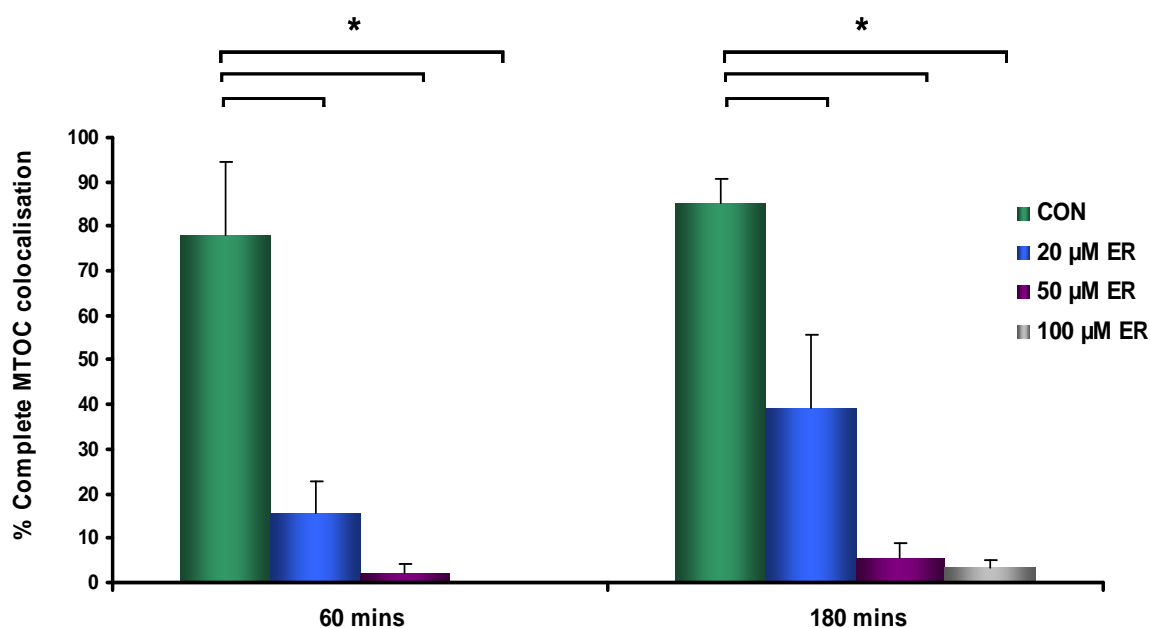


Figure 4.8. Effect of ER-27319 on Ad5 colocalisation with the MTOC.

The percentage of SKOV3 cells with complete colocalisation of Ad5 with pericentrin was calculated by analysing at least 5 separate 40x microscope fields per experimental condition. * $p < 0.05$ as compared to control conditions at the individual time points as determined by one-way ANOVA and Dunnett's multiple comparison post-test. Error bars represent SEM ($n = 5$).

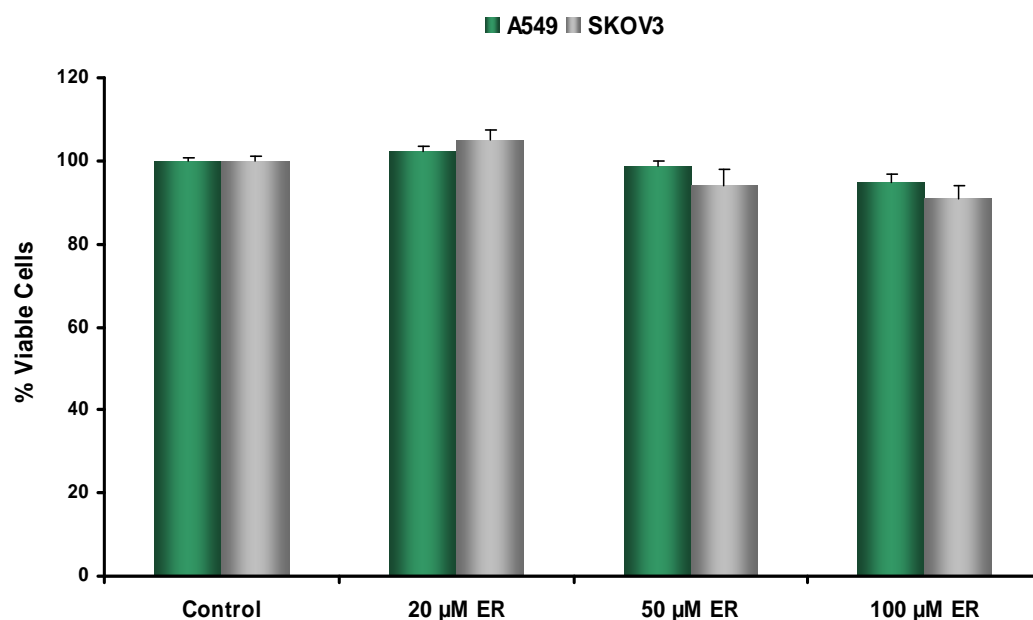


Figure 4.9. Effect of ER-27319 on cell viability after 4 h.

Cells were incubated with 20 µM, 50 µM or 100 µM ER-27319 for 4 h and a cell viability MTT assay was performed. Error bars represent SEM ($n = 4$).

4.2.4 Effect of the Syk inhibitor BAY 61-3606 on FX-mediated Ad5 infectivity

To investigate whether the inhibition of Ad5:FX gene transfer caused by ER-27319 was as a result of the compound blocking Syk activity, the effects of an alternative Syk inhibitor, BAY 61-3606 (2-[7-(3,4-dimethoxyphenyl)-imidazo[1,2-c]pyrimidin-5-ylamino]-nicotinamide dihydrochloride), on FX-mediated Ad5 infectivity were analysed. The mechanisms of action of both compounds differ (Moriya *et al.*, 1997; Yamamoto *et al.*, 2003). ER-27319 is reported to inhibit the tyrosine phosphorylation of Syk induced by the IgE receptor, Fcε receptor I (FcεRI) in mast cells but not in human peripheral B cells, whilst the more potent and highly selective inhibitor BAY 61-3606 prevents Syk activity in an ATP competitive manner in mast cells and basophils and shows efficacy in monocytes and eosinophils (Moriya *et al.*, 1997; Yamamoto *et al.*, 2003). Therefore, fluorescently labelled-Ad5 binding and intracellular transport in the presence of FX and increasing doses of BAY 61-3606 were assessed in SKOV3 cells using confocal microscopy. Ad5 cellular binding and trafficking to the nucleus in the presence of the inhibitor did not differ to Ad5 plus FX control conditions (Figure 4.10). Next, the effect of BAY 61-3606 on FX-mediated Ad5 transduction in SKOV3 cells was analysed. There was no significant difference in Ad5 gene transfer in the absence or presence of the kinase inhibitor, hence BAY 61-3606 did not affect FX-mediated Ad5 infectivity (Figure 4.11).

4.2.5 Syk gene and protein expression

Syk expression at the gene and protein level was next analysed in SKOV3 and A549 cells. In these experiments human colorectal adenocarcinoma SW620 cells were employed as a positive control as previous studies have shown them to have high levels of Syk (Leroy *et al.*, 2009). First, relative expression of Syk was investigated by qRT-PCR performed on cDNA derived from the three cell types. qRT-PCR demonstrated high levels of Syk expression in positive control SW620 cells, whereas the presence of Syk in SKOV3 and A549 was undetectable (Figure 4.12). Western blot analysis was performed to assess the expression of the Syk protein in SW620, SKOV3 and A549 cell lysates. In concordance with the qRT-PCR results Syk was detected in SW620 cells, whilst both SKOV3 and A549 cell lysates were negative for Syk protein expression (Figure 4.12).

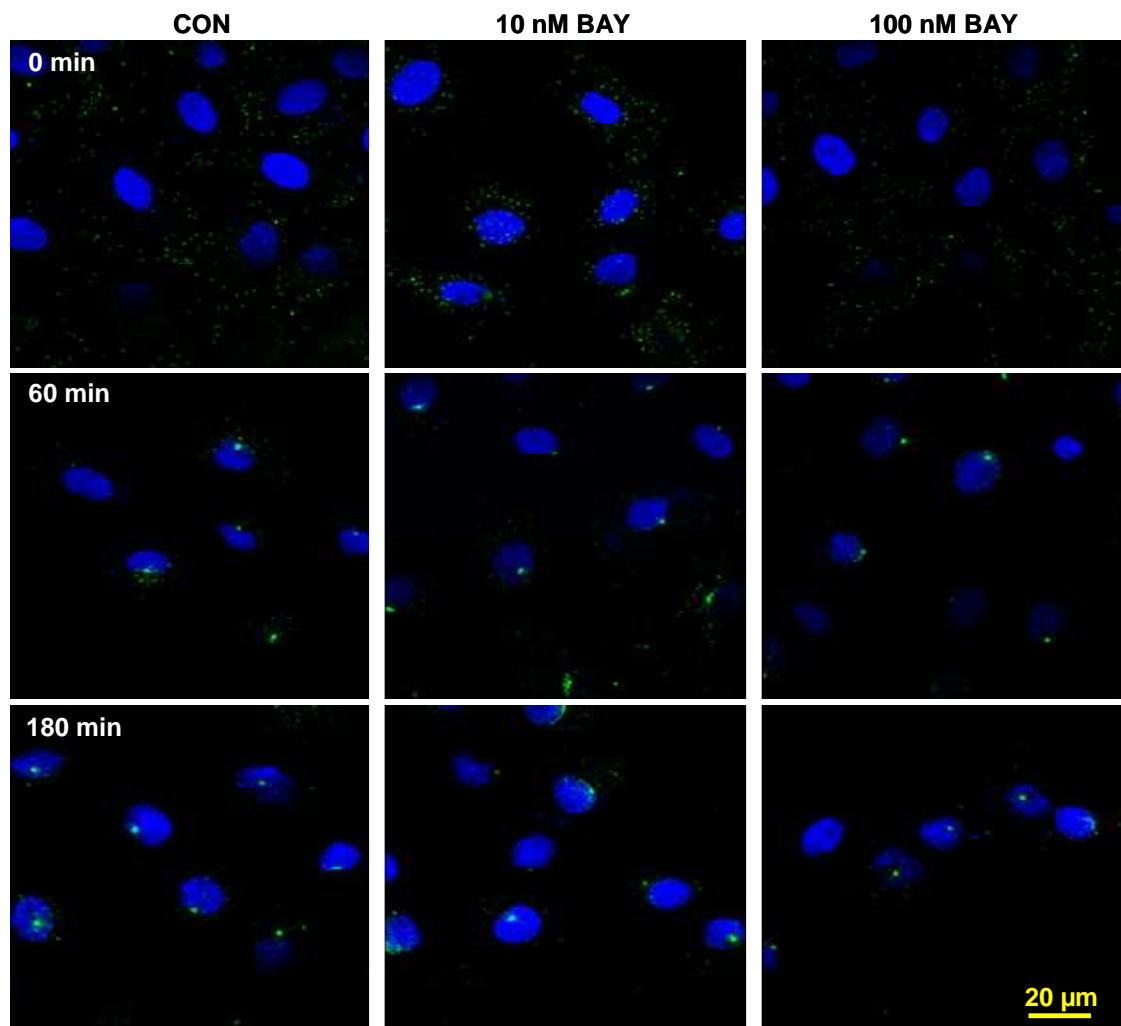


Figure 4.10. Effect of BAY 61-3606 on FX-mediated Ad5 intracellular transport.

SKOV3 cells were incubated with BAY 61-3606 for 30 min at 37°C, washed, then 10,000 vp/cell of Alexa488-labelled Ad5 (green) in the presence of FX with BAY 61-3606 were allowed to bind cells for 1 h at 4°C, followed by incubation at 37°C for 0, 60 or 180 min prior to fixation. 63x magnification, scale bar = 20 μm, applicable to all images.

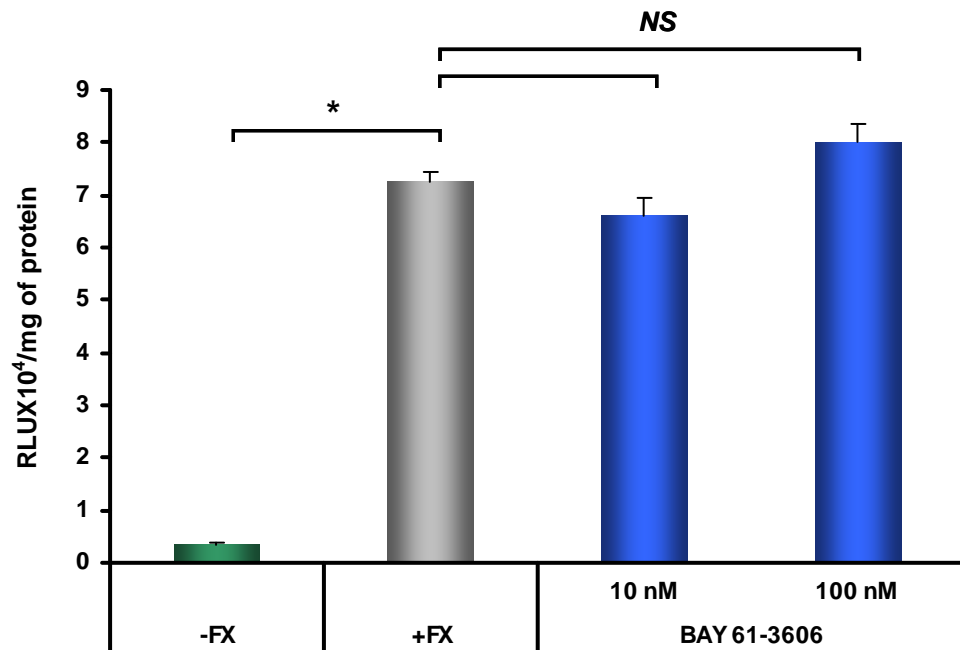
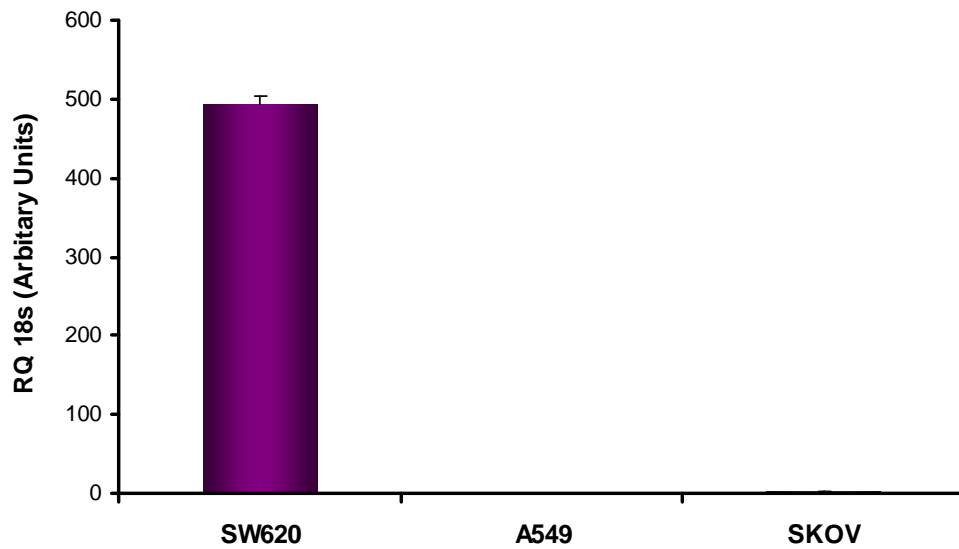


Figure 4.11. Effect of BAY 61-3606 on FX-mediated Ad5 transduction.

SKOV3 cells were incubated BAY 61-3606 for 30 min at 37°C, washed, then incubated with 1000 vp/cell Ad5 +/- FX and BAY 61-3606 for 3 h at 37°C. Ad5 transgene expression was quantified 48 h post-infection. Error bars represent SEM (n = 4). *p<0.05 as compared to plus FX conditions, as determined by one-way ANOVA and Dunnett's multiple comparison post-test. NS = non significant, p>0.05.

(A)



(B)

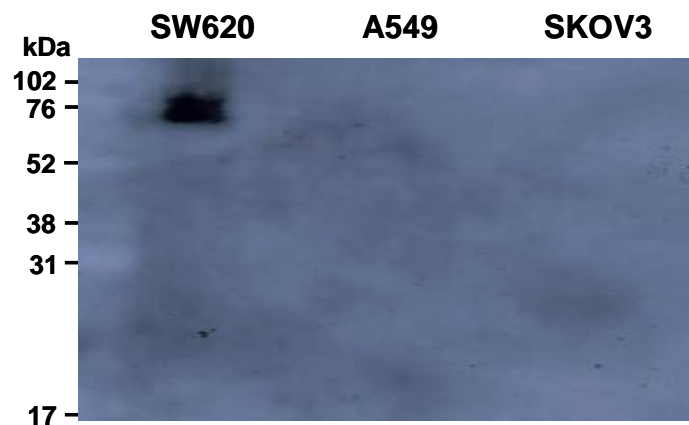


Figure 4.12. Syk kinase expression in SW620, A549 and SKOV3 cells.

(A) RNA was extracted from SW620, A549 and SKOV3 cells and converted to cDNA. qRT-PCR was performed on the samples to detect Syk. Error bars represent SEM (n = 4). (B) SW620, A549 and SKOV3 cell lysates were subjected to western immunoblotting and detection with an anti-Syk antibody. 70 μ g of each protein sample was loaded onto a 10% gel and Syk was probed with 2 μ g/ml of the primary mouse monoclonal anti-Syk antibody and a rabbit anti-mouse HRP secondary antibody (1:1000 dilution).

4.2.6 Mechanism of action of ER-27319

Through personal correspondence with Dr. Juan Rivera (National Institute of Health, Bethesda, Maryland, USA) additional information on the mechanism of action of ER-27319 was obtained. Dr. Juan Rivera was an author of the paper entitled “ER-27319, an acridone-related compound, inhibits release of antigen-induced allergic mediators from mast cells by selective inhibition of Fcε receptor I-mediated activation of Syk”. From this communication it was noted that ER-27319 does not bind directly to Syk or interfere with the Syk ATP binding site. The compound selectively binds to the immunoreceptor tyrosine-based activation motif (ITAM) of the FcεRI gamma subunit in mast cells and does not directly interfere with Syk activity (Figure 4.13). This ITAM is encoded for by the consensus amino acid sequence (D/E)-x-x-Y-x-x-(L/I)-(x_{n=6-8})-Y-x-x-(L/I) in which x can represent any amino acid. SKOV3 and A549 cells are reported to be negative for FcεRI expression, as documented on the NCI-60 database (http://dtp.nci.nih.gov/docs/misc/common_files/cell_list.html).

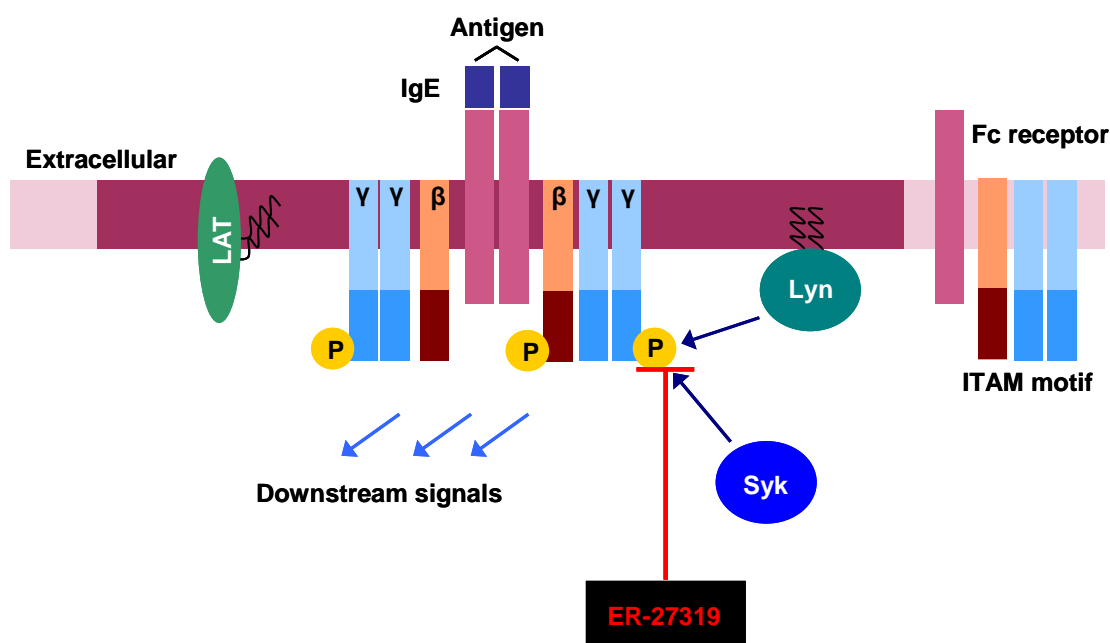


Figure 4.13. Mechanism of action of ER-27319 in mast cells.

Antigen-induced receptor dimerisation of the Fc receptor leads to phosphorylation of the receptors' ITAMs by Src-family protein tyrosine kinases (for example, Lyn, Lck and Fyn). Phosphorylated ITAMs act as a membrane docking site for cytoplasmic Syk. ER-27319 binds to the ITAMs of the FcεRI gamma subunit, thereby blocking the Syk binding site and preventing Syk from becoming activated.

4.2.7 ITAM-containing viral proteins

It was postulated that ER-27319 may be binding to an alternative ITAM-containing protein present in these cells or on Ad5 itself and thereby disrupting viral intracellular transport. Previous studies have reported ITAMs expressed in several viral proteins including the mouse mammary tumour virus (MMTV) envelope protein (Env) (Katz *et al.*, 2005), the Kaposi's sarcoma-associated herpesvirus (KSHV) K1 protein (Lee *et al.*, 1998), the Epstein barr virus (EBV) latent membrane protein 2A (LMP2A) (Fruehling *et al.*, 1997), the Simian Immunodeficiency Virus (SIV) negative regulatory factor protein (Dehghani *et al.*, 2002), the Bovine leukemia virus (BLV) gp30 protein, Hantaan virus G1 (Mou *et al.*, 2007) as well as several others. Therefore human Ad subgroup C protein sequences were analysed using the SwissProt database for the presence of conventional ITAM sequences and "ITAM-like" motifs with different numbers of residues (n) between the two Y-x-x-I/L modules. Sequence scanning of the Ad2 and Ad5 proteomes were performed in search of amino acids encoding for potential ITAMs. Two ITAM-like sequences were found on the hexon protein (Figure 4.14 and Table 4.3). Although previous work has described flexibility in the ITAM encoding sequence, neither of the potential Ad5 ITAMs strictly followed that reported for FcεRI gamma subunit, instead of the of the conventional 7 amino acid residues between the two Y-x-x-I/L modules as in FcεRI gamma, the hexon ITAM-like sequences expressed 17 or 22 amino acids (Table 4.3 and Figure 4.14).

Table 4.2. ITAM containing viral proteins.

Viral proteins encoding ITAM sequences. The canonical ITAM residues are highlighted in red.

Virus protein	Amino acid sequence	Reference
MMTV Env	AYDYAAIIVKRPPYVLL	(Katz <i>et al.</i> , 2005)
EBV LMP2A	HSDYQPLGTQDQSLYLGL	(Fruehling <i>et al.</i> , 1997)
BLV gp30	DSDYQALLPSAPEIYSHLSPTKPDYINL	(Reichert <i>et al.</i> , 2001)
SIV Nef	GDLYERLLRARGETYGRL	(Dehghani <i>et al.</i> , 2002)
Hantavirus-G1 (NY1)	GCYRTLGVFRYKSRCYVGL	(Humphrey <i>et al.</i> , 2005)
Rhadinovirus R1	HNEYNHLLNELNMIEQYDWL	(Damania <i>et al.</i> , 1999)

Table 4.3. Searching the Ad proteome for ITAMs.

The Ad5 proteome was scanned using the SwissProt database for the presence of ITAM sequences (Yxx(L/I)_{x_n}Yxx(L/I)). The canonical ITAM residues are highlighted in blue.

Ad capsid protein	Amino acid sequence	x(n length)
Hexon	QWSYMHISGQDASEYLSPGLVQFARATETYFSL	22
Hexon	ASTYFDIRGVLDRGPTFKPYSGTAYNAL	17

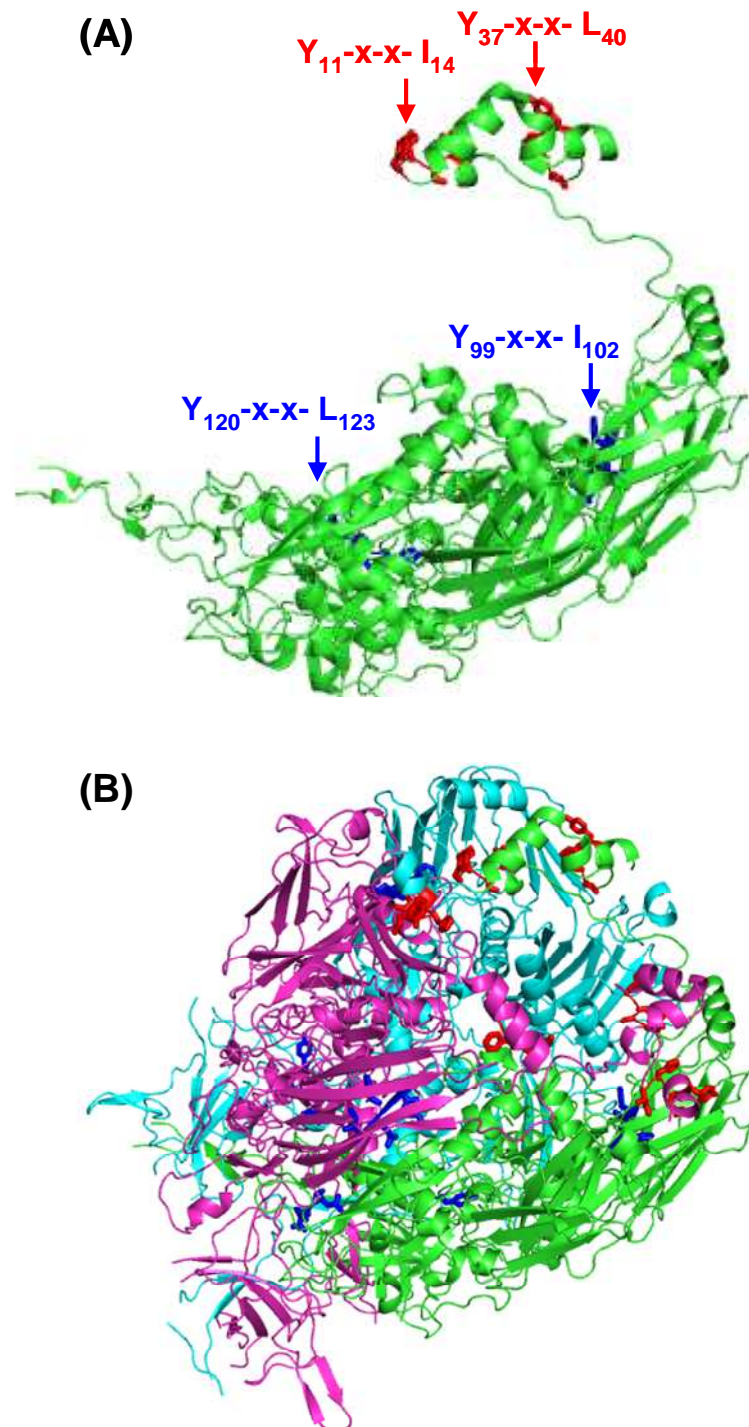


Figure 4.14. Ad5 hexon ITAMs.

(A) Ribbon diagram of an individual Ad5 hexon monomer (green) highlighting the positions of the four Yxx(L/I) amino acid motifs (blue and red). (B) Ribbon diagram of the Ad5 hexon trimer (monomers in green, cyan and pink) highlighting the relative positions of the ITAM-like motifs (blue and red). These images were generated using POLYVIEW-3D (<http://polyview.cchmc.org/polyview3d.html>) (Porollo *et al.*, 2007).

4.2.8 ITAM containing cellular proteins

By performing literature searches the presence of ITAM amino acid sequences in cellular proteins were investigated. These are described in Table 4.4. The NCI-60 database was employed to investigate the possible expression of these ITAM-containing cellular proteins in SKOV3 and A549 cells, as these cell types were used to define the original phenotypic effects. The proteins ezrin, radixin and moesin (ERM) were highlighted as the most likely ITAM-containing protein candidates to be present in SKOV3 and A549 cells, thus this ERM family of proteins were investigated further.

Table 4.4. ITAM-containing cellular proteins.

Proteins encoding ITAM sequences. Canonical ITAM residues are highlighted in red.

Protein	Amino acid sequence	Reference
CD3 γ	DQLYQP LKDREDDQYSHL	(Haks <i>et al.</i> , 2002)
CD3 δ	DQVYQP LRDRDDAQYSHL	(Dave <i>et al.</i> , 1997)
CD3 ϵ	NPDYEPI RKGQRDLYSGL	(Sommers <i>et al.</i> , 2000)
CD3 ζ -1	NQLYNE LNLGRREEYDVL	(Yudushkin <i>et al.</i> , 2010)
CD3 ζ -2	EGLYNE LQKDKMAEAYSEI	(Lysechko <i>et al.</i> , 2005)
CD3 ζ -3	DGLYQGL LSTATKDTYDAL	(Gil <i>et al.</i> , 2001)
Fc ϵ RI β	DRVYEEL NIYSATYSEL	(Furumoto <i>et al.</i> , 2004)
Fc ϵ RI γ	DGVYTG LSTRNQETYETL	(Sakurai <i>et al.</i> , 2004)
DAP12	ESPYQEL LQGQRSDVYSDL	(Lanier <i>et al.</i> , 2000)
Ig α	ENLYEGL NLDDCSMYEDI	(Kraus <i>et al.</i> , 2001)
Ig β	DHTYEG LDIDQTATYEDI	(Gazumyan <i>et al.</i> , 2006)
Merlin	EMEY LKI AQDLEMYGVNYFAI	(Barrow <i>et al.</i> , 2006)
Ezrin	MLEY LKI AQDLEMYGINYFEI	(Rozsnyay <i>et al.</i> , 1996)
Radixin	MMEY LKI AQDLEMYGVNYFEI	(Urzainqui <i>et al.</i> , 2002)
Moesin	VLEY LKI AQDLEMYGVNYFSI	(Urzainqui <i>et al.</i> , 2002)

4.2.9 Ezrin, radixin and moesin gene expression

ERM proteins are important regulators of the cell cortex, capable of interacting with both the plasma membrane and filamentous actin (Figure 4.15). Furthermore, these proteins can control signalling pathways through their ability to bind transmembrane receptors and link them to downstream signalling components (Dransfield *et al.*, 1997; Ruppelt *et al.*, 2007; Tang *et al.*, 2007). Ezrin, radixin and moesin gene expression in SKOV3 and A549 cells was therefore assessed. Expression was investigated by qRT-PCR performed on cDNA, derived from the both cell types. All three members of the ERM family were present in both SKOV3 and A549 cells (Figure 4.16). Moesin showed the highest levels of expression, in particular in SKOV3 cells. Ezrin was found to be more highly expressed in SKOV3 cells than A549s, whilst radixin was expressed in lower quantities in both cell types. Next ERM protein expression was assessed by western blot analysis. ERM proteins were expressed at the protein level in both SKOV3 and A549 cells (Figure 4.17).

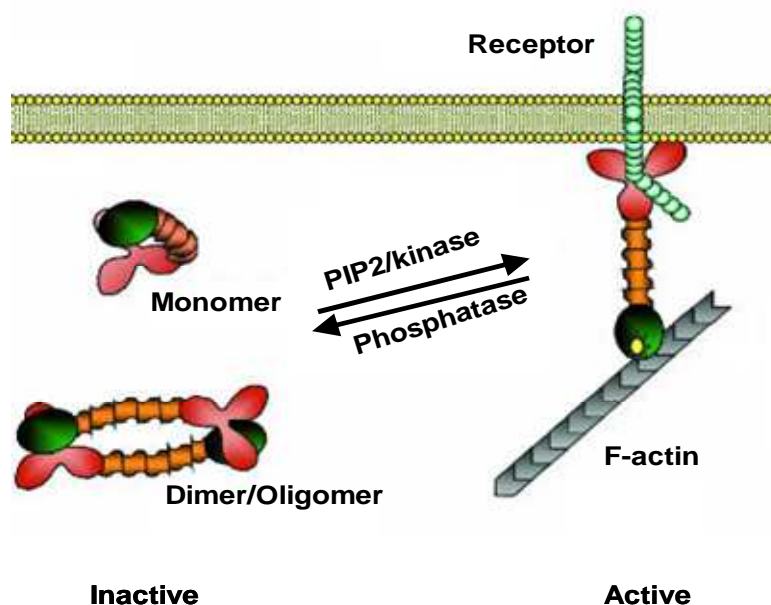


Figure 4.15. Schematic of ERM activation.

In the active conformation, the N-terminal domain of ERM proteins (red) binds to the C-terminal actin-binding domain (green). The α -helical domain is in orange. Phosphatidylinositol 4,5 bis-phosphate (PIP2) binding to the N-terminal and phosphorylation of the C-terminal induces and stabilises the unfolded active conformation, allowing the N-terminal domain to bind transmembrane receptors and the actin-binding domain to interact with actin filaments. This figure was adapted from Ivetic *et al.* (Ivetic *et al.*, 2004).

4.2.10 Effects of ER-27319 on ERM protein expression

The effects of ER-27319 on viral intracellular trafficking and the expression of ezrin, radixin and moesin were investigated. SKOV3 cells were incubated with ER-27319 and fluorescently labelled-Ad5 in the presence of FX for 1 h at 4°C and then fixed after 0 min or 180 min at 37°C and stained using antibodies against ezrin, radixin or moesin. IgG controls for all antibodies were negative for unspecific staining. At the 0 min time point there was no specific colocalisation of Ad5 with the ERM proteins (Figure 4.18). As previously shown, the compound severely disrupted Ad5 intracellular trafficking by 180 min. The compound did not cause any obvious differences in the expression or localisation of the ERM proteins compared to control conditions (Figure 4.18). However the staining of all three proteins was variable with differences in their expression even within the untreated control conditions at the different time points, making it difficult to draw a clear conclusion, however under these conditions no gross difference was observed.

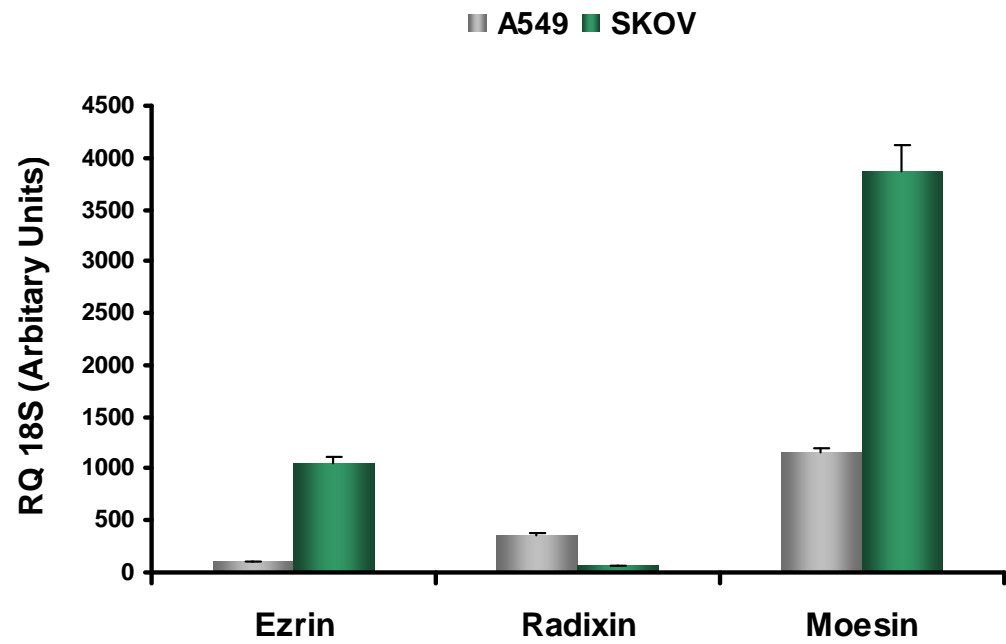


Figure 4.16. ERM gene expression in A549 and SKOV3 cells.

RNA was extracted from A549 and SKOV3 cells and converted to cDNA. qRT-PCR was performed on the samples to detect ezrin, radixin and moesin expression. Error bars represent SEM (n = 4).

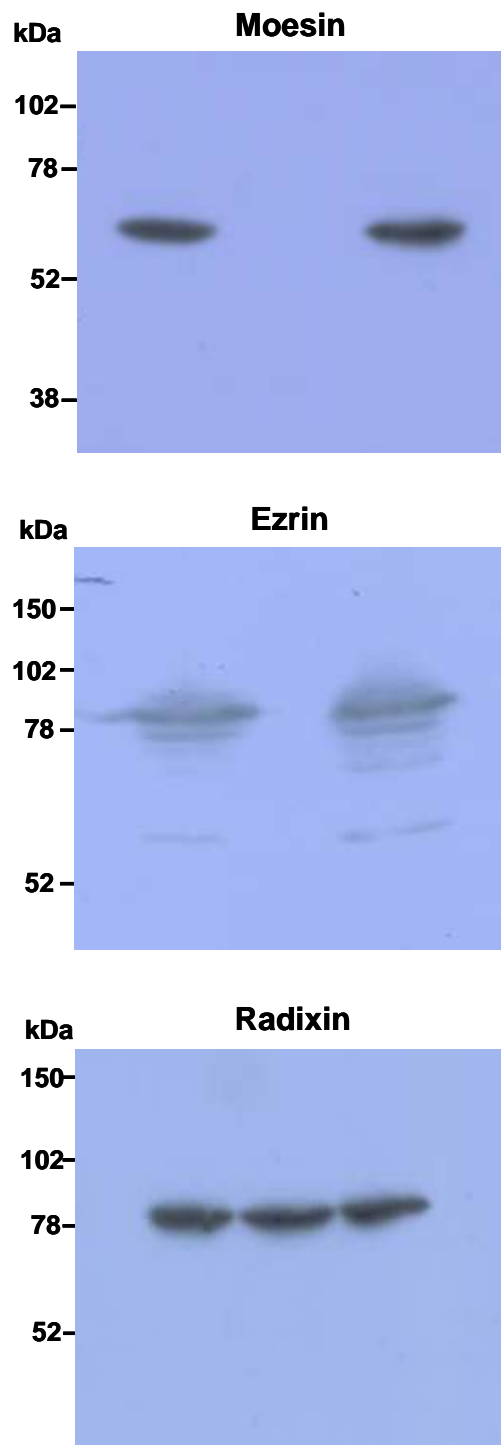


Figure 4.17. Ezrin, radixin and moesin protein expression in SKOV3 cells.

SKOV3 cell lysates were subjected to western immunoblotting and detection with an anti-ezrin, anti-radixin or anti-moesin antibody. Lanes represent replicate SKOV3 cell lysate samples. 50 μ g of each protein sample was loaded onto a 10% gel and probed with either the primary rabbit polyclonal antibody anti-ezrin (1:750 dilution), the rabbit monoclonal anti-radixin (1:1000 dilution) or the rabbit monoclonal anti-moesin (1:2500 dilution) and a swine anti-rabbit HRP secondary antibody (1:1000 dilution).

(A)

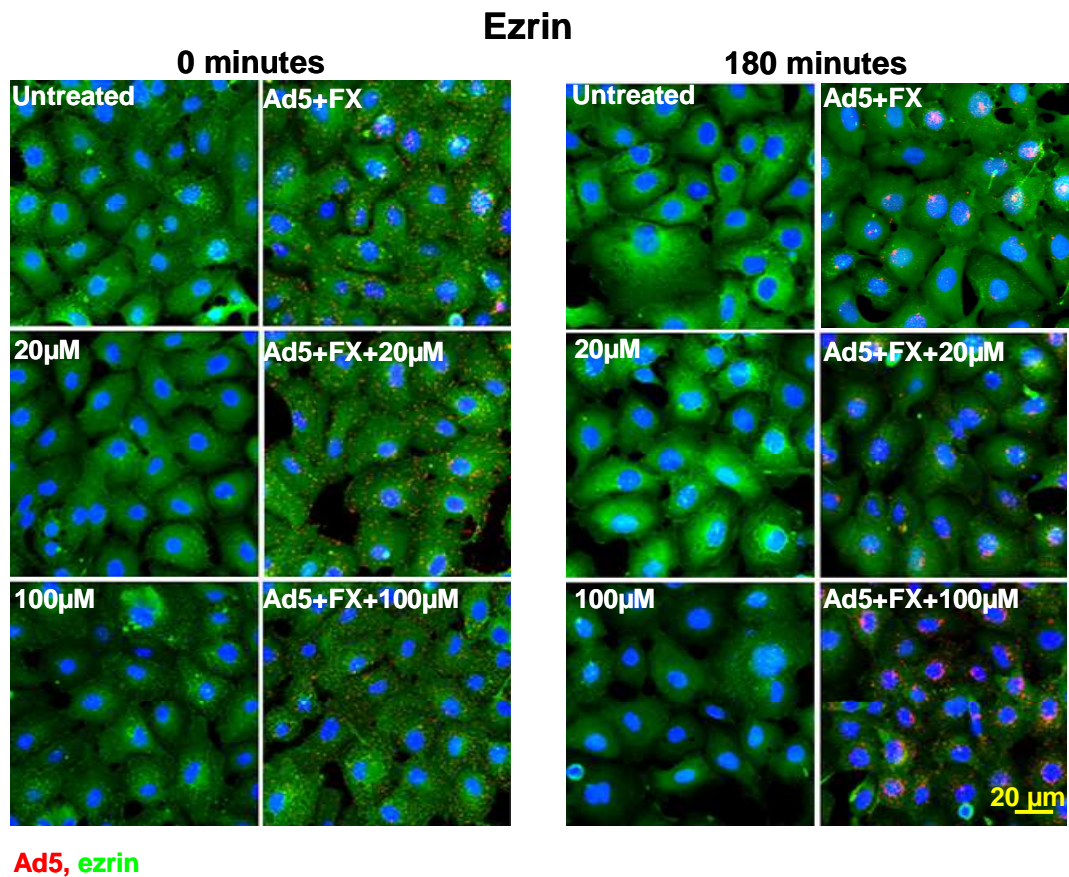
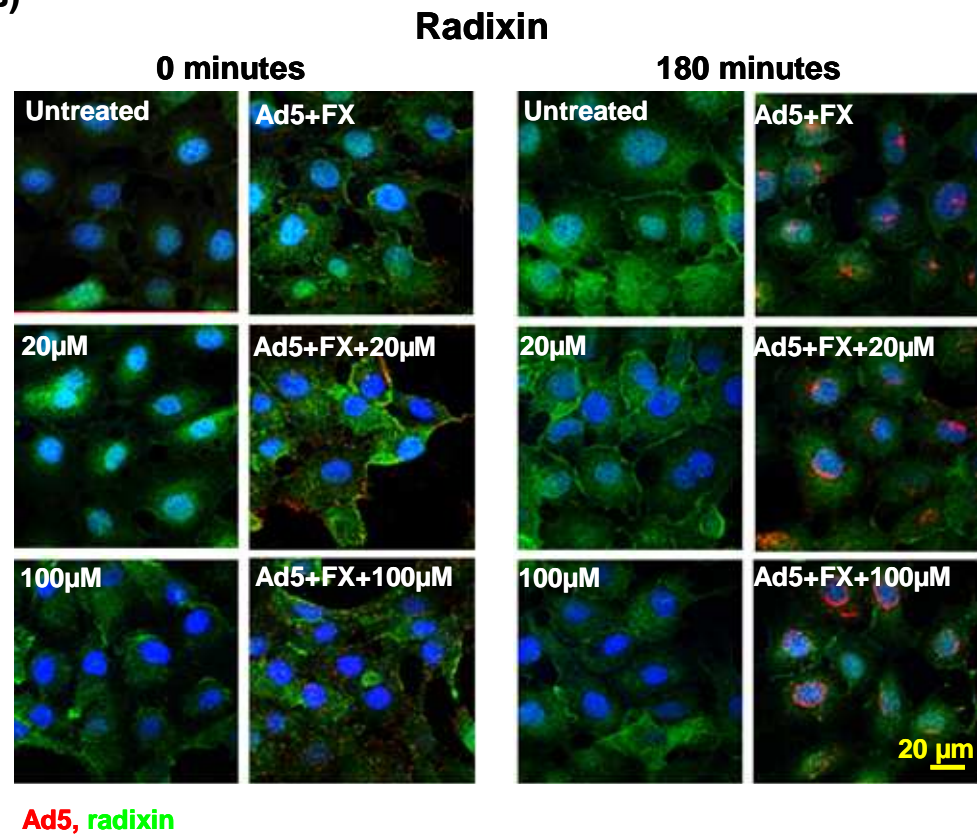


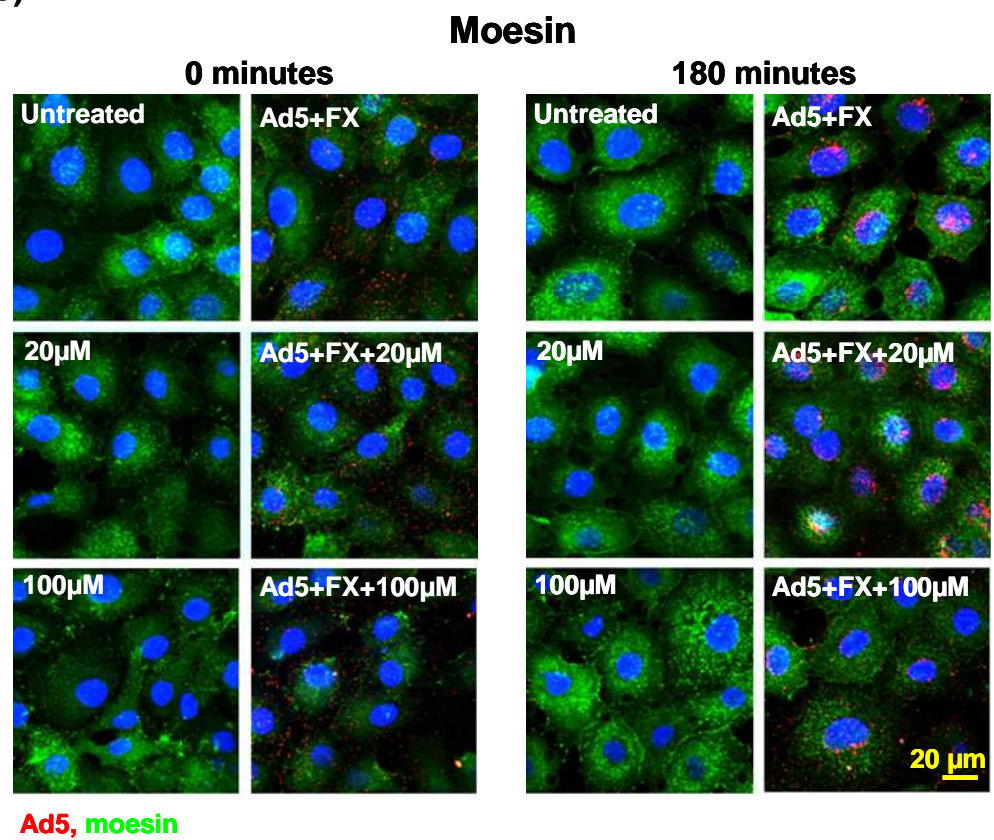
Figure 4.18. Effect of ER-27319 on ERM proteins expression and FX-mediated Ad5 cellular trafficking.

SKOV3 cells were incubated with media alone, 20 μ M or 100 μ M ER-27319 for 30 min at 37°C then 10,000 vp/cell of Alexa Fluor-555-labelled Ad5 (red) in the presence of FX with 20 μ M or 100 μ M ER-27319 were allowed to bind cells for 1 h at 4°C, followed by incubation at 37°C for 3 h prior to fixation. Cells were stained using (A) 1:200 dilution of a polyclonal rabbit anti-ezrin antibody (green), (B) 1:200 dilution of a monoclonal rabbit anti-radixin antibody (green) or (C) 1:200 dilution of a monoclonal anti-moesin (green) antibody. Nuclei were counterstained using DAPI.

(B)



(C)



4.3 Discussion

Among the first consequences of viral binding to cellular receptors is the activation of key intracellular signalling pathways. This study was aimed at investigating the involvement of a broad range of kinases and cellular proteins following Ad5:FX engagement with HSPGs, by employing small molecule inhibitors to decipher dependencies on individual signalling molecules. The study was also designed to develop Ad5 infectivity screening technologies prior to the initiation of Chapter 5.

Initially compound inhibitors of PKA, PI3K and p38MAPK were tested for their effects on Ad5 intracellular transport in the presence of FX. These kinases have previously been reported to have a critical role in Ad5 trafficking and nuclear targeting via the CAR pathway (Li *et al.*, 1998b; Suomalainen *et al.*, 2001). In previous experiments, cells were preincubated with the kinase inhibitors at 37°C for 30 min and drugs were kept present throughout virus binding, internalisation and gene delivery (Li *et al.*, 1998b; Suomalainen *et al.*, 2001), therefore this experiment was designed in a similar manner using the same concentrations i.e. 40 µM of the PKA inhibitor H89 dihydrochloride, 100 µM of the PI3K inhibitor LY 294002 hydrochloride or 10 µM of the p38MAPK inhibitor SB 203580. Coincubation of cells with the compounds in the presence of Ad5 and FX disrupted efficient viral intracellular transport as demonstrated by the decreased levels of MTOC colocalisation by 3 h post-infection compared to control conditions. In the presence of the PI3K or p38MAPK inhibitors MTOC colocalisation was reduced by greater than 40%, whilst in the presence of the PKA inhibitor by almost 70%, indicating a critical role for these kinases in efficient Ad5 nuclear targeting via the FX pathway (Suomalainen *et al.*, 2001). In addition to the study by Bradshaw *et al.*, reporting an important role for the penton base RGD motif for optimal cell entry in the presence of FX, these data suggest overlap with classical *in vitro* CAR-mediated infection mechanisms (Bradshaw *et al.*, 2010).

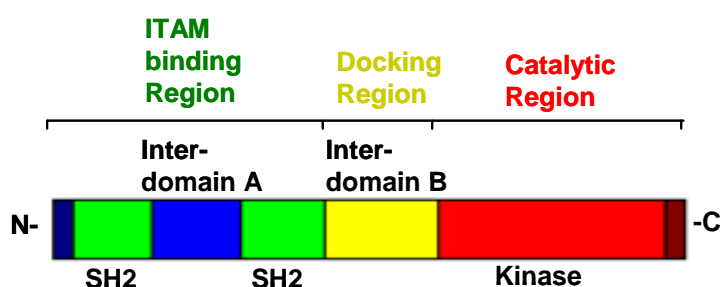
Next, a broad library of kinase inhibitors (n = 80) were screened to evaluate any having an effect on Ad5 gene transfer in the presence of FX in SKOV3 cells. Similarly to the previous experiment, cells were preincubated with the inhibitors for 30 min prior to the addition of virus. However in this case, as the number of compounds to be tested was quite large, all compounds were used at the same dose. An average concentration of ~10 µM was recommended by the manufacturer for several of the compounds, therefore cells were first incubated with Ad5 in the presence of FX and 20 µM compound in 100 µl serum free media for 3 h, followed by the addition of 100 µl media containing 20% serum, thus giving

a final concentration of 10 μM compound in 10% serum for the remainder of the assay. At these concentrations several compounds previously described as important for Ad5 infection were not highlighted as having a role in FX-mediated Ad5 gene transfer including inhibitors of MEK (e.g. U0126) (Farmer *et al.*, 2009), PI3K (e.g. LY 294002 hydrochloride or PD98059) (Li *et al.*, 1998b) and p38MAPK (e.g. SB 203580 hydrochloride) (Suomalainen *et al.*, 2001). This could be due to differences in experimental design, for instance other studies have used higher concentrations of compound ($> 20 \mu\text{M}$), investigated earlier stages of Ad5 infection and more subtle effects of kinase inhibition using confocal or electron microscopy (Farmer *et al.*, 2009; Suomalainen *et al.*, 2001). This was highlighted by the fact that in this study at higher concentrations H89 dihydrochloride and LY 294002 hydrochloride resulted in inefficient viral trafficking toward the nucleus by 3 h, however at lower concentrations did not significantly decrease Ad5 gene transfer at 48 h post infection. However, it cannot be ruled out that kinases known to be activated following Ad5 binding to CAR are not the same as those involved in Ad5:FX engagement with HSPGs, or perhaps there are subtle differences between the pathways. On the other hand, some of the inhibitors used in this screen were employed at concentrations above their previously reported IC_{50} values and in turn may have resulted in non-specific effects and caused substantial cytotoxicity thereby making full interpretation of their effects on FX-mediated Ad5 gene transfer difficult. For example the highly potent MEK inhibitor PD 198306 has an IC_{50} value of 8 nM, whilst at concentrations above 1 μM can decrease ERK, c-Src, cdks and PI3K activity (Ciruela *et al.*, 2003). The cdk4 inhibitor Ryuvudine, has an IC_{50} value of 6 μM for cdk4 in a range of cancer cell lines but has also been reported to have cytotoxic potential (Ryu *et al.*, 2000). Therefore, the inhibitor chosen for further study was the synthetic compound ER-27319 as this resulted in $> 90\%$ decrease in FX-mediated Ad5 gene transfer, whilst causing minimal toxicity.

ER-27319 was previously reported to selectively inhibit Syk activity (Moriya *et al.*, 1997). Syk is a 72 kDa, non-receptor tyrosine kinase that acts as a key mediator of immunoreceptor signalling. This cytoplasmic protein is expressed prevalently in haematopoietic cells but is also found in a wide range of non-haematopoietic cells including fibroblasts (Yamada *et al.*, 2001), osteoclasts (Mócsai *et al.*, 2004), hepatocytes (Tsuchida *et al.*, 2000), endothelial (Yanagi *et al.*, 2001), neuron-like cells (Tsujimura *et al.*, 2001) and epithelial cells (Ulanova *et al.*, 2005) suggesting Syk has a broad range of functions in multiple biologic processes beyond the immune system. Syk is classically activated via ITAMs, present either in the cytoplasmic tail of the receptor itself or on

receptor-associated transmembrane adaptors (Figure 4.19). In addition, Syk has been reported to be activated through G-protein-coupled receptors (Wan *et al.*, 1996) and by integrins which do not contain conventional ITAMs but instead employ ITAM-containing adaptor proteins such as DAP12 or FcR γ (Mocsai *et al.*, 2006). Previously an involvement of Syk kinase in relation to Ad5 infectivity has not been described. Therefore, it was decided that investigation into a role for Syk would be of interest and ER-27319 was chosen for additional experimentation.

(A)



(B)

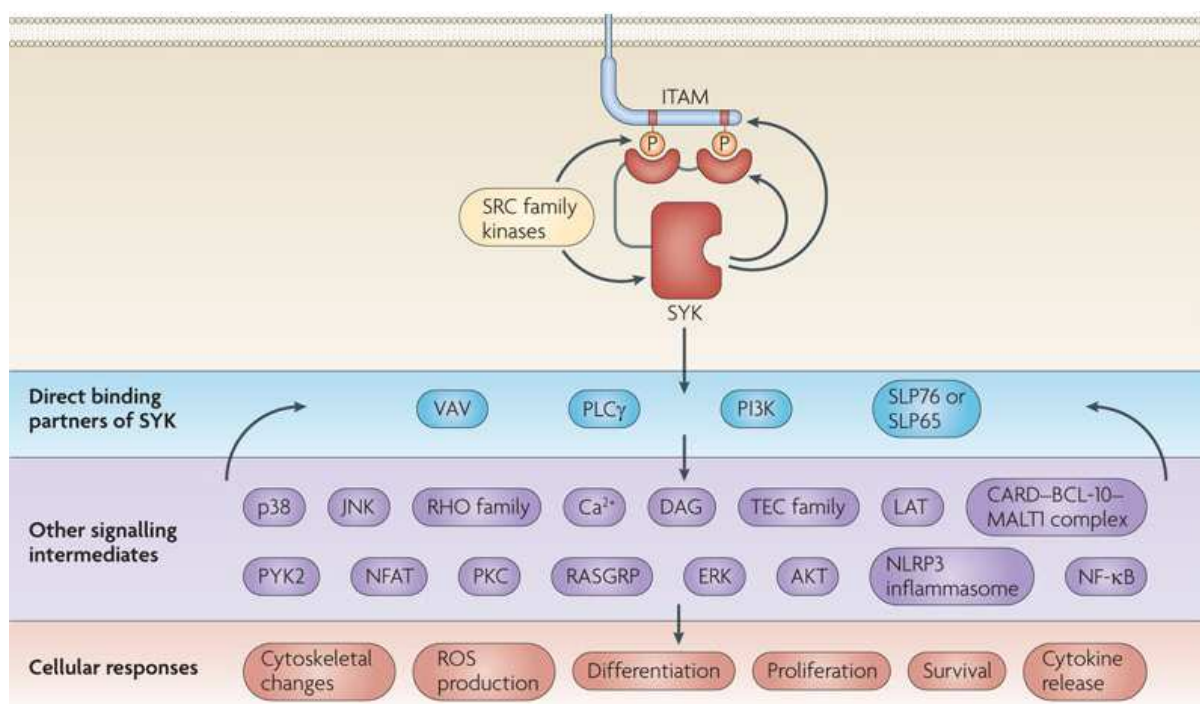


Figure 4.19. Spleen tyrosine kinase.

(A) Syk domain structure (B) Schematic of the Syk signalling pathway. Figure taken from Mocsai *et al.* 2010 (Mócsai *et al.*, 2010).

In the kinase screen experiment, ER-27319 was tested at a concentration of 20 μM for the first three and a half hours, followed by 10 μM for the remainder of the assay. These doses were similar to those used in a previous *in vitro* study in which ER-27319 was reported to have an IC_{50} value of 10 μM for inhibition of Syk in human and rat mast cells (Moriya *et al.*, 1997). Although 48 h coincubation with this compound did result in a decrease in cell viability, this was not thought to be the primary reason for the significant reduction in FX-mediated Ad5 transduction in SKOV3 cells. Consequently, in order to analyse the effects of the compound after shorter incubations and the effects on the early stages to Ad5 infection, intracellular transport of fluorescently-labelled Ad5 in the presence of FX was investigated. When cells were incubated with increasing doses of ER-27319 in the presence of Ad5 and FX, intracellular trafficking was substantially disrupted. The compound prevented efficient colocalisation with the MTOC by 180 min as assessed visually and quantitatively, therefore in contrast to Ad5 plus FX control conditions. For Ad5 to reach the nucleus a series of sequential steps are required including endocytosis, partial capsid disassembly, endosomal escape, microtubule based transport to the MTOC and nuclear import. This inhibitor appeared to cause a post-entry block in viral infectivity and had an effect at the later stages of trafficking, hindering MTOC accumulation. It appeared as though the virus was trapped in an alternative cellular compartment in a perinuclear region and at 180 min in SKOV3 cells this is particularly evident. This data demonstrates the ability of the ER-27319 to prevent efficient Ad5 intracellular transport and infection in the presence of FX.

In order to investigate the effects of ER-27319 on Ad5 infectivity it was important to understand the compound's mode of action. In a previous study ER-27319 is reported to selectively inhibit the tyrosine phosphorylation and activation of Syk induced by the Fc ϵ RI receptor in mast cells (Moriya *et al.*, 1997). Syk is characterised by a C-terminal kinase domain, two N-terminal Src homology (SH2) domains and two intervening domains, A and B (Figure 4.19). The tandem SH2 domains bind to diphosphorylated ITAMs (D/E)-x-x-Y-x-x-(L/I)-(x_{n=6-8})-Y-x-x-(L/I) of the cytoplasmic region of receptors. The tyrosines embedded within this motif are necessary and sufficient for ITAM signalling. This triggers Syk activation and initiates downstream signalling. In the study by Moriya *et al.* the compound prevented the phosphorylation of Syk induced by the phosphorylated ITAM of the Fc ϵ RI γ subunit (Moriya *et al.*, 1997). ER-27319 was described as specific for Syk and at concentrations up to 100 μM it had no effect on ZAP-70, another member of the Syk family or the downstream target PLC- γ 1 in Jurkat T cells (Law *et al.*, 1996; Moriya *et al.*, 1997). The compound did not affect the activity of Lyn kinase, a Src family member, which is

responsible for the phosphorylation of FcεRI receptor β and γ subunits leading to Syk binding, indicating it was not preventing receptor phosphorylation (Moriya *et al.*, 1997).

In order to further analyse the effects of using a Syk inhibitor on Ad5 intracellular transport and gene transfer, an alternative kinase inhibitor BAY 61-3606 was utilised. BAY 61-3606 is reported to be a potent and specific inhibitor of Syk acting in an ATP-competitive manner (Yamamoto *et al.*, 2003). It has an IC₅₀ value of 10 nM in mast cells and demonstrated greater than 626-fold selectivity over other tyrosine kinases such as Lyn and Src (Yamamoto *et al.*, 2003). It also has been shown to be effective in inhibiting the release of various inflammatory mediators in basophils, B cells and monocytes (Yamamoto *et al.*, 2003). Therefore although both inhibitors are reported to decrease Syk activity it is evident the mechanism by which BAY 61-3606 acts differs from that of ER-27319. This compound was employed to investigate whether it would affect FX-mediated Ad5 infectivity. In this study, the coincubation of SKOV3 cells with increasing doses of BAY 61-3606 did not affect Ad5 intracellular trafficking or FX-mediated Ad5 gene transfer at 48 h post-infection. This data suggests that ER-27319 may not be disrupting FX-mediated infectivity via an effect directly related to Syk activity.

To investigate this, the expression levels of Syk in our cells were investigated by qRT-PCR and western blot analysis. Syk has previously been shown to be present on a range of non-haematopoietic cell lineages including human mammary epithelial cells (Ruschel *et al.*, 2004) and several types of airway epithelial cells (Ulanova *et al.*, 2005). However, qRT-PCR and western blotting of SKOV3 and A549 cells revealed no detectable Syk gene or protein expression. This is in agreement with previous studies (Ulanova *et al.*, 2005). Therefore it was confirmed that ER-27319 was not causing its effects via Syk inhibition.

In order to find out additional information on the precise mechanism of action of ER-27319 the authors of the PNAS publication entitled “ER-27319, an acridone-related compound, inhibits release of antigen-induced allergic mediators from mast cells by selective inhibition of Fcε receptor I-mediated activation of Syk” were contacted. The compound does not bind directly to Syk but instead binds to the ITAM of the FcεRI gamma subunit, thereby preventing the interaction between the Syk SH2 domains and the doubly phosphorylated ITAMs. In the study by Moriya *et al.* the compound did not prevent activation of Syk via binding to phosphorylated Igβ ITAMs, therefore implying a specificity in the interaction between ER-27319 and the ITAM of the FcεRI gamma subunit. However, Syk possesses high structural flexibility and can recognise a variety of

phosphorylated ITAMs that vary both in sequence and in the length of the intervening amino acids between the SH2 binding motifs (Table 4.4) (Kumaran *et al.*, 2003). In a study by de Mol *et al.*, the seven amino acids between the phosphorylated SH2 binding motifs YETL and YTGL of the FcεRI gamma chain ITAM were replaced by a non-peptidic flexible and a rigid propynylbenzoy linker of similar length (de Mol *et al.*, 2005). Both ligands exhibited comparable affinities for Syk thereby indicating that the spacer region between the two phosphotyrosines do not contribute to binding. Therefore it was hypothesised that ER-27319 may also bind to additional ITAM-containing proteins other than that of the FcεRI gamma subunit. This hypothesis was developed into our model system.

Several viral ITAM signalling domains have been previously described. These are, in general, thought to enhance viral pathogenesis by interfering with normal antigen receptor signalling. A study reported the presence of an ITAM signalling domain encoded within the β-retrovirus MMTV *env* gene which can associate with Syk and participates in virus-induced mammary tumours (Katz *et al.*, 2005; Ross *et al.*, 2006). Mutation of this ITAM prevented the induction of tumours and altered patterns of oncogenic activation (Katz *et al.*, 2005; Ross *et al.*, 2006). In addition, the K1 protein of KSHV contains an ITAM sequence capable of binding to SH2 domain containing proteins (Lee *et al.*, 1998). The EBV LMP2A also possesses an ITAM to which Syk can bind (Fruehling *et al.*, 1997) and regulates downstream PI3K/Akt pathway signalling (Swart *et al.*, 2000). Several other viruses including rhadinovirus, bovine leukaemia virus, Hantaan virus and African horse sickness virus contain ITAM domains. Therefore, due to the variety of viruses which express functional ITAMs, the possible presence of a conventional ITAM sequence or the “less stringent” ITAM-like sequence, Y-X-X-(L/I)-(X_n)-Y-X-X-(L/I), on the Ad5 capsid proteome was investigated. Two ITAM-like sequences were identified on the hexon protein. However, neither QWSYMHISGQDASEYLSPLVQFARATETYFSL or ASTYFDIRGVLDRGPTFKPYSGTAYNAL conformed to the canonical ITAM sequence, having variation in the spacing between the Y-X-X-(L/I) motifs. However, the possibility of a direct interaction between ER-27319 and the Ad5 capsid could be further investigated using SPR. This could be performed by coating a biacore sensor chip with Ad5 and passing 20 μM ER-27319 over the chip to assess potential binding.

Rather than ER-27319 binding to a virus ITAM it was postulated that it could be binding to a cellular ITAM-containing protein and thereby disrupting efficient FX-mediated Ad5 trafficking. The previously reported cellular proteins possessing an ITAM domain are

listed in Table 4.4. The majority of these are immunoreceptors and transmembrane adaptor molecules but several more ubiquitously expressed intracellular proteins are also included. Employing the NCI-60 database (http://ntp.nci.nih.gov/docs/misc/common_files/cell_list.html) as a tool to scan for the presence of ITAM-containing proteins in SKOV3 and A549 cells, it was found that the ezrin, radixin and moesin were the most likely candidates to be expressed in both cell types. The ERM family of proteins act as regulated “cross-linkers” between the plasma membrane and the cortical actin cytoskeleton. They arose from gene duplication in vertebrates and their structures are closely related, featuring a N-terminal membrane binding domain of approximately 300 amino acids known as FERM (Four point one Ezrin, Radixin, Moesin) and a C-terminal domain containing a major F-actin binding site (Funayama *et al.*, 1991; Gary *et al.*, 1995; Gould *et al.*, 1989; Lankes *et al.*, 1991). ERMs have widely distributed expression patterns. *In vivo*, ezrin is most highly enriched on the apical side of polarised epithelial cells, whilst radixin is abundant in the liver and moesin is predominantly found in endothelial cells but is also present in a subset of epithelial cells (Amieva *et al.*, 1994; Berryman *et al.*, 1993). Of note, ezrin and moesin can bind to heparin and the ezrin N-terminal domain can link syndecan-2, a HSPG, to the actin cytoskeleton (Granés *et al.*, 2003; Lankes *et al.*, 1988; Lankes *et al.*, 1991). Previous work has demonstrated the expression of all three ERM proteins in a range of cultured epithelial and fibroblastic cells (Hayashi *et al.*, 1999; Maeda *et al.*, 1999). In this study qRT-PCR and western blot analysis confirmed the presence of ezrin, radixin and moesin in both SKOV3 and A549 cells. Both moesin and ezrin have been reported to directly interact with Syk in an ITAM dependent manner and mediate signalling by the leukocyte adhesion receptor P-selectin glycoprotein ligand 1 (Urzainqui *et al.*, 2002). Therefore this family of ITAM-containing proteins were investigated as potential targets for ER-27319 induced effects on Ad5 infectivity.

It is of interest that in the recent publication by Farmer *et al.* the authors speculate that p44/42 MAPK does not exert its effects on the subcellular localisation of integrins through a direct interaction but perhaps instead via an intracellular integrin activation protein such as talin, a protein which mediates integrin inside-out signalling by direct binding of its FERM domain to the cytoplasmic tail of integrins (Calderwood *et al.*, 2002; Farmer *et al.*, 2009). However, currently this is only a hypothesis and requires additional study. Radixin also demonstrates integrin activation activity, being capable of binding to integrin $\alpha_M\beta_2$, thereby enhancing its adhesive activity (Tang *et al.*, 2007).

We investigated whether ER-271319 in the absence or presence of Ad5 plus FX could alter the cellular distribution of ERM expression. In cultured epithelial cells ERMs are reported to be expressed both in the cytoplasm and at the plasma membrane where they are localised to actin rich regions such as microvilli, ruffling membranes, cell-cell borders and cleavage furrows (Hayashi *et al.*, 1999). ERMs can exist in an inactive or active conformation (Gary *et al.*, 1995). Binding to the membrane lipid phosphatidylinositol 4,5-biphosphate (PIP₂) results in the phosphorylation of a conserved threonine in the actin binding site and localisation of ERMs to actin-rich membrane extensions (Barret *et al.*, 2000; Hayashi *et al.*, 1999). This also involves the small GTP-binding protein Rho (Matsui *et al.*, 1998). In addition, ERM proteins are reported to be phosphorylated on tyrosine residues *in vivo* (Thuillier *et al.*, 1994). Conversely, dephosphorylation leads to their translocation to the cytoplasm (Fievet *et al.*, 2004). It was hypothesised that as ERMs play a role in the regulation of the plasma membrane, cytoskeleton and signalling cascades, they may have a role in the early stages of Ad5 infection. Furthermore, it was postulated that ER-27319 could interfere with the efficient activation of ERMs, disrupting their function in virus infected cells. Unfortunately, from immunocytochemistry results analysing the distribution of ezrin, radixin and moesin in SKOV3 cells it was difficult to draw a clear conclusion as to whether ERM expression is altered in the presence of Ad5 or ER-27319 compared to untreated control conditions. There is substantial variation in the expression of all three proteins in untreated cells at the different time points. For example with regards to ezrin staining at 0 min in control cells, the expression is evenly distributed throughout the cytoplasm, whereas at 180 min it is more concentrated around the nuclei. These disparities made it almost impossible to dissect any subtle changes which may be occurring.

For immunocytochemistry and confocal experiments, cells were fixed in 4% PFA for 15 min and permeabilised in 0.1% Tween20 for 10 min prior to staining for the ERM markers. Ideally this would immobilise the antigens, whilst still retaining authentic cellular and subcellular architecture and permitting the antibody unhindered access. However it may be that these conditions were too severe. Alternative fixation methods were investigated. In a study by Hayashi *et al.* several fixatives were assessed for their ability to inactivate enzymes such as phosphatases without strong chemical modification and the effects on the distribution of C-terminally phosphorylated ERMs were analysed (Hayashi *et al.*, 1999). The fixatives included 1% or 4% PFA, ethanol/acetone, methanol and trichloroacetic acid (TCA). The antibody used specifically recognised C-terminally phosphorylated ERMs but not non-phosphorylated ERM proteins. This antibody did not produce any

immunofluorescence signals in PFA-treated cells and only gave rise to signals in TCA fixed cells indicating a sensitivity of these proteins to fixation methods (Hayashi *et al.*, 1999). It would be of interest in future work to employ this TCA method of fixation and analyse ERM distribution in SKOV3 and A549 cells. In addition, to specifically look at the role of ERM protein function in Ad5 infectivity, siRNA silencing or chemical inhibition of these proteins would be attractive options.

Finally, taking a different approach to investigating the mechanism of action of ER-27319 the compounds structure was assessed. This is a synthetic, acridone-related compound (Moriya *et al.*, 1997). Acridone (10*H*-acridin-9-one) is a tricyclic ring, having nitrogen at 10th position and ketone group at 9th position (Figure 4.20). Its derivatives have previously been reported to possess antiviral activity against both RNA and DNA viruses including Semliki forest, coxsackie B, Western equine encephalitis, herpes simplex, Epstein barr, pseudorabies, dengue viruses and cytomegalovirus (Akanitapichat *et al.*, 2000; Itoigawa *et al.*, 2003; Kramer *et al.*, 1976; Lowden *et al.*, 2003). Several different targets and metabolic points have been suggested as potential mediators of these effects. Acridone-related compounds are reported as acting on nucleotides by intercalating viral DNA and RNA strands (Stankiewicz-Drogoń *et al.*, 2010; Stankiewicz-Drogon *et al.*, 2008), as DNA topoisomerase II inhibitors (Goodell *et al.*, 2006) and as inducers of interferon (Storch *et al.*, 1986). Moreover, a study by Zarubaev *et al.* demonstrated a direct antiviral effect of 10-carboxymethyl-9-acridanone (cycloferon) against Ad6 in HepG2 cells (Zarubaev *et al.*, 2003). Treatment with the drug significantly reduced the yield of infectious virus *in vitro* and affected the structure of intranuclear virus-specific inclusions. The authors suggest the ability of the drug to suppress the late stages of the adenoviral cycle, late DNA replication and/or packaging into virions during viral assembly (Zarubaev *et al.*, 2003). Many of the potential modes of action for these compounds appear to involve post-nuclear entry, transcription and replication stages of viral infection. In the current study it appears as though ER-27319 is causing effect prior to nuclear import, however due to its structural similarity to other acridone derivatives previously described, a similar nuclear target can not be ruled out and is of certain interest.

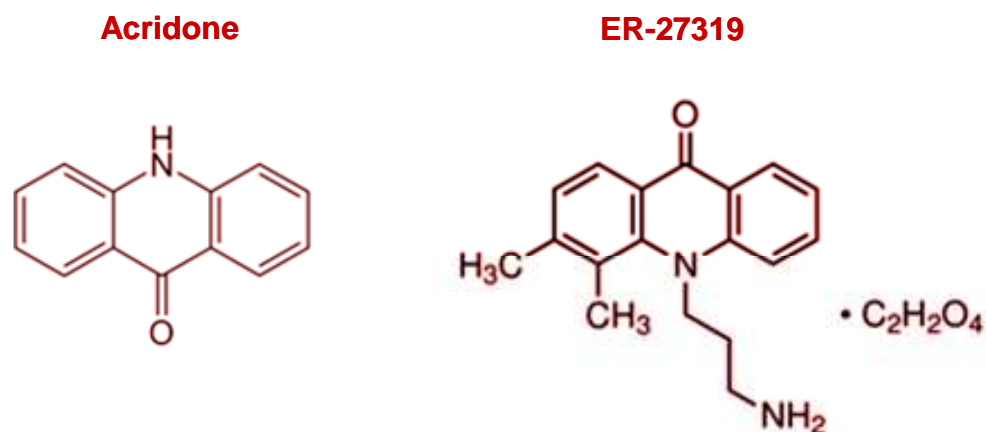


Figure 4.20. Compound structure.

Chemical structure of acridone and its derivative ER-27319.

The dynamics of intracellular transport depend on virus binding and extracellular signals transmitted via plasma membrane receptors being relayed by the corresponding signalling cascades and cellular proteins. In this study, several kinases including PKA, PI3K and p38MAPK were identified as critical to efficient FX-mediated Ad5 intracellular transport. These are no doubt part of extensive signalling pathways along with the reorganisation of cellular proteins required for effective viral infection. The identification of the compound ER-27319 as an inhibitor of Ad5 nuclear targeting and gene transfer was a novel finding, however a major challenge within this project was to identify the substrates of ER-27319, in order to obtain a comprehensive understanding of how this inhibitor was causing effect. Unfortunately within the time frame of this project it was not possible to conclude the precise mechanism of action of ER27319 and determine how it was causing such dramatic effects on Ad5 intracellular trafficking and nuclear targeting. Several aspects of this investigation warrant further study, such as the role of ERM proteins in Ad5 infection, as selective targeting of such cellular components or signalling pathways could have potential as antiviral therapies. Understanding the intricacies of Ad5 infection is a difficult process but will ultimately aid in the prediction and manipulation of the host response.

Chapter 5

Identification of small molecule inhibitors of FX-mediated Ad5 gene transfer

5.1 Introduction

A large body of recent work has focused on precluding FX-mediated Ad5 transduction, by investigating strategies to block the direct interaction of the Ad hexon with the coagulation factor. Methods such as genetic manipulation of the virus capsid or polymer conjugated Ad complexes have been studied, as discussed earlier in this thesis (Alba *et al.*, 2009; Short *et al.*, 2010; Subr *et al.*, 2009). The use of pharmacological agents including heparin, warfarin and X-bp in animal studies have highlighted the efficacy of a drug intervention approach, however such drugs are not ideal therapies in a gene therapy clinical setting due to anticoagulation properties and toxicity profiles (Atoda *et al.*, 1998; Bradshaw *et al.*, 2010; Waddington *et al.*, 2008). Less attention has been placed on investigating novel therapeutically viable pharmacological approaches to block Ad transduction in the presence of FX but this area may hold great promise. Therefore, this study was aimed at identifying an inhibitor of FX-mediated Ad5 transgene expression, with ultimately the *in vivo* utility of this approach.

During the past two decades a fundamental change has occurred in the drug discovery process, with a growing trend toward the use of high throughput screens (HTS). HTS of large compound libraries in search of lead candidates is a phenomenon which has invaded a diverse range of fields, both in the pharmaceutical and academic sectors (Andersson *et al.*, 2010; Inglese *et al.*, 2007; Johnston *et al.*, 2002). The aim being to test a great number of compounds against target molecules in a short period of time, by combining automation with translation of well defined traditional bench top assays into miniaturized 96-, 384- or 1,536-microwell plate formats and large scale data analysis. HTS is a multilevel process, comprising several key stages; target validation, assay development, primary and secondary screening, data analysis, absorption, distribution, metabolism and excretion (ADME) investigation, toxicology assessments and generation of lead compounds (Johnston *et al.*, 2002). The primary screen is therefore just the initial step of an integrated process (Figure 5.1). Here, a HTS strategy was devised in order to assay > 10,000 compounds in search of those which prevented Ad5 transduction via the FX pathway.

The well documented Ad5:FX interaction resulting in Ad5 binding to hepatocytes *in vivo* indicates that several steps of this pathway may serve as potential targets for intervention (Bradshaw *et al.*, 2010; Kalyuzhniy *et al.*, 2008; Vigant *et al.*, 2008; Waddington *et al.*, 2008). The drugability of a given target is critical to the success of any HTS and the ability of X-bp to bind to the FX Gla domain and decrease Ad5 liver gene transfer in mice for

example, highlights the feasibility of the Ad5:FX pathway to be effectively modulated by a ligand (Liu *et al.*, 2009; Waddington *et al.*, 2008). Having a well defined target, this study commenced at the assay development stage in the HTS process.

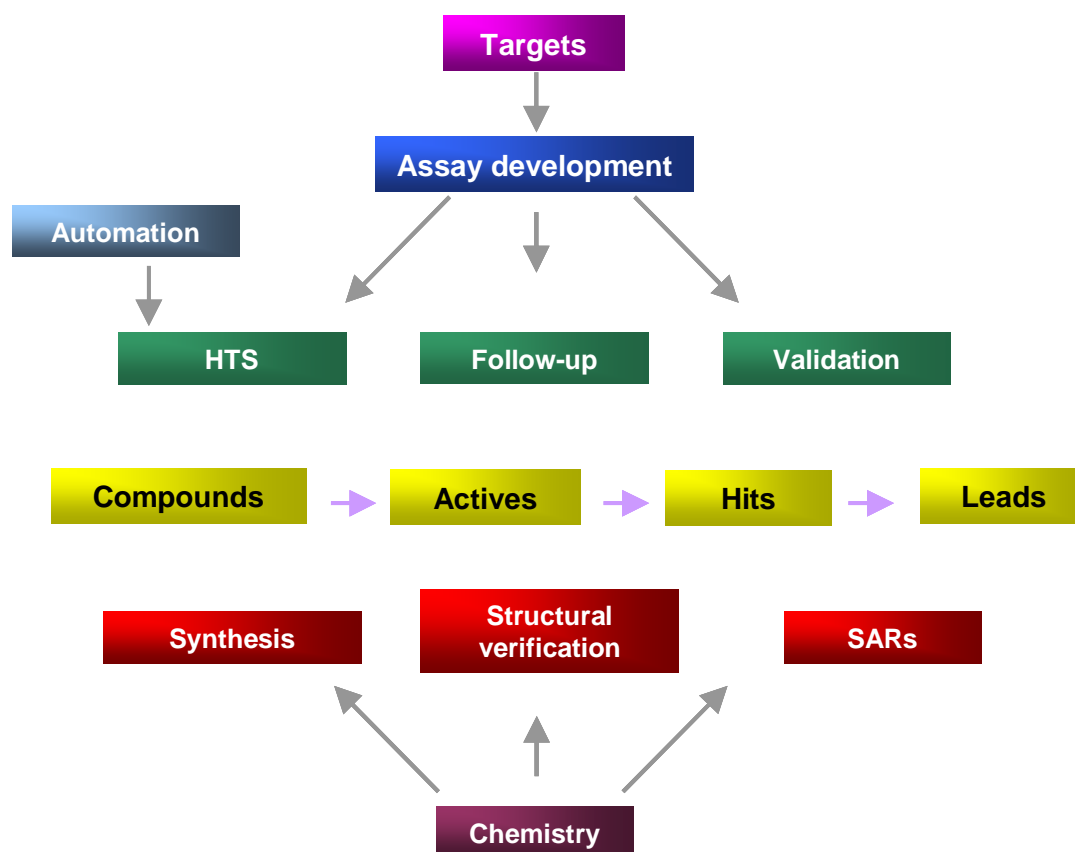


Figure 5.1. Steps of the HTS process.

Graphical summary of the integrated steps involved in the HTS process.

A suitable starting library is of critical importance (Bleicher *et al.*, 2003; McGovern *et al.*, 2002). Previously the generation of compounds was directed by chemical structures and selectivities rather than on pharmacological properties. In this regard, *in vitro* affinities were optimised at the expense of solubility, metabolic stability and permeability properties and often compounds which appear to be promising lead candidates are not always suitable for further medicinal chemistry exploration, which precludes their progression (Bleicher *et al.*, 2003). In addition, seemingly attractive hits can fail to exhibit obedient structure-activity relationships (SAR) which can lead to the termination of such compounds, as without a well defined target, SAR is the only available means of compound optimisation. Hits develop into lead compounds through comprehensive assessment of their chemical integrity, biological actions, synthetic assessibility, SAR and ADME properties

(Hodgson, 2001). Screening libraries of compounds with drug-like properties is preferable, possessing improved ADME and toxicity properties they are likely to reduce the number of false positives or nuisance compounds (cytotoxic, detergents or positively charged compounds) identified in the primary screen and the rate of attrition at the later stages. The library chosen for this screen was the Pharmacological Diversity Drug-like Set from Enamine (additional information describing this library, including chemical structures can be obtained from <http://www.enamine.net>). Design of this set was based on pharmacological properties rather than on the chemical structure of compounds. For each compound a profile of 3081 predicted pharmacological properties was generated by Enamine and any compounds possessing toxic signatures were removed, then pharmacological profiles were clustered for the rest of the structures, thereby generating a varied assortment of 10,240 low molecular weight (majority < 500 Da) drug-like compounds.

Today, robust cell-based screening approaches are commonly used to identify biologically active compounds in viral screens (Andersson *et al.*, 2010; Baldick *et al.*, 2010; Basu *et al.*, 2011). Despite often being more labour intensive (production of large quantities of cells and virus, the inherent variability of assay performance due to differences in cell passage number and handling etc.) they have the benefit of more realistic screening parameters compared to virtual screening technologies, without a preconceived idea of the compounds mechanism of action or safety profile. Configuring assays to function within the constraints imposed by HTS (simple protocol with few steps, low volumes, microtitre plate format, short assay time, easily measured readout) can be difficult and only a subset of biological assays are amenable (Inglese *et al.*, 2007). In this study the FX-mediated Ad5 transduction pathway and routinely used cell-based infectivity protocols were exploited to design a robust Ad5 fluorescence reporter gene based HTS using SKOV3 cells (CAR^{low}) in the presence of FX.

Identification of a novel small molecule inhibitor of FX-mediated Ad5 transduction could have several benefits over alternative methods of liver detargeting. An attractive incentive for using a pharmacological approach to prevent Ad5 hepatic gene transfer, is that there is no requirement for genetic manipulation of Ad5 capsid proteins, which can often be very time consuming and interfere with large scale virus production (Alba *et al.*, 2009). As for regulatory issues regarding the use of such viruses in the clinic, capsid modified Ad5 vectors would require additional toxicology and safety studies to be performed. Regarding polymer conjugated Ad complexes, this process involves coating the entire capsid in a

synthetic shield, which may result in decreased affinity of the virus not only to FX but alternative native receptors. The use of alternative Ad serotypes devoid of FX binding is also a viable option, however a vast array of safety and clinical data has been obtained using Ad5, for which novel and less commonly used vectors lack. Identification of a safe compound which specifically blocks Ad5 binding to FX or FX-mediated Ad5 gene transfer may hold great promise for preventing unwanted liver transduction and decreasing Ad5 related hepatotoxicity in the clinical setting.

As the screen is designed to identify inhibitors of FX-mediated Ad5 transduction, any hits may also have potential value as a treatment against naturally occurring disseminated Ad infection. In healthy individuals Ad infection is mostly self-limiting, however in immune compromised individuals (e.g. suffers of hereditary immunodeficiencies, AIDS patients or haematopoietic stem cell transplant recipients undergoing immunosuppressive treatment) Ads exploit the impaired immunological response and can cause more prolonged, severe and even life threatening disease. Infections can manifest in diverse clinical syndromes, ranging from upper and lower respiratory tract disease, (kerato)conjunctivitis or gastroenteritis to more serious complications including hemorrhagic cystitis, hepatitis, myocarditis, coagulopathy, encephalopathy, nephritis or multi-organ failure (Abzug *et al.*, 1991; Chuang *et al.*, 2003; Echavarría, 2008; Straussberg *et al.*, 2001). Disseminated Ad infections are often fatal, reaching a mortality rate of 50%, whilst pediatric transplantation patients are yet more prone to the disseminated disease, with mortality rates up to 83% in immunodeficient children (Chakrabarti *et al.*, 2002; Munoz *et al.*, 1998). Despite this, Ad can be detected in peripheral blood 3 weeks prior to the onset of clinical symptoms, thereby leaving a wide therapeutic window by which to treat the potentially life threatening disseminated infection (Lion *et al.*, 2003).

There are currently no formally approved antiviral agents available that specifically treat Ad infection. In some clinical cases cidofovir ((S)-1-(3-hydroxy-2-phosphonylmethoxypropyl)cytosine) and ribavirin (1- β -d-ribofuranosyl-1,2,4-triazole-3-carboxamide) have been employed and have demonstrated some efficacy against Ad infection (Lenaerts *et al.*, 2006; Neofytos *et al.*, 2007). Ribavirin is a purine nucleoside analogue that shows efficacy against RNA and DNA viruses (Lenaerts *et al.*, 2006; Pawlotsky *et al.*, 2004). Cidofovir is an acyclic nucleoside phosphonate analogue that is used as a broad-spectrum antiviral agent (Baba *et al.*, 1987; De Clercq, 2003). However the efficacy of these compounds is contentious as they have not been rigorously tested in randomised controlled clinical trials for their efficacy in treating Ad infection (reviewed by

Lenaerts *et al.* (Lenaerts *et al.*, 2008)). This suggests a gap in the market for a selective anti-adenoviral compound, as such potential screen hits may warrant investigation in this regard.

In recent years, several low molecular weight compounds identified from HTS assays have shown successes in modulating viral functions (Baldick *et al.*, 2010; Basu *et al.*, 2011; Hoffmann *et al.*, 2011; Larson *et al.*, 2008; Micheva-Viteva *et al.*, 2011; Mueller *et al.*, 2008; Thompson *et al.*, 2010). One such study developed a fluorescence-based assay using hepatitis C virus (HCV) with a firefly reporter to screen 1 million small molecules for blockers of HCV entry and identified a potent and selective HCV inhibitor from the HTS process (Baldick *et al.*, 2010). Another study employed 200,000 compounds and tested the library in a cell-based system to identify small molecule antagonists of HIV-1 latency (Micheva-Viteva *et al.*, 2011). These reported successes highlight the feasibility of using a HTS to find an inhibitor of FX-mediated Ad5 transduction.

Advancements in the understanding of the mechanisms underlying Ad5 liver transduction has created several targets for drug discovery. The aim of this study was to screen a pharmacologically diverse library of drug-like compounds to identify a safe inhibitor of FX-mediated Ad5 transduction. To efficiently ascertain whether compounds exert such biological activity, a robust fluorescence-based HTS was developed using SKOV3 cells (CAR^{low}) seeded in a 384-well microplate format to analyse FX-mediated Ad5GFP infection.

5.2 Results

5.2.1 Design and optimisation of an assay compatible with HTS

It has been previously described in this thesis and several publications that co-incubation of Ad5 with 10 µg/ml FX causes a substantial increase in Ad5 transduction *in vitro* and *in vivo* compared to Ad5 alone (Bradshaw *et al.*, 2010; Waddington *et al.*, 2008). In this study, initial optimisation and validation experiments were performed to convert this frequently employed assay into a high throughput SKOV3 cell-based screen in order to test 10,240 compounds for their ability to inhibit FX-mediated Ad5 gene transfer.

5.2.2 Plates – 384-well assay format to increase assay robustness

Several different types of well plates were tested for their suitability in the HTS assay set-up. These included both 96- and 384-well formats; CellBIND 96-well flat clear bottom black, low volume 384-well flat clear bottom black, CellBIND® 384-well flat clear bottom black, 384-well optical imaging flat clear bottom black and Greiner Bio One 384 µ-clear flat bottom black cell culture microplates. 384 µ-clear flat bottom black cell culture microplates (catalogue number 781091, Greiner Bio One) were chosen for the HTS. The SKOV3 cells adhered to these plates and they allowed for high quality fluorescence imaging using the IN Cell Analyser 2000. Furthermore the 384-well set up increased the robustness of the assay, decreasing amounts of reagents required (cells, number of plates, volumes of media, compound, virus, FX and storage space etc.) and this format was time and cost effective.

5.2.3 Cells – optimal seeding densities

To examine the effects of cell density, SKOV3 cells were seeded at densities ranging from 750 cell/well to 5000 cell/well in 384-well plates. At a density of 1500 cell/well the cells adhered to the plates, were not washed off during liquid dispensing and aspirating steps and were not over confluent at 72 h after seeding, thus allowing for clear image acquisition using the IN Cell Analyser 2000 and accurate segmentation of cells with the IN Cell Developer Toolbox V1.6 analysis software. Therefore a density of 1500 cell/well in 50 µl media was chosen for the HTS assay. Prior to starting the assay the cells were tested for mycoplasma infection and found to be negative.

5.2.4 Control-based method of normalisation

In vitro FX has been reported to cause up to log-fold increases in Ad5 transduction compared to conditions in the absence of FX (Bradshaw *et al.*, 2010; Parker *et al.*, 2006; Waddington *et al.*, 2008). When tested in this study in SKOV3 cells, 1000 vp/cell of Ad5 in the presence of 10 µg/ml FX resulted in high levels of GFP expression, whilst in the absence of FX the levels were low (~41-fold difference) (Figure 5.2). GFP expression was treated as the primary readout, with clear positive and negative controls and a large signal window in which to investigate compounds inhibiting FX-mediated Ad5 gene expression. Therefore, this assay was very accommodating to the control-based method of normalisation and this method was chosen as standard approach for dealing with sources of HTS variability; fixed positive and negative controls on each plate, allowing for the normalisation of the test data to the controls and representation of data as percentage inhibition of FX-mediated Ad5GFP expression.

5.2.5 Designing robotic liquid handling protocols

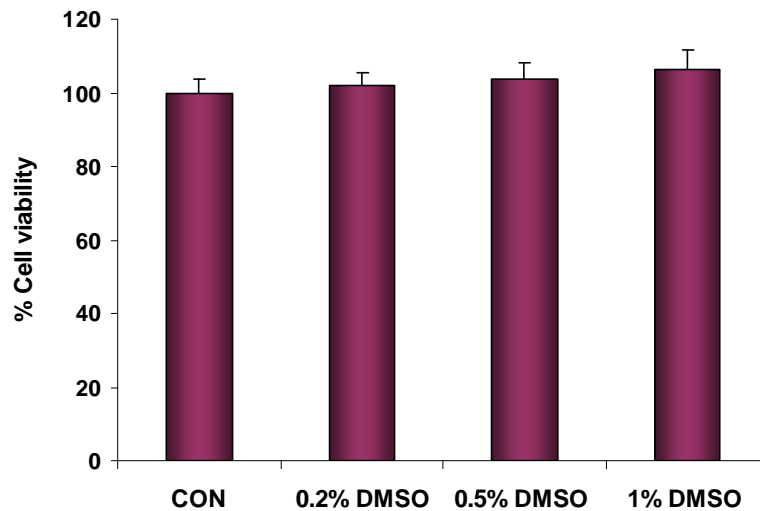
As the compounds were dissolved in 100% DMSO it was important to investigate the levels of this organic solvent tolerable to the cells and the activity of the assay in order to minimise the number of dilution plates required and to facilitate assay automation. The impact of DMSO concentrations was examined prior to designing liquid handling protocols and the production of replicate mother plates. This was performed by manually infecting cells with 1000 vp/cell of Ad5 in the absence or presence of FX and increasing concentrations of DMSO (0.2 – 1%). A concentration of 1% DMSO was well tolerated by the cells as assessed by MTT assay and did not effect FX-mediated Ad5GFP expression after 48 h (Figure 5.2). Therefore, a final DMSO concentration of 1% was compatible with this assay.

A major focus of the experiment was to design the robotic liquid handling protocols in the minimum number of steps possible, whilst still maintaining assay integrity in order to decrease random variability (e.g. errors which arise due to technical or instrumental issues) and systemic variability (e.g. errors which arise due to differences between reagent lots, buffer preparations or incubation times) that contribute to ‘noise’ associated with experimental data. Furthermore, this was a key factor in order to keep costs down, an important consideration when performing a HTS. Consequently, 32 mother plates were produced, in which compounds were at 100 µM in 100% DMSO, leaving the outer

columns 1, 2, 23 and 24 empty to later allow for easy incorporation of assay plate controls. In order to facilitate assay automation, daughter plates were produced, in which Ad5 was incubated with the compound or DMSO, whilst in the assay plate FX or serum free media alone was preincubated on the cells. The contents of the daughter plates were added to the relevant wells of the assay plates, followed by the control additions. This gave a final concentration of 1000 vp/cell of Ad5 in the absence or presence of 10 µg/ml FX plus 10 µM compound. An important quality control feature of a HTS is good plate design. All assay plates contained an equal number of positive (16 wells of Ad5) and negative (16 wells of Ad5+FX+DMSO) controls, the locations of which in columns 2 were reversed in column 23 in an attempt to reduce the influence of potential intra-plate positional and row effects (Figure 5.3). No positive or negative control or test wells were located on the outer most columns (1 and 24) to decrease intra-plate edge related variability. In an effort to monitor and reduce the influence of inter-plate variability and the incidence of false positives, three replicates of each plate containing the controls and test compounds were produced providing an $n = 3$ for each compound.

In an additional attempt to aid assay automation, instead of washing cells and re-adding the compounds after 3 h incubation at 37°C, an equal volume of media containing 20% serum was added to the cells, resulting in a final compound concentration of 5 µM in 10% serum containing media on the cells. At no point during the assay did the concentration of DMSO exceed 1% and for the majority of the time (~45 h) remained at 0.5%. Following 48 h incubation at 37°C, the media was removed, the cells were washed in PBS and fixed in 4% PFA prior to staining with 10 µg/ml Hoechst 33342 and 10 µg/ml propidium iodide. Throughout the liquid handling steps the cells remained adherent to the plates and the fixation and staining provided good conditions for imaging.

(A)



(B)

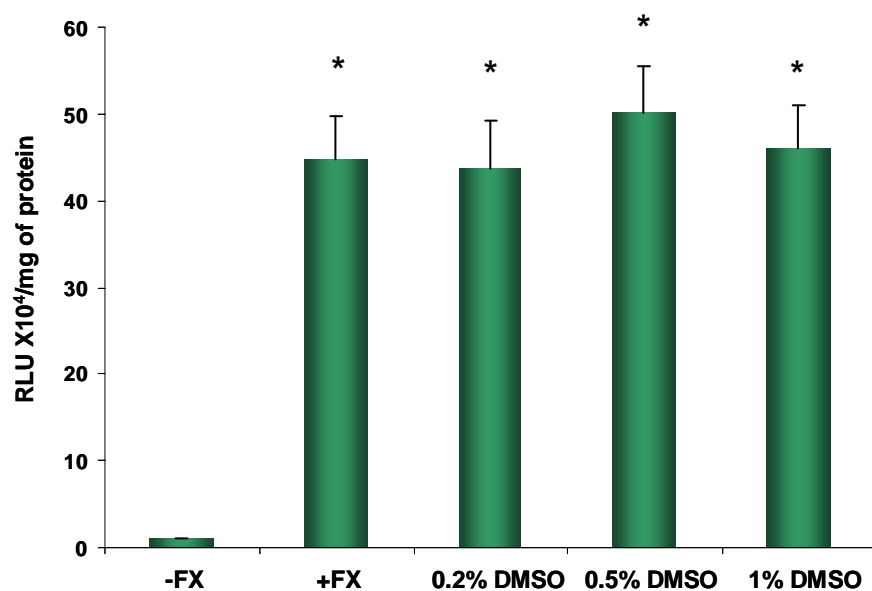


Figure 5.2. Effect of DMSO on SKOV3 cell viability and assay activity.

(A) SKOV3 cells were incubated with increasing concentrations of DMSO for 48 h and then a MTT assay was performed. (B) Cells were infected with 1000 vp/cell of Ad5 in the absence or presence of FX plus DMSO. Ad5 transgene expression was measured 48 h post-infection. * $p < 0.05$ as compared to non-FX conditions as determined by one-way ANOVA and Dunnett's multiple comparison post-test. Error bars represent SEM ($n = 3/\text{group}$).

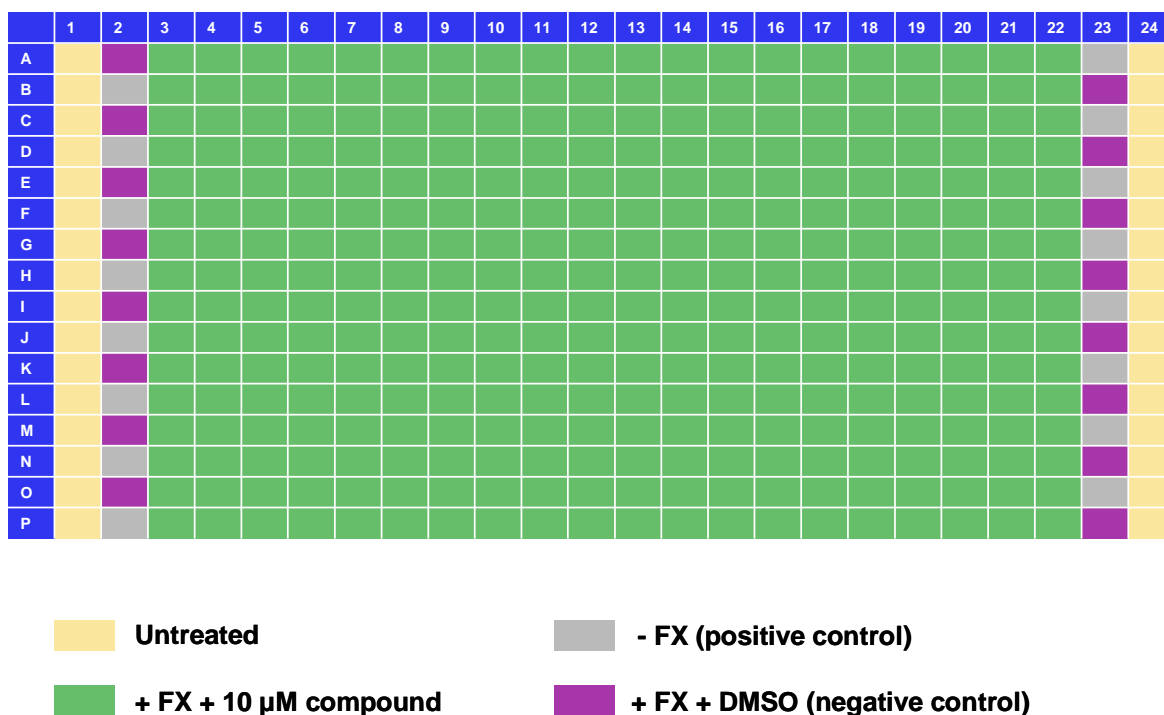


Figure 5.3. Assay plate layout.

Schematic of the 384-well assay plate, highlighting the position of the positive and negative controls. Yellow = untreated controls, green = compounds, purple = negative controls and grey = positive controls.

5.2.6 Design of imaging analysis conditions

5.2.6.1 Acquiring

The image acquisition settings on the IN Cell Analyser 2000 were developed and optimised to produce a robust assay delivering high quality fluorescence images. A single 10x image of the centre of each well of the 384-well plate was captured of Hoechst 33342 nuclear staining (40 ms exposure time), GFP expression (60 ms exposure time) and propidium iodide non-viable nuclear staining (45 ms exposure time). The conditions were optimised in order to capture both the MIN and MAX GFP control wells without saturation or under-exposure, whilst maximising the signal window. Fast hardware autofocus options were chosen, which optimise the quality of the images, and along with the short exposure times contributed to the speed of acquisition. An individual 384-well plate took approximately 15 min to image using the optimised automated conditions. Each acquisition captured thousands of cells (average > 3,500 cells per field of view), thus providing a reasonable size database by which to calculate results.

5.2.6.2 Analysis

Images were analysed using IN Cell Developer Toolbox V1.6 software, a high content cellular analysis package that utilises a vast array of user-definable parameters, calculations, measures and output formats to allow for individualised assay analysis. The primary output measure of this assay was chosen as GFP intensity normalised to viable cell count per field of view. Therefore in order to obtain an accurate measure, precise segmentation of the cells and GFP was critical. Nuclear staining with Hoechst 33342 and non-viable nuclear staining with propidium iodide enabled per cell data to be obtained. As nuclei were more uniform in shape and more easily separated from one another than the heterogeneous SKOV3 cell population, the stained nuclei were first segmented based on size and shape, and then the segmented nuclei were used to seed the segmentation of individual cells (Figure 5.4). During the optimisation steps, the bright-field images of cells were also used as an approximate outline of cell shape. Cells were classed as viable or non-viable depending on propidium iodide staining. GFP expression was segmented based on the signal intensity (Figure 5.4). Intensity-based measurements can fluctuate or decrease for a given set of plates depending on whether or not the plates were assayed on the same day, therefore it was important to perform preliminary checks of GFP intensity prior to starting the analysis on any given day. Several measures/classifications were defined and results were calculated. In order to prevent skewing of results due to compound toxicity non-viable cells were discarded from the analysis and a measure of GFP intensity per viable cell per field of view was calculated (Figure 5.5). Under optimised conditions each 384-well plate took approximately 25 min to analyse with the IN Cell Developer Toolbox software. Sufficient viable cell counts and the positive and negative controls widely separated from each other allowed for a reproducible signal window (Figure 5.6). The signal was normalised to controls on each plate and the final readout reported as percentage inhibition of FX-mediated Ad5GFP expression. Low levels of GFP expression in the absence of FX in this CAR^{low} cell line compared to in the presence of FX and the analysis design enabled consistently high signal-to-background ratios (calculated by the equation $\text{average}_{\text{MAX}}/\text{average}_{\text{MIN}}$ control), a commonly used parameter employed to estimate the separation or range of an assay signal window (Sittampalam *et al.*, 1997).

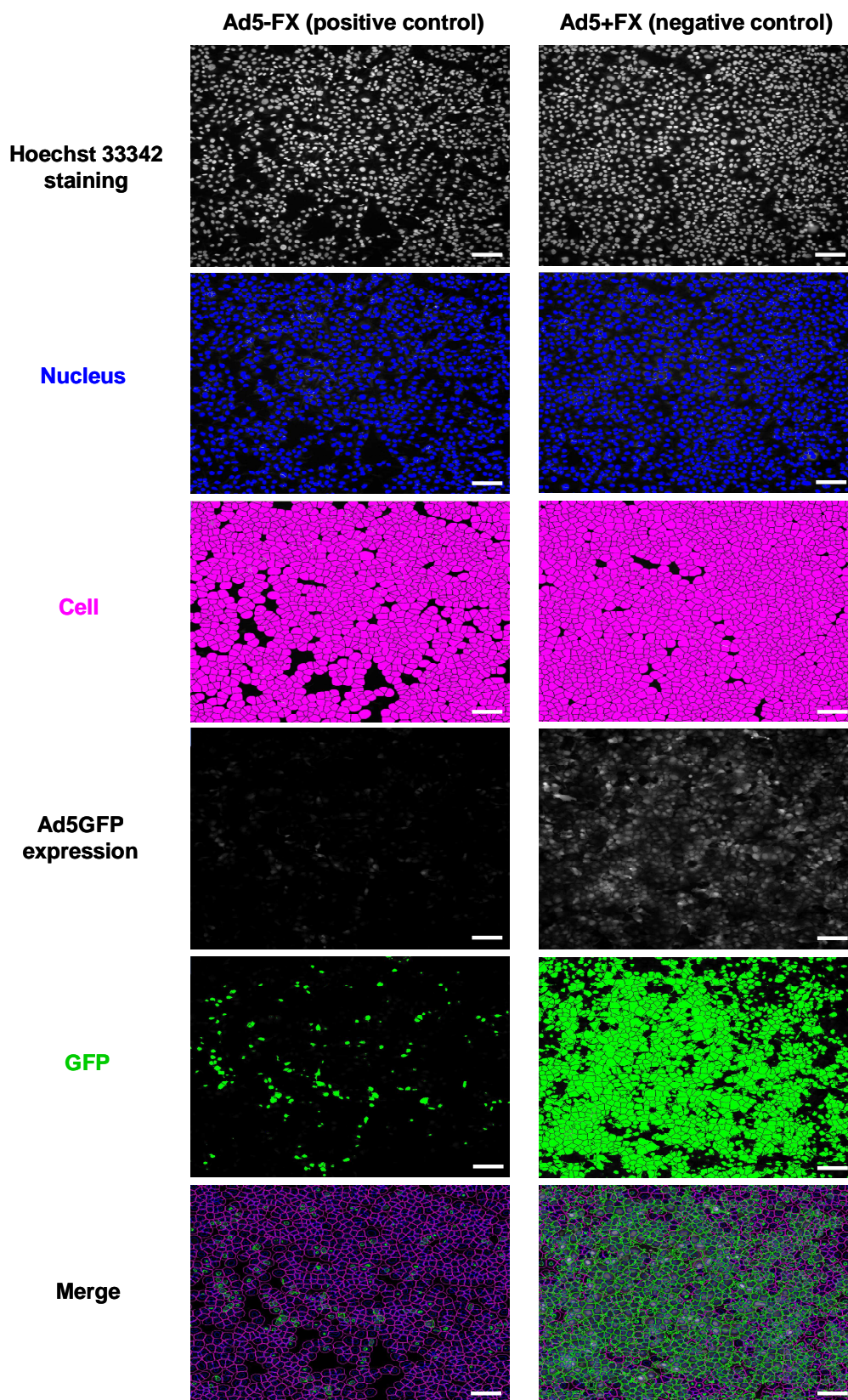


Figure 5.4. Design of image analysis conditions – signal window.

SKOV3 cells were infected with 1000 vp/cell of Ad5GFP in the absence or presence of FX. At 48 h post-infection cells were fixed and stained with Hoechst 33342. Cells were imaged using the IN Cell Analyser 2000 and images were analysed using the IN Cell Developer Toolbox. Nuclei (blue), cells (pink) and GFP expression (green) were segmented based on their staining, size, shape and intensity. 10x magnification, scale bars = 50 μ m.

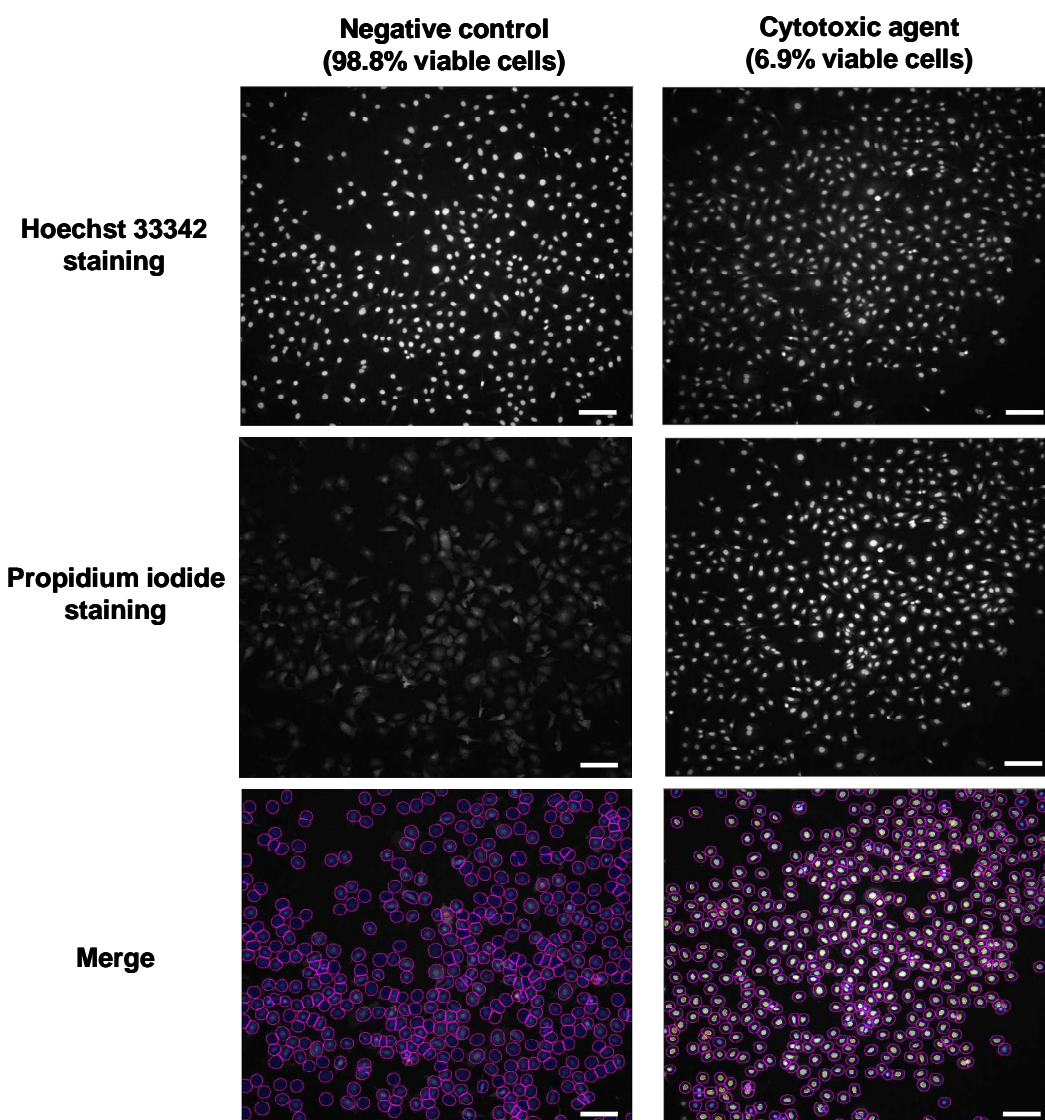
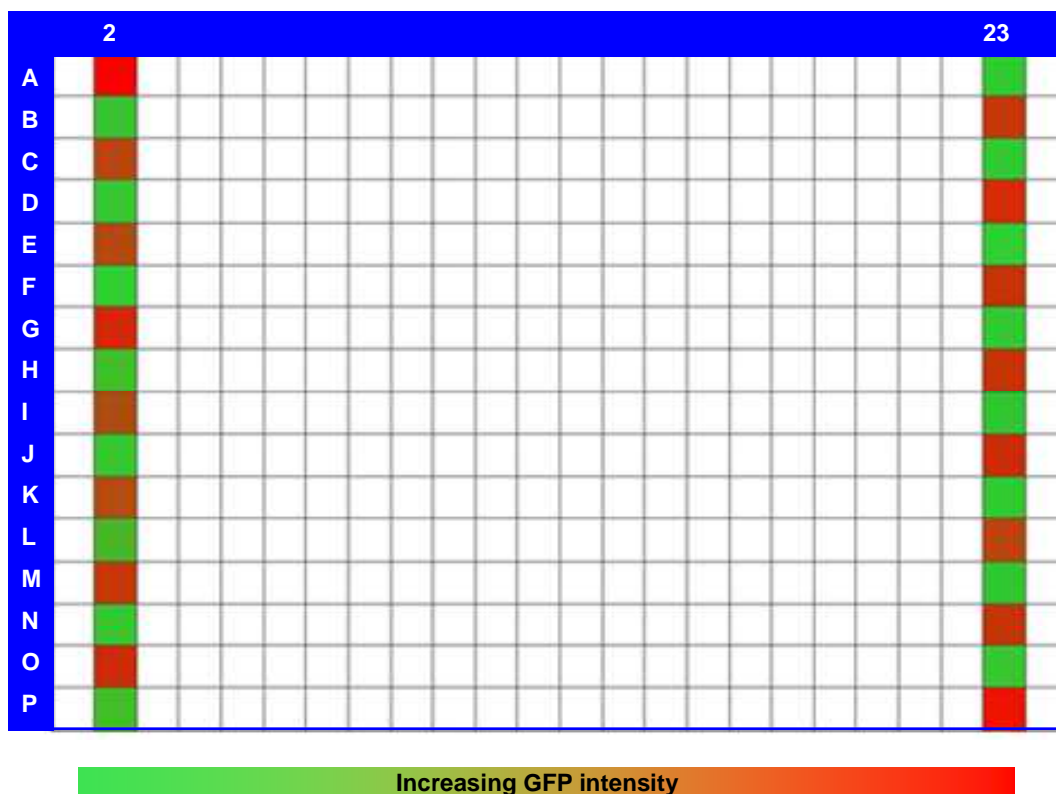


Figure 5.5. Design of image analysis conditions – defining non viable cells.

SKOV3 cells were infected with 1000 vp/cell of Ad5 in the absence or presence of 40 μ M T0501-7827 (Enamine, Ukraine), a cytotoxic compound. After 48 h cells were fixed and stained with Hoechst 33342 and propidium iodide. Cells were imaged using the IN Cell Analyser 2000 and images were analysed using the IN Cell Developer Toolbox. Nuclei were segmented based on Hoechst 33342 staining and non-viable cells were segmented based on propidium iodide staining. Once parameters were defined, the IN Cell Developer Toolbox was used to calculate the number of viable cells. 10x magnification, scale bars = 50 μ m.

(A)



(B)

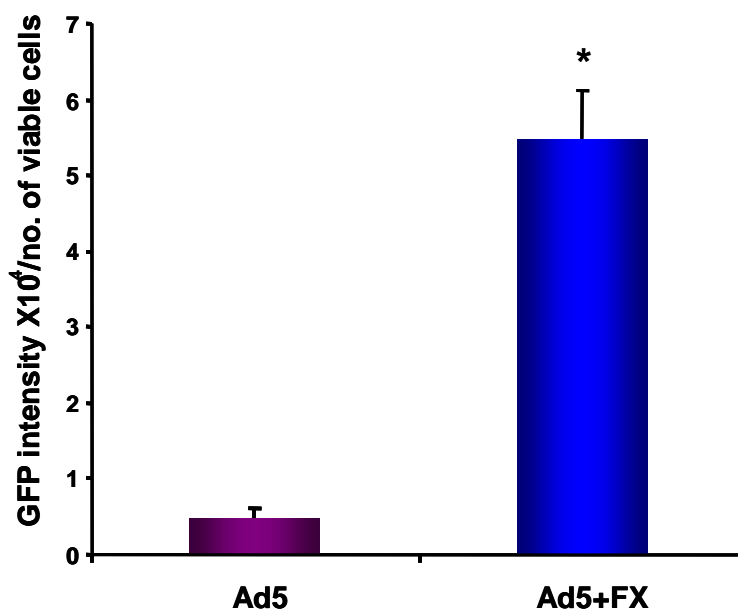


Figure 5.6. Testing screening control conditions.

SKOV3 cells were infected with 1000 vp/cell of Ad5GFP in the absence or presence of FX. At 48 h post-infection cells were fixed and stained with Hoechst 33342, imaged using the IN Cell Analyser 2000 and analysed using Developer Toolbox. (A) Trellis heat map of the assay plate highlighting the plus and minus FX control conditions. (B) Quantification of GFP intensity normalised to the number of viable cells per field of view for the positive and negative control wells. * $p < 0.05$ as compared to non-FX conditions. Error bars represent SEM (n = 16).

Table 5.1. Traditional screening assay versus the HTS format.

Parameters	Traditional screening assay	High throughput screening assay
Plate	Up to 96 well, clear	384 well, black, clear bottom
Cells	2×10^4	1.5×10^3
Virus	1000 – 10000 vp/cell	1000 vp/cell
Well volume	200 μ l	50 μ l
FX	10 μ g/ml	10 μ g/ml
Liquid handling	Manual Assay components added singly	Robotic Assay components added simultaneously
Compound stock	Dry powder, individual tubes	Dissolved in DMSO, preplated
Controls	Row B	Column 2 and 23
Incubation times	3 h, 45 h	3 h, 45 h
Reporter gene	β -gal, GFP, luciferase	GFP
Data normalisation	To protein content - measured by BCA assay	To % viable cells - imaging Hoescht 33342 and propidium iodide staining
Detection method	Victor Wallac2	IN Cell Analyser 2000, Developer Toolbox software
Readout	RLU/mg of protein	GFP intensity/no. viable cells
Toxicity analysed	No	Yes
No. screened	20-80 compounds/week	1000-3000 compounds/week

5.2.7 Assay validation

Using the assay conditions outlined above, the optimised HTS protocol was tested using a small subset of compounds selected from the Pharmacological Diversity Drug-like Set compound library in order to validate the assay format. Principle component analysis (PCA) plots were generated by Dr. Murray Robertson (University of Strathclyde, Glasgow), describing the diversity in chemical space of the 10,240 compounds from the library (Figure 5.7). Chemicals can be characterised by a wide range of ‘descriptors’. Here ‘chemical space’, a term often used in place of ‘multi-dimensional descriptor space’, is a region defined by a particular choice of descriptors and the limits placed on them (Dobson, 2004). In this instance these parameters included the molecular mass, lipophilicity and topological features of each compound. From this 80 compounds were initially chosen to assay based on the spread of compound chemical space within the library (compound I.Ds supplied in the appendices to this thesis). When the 80 compounds were plotted within a worldwide database for >80,000 various marketed and developmental drugs, the so called World Drug Index (WDI) (Derwent WDI, Derwent Information Ltd., 14 Great Queen Street, London, WC2B 5DF, U.K), compounds were in a relatively small area of chemical

space compared to the substantially larger dataset. As the compounds from this library are designed as ‘drug-like’ small molecules this was as expected.

The 80 compounds were assayed on the same day across four 384-well plates to compare the variability of the assay format and reproducibility of inter and intra-plate controls (Figure 5.8). The positive and negative controls were positioned in columns 2 and 23 (as described in section 5.2.5) and 20 compounds were tested in triplicate across the plates. The assay provided a robust and reproducible assay signal window; in the presence of FX there was an approximate 16-fold increase in GFP intensity/no. of viable cells compared to conditions in the absence of FX. The Z’ factor is the most widely used method to assess HTS quality, being reflective of both the assay signal dynamic range and the data variation associated with the signal measurements (Zhang *et al.*, 1999). The Z’ factor is calculated by the equation:

$$Z' = 1 - (3 \times SD_{\text{MAX CONTROL}} + 3 \times SD_{\text{MIN CONTROL}}) / (\text{Average}_{\text{MAX CONTROL}} - \text{Average}_{\text{MIN CONTROL}})$$

(SD = standard deviation)

The individual Z’ factors from each of the four plates were 0.48, 0.6, 0.63 and 0.58 (average = 0.57). The combination of a high signal-to-background ratio and an average Z’ factor > 0.5 indicates the control-based method of data processing and hit identification strategy would be suitable for the HTS and the assay is robust and reliable. Whilst several of the 80 compounds in this screen caused a significant decrease in GFP intensity/no. of viable cells compared to plus FX conditions, only compound numbers 48 and 64 reached the 75% inhibition of FX-mediated Ad5 transduction cut-off, and as expected the majority of compounds were inactive in this assay (Figure 5.8). These data validate the HTS protocol and the activity of the Pharmacological Diversity Drug-like Set compound library.

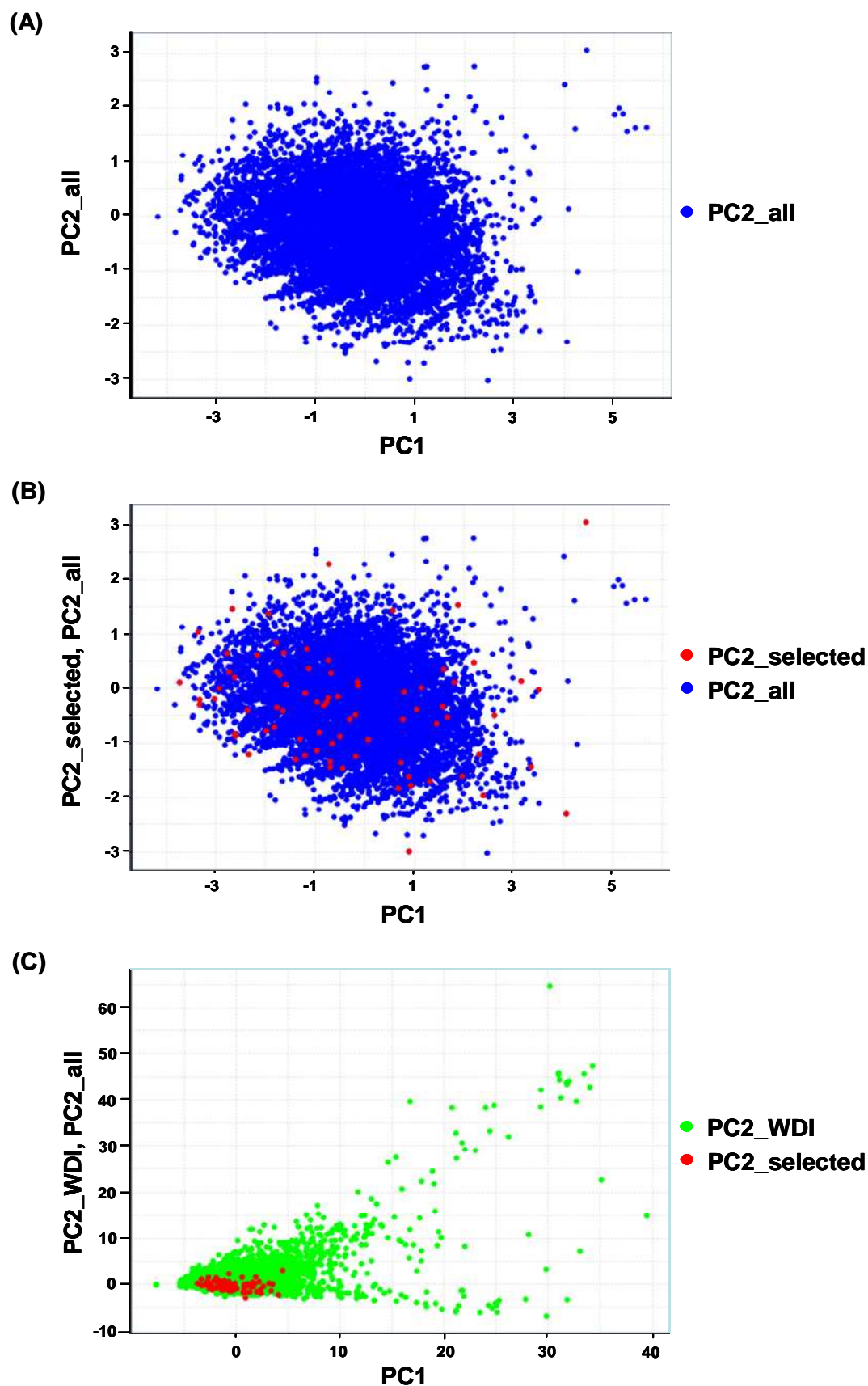


Figure 5.7. Principle component analysis of the compound library.

PCA plots of (A) the chemical spread of the 10,240 compounds in the library (blue), (B) 80 of the most diverse compounds from within the set (red) and (C) the 80 diverse compounds (red) plotted against the WDI (green).

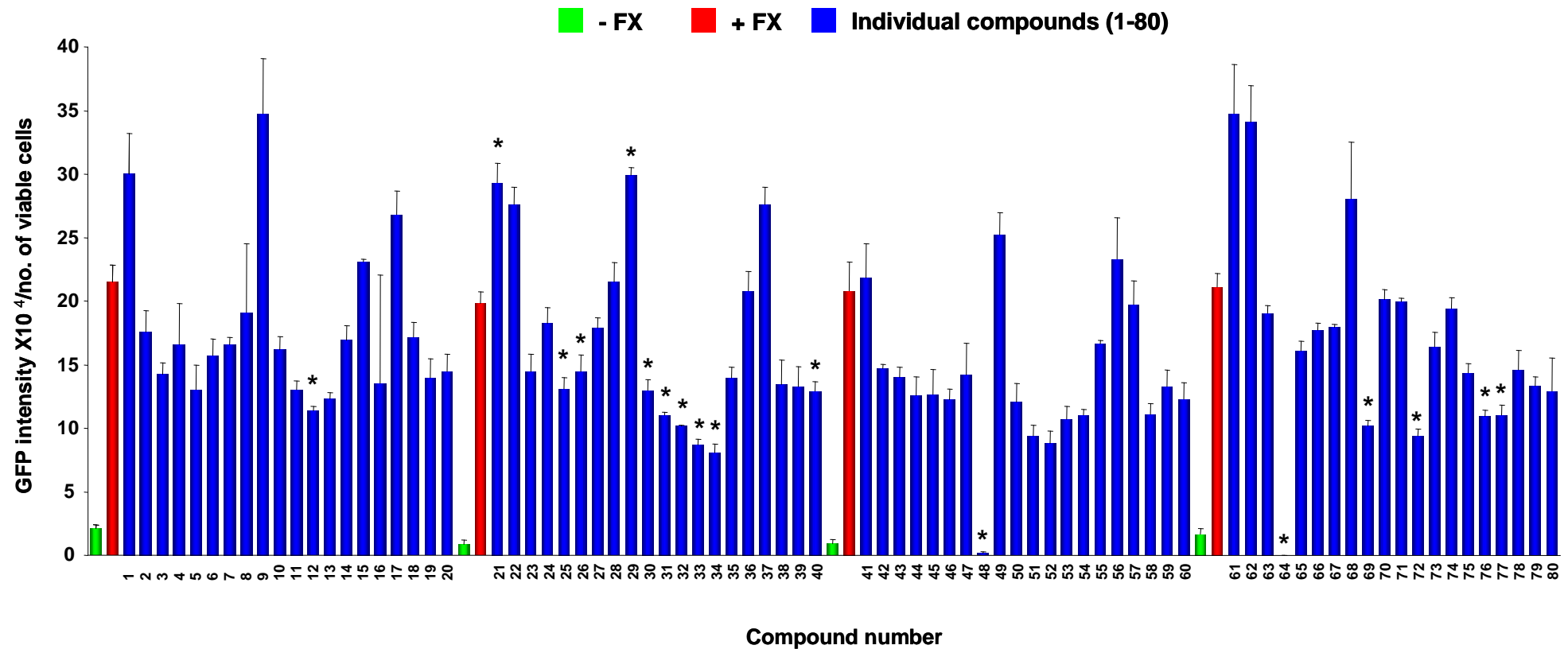


Figure 5.8. 80 compound screen in SKOV3 cells to validate the HTS method.

A collection of 80 diverse compounds from the Pharmacological Diversity Drug-like Set compound library were tested on SKOV3 cells for their ability to inhibit FX-mediated Ad5 transduction using the HTS assay protocol. * $p < 0.05$ compared to plus FX conditions as determined by one-way ANOVA and Bonferroni's post-test. Error bars represent SEM (n = 3).

5.2.8 HTS to identify inhibitors of FX-mediated Ad5 gene transfer

Based on the preliminary data and assay optimisation studies, 10,240 compounds from the Pharmacological Diversity Drug-like Set library were screened in the HTS at a single concentration of 10 μ M in triplicate wells. Over 96 384-well assay plates were run throughout the screen over a period of several weeks. Employing a 75% inhibition of FX-mediated Ad5GFP expression as the criterion for further evaluation, 288 compounds were identified as hits (Figure 5.9 and Figure 5.10). The vast majority of compounds screened in this assay were considered inactive, as defined by the assay parameters i.e. caused no inhibition (Figure 5.10). In total the number of compounds causing $\leq 0\%$ inhibition of FX-mediated Ad5GFP expression was 7,603, whilst 2,349 compounds appeared to cause some inhibition ($> 0\% < 75\%$) but did not reach the stringent 75% cut-off for selection for further screening (Figure 5.10).

The 288 compounds resulting in over 75% inhibition equated to a ~2.8% hit rate for the HTS. In the presence of the 288 compounds FX-mediated Ad5GFP expression was significantly decreased compared to plus FX control conditions as determined by Student t-tests (Figure 5.10B). However this 2.8% hit rate was higher than was expected ($< 1\%$ (Koresawa *et al.*, 2004; Sills *et al.*, 2002; Yarrow *et al.*, 2003)), suggesting cytotoxic compounds or false positives from assay variation were included. Nonetheless, in an attempt to avoid missing potential hits the 288 compounds were selected for further analysis and their effects were re-evaluated in a secondary assay using a similar screening format.

5.2.9 Enhancers of FX-mediated Ad5 gene transfer

A number of the compounds screened in this assay caused a substantial increase in FX-mediated Ad5GFP expression, with compounds enhancing Ad5 gene transfer by up to 10-fold (Table 5.2 and Figure 5.11). Further study and statistical analysis of compounds which enhance Ad5 gene transfer was outside the scope of this study.

Table 5.2. Summary of compounds enhancing FX-mediated Ad5 gene transfer.

Fold increase	1	2	3	4	5	6	7	8	9	10
No. of compounds	4370	1945	762	273	122	67	39	9	10	6

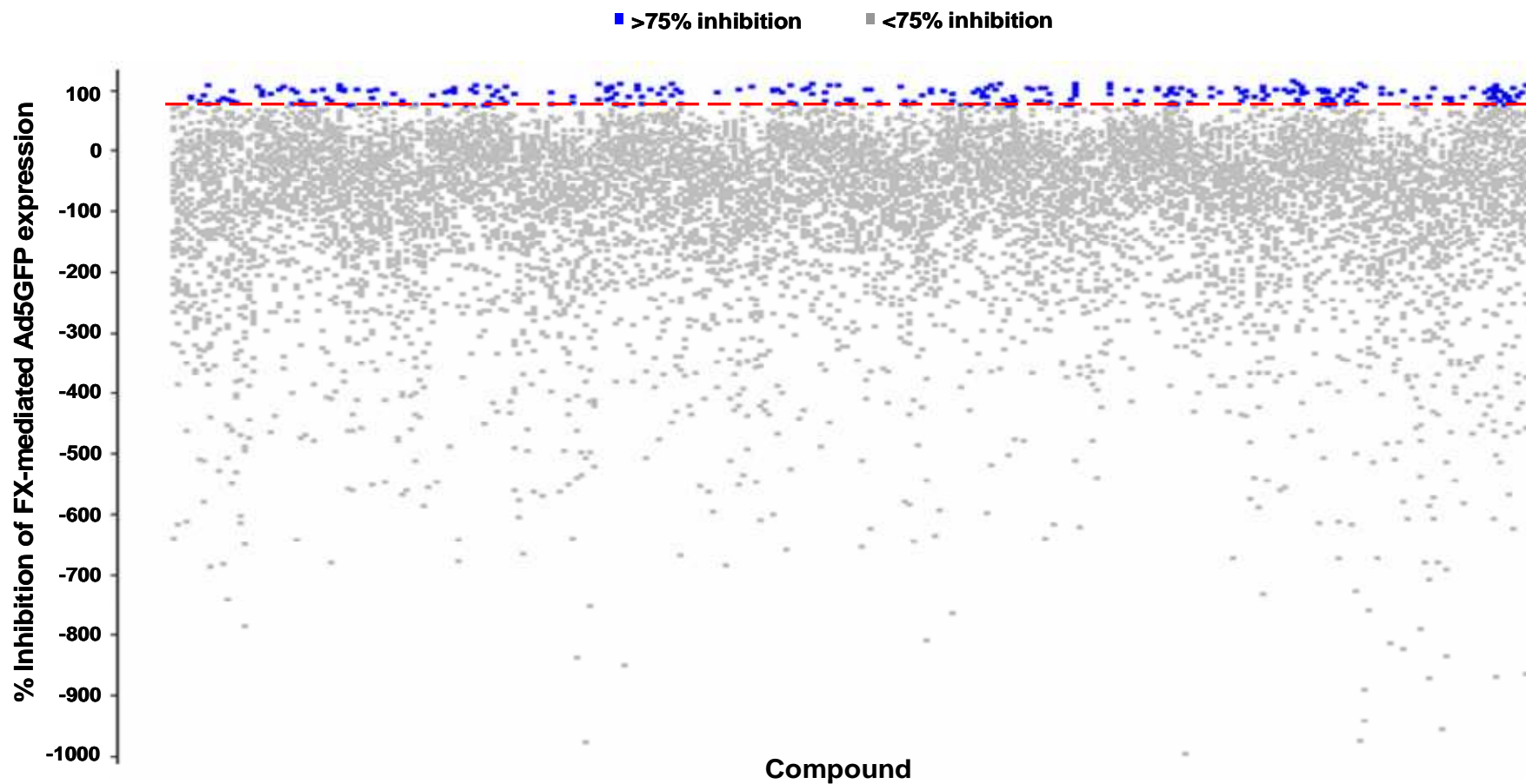
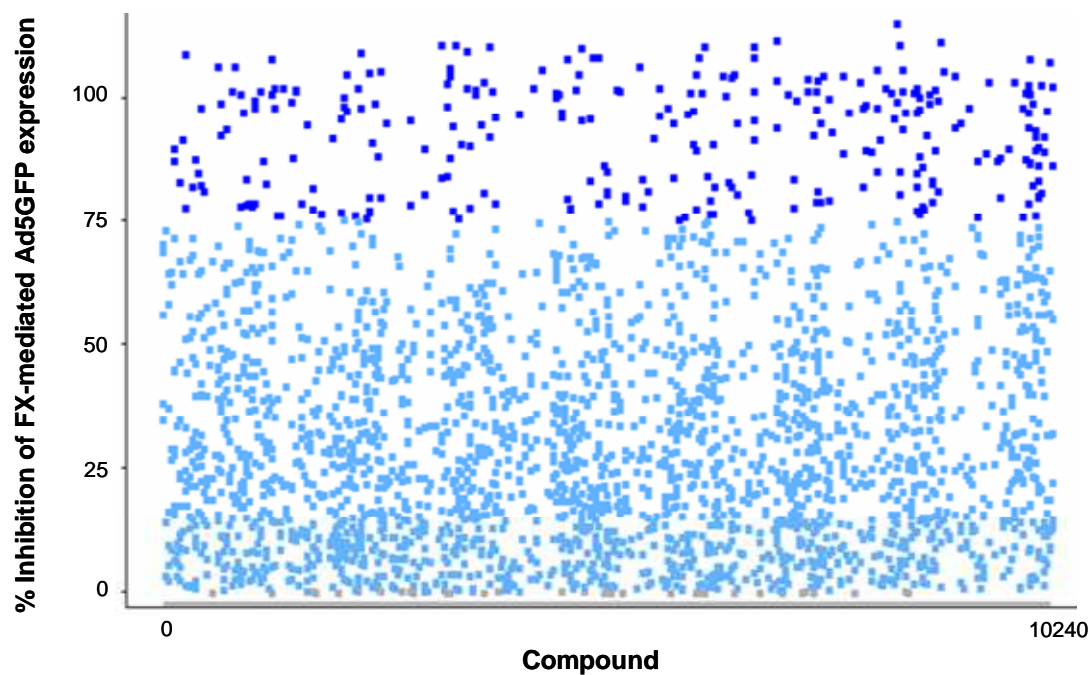


Figure 5.9. HTS of the Pharmacological Diversity Drug-like Set.

SKOV3 cells were infected with 1000 vp/cell of Ad5GFP in the absence or presence of FX plus 10 μ M compound. At 48 h the cells from the 10,240 compounds tested were fixed and stained with Hoechst 33342 and propidium iodide, then screened for their ability to inhibit FX-mediated Ad5GFP expression using the IN Cell Analyser 2000 and Developer Toolbox analysis software. Compounds causing > 75% inhibition, as indicated by the red line, are highlighted in blue.

(A)



(B)

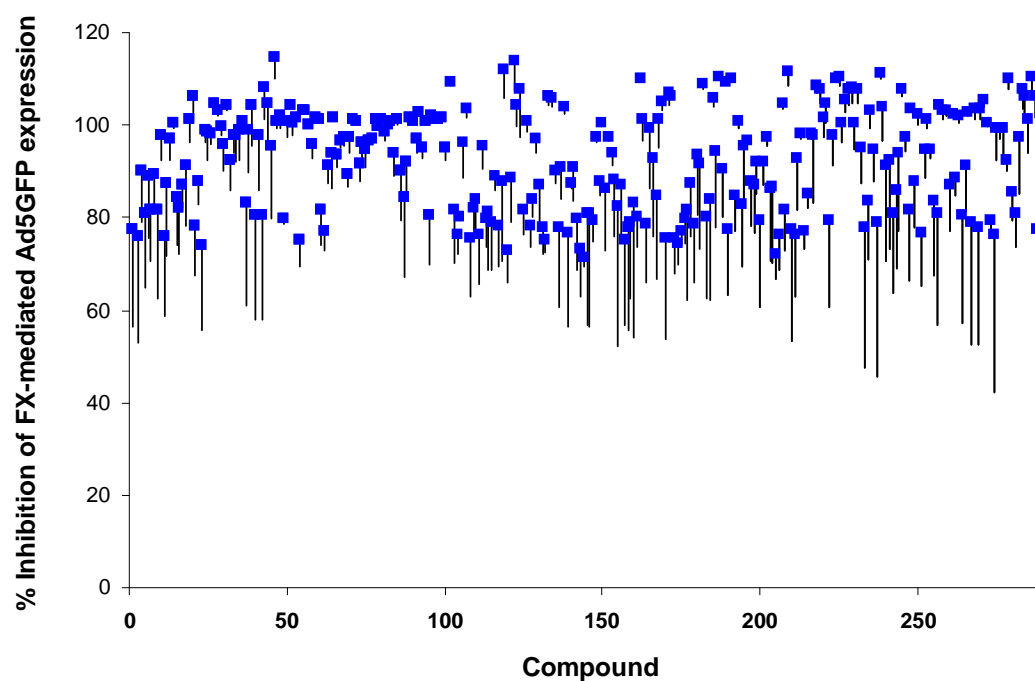


Figure 5.10. HTS inhibitors of FX-mediated Ad5 gene transfer.

(A) Graphical summary of HTS data, highlighting compounds causing > 75% inhibition in blue, those causing between 0 and 75% inhibition in light blue and those causing no inhibition in grey (B) The 288 compounds causing > 75% inhibition. Error bars represent SEM (n = 3/compound).

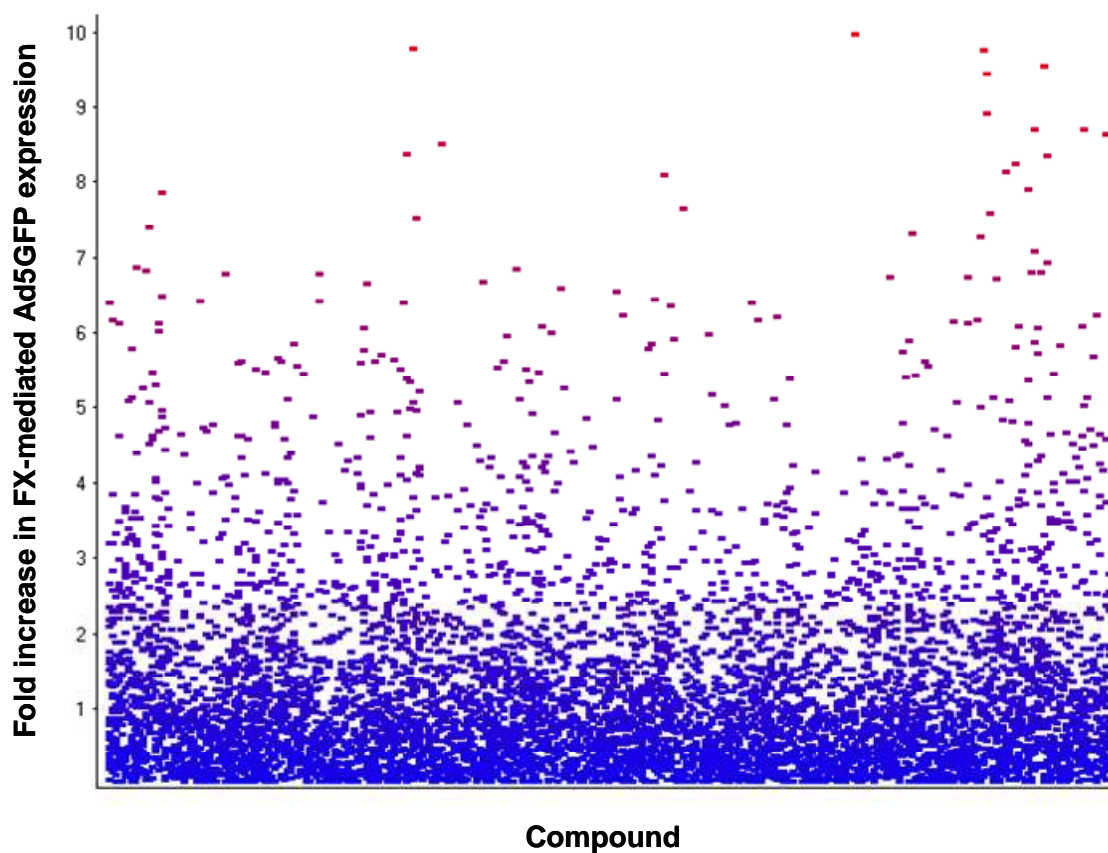


Figure 5.11. HTS enhancers of FX-mediated Ad5 gene transfer.

Graphical summary of the HTS data showing the large number of compounds from the Pharmacological Diversity Drug-like Set which caused an increase in FX-mediated Ad5GFP expression.

5.2.10 HTS quality control

Minimal assay signal variation and high signal-to-background ratios are important factors in HTS. There was a high signal-to-background ratio for each of the 32 sets of plates assayed, the minimum being 7.5:1 and in most cases were several fold higher with the average being 29.82 ± 3.93 -fold (Table 5.3). The magnitude of the signal window and its reproducibility further confirms the suitability of this assay to the control-based method of data normalisation.

A plot of the percent inhibition from the 32 sets of assay plates classified by plate row and the plate row median data value indicates that the assay was well behaved and the majority of compounds were inactive and exhibited activity levels similar to the plus FX control conditions (i.e. $\leq 0\%$ inhibition of FX-mediated Ad5 gene transfer) (Figure 5.12). There was a minimal trend toward positional bias depending of the plate row, with every second row (rows B, D, F, H, J, L, N and P) having a increased median activity value compared to the next (rows A, C, E, G, I, K, M and O) (Figure 5.12). Systemic positional bias such as row, column or edge effects can result in false positives or negatives in such large datasets. Therefore all 288 compounds identified as hits from the HTS were selected for further analysis to minimise the risk of bypassing potential true hits.

Table 5.3. HTS data quality control review.

A summary of the signal-to-background ratios for each of the 32 sets of 384-well plates assayed.

Plate I.D.	Signal-to-background ratio
1	13.26
2	15.93
3	50.25
4	20.03
5	25.22
6	40.05
7	30.00
8	21.89
9	52.30
10	7.54
11	20.53
12	32.32
13	9.81
14	8.73
15	10.02
16	17.55
17	15.46
18	15.04
19	12.69
20	38.65
21	35.43
22	35.93
23	97.81
24	13.57
25	10.21
26	36.48
27	9.68
28	37.69
29	38.57
30	27.96
31	61.401
32	92.14
Average	29.81771 ± 3.93

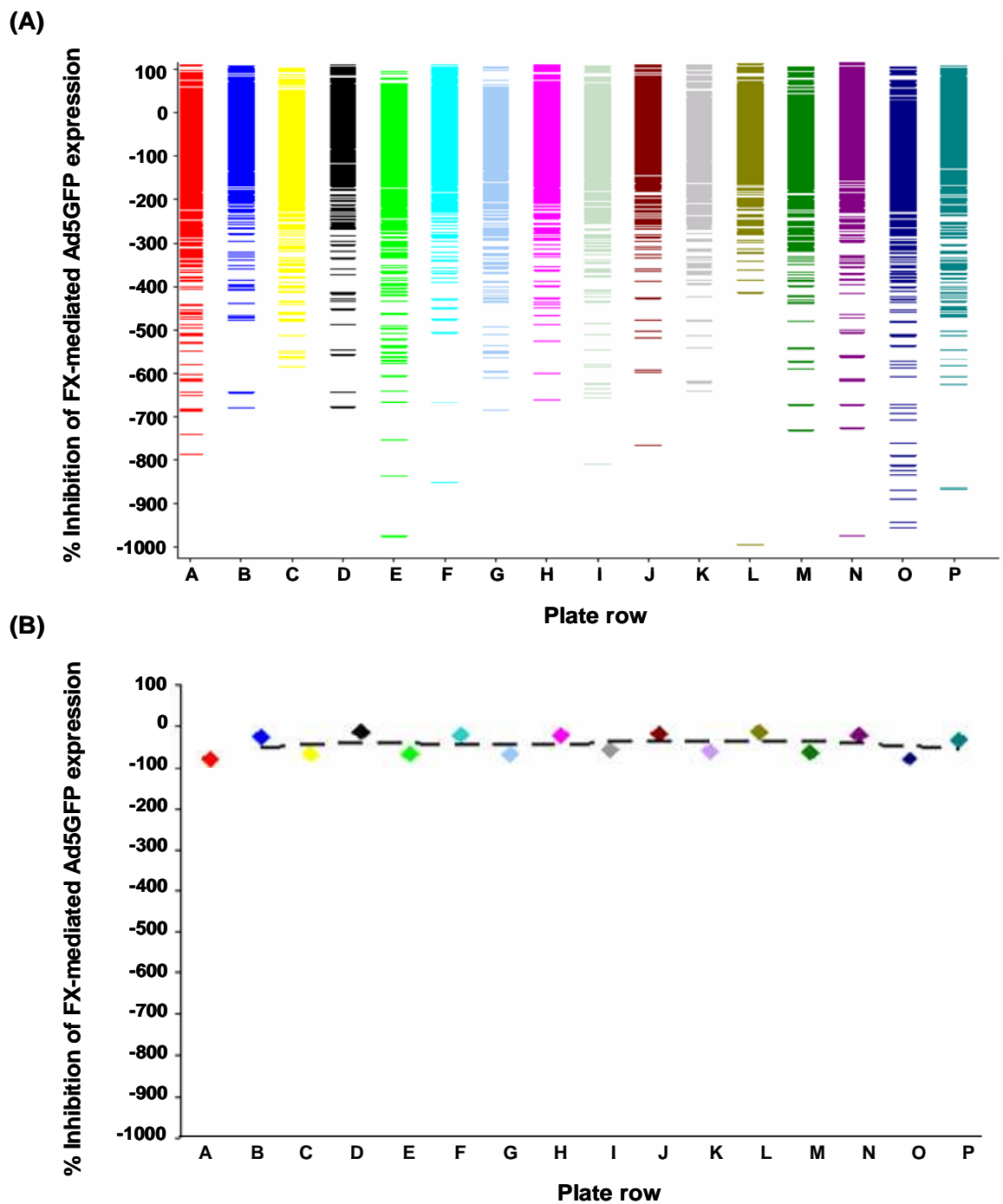


Figure 5.12. Plate positional effects.

(A) Graphical summary of the HTS data categorised by plate row A to P. Each row is separated by colour. (B) Plot of plate row median percentage inhibition of FX-mediated Ad5GFP expression with the median trendline.

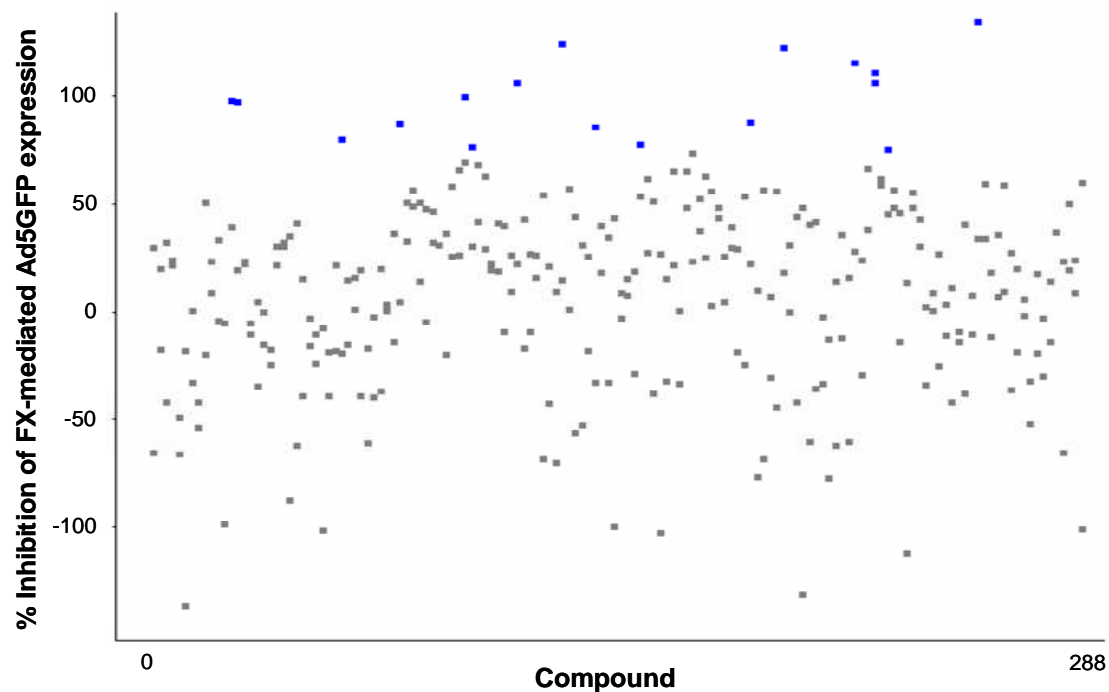
5.2.11 Secondary screening of compounds

In the secondary assay the 288 most active compounds from the initial screen were retested at the same concentration of 10 μM in triplicate wells using the same assay format. The secondary screen was repeated twice on separate occasions. On completion of these assays the majority of compounds described as hits from the primary screen were disqualified as false positives; either not causing any inhibition (103 of the 288 compounds – 36%) or as causing less than 75% inhibition of FX-mediated Ad5 gene transfer (167 of the 288 compounds – 58%) (Figure 5.13). Several marginal hits from the primary screen did not reach the cut-off of 75% inhibition when retested, with 28 of the 288 compounds causing 50-75% inhibition (Figure 5.13). A total of 17 compounds were identified as reproducibly causing greater than 75% inhibition in this assay and causing a significant decrease compared to plus FX conditions as determined by one-way ANOVA and Dunnett's multiple comparison post-test. Therefore these preliminary hits were selected for further analysis (Figure 5.14).

5.2.12 Effects of preliminary hits on cell viability

The 17 compounds identified as preliminary hits from the HTS assays, were assessed for effects on cell viability by propidium iodide nuclear staining and MTT assay. Two of the compounds were found to be toxic to cells (making a total of 3 of the 288 compounds in the secondary screen causing cytotoxicity - ~1%) (Figure 5.15). Therefore, a further two compounds were disqualified from the preliminary hit list and the remaining 15 compounds were selected for further analysis and manual testing.

(A)



(B)

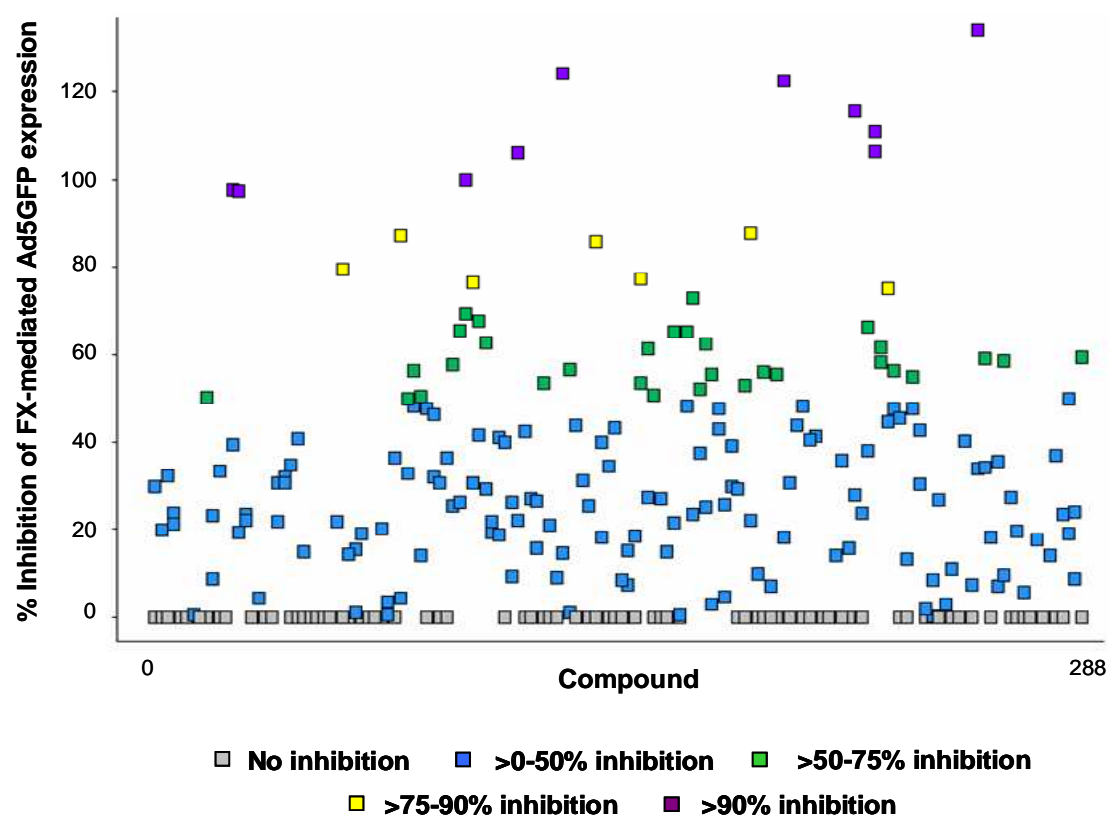


Figure 5.13. Secondary screen.

(A) The 288 active compounds from the HTS were rescreened in a secondary assay using the same format as before. Compounds causing > 75% inhibition are highlighted in blue. (B) Inhibitors of FX-mediated Ad5GFP expression categorised by the percentage inhibition and separated by colour.

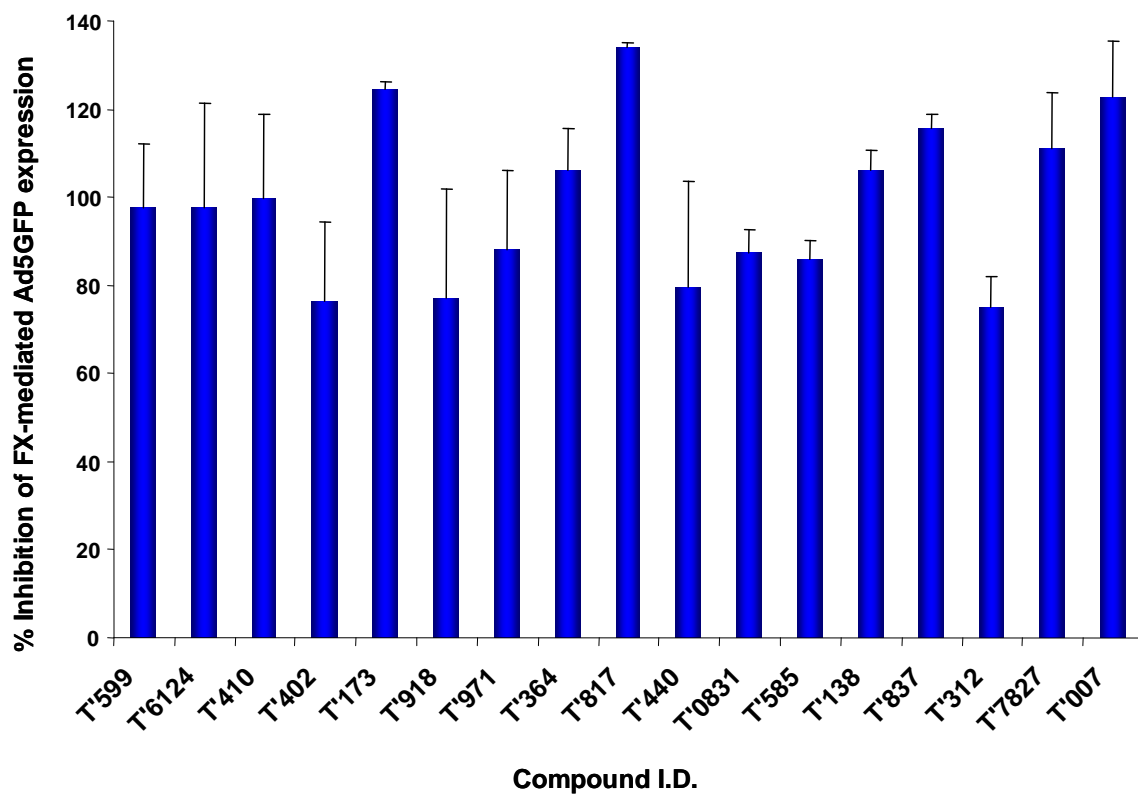


Figure 5.14. Preliminary hits.

The 17 compounds which caused > 75% inhibition in the secondary screen. Error bars represent SEM (n = 3/compound).

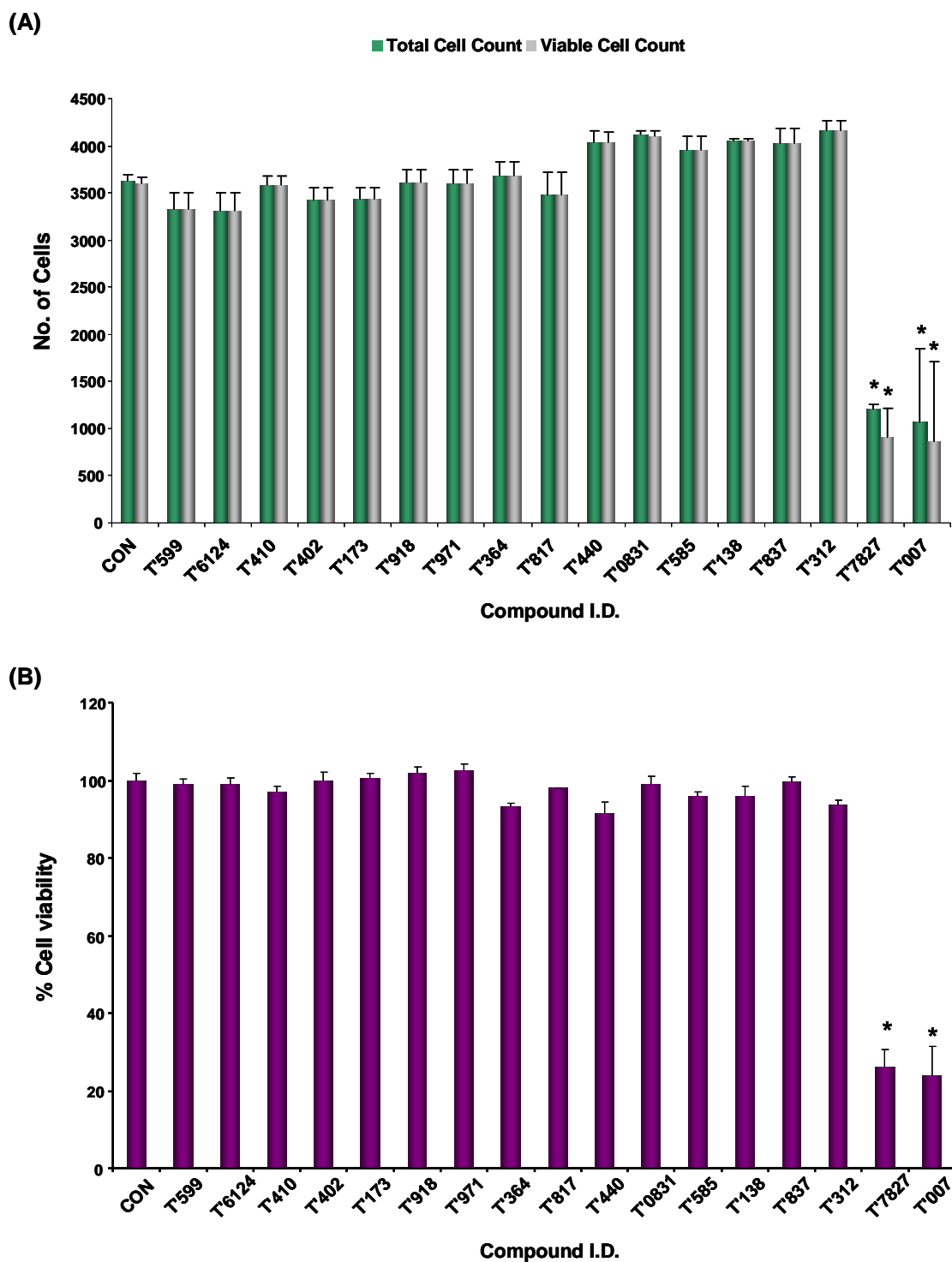


Figure 5.15. Effects of preliminary hits on cell viability.

SKOV3 cells were incubated with 10 μ M compound for 3 h, followed by incubation with 5 μ M compound for a further 45 h when cell viability was assessed. (A) Cells were fixed in 4% PFA and stained with Hoechst 33342 and propidium iodide. Cells were imaged using the IN Cell Analyser 2000 and total cell counts and viable cell counts were performed using the IN Cell Developer Toolbox software. (B) MTT assay was performed. * $p < 0.05$ as compared to control conditions as determined by one-way ANOVA and Dunnett's multiple comparison post-test. Error bars represent SEM ($n = 3$ /compound).

5.2.13 Manual testing of preliminary HTS hits

In order to confirm the activity of the 15 compound hits from the HTS it was important to test them in the standard 96-well manual assay format, without the use of assay automation such as robotic liquid handling equipment and high content cellular screening analysis equipment including the IN Cell Analyser and IN Cell Developer Toolbox software. This assay was repeated three times. This assay further narrowed down the preliminary hits to five compounds validated as causing > 75% inhibition of FX-mediated Ad5 gene transfer (Figure 5.16). The five inhibitors were identified as T5424837 (abbreviated to T'837), T5550585 (T'585), T5660138 (T'138), T0503-0831 (T'0831) and T5960817 (T'817) from the Pharmacological Diversity Drug-like Set library. The compounds had molecular weights ranging from 334 to 423 Da (Figure 5.16).

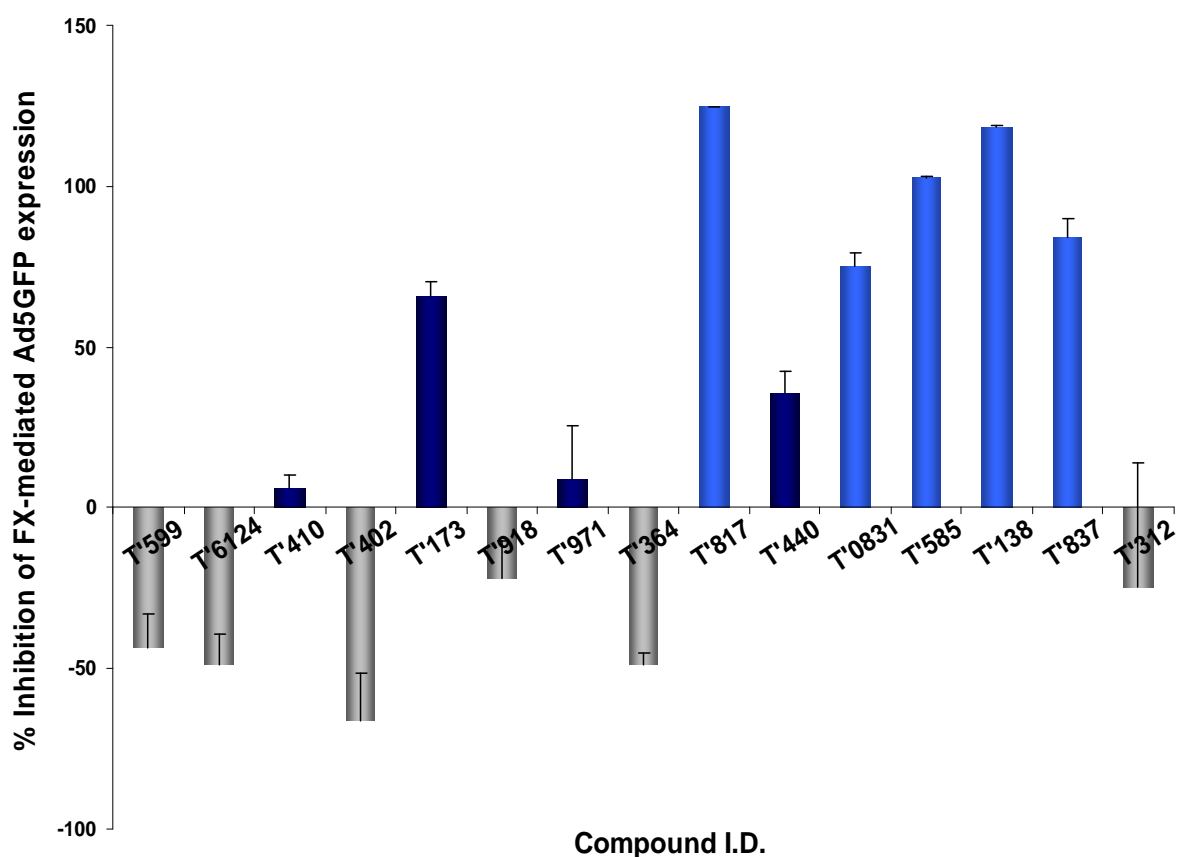


Figure 5.16. Manual testing of preliminary hits.

SKOV3 cells seeded in 96-well plates were infected with 1000 vp/cell of Ad5GFP in the absence and presence of FX plus 10 μ M compound in 100 μ l serum free media. After 3 h 100 μ l media containing 20% serum was added to cells. After 48 h cells were washed in PBS and lysed. GFP expression from the cell lysates was analysed using the Victor Wallac2 plate reader at 450 nm absorbance. Blue = compounds causing > 75% inhibition, grey = no inhibition and navy = < 75% inhibition. Error bars represent SEM (n = 4/compound).

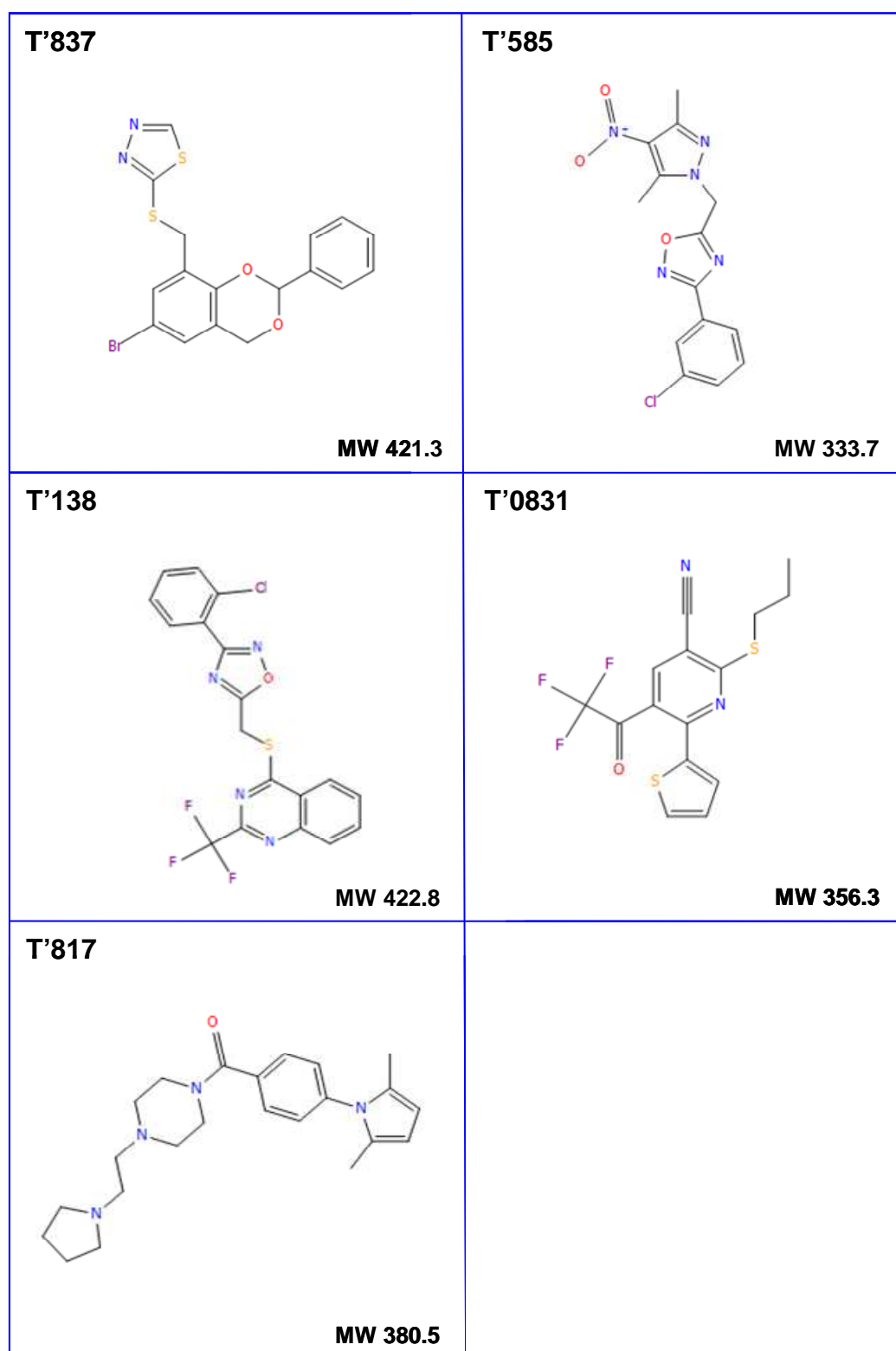


Figure 5.17. Structures of the 5 candidate hit compounds.

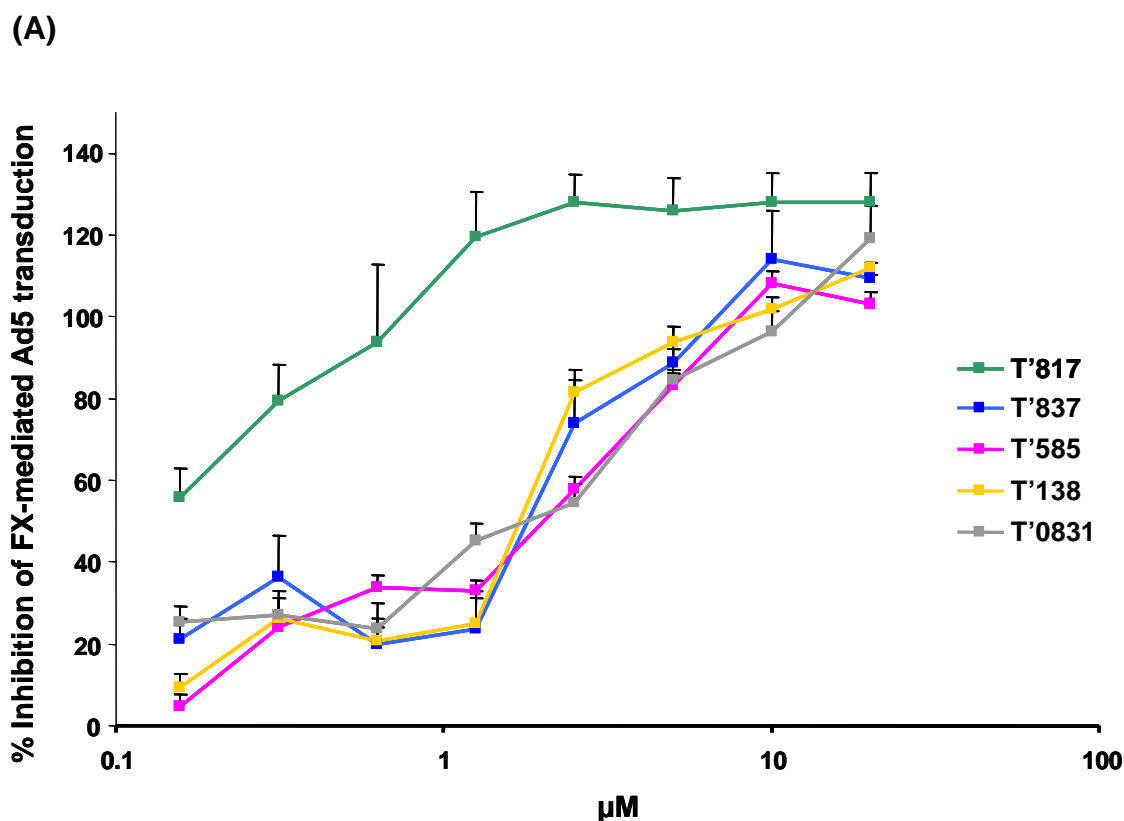
The chemical structures of the 5 compounds identified as consistently causing > 75% inhibition of FX-mediated Ad5 gene transfer.

5.2.14 IC₅₀ determination of the candidate hit compounds

In an attempt to rank the compounds by percentage inhibition and potency of the effect, eight serial 2-fold dilutions of each of the five compounds were prepared and assayed on SKOV3 cells with FX-mediated Ad5 transgene expression as the readout. Instead of using Ad5GFP, Ad5lacZ was employed in this assay and this did not hinder the compounds activity, as assessed by % inhibition of FX-mediated Ad5 transgene expression, indicating their effects are independent of the viral reporter gene. All compounds ablated FX-mediated Ad5 transduction at the top concentrations of 10 and 20 μM , having IC₅₀ values below 4.5 μM . Compound T'817 was the most potent with an IC₅₀ value of 0.47. The other four compounds produced very similar dose response curves, with low levels of inhibition at the lowest concentration of 0.15 μM .

5.2.15 Effect of candidate hit compounds on FX-mediated Ad5 intracellular transport

In order to gain more information of the mechanism of action of the five hit compounds, their effects on fluorescently-labelled Ad5 trafficking in the presence of FX was assessed in SKOV3 cells. Compounds were tested at 10 μM and effects were analysed at 0, 15, 60 and 180 min time points. Apart from compound T'817 none of the hits caused a substantial decrease in Ad5 binding to the cell surface as assessed visually. However, intracellular trafficking at all subsequent time points appeared to be disrupted by each of the inhibitors, with the most severe effects seen with T'817. Instead of forming a punctuate spot at the MTOC by 60 min, the virus was more diffusely situated in the perinuclear region in the presence of each of the compound compared to the plus FX conditions. When the percentage of cells with which the virus particles colocalised with the MTOC were quantified it was found that colocalisation was significantly reduced at 15, 60 and 180 min with all inhibitors. These data from visual assessments of viral trafficking assays indicate that the compound T'817 decreases cellular binding, whilst the other four compounds T'837, T'585, T'138 and T'0831 are causing their principle effect post-cell binding and disrupt intracellular trafficking to the nucleus.



(B)

Name	Compound I.D.	IC ₅₀
T'817	T5960817	0.47
T'837	T5424837	2.47
T'585	T5550585	2.78
T'138	T5660138	2.02
T'0831	T0503-0831	4.47

Figure 5.18. IC₅₀ determination of the candidate hit compounds.

(A) Cells were infected with 1000 vp/cell of Ad5lacZ in the absence or presence of FX plus 0.15, 0.3, 0.6, 1.25, 2.5, 5, 10 or 20 µM compound in 100 µl serum free media. After 3 h 100 µl media containing 20% serum was added to cells. Transgene expression was measured 48 h post-infection. Data was normalised to minus and plus FX control conditions and represented at percentage inhibition. Error bars represent SEM (n = 4/compound). (B) Table represents the IC₅₀ values for each of the compounds. The IC₅₀ was calculated by fitting a 4-parametre logistic non-linear regression model equation using MasterPlex ReaderFit analysis software (Hitachi Solutions America, Ltd., MiraiBio Group).

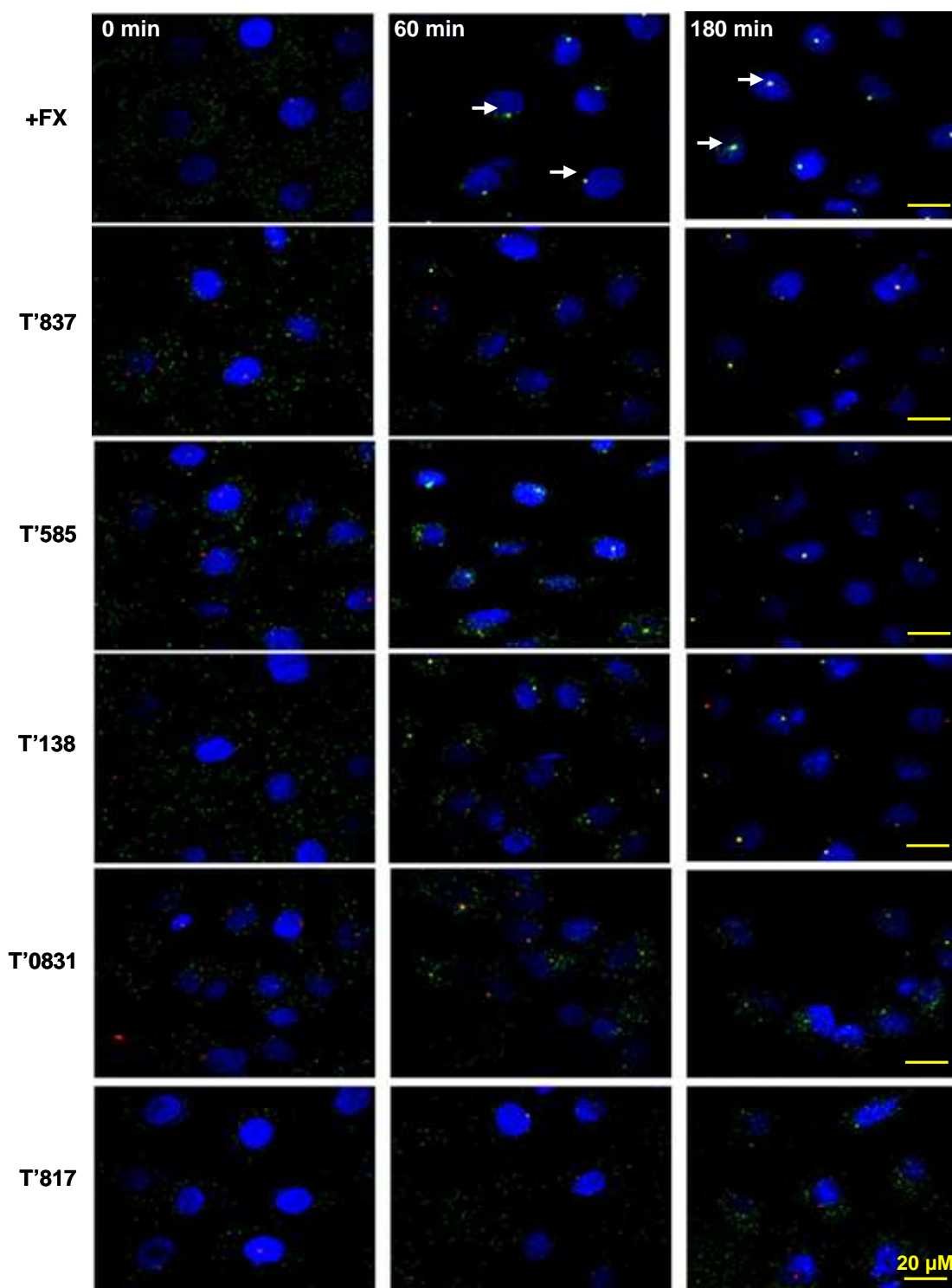


Figure 5.19. Effects of candidate hits on FX-mediated Ad5 intracellular trafficking.

Cells were incubated with 10,000 vp/cell of Alexa488-labelled Ad5 (green) in the presence of FX and 10 μ M compound for 1 h at 4°C, followed by incubation at 37°C for 0, 60 or 180 min prior to staining for pericentrin (red). Images were captured on a confocal microscope at 63x magnification, scale bar = 20 μ m, applicable to all panels. White arrows highlight examples of Ad5 accumulation at the MTOC.

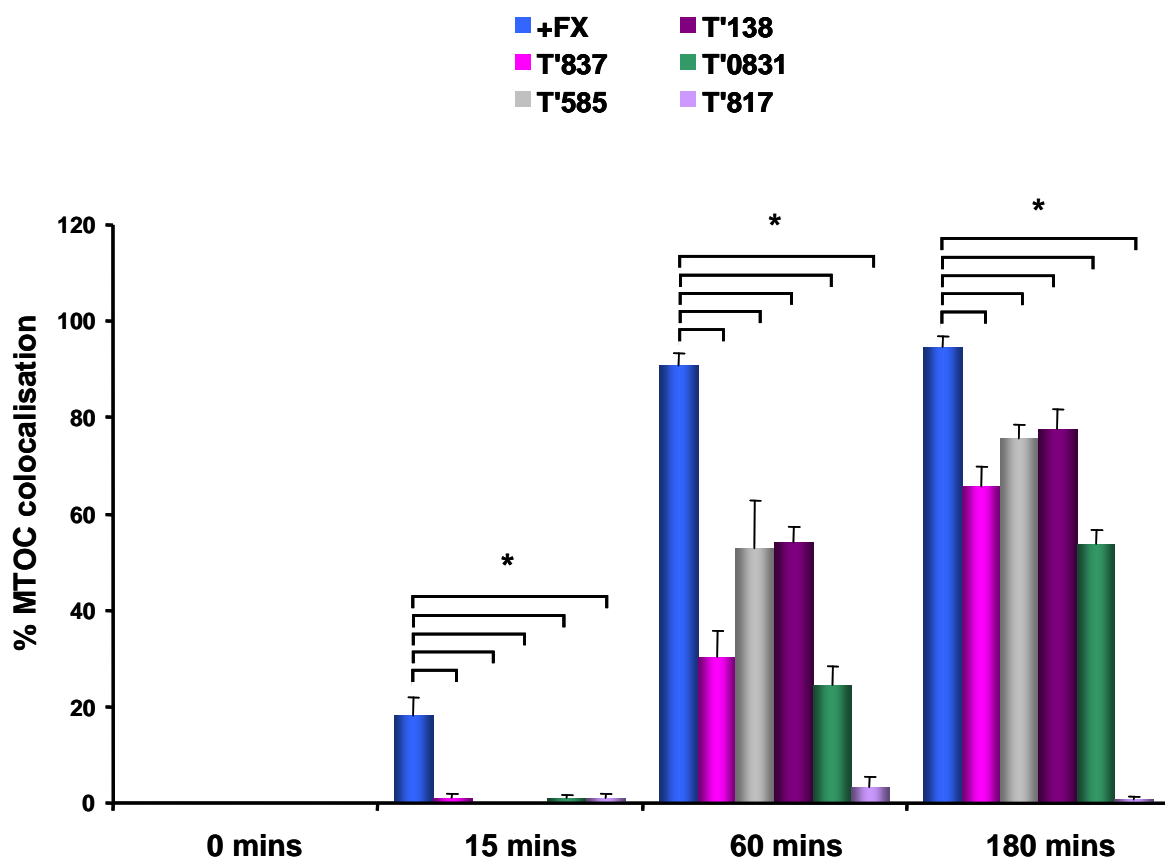


Figure 5.20. Effect of candidate hits on Ad5 colocalisation with the MTOC.

The percentage of SKOV3 cells with complete colocalisation of Ad5 with pericentrin was calculated by analysing at least 5 separate 40x microscope fields per experimental condition. * $p < 0.05$ as compared to control conditions at the individual time points as determined by one-way ANOVA and Dunnett's multiple comparison post-test. Error bars represent SEM ($n=5/\text{condition}$).

5.2.16 Structural analysis and determination of hit compounds

Structural analysis of the compounds and follow up library design was performed by Dmytro Kovalsky (Enamine, Ukraine). Structural analysis of the five candidate hits revealed that compounds T'817 and T'0831 may have bias toward promiscuity (Baell *et al.*, 2010; McGovern *et al.*, 2002). T'0831 had several hydrophobic features in a very compact spatial shape, which can confer bias toward hydrophobic cavities on protein surfaces. This could be the source of the observed activity and therefore may be unlikely to produce highly specific and potent interactions. On reorder from Enamine, compound T'817 no longer showed any inhibition of FX-mediated Ad5 gene transfer. This may be a result of impurities within the initial batch, decomposition over time attributing to the activity or the promiscuous nature of the compound (Baell *et al.*, 2010; McGovern *et al.*, 2002). On the other hand, upon batch reorder the effects of compounds T'585, T'138 and T'837 were reproducible and furthermore they display certain common structural features which increased their chances to be true positives and may indicate a common mode of action. Therefore, T'817 and T'0831 were no longer investigated in this study and additional work focused on validating T'585, T'138 and T'837.

A pharmacophore model is one which represents the key physico-chemical interactions that mediate biological activity (Acharya *et al.*, 2011). An initial pharmacophore model based on T'585, T'138 and T'837 was generated and a follow up library designed around each compound. The model was established in collaboration with Dmytro Kovalsky (Enamine, Ukraine). Compounds T'585 and T'138 share a similar 3-phenyl-5-methylene-1,2,4-oxadiazole moiety, whereas T'138 and T'837 have similar substituted condensed heterocyclic systems bridged to a 5-membered heterocyclic ring via two atom linkers (Figure 5.21). Hence, compound T'138 has features that overlap with both the other two hits. In an attempt to align all three molecules simultaneously, a pharmacophore hypothesis was suggested (Figure 5.21). The minimal core can be defined as two heterocyclic moieties bridged via 1-2 atom linker. The first moiety is a 5-membered electron ring heterocycle which may serve as a H-bond acceptor as well as a participant in Van der Waals contacts and the second moiety is larger by volume, lipophilic, condensed heterocycle that may serve as bulk Van der Waals contributor. The quinazoline (two fused six-membered aromatic rings; a benzene ring and a pyrimidine ring) and 1,3-benzodioxane of T'138 and T'837, respectively, are examples of this. The 4-nitro-3,5-dimethyl-1,2-pyrazole of T'585 is a bulky group that also obeys this model. An additional enforcement is provided by substitutions on both sides of the minimalist core. With T'585 additional interaction is

achieved by *m*-Cl-phenyl group attached to 5-position of oxazole. With T'837 2-phenyl and 5-Br groups of 1,3-benzodioxane moiety can be a source of extensive van der Waals contacts. Finally, T'138 has substitutions on both heterocyclic moieties. Based on these considerations, additional compounds that resemble the minimalistic core with various substitutions on the periphery were identified in Enamines stock collection. 28 compounds were selected as a follow up library.

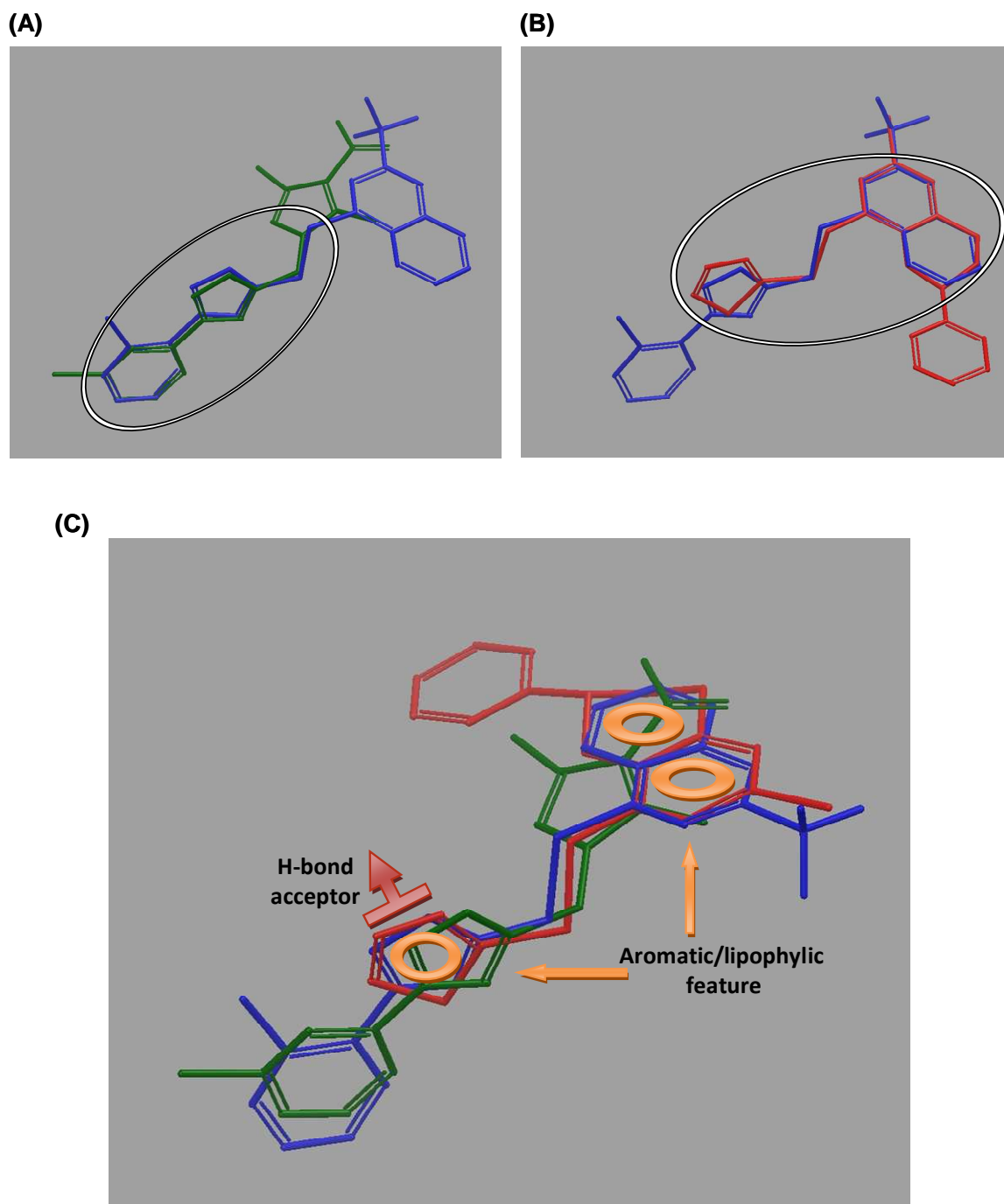


Figure 5.21. Structural alignments.

(A) T'585 (green) with T'138 (blue) (B) T'138 (blue) and T'837 (red). Zones of high topological identity are highlighted. (C) Structural alignment of all three hits. Common minimal pharmacophore core is shown: 5-membered heterocycle with hydrogen bond acceptor and aromatic feature linked to a bulky lipophylic feature. Figure provided by Dmytro Kovalskyy (Enamine, Ukraine).

5.2.17 Assessing the activity of hit T5424837 analogues

In an attempt to further validate the activity of T'837 and to perform some preliminary SAR analysis, T'837 and seven chemically related compounds were ordered from Enamine and tested for their ability to decrease Ad5 gene transfer in the presence of FX. As in previous experiments, T'837 decreased FX-mediated Ad5 transduction in SKOV3 cells (Figure 5.22). All of the analogues caused inhibition ranging from 35 to 85% (Figure 5.22). Three compounds T'5243639 (T'639), T'5306163 (T'163) and T'5677956 (T'956) resulted in levels of inhibition similar to the parent compound (Figure 5.22 and Figure 5.23). These data validates the parent T'837 compound and suggests potential for more potent analogues.

In an attempt to rank the compounds based on inhibition and potency, the IC_{50} of T'639, T'163 and T'956 were determined and compared to the parent compound. All inhibitors produced similar dose response curves, with values ranging from ~1 to 5 μ M (Figure 5.22A and B). The IC_{50} for T'837 (2.35 μ M) was very similar to the previously tested batch of compound (2.47 μ M). T'956 caused the greatest level of inhibition and had an IC_{50} of 3 μ M, therefore this analogue, in addition to T'837 was chosen for further studies. This compound is structurally very similar to the parent, with the addition of a benzyl ring (Figure 5.22B).

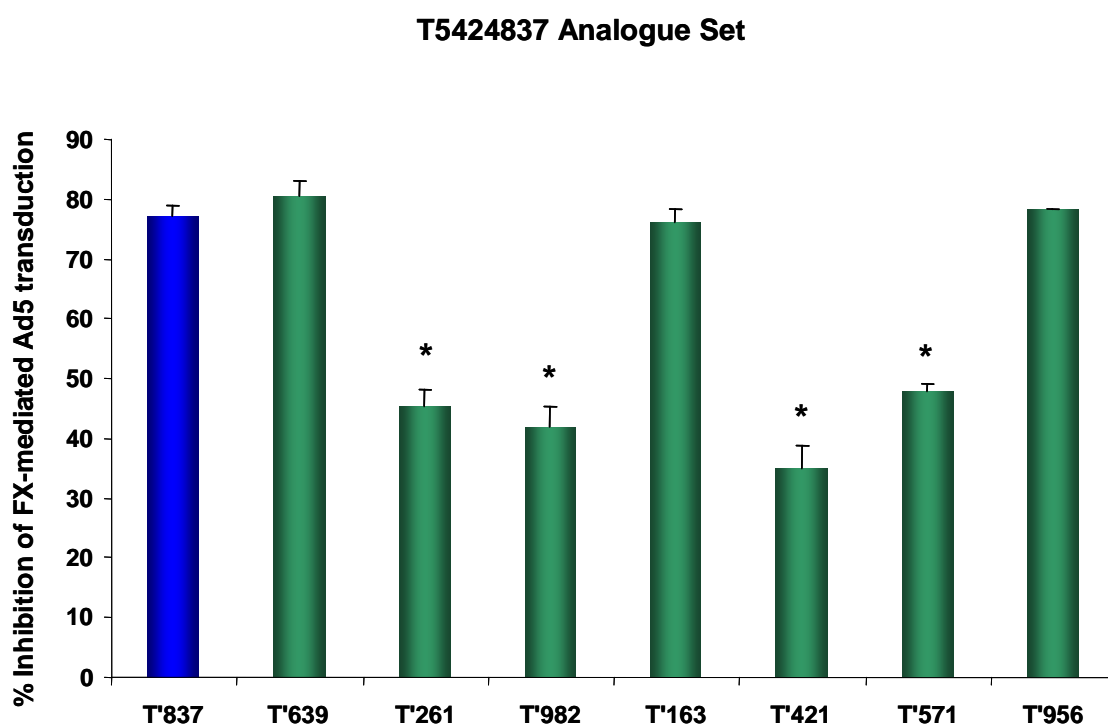


Figure 5.22. Assessing the activity of T'837 analogues.

Cells were infected with 1000 vp/cell of Ad5lacZ in the absence or presence of FX plus 10 μ M compound T'837 or 7 of its chemical analogues in 100 μ l serum free media. After 3 h 100 μ l media containing 20% serum was added to cells. Transgene expression was measured 48 h post-infection. Data was normalised to minus and plus FX control conditions and represented as percentage inhibition. * $p < 0.05$ as compared to the parent compound T'837 conditions as determined by one-way ANOVA and Dunnett's multiple comparison post-test. Error bars represent SEM ($n = 4/\text{compound}$).

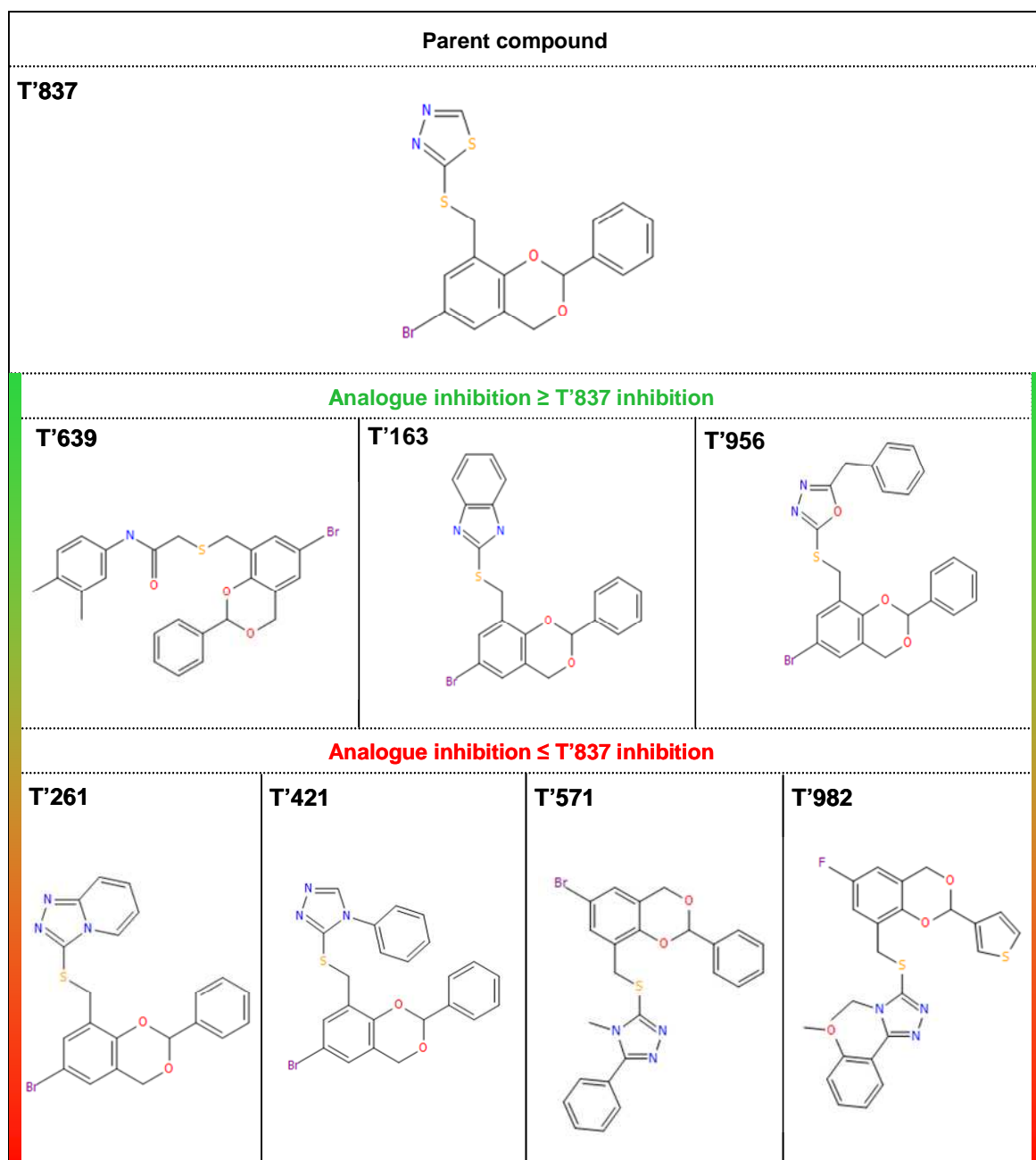
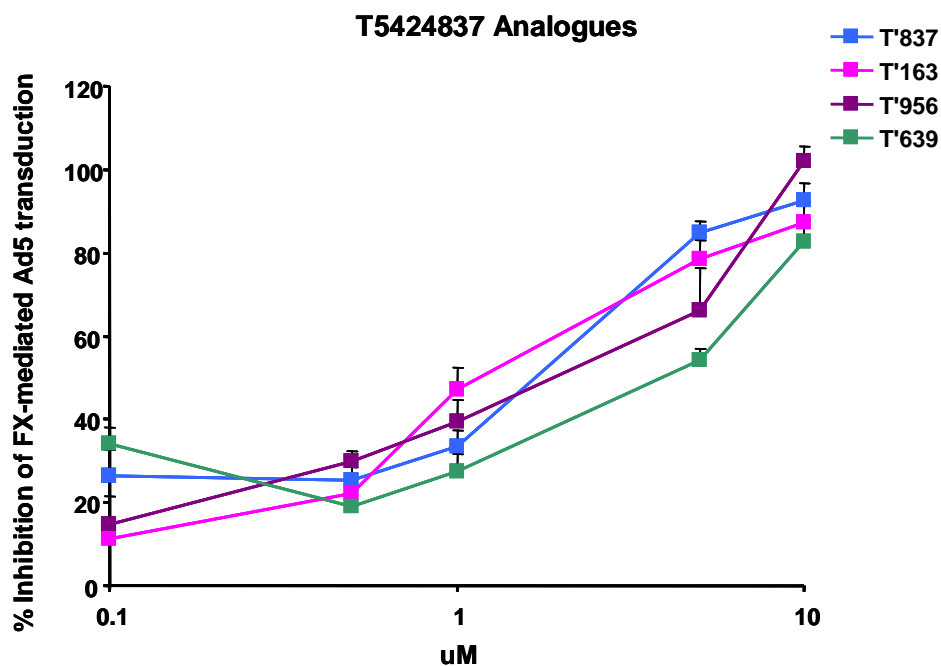


Figure 5.23. Chemical structures of T'837 analogues.

The structures of T'837 and 7 chemically related compounds are shown. The analogues are categorised by their percentage inhibition of FX-mediated Ad5 transduction in SKOV3 cells relative to the parent compound T'837.

(A)



(B)

Name	Compound I.D.	IC ₅₀
T'837	T5424837	2.35
T'163	T5306163	1.03
T'956	T5677956	3.02
T'639	T5243639	5.22

(C)

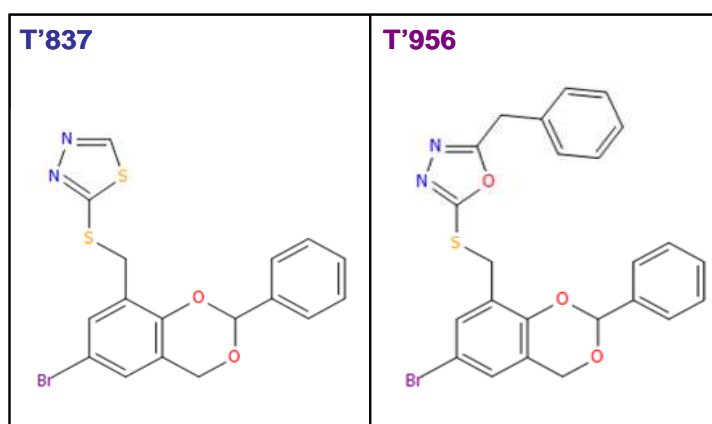


Figure 5.24. IC₅₀ determination of compound T'837 and analogues.

(A) Cells were infected with Ad5 in the absence or presence of FX plus 0.1, 0.5, 1, 5 or 10 μM T'837 or chemically related compounds in 100 μl serum free media. After 3 h 100 μl media containing 20% serum was added to cells. Transgene expression was measured after 48 h. Data was normalised to minus and plus FX control conditions and represented as percentage inhibition. Error bars represent SEM (n = 4). (B) Table represents the IC₅₀ values for each of the compounds. The IC₅₀ was calculated by fitting a 4-parametre logistic non-linear regression model equation using MasterPlex ReaderFit analysis software. (C) Structures of T'837 and T'956.

5.2.18 Assessing the activity of hit T5660138 analogues

The ability of T'138 to inhibit Ad5 transduction in the presence of FX was compared to that of 10 chemically related compounds purchased from Enamine. All compounds possessed the same basic structure as the T'138 parent, in addition to having several extra peripheral groups. This allowed for further validation of T'138 whilst simultaneously investigating key functional groups within its structure. Several of the analogues (T'287, T'489, T'137 and T'432) caused no inhibition (Figure 5.25 and Figure 5.26). The three compounds T'494, T'136, and T'376 inhibited FX-mediated Ad5 transduction to similar levels as the parent compound (~95 to 100%) (Figure 5.25 and Figure 5.26).

Next, serial dilutions (ranging from 10 to 0.1 μM) of the three most active analogues and T'138 were prepared and assayed in SKOV3 cells in an effort to grade the compounds in terms of percentage inhibition and potency of the effect. From this analysis, T'136 was found to be the most potent, having an IC_{50} value of 1 μM compared to 4.01 μM for the parent, 4.91 μM for T'376 and 5.33 μM for T'494. T'136, a *m*-Cl substituted analogue, showed 4-fold improved IC_{50} suggesting favourable hydrophobic contacts with the receptor and was the most effective compound in this assay, therefore it was selected for further investigation in conjunction to the parent T'138.

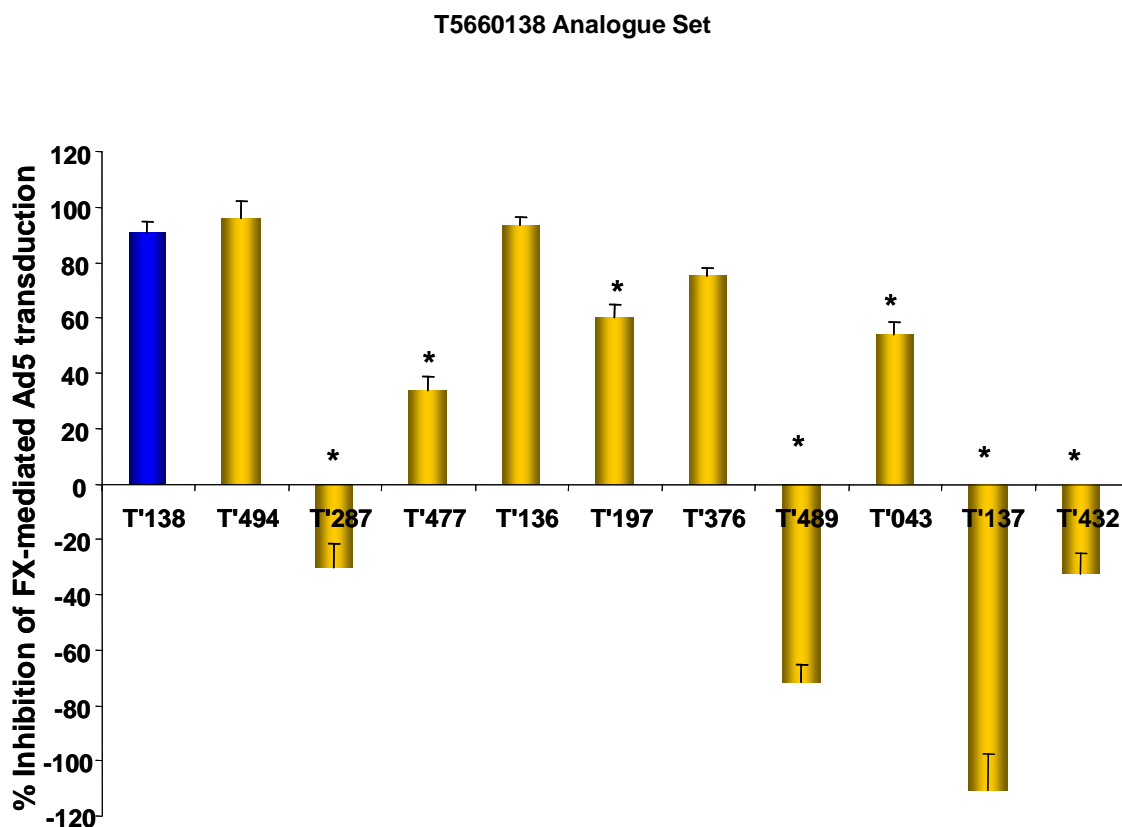


Figure 5.25. Assessing the activity of T'138 analogues.

Cells were infected with 1000 vp/cell of Ad5lacZ in the absence or presence of FX plus 10 μ M compound T'138 or 10 of its chemical analogues in 100 μ l serum free media. After 3 h 100 μ l media containing 20% serum was added to cells. Transgene expression was measured 48 h post-infection. Data was normalised to minus and plus FX control conditions and represented as percentage inhibition. * $p < 0.05$ as compared to the parent compound T'138 conditions as determined by one-way ANOVA and Dunnett's multiple comparison post-test. Error bars represent SEM ($n = 4/\text{compound}$).

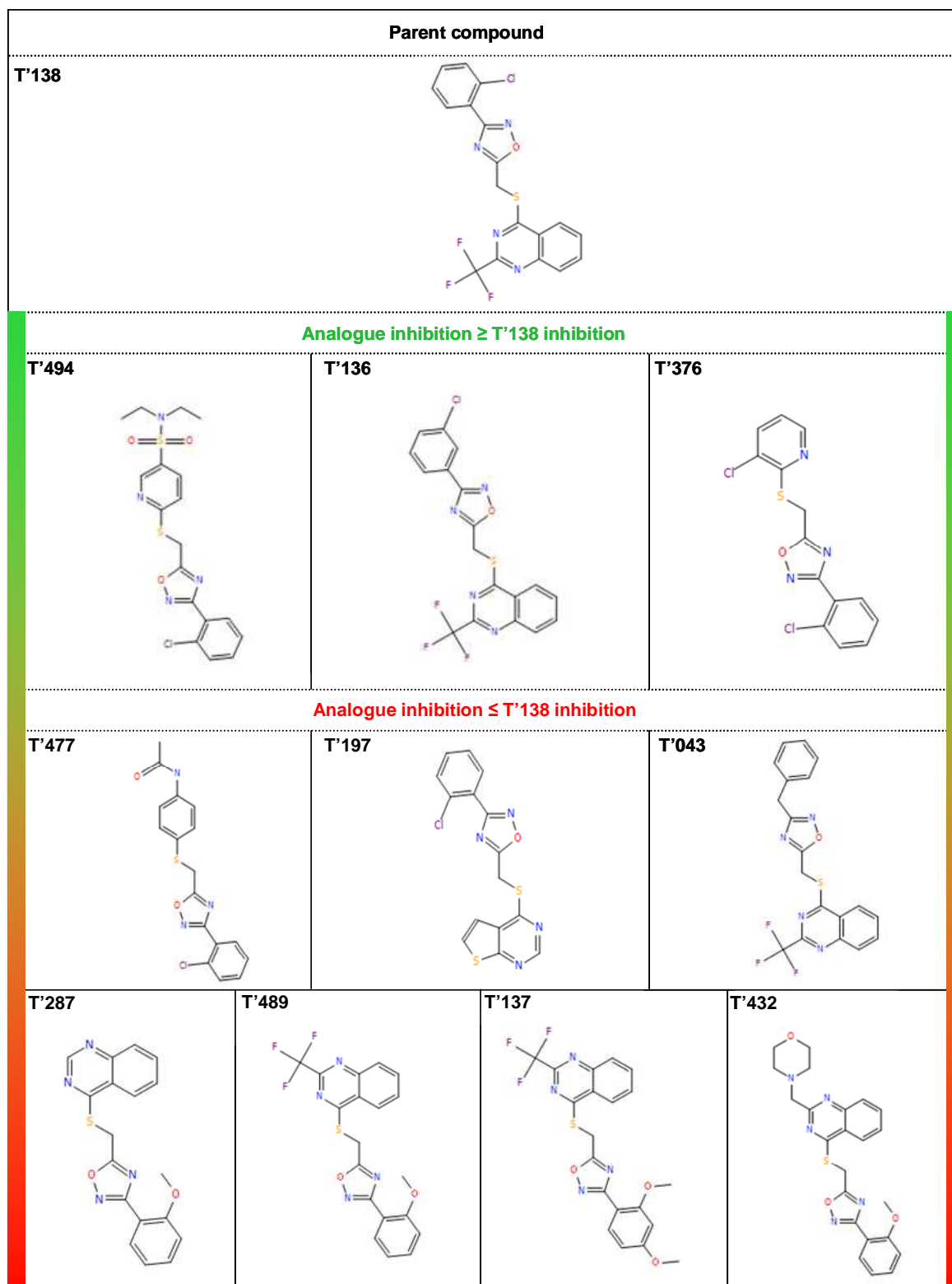
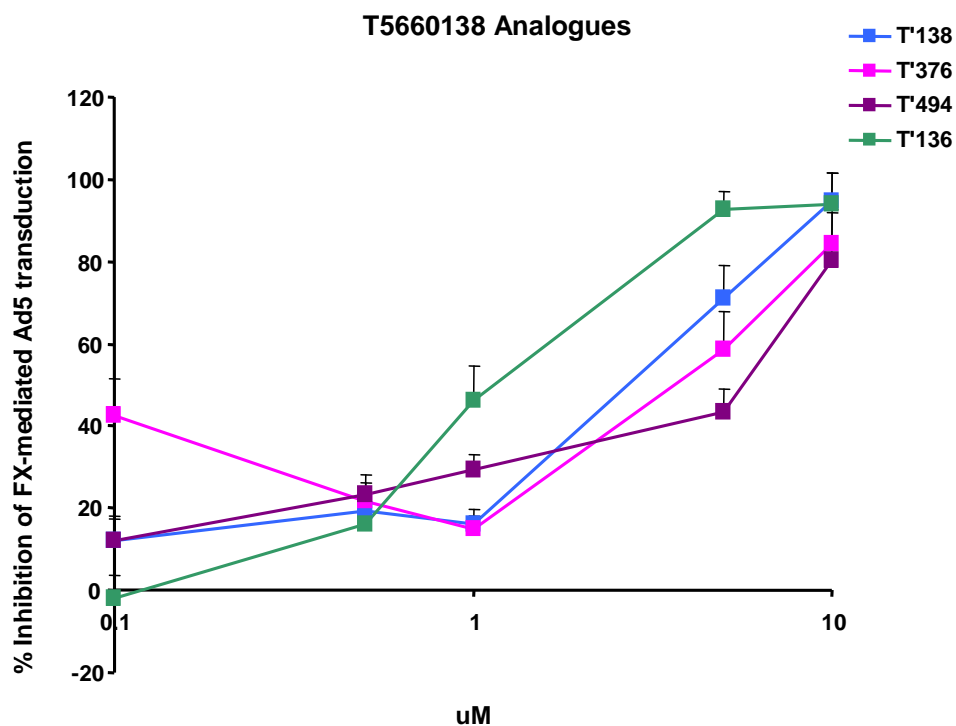


Figure 5.26. Chemical structures of T'138 analogues.

The structures of T'138 and 10 chemically related compounds are shown. The analogues are categorised by their percentage inhibition of FX-mediated Ad5 transduction in SKOV3 cells relative to the parent compound T'138.



(B)

Name	Compound I.D.	IC ₅₀
T'138	T5660138	4.01
T'376	T6314376	4.91
T'494	T7008494	5.33
T'136	T5660136	1.00

(C)

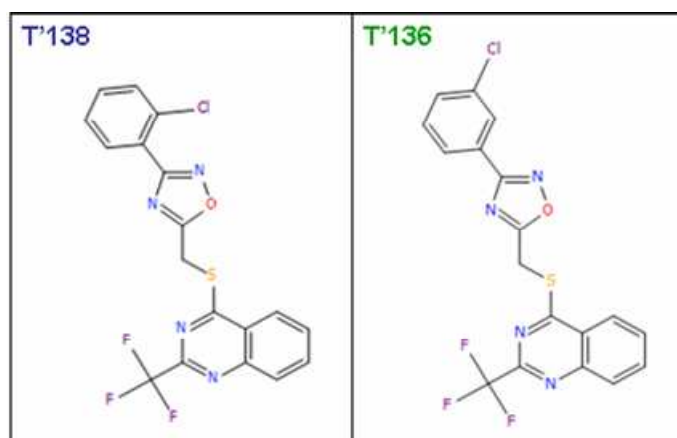


Figure 5.27. IC₅₀ determination of compound T'138 and analogues.

(A) Cells were infected with Ad5 in the absence or presence of FX plus 0.1, 0.5, 1, 5 or 10 μM T'138 or the most active analogues in 100 μl serum free media. After 3 h 100 μl media containing 20% serum was added to cells. Transgene expression was measured after 48 h. Data was normalised to minus and plus FX control conditions and represented as percentage inhibition. Error bars represent SEM (n = 4/compound). (B) Table represents the IC₅₀ values for each of the compounds. (C) Structures of T'138 and T'136.

5.2.19 Assessing the activity of hit T5550585 analogues

The third hit compound T'585 along with 11 additional chemical analogues were studied. As previously shown T'585 ablated FX-mediated Ad5 transduction (Figure 5.16 and Figure 5.28), as did another closely related compound T'402 (Figure 5.28 and Figure 5.29). Of the remaining 10 analogues, 5 compounds (T'006, T'327, T'011, T'009 and T'883) showed some inhibition of Ad5 gene transfer but to significantly lower levels than the parent, whilst 5 compounds (T'756, T'001, T'820, T'238 and T'036) resulted in no inhibition (Figure 5.28).

Compounds T'402 and T'585 are structurally very similar with only a change in the positioning of a chlorine atom (Figure 5.29). In order to investigate whether this minor chemical alteration could affect the activity of the compound, dose response curves were generated comparing the two most active inhibitors in this series. Whilst the shape of the dose response curve was very similar for both compounds, T'402 was slightly more potent, producing an IC_{50} value of 4.43 μ M versus 4.67 μ M of T'585 (Figure 5.30). Due to the effect of this compound, T'402 along with T'585 was selected for additional experimentation.

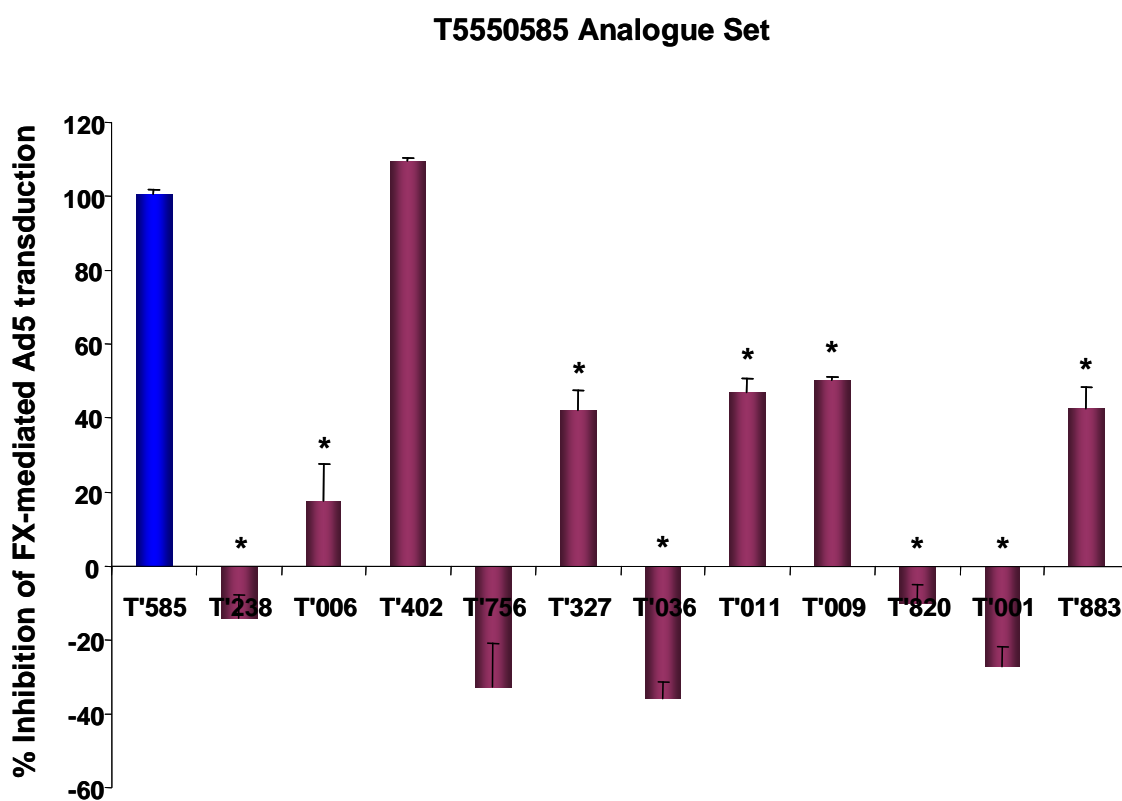


Figure 5.28. Assessing the activity of T'585 analogues.

Cells were infected with 1000 vp/cell of Ad5lacZ in the absence or presence of FX plus 10 μ M compound T'585 or 11 of its chemical analogues in 100 μ l serum free media. After 3 h 100 μ l media containing 20% serum was added to cells. Transgene expression was measured 48 h post-infection. Data was normalised to minus and plus FX control conditions and represented as percentage inhibition. * $p < 0.05$ as compared to the parent compound T'585 conditions as determined by one-way ANOVA and Dunnett's multiple comparison post-test. Error bars represent SEM ($n = 4/\text{compound}$).

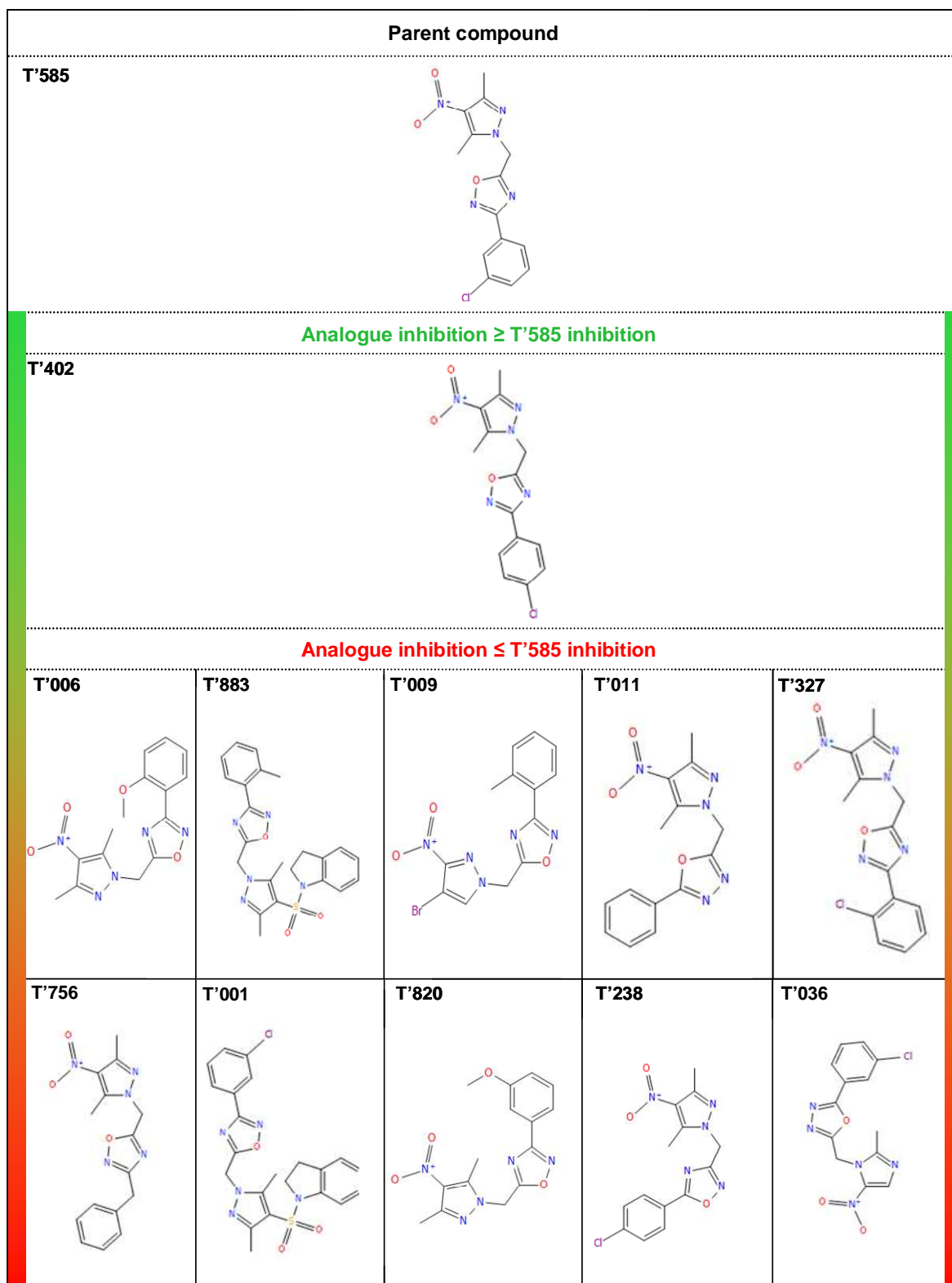
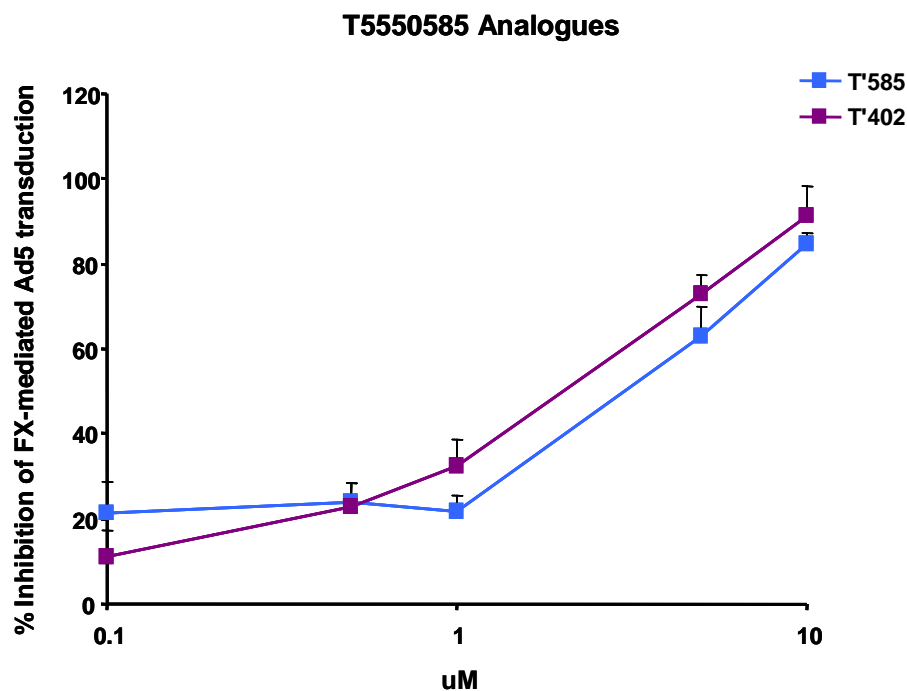


Figure 5.29. Chemical structures of T'585 analogues.

The structures of T'585 and 11 chemically related compounds are shown. The analogues are categorised by their percentage inhibition of FX-mediated Ad5 transduction in SKOV3 cells relative to the parent compound T'585.

(A)



(B)

Name	Compound I.D.	IC ₅₀
T'585	T5550585	4.67
T'402	T5572402	4.43

(C)

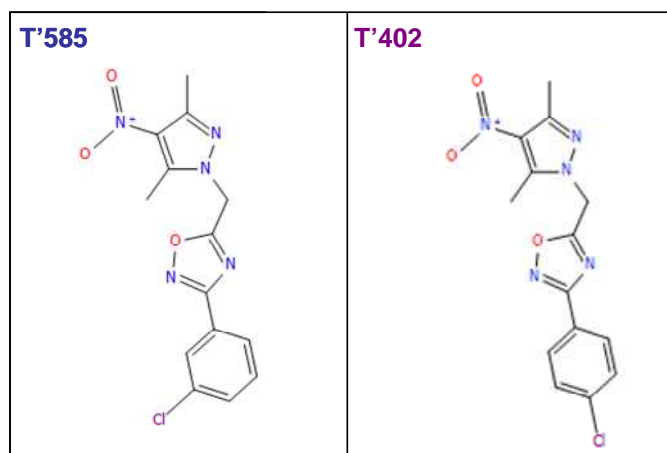


Figure 5.30. IC₅₀ determination of compound T'585 and analogue.

(A) Cells were infected with Ad5 in the absence or presence of FX plus 0.1, 0.5, 1, 5 or 10 μM T'585 or its analogue T'402 in 100 μl serum free media. After 3 h 100 μl media containing 20% serum was added to cells. Transgene expression was measured after 48 h. Data was normalised to minus and plus FX control conditions and represented as percentage inhibition. Error bars represent SEM (n = 4/compound). (B) Table represents the IC₅₀ values for each of the compounds. (C) Structures of T'585 and T'402.

5.2.20 Investigation of compound effect on Ad5:FX binding

To investigate if the three hit compounds (T'837, T'138 and T'585) and their active related analogues (T'956, T'136 and T'402) were interfering with Ad5 binding to FX, SPR analysis was performed with the assistance of Dr. Sharon Kelly (University of Glasgow). FX was covalently immobilised on a biosensor chip and running buffer, 10 μ M compound or an equivalent volume of DMSO was passed over the chip in order to assess if the compound was binding directly to FX (Figure 5.31). Directly after injection of each compound the chip was regenerated with EDTA and running buffer. There was a negligible increase in response units (average < 5 RU) after injection of each of the six compounds (Figure 5.31) However this was thought likely to be the result of the injection process and not due to a true interaction between the compound and the FX bound to the chip.

In order to investigate if the compound was interacting with the virus and thereby hindering Ad5 binding to FX, 10 μ M compound or an equivalent volume of DMSO was preincubated with Ad5. Ad5 in the presence of each of the six compounds or DMSO was injected over the FX on the chip. Under Ad5 plus DMSO control conditions, there was a large increase in response units (up to ~60 RU), indicating virus binding to the FX immobilised on the chip (Figure 5.32). When Ad5 in the presence of each of the six compounds was passed over the chip, the increase in response units remained at similar levels (Figure 5.32). These data suggest that incubation of Ad5 with the transduction inhibitors T'837, T'138, T'585 T'956, T'136 and T'402 does not interfere with Ad5 binding directly to FX.

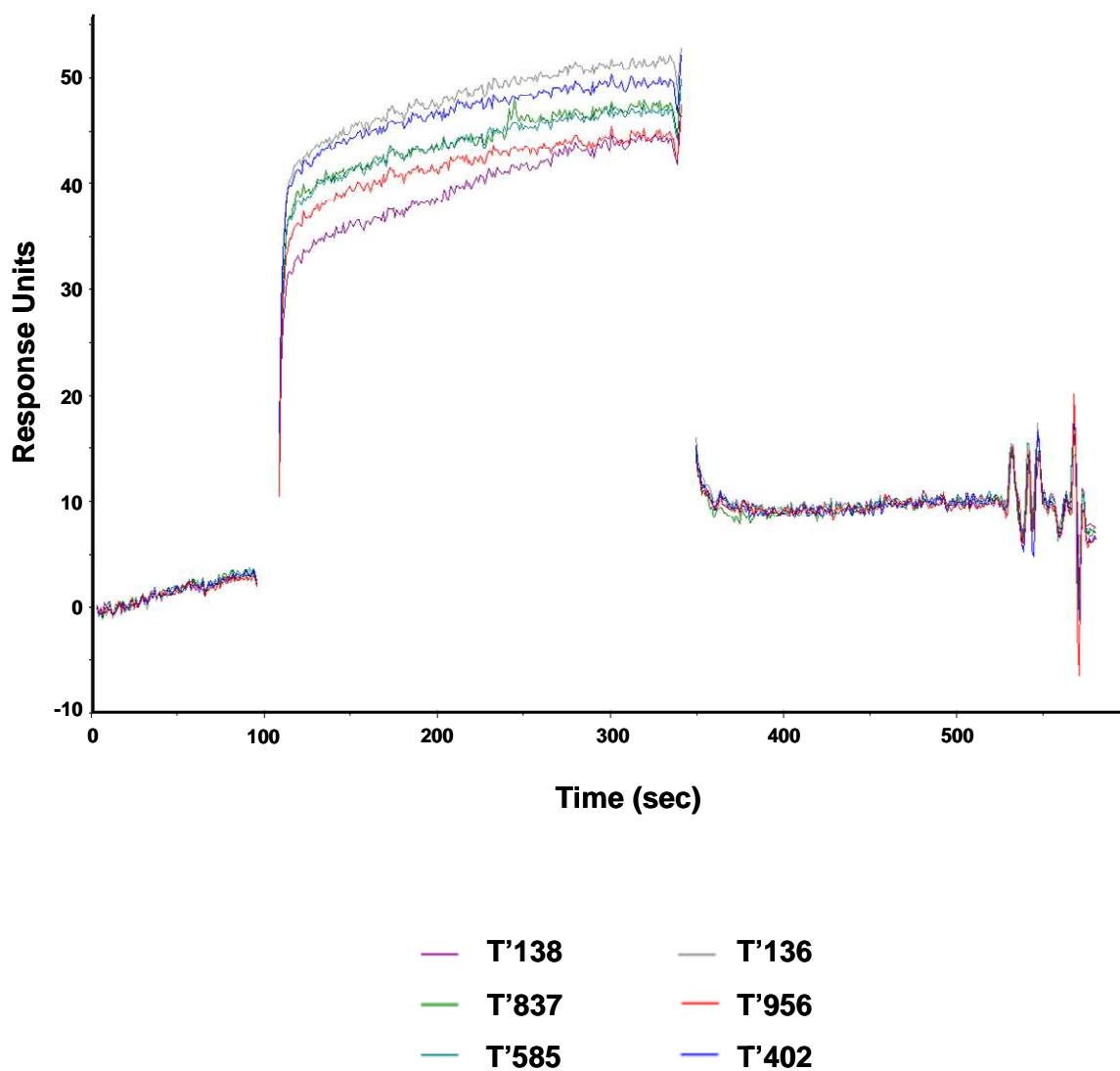


Figure 5.31. SPR analysis of compound binding to FX.

Sensorgram of 10 μM T'837, T'138, T'585, T'956, T'136 and T'402 injected over FX immobilised to a biosensor chip for ~ 200 sec at a flow rate of 30 $\mu\text{l}/\text{min}$. Sensorgrams are subtracted for the control DMSO injection.

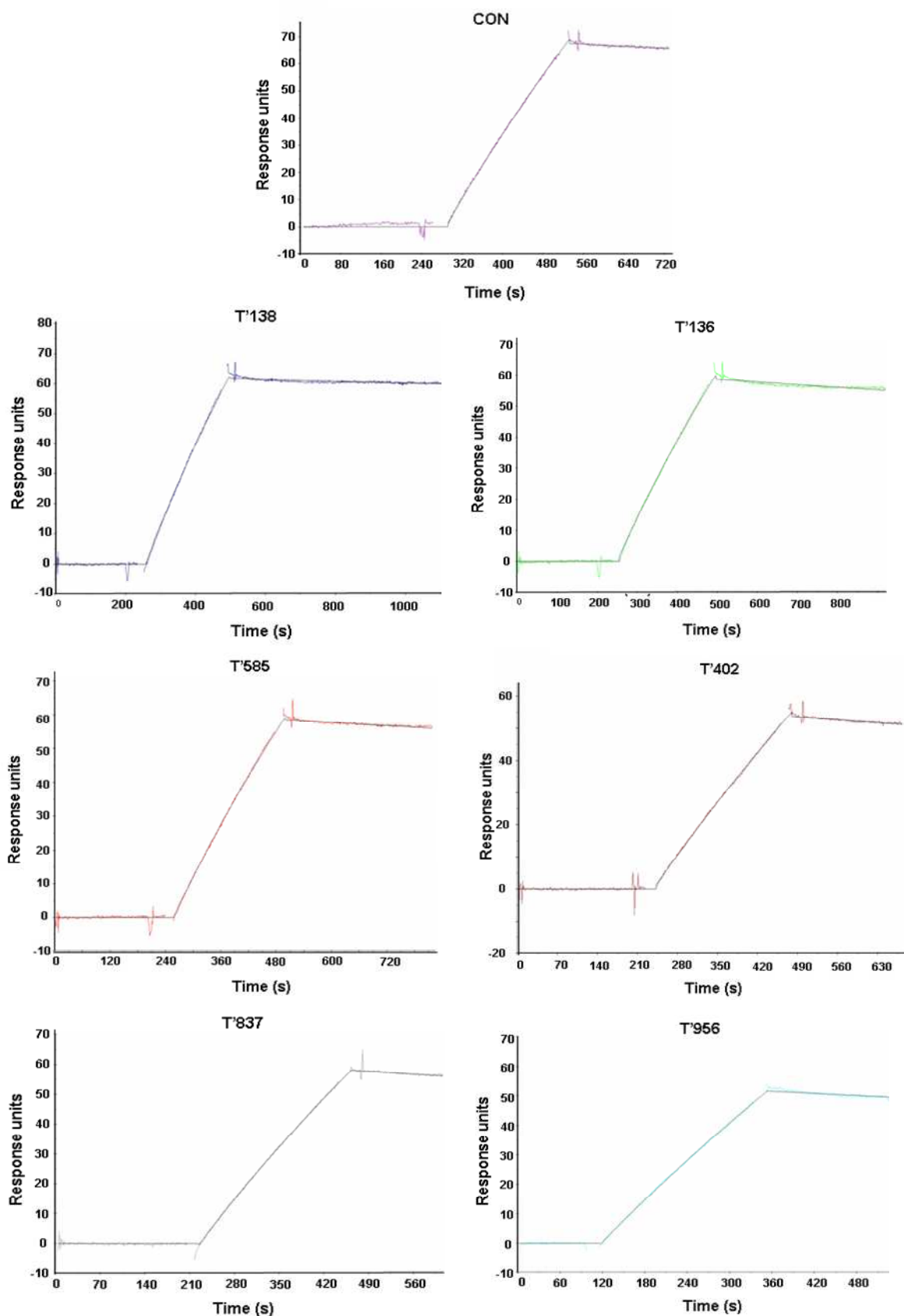


Figure 5.32. Effect of compounds on Ad5 binding to FX by SPR.

Sensorgrams of Ad5 in the presence of 10 μ M T'837, T'138, T'585 T'956, T'136 and T'402 or DMSO injected over FX for \sim 200 sec at a flow rate of 30 μ l/min.

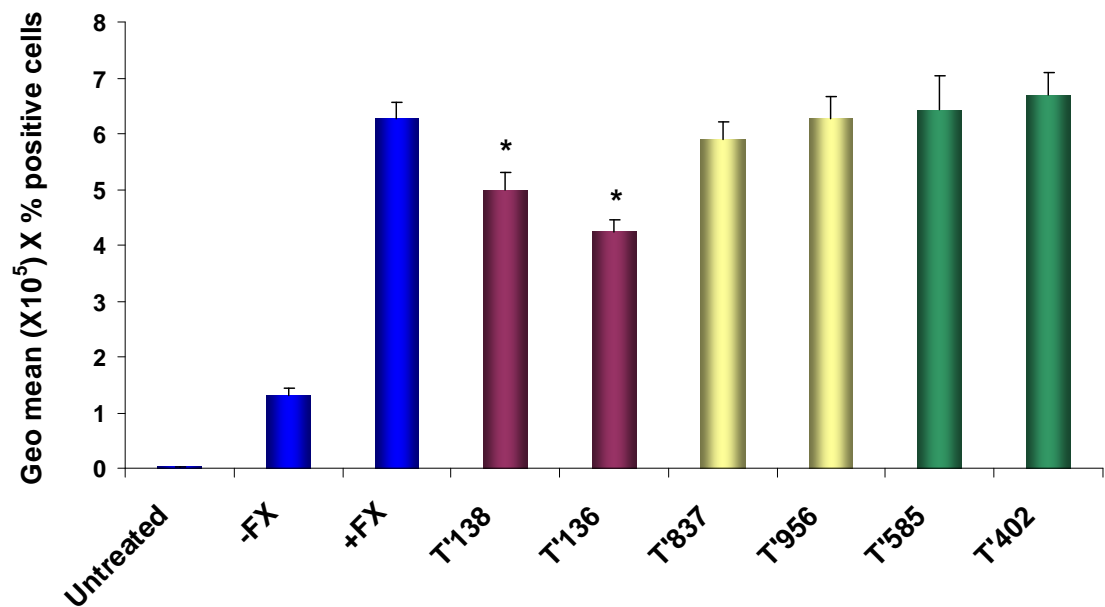
5.2.21 Effect of hit compounds on FX-mediated Ad5 cellular binding

To quantitatively assess if any of the six hit compounds, T'837, T'138, T'585 T'956, T'136 and T'402, caused their effect on Ad5 infectivity at the stage of Ad5:cellular binding, SKOV3 cells were incubated with 5000 vp/cell of fluorescently labelled Ad5 in the absence or presence of FX plus 10 μ M compound for 1 h at 4°C. Of the six compounds, T'138 and T'136 caused a significant decrease in FX-mediated Ad5 cell binding compared to plus FX conditions (Figure 5.33). This equated to ~25 % (T'138) and ~40% (T'136) inhibition of FX-mediated binding when normalised to minus and plus FX control conditions. The other compounds (T'837, T'956, T'585 and T'402) caused no significant difference compared to conditions in the presence of FX (Figure 5.33).

5.2.22 Effect of compounds on CAR-mediated Ad5 transduction

In order to assess if the compounds could block Ad5 transduction via the classical *in vitro* receptor CAR in addition to FX-mediated transduction, A549 cells were incubated with 1000 vp/cell of Ad5 in the presence of 10 μ M T'837, T'138, T'585 T'956, T'136 and T'402 with and without FX (Figure 5.33). Transgene expression was measured after 48 h. A549 cells express significant levels of CAR (Hidaka *et al.*, 1999), therefore are a commonly used cell line to study CAR-mediated transduction, whilst also being positive for HSPGs and thus susceptible to FX-mediated Ad5 transduction (Bradshaw *et al.*, 2010). Under control conditions, Ad5 transduction was significantly increased in the presence of FX (~6 fold) (Figure 5.33). All six compounds ablated Ad5 transduction in the absence and presence of FX. This data shows the ability of all six compounds to inhibit both CAR and FX-mediated Ad5 gene transfer.

(A)



(B)

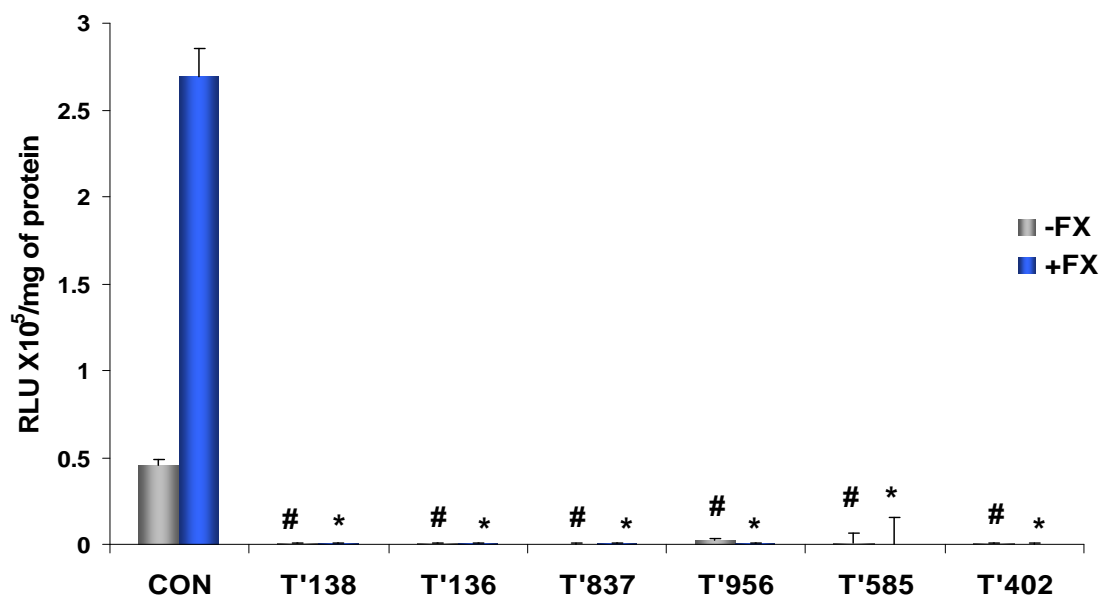


Figure 5.33. Effect of compounds on FX-mediated Ad5 binding to SKOV3 cells and transduction in A549 cells.

Binding of 5000 vp/cell of Ad5 to SKOV3 cells for 1 h at 4°C in the absence or presence of FX plus 10 μM compound was analysed. (B) A549 cells were infected with Ad5 in the absence or presence of FX plus 10 μM compound in 100 μl serum free media. After 3 h 100 μl media containing 20% serum was added to cells. Transgene expression was measured after 48 h. *p<0.05 as compared to plus FX or #p<0.05 as compared to minus FX conditions as determined by one-way ANOVA and Dunnett's multiple comparison post-test. Error bars represent SEM (n = 4/condition).

5.2.23 Effect of compounds on Ad5 transduction *in vivo*

To investigate whether the compounds were active *in vivo* and decreased Ad5 transduction and liver transduction, MF1 mice were injected intravenously with a high dose of 1×10^{11} vp/mouse of Ad5 luciferase in the absence or presence of 10 μ M T'138, T'136, T'585, T'402, T'837, T'956 or an equivalent volume of DMSO. Luciferase transgene expression was visualised by whole-body bioluminescence imaging and quantified 48 h after administration. Mice were injected on two separate days using an identical experimental procedure and the data pooled from both experiments. Group sizes: PBS n = 7, Ad5 n = 6, Ad5+DMSO n = 6, Ad5+T'138 n = 6, Ad5+T'136 n = 7, Ad5+T'837 n = 7, Ad5+T'956 n = 6, Ad5+T'585 n = 7 and Ad5+T'402 n = 6. As expected, Ad5 targeted the liver as evidenced by the high levels of luciferase expression visually and quantitatively assessed by whole-body bioluminescence imaging at 48 h post-injection (Figure 5.34 and Figure 5.35). There was no significant difference seen in the Ad5 plus DMSO control group, indicating that the vehicle did not cause an effect on Ad5 transduction *in vivo* (Figure 5.34 and Figure 5.35). However in the presence of 10 μ M T'138 and T'136 there were 6.7-fold and 4.6-fold decreases respectively in luciferase expression compared to Ad5 and Ad5 plus DMSO control conditions. This indicates that these two closely related compounds have activity and cause an effect *in vivo* on liver gene transfer of Ad5. The other four compounds T'585, T'402, T'837 or T'956 caused no significant decrease in Ad5 transduction compared to the animals in the Ad5 control groups under these conditions (Figure 5.34 and Figure 5.35).

5.2.24 Effect of compounds on Ad5 liver accumulation *in vivo*

To assess whether the compounds affected Ad5 liver accumulation, tissues were harvested 48 h post-injection of Ad5 in the absence or presence of 10 μ M T'138, T'136, T'585, T'402, T'837, T'956 or DMSO and homogenates produced. DNA was extracted from liver tissue homogenates and vector genomes were quantified by qPCR. QPCR was performed with Ad5 hexon specific primers, thus provided an accurate measure of Ad5 vector genome accumulation in the liver. DMSO caused no affect on the level of Ad5 genomes in the liver compared to the Ad5 alone group (Figure 5.35). In contrast, liver accumulation by Ad5 was significantly decreased following incubation with 10 μ M T'138. Neither the T'138 analogue T'136 nor the other four compounds T'585, T'402, T'837 or T'956 significantly reduced vector genomes present in the liver.

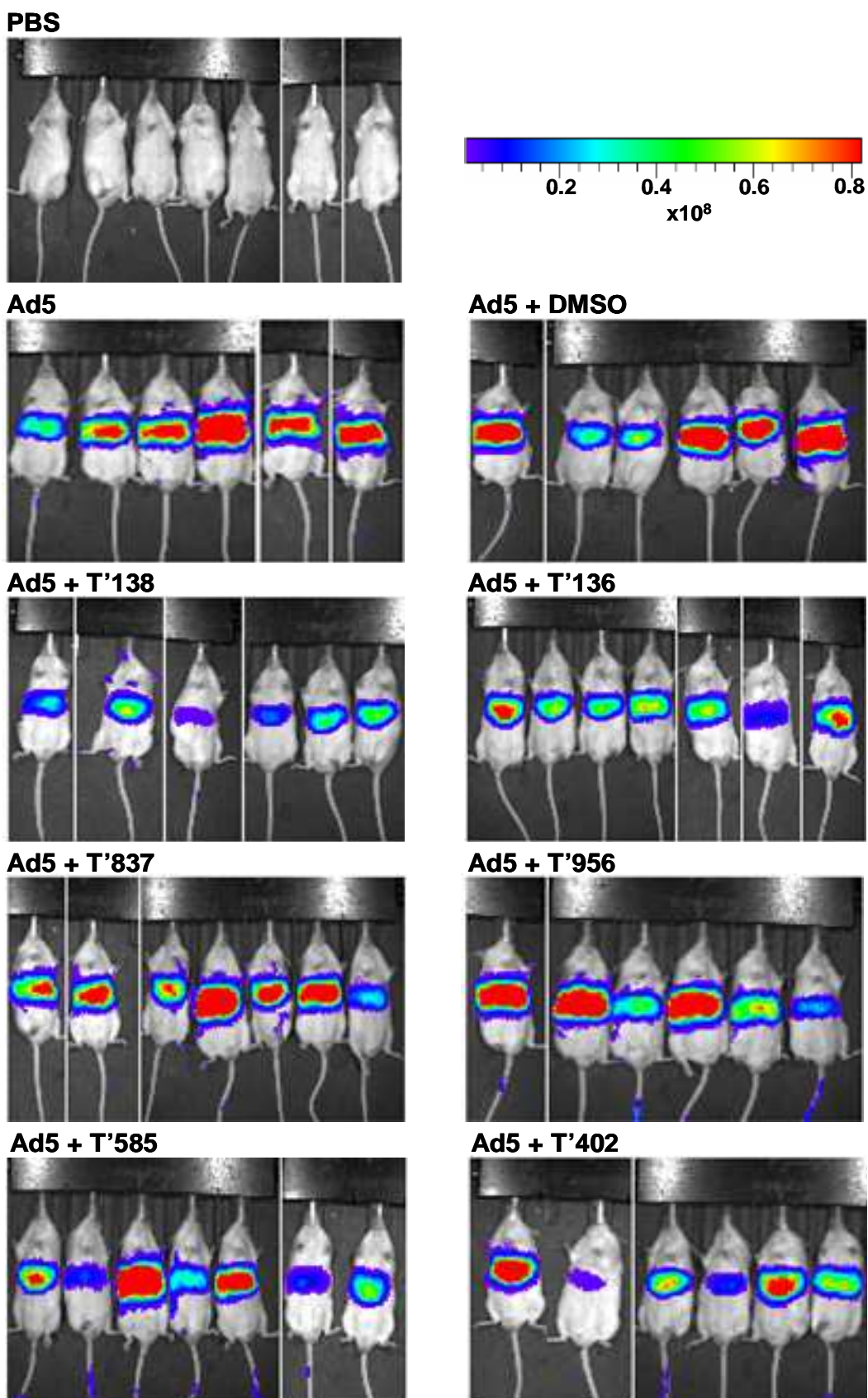


Figure 5.34. Effect of hit compounds on *in vivo* Ad5 transduction in MF1 mice. Luciferase expression visualised by whole-body bioluminescence imaging 48 h after intravascular administration of PBS, 1×10^{11} vp/mouse Ad5 alone or Ad5 in the presence of 10 μ M T'138, T'136, T'585, T'402, T'837, T'956 or DMSO in MF1 mice.

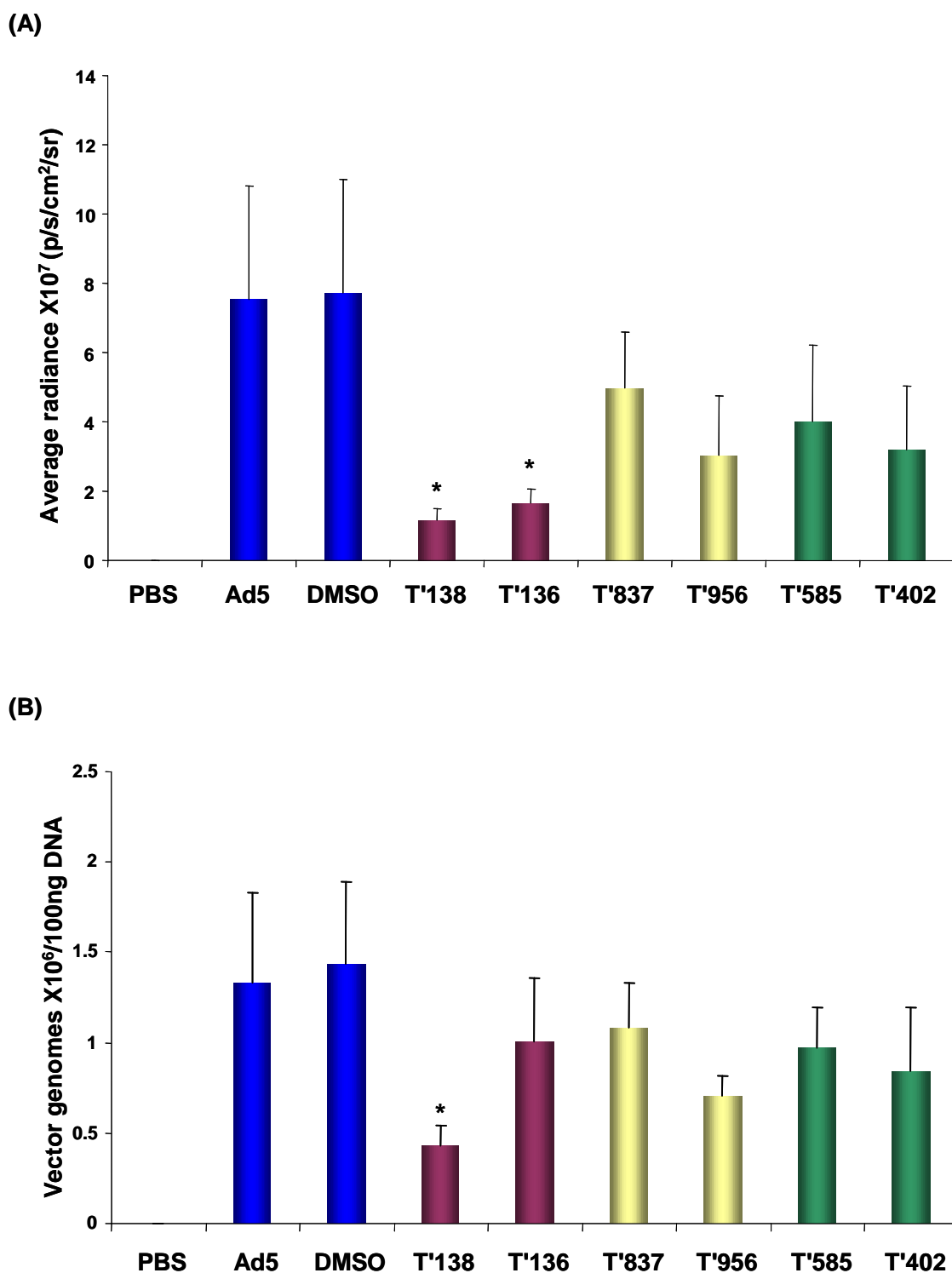


Figure 5.35. Liver Ad5 accumulation and transduction at 48 h *in vivo*.

(A) Luciferase expression as assessed by whole-body bioluminescence imaging was quantified at 48 h post-administration of PBS, Ad5 alone or Ad5 in the presence of 10 μ M T'138, T'136, T'585, T'402, T'837, T'956 or DMSO. (B) Viral and total genomic DNA was extracted from liver samples taken 48 h post-injection. Vector genome accumulation was quantified by qPCR. * $p < 0.05$ versus Ad5 as determined by Student's t-test. Error bars represent SEM (n = 6/group).

5.3 Discussion

Intravascular delivery of Ad5 is an attractive route for targeting the vasculature at defined sites, if not the only route suitable for targeting the multitude of micro-metastases required for many cancer gene therapy applications. Following contact with blood, Ad5 interacts with FX and mediates liver gene transfer (Kalyuzhniy *et al.*, 2008; Waddington *et al.*, 2008). The initial aim of this study was to use a HTS to identify a small molecule which specifically blocked FX-mediated Ad5 gene transfer to prevent liver transduction. Furthermore, such an inhibitor may hold promise as an anti-adenoviral agent for the treatment of life threatening disseminated Ad5 infections in the bloodstream. While it remains unclear whether FX binding by the virus is used for Ad5 dissemination, blocking this pathway may have fundamental beneficial effects for disseminated Ad pathogenesis in addition to gene therapy applications.

During the initial phase of this study the traditional methods of assessing Ad5 transduction in the presence of FX were adapted to generate an assay amenable to a HTS format. This set-up stage is one of the most crucial aspects of a HTS and warrants adequate time to be spent on optimisation (Sharlow *et al.*, 2008; Shun *et al.*, 2011). Here, an efficient, automated 384-well cell-based assay was developed and optimised using GFP as the output measure. Figure 5.36 highlights the different stages of assay development which were undertaken. Cell-based screen implementation presents several challenges, including the production of sufficient cells and virus for HTS, plating and adherence of cells for the assay, effects of compound exposure, cytotoxicity and capture of the assay signal (Johnston *et al.*, 2002). Identifying systemic errors prior to the commencement of the screen is vital and efforts were made to control the variability of the assay in the context of several factors, including: DMSO tolerance, reagents and signal stability (Figure 5.36). Having an easily quantifiable readout simplifies and greatly aids in the efficiency of the screening process (Johnston *et al.*, 2002; Trask *et al.*, 2009). In the presence of FX Ad5GFP transgene expression was substantially increased compared to non-FX conditions, providing a robust and reproducible signal window (average of ~30 fold signal-background ratio) and therefore the control-based method of normalisation of data was chosen (Shun *et al.*, 2011). Non-control-based methods of data normalisation such as the Z-score and B-score (both plate-based statistical methods) are also frequently used HTS methods, which can reduce the impact of systemic row/column effects (Brideau *et al.*, 2003; Zhijin Wu *et al.*, 2008), but from preliminary testing this was not a major problem and control-based normalisation was most suited to this assay (Shun *et al.*, 2011).

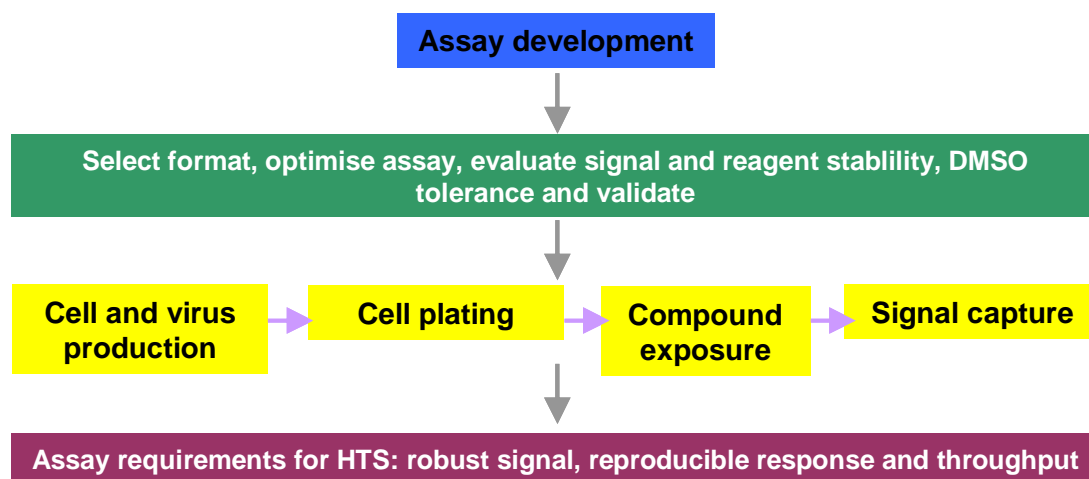


Figure 5.36. Cell-based assay development.

Additional challenges to the development and implementation of cell-based screens beyond those associated with biochemical HTS formats. Figure adapted from Johnston *et al.* (Johnston *et al.*, 2002).

Many factors beyond biological activity can affect the data quality from HTS. The multiple automated steps involving the liquid handling robotics, with aspirations, dispersions and fluid transfers, the programmed high content cellular imaging and handling of large databases all contribute to systemic variation. The small scale screen of 80 compounds was performed in order to test and validate the HTS protocol. The reproducibility of controls, the high signal-to-background ratio and an average Z' factor of > 5 indicated that the assay was suited to a HTS format.

From the primary screen, 288 of the 10,240 compounds tested resulted in $> 75\%$ inhibition of FX-mediated transduction and were identified as preliminary hits. An initial hit rate of $\sim 2.8\%$ was higher than expected. Despite this, the main focus of the primary assay was to create a list of potential hits, in a cost and time effective manner, therefore in an attempt not to miss any such molecules all 288 were selected for two rounds of secondary screening. In order to distinguish assay variability from biological activity, the compounds showing potential were tested on multiple occasions, in secondary screens and manually using traditional routinely used methods. The false-positive rate (i.e. false-positive rate = $[\text{number of primary HTS actives} - \text{number of confirmed hits}] \times 100 / \text{number of primary HTS actives}$) was $\sim 94\%$. From the 15 hits identified in the secondary screen as being non-toxic and achieving $> 75\%$ inhibition, only five were demonstrated to be active when tested without the use of automated techniques, thus discarding a further two-thirds of the positive compounds. False positives from HTS are a common problem, the consequences of which depend on the time and resources spent on their identification and elimination in

the follow up hit characterisation stage (Brideau *et al.*, 2003; Coan *et al.*, 2009; Zhang *et al.*, 1999). A graphical summary of the hit identification process is given in Figure 5.37. These data highlight the necessity of repeated testing of seemingly attractive compounds and the requirement for hit validation. However despite the high attrition rate, five repeat positive hits were identified from a screen of 10,240 molecules (0.048% hit rate).

Upon further analysis, the compounds T'817, T'0831, T'138, T'585 and T'837 were identified as ablating Ad5 transduction in presence of FX, all of which had IC_{50} values < 5.5 μ M. The compounds T'138, T'585 and T'837 primarily interfered with a post-binding stage of the Ad infection pathway and all affected efficient virus trafficking to the MTOC, as demonstrated by confocal microscopy. From this early investigation of candidate hits, T'817 appeared to be the most effective, having the most potent effect on Ad5 transduction ($IC_{50} = 0.47$), intracellular trafficking and completely prevented Ad5 accumulation at the MTOC. However, an additional factor which can contribute to false positives is the presence of promiscuous compounds within the library itself (McGovern *et al.*, 2002). Following post-screen structural analysis T'817 and T'0831 were eliminated due to the presence of sub-structural properties resembling those of 'frequent false hitters' from other screens (Baell *et al.*, 2010; McGovern *et al.*, 2002). Attempts to develop such peculiar or promiscuous compounds into viable leads are often futile, and a great amount of time and resources can be wasted on the characterisation of 'fake' hits (McGovern *et al.*, 2002). Therefore, efforts were focused on validating the other three HTS hits, T'138, T'585 and T'837. Interestingly these three compounds share structural features and fit within the one pharmacophore model established by Enamine. This was seen as encouraging and improved the chances of them being true hits. Moreover, the fact that T'138 had similar features to both T'585 and T'837 was a very positive aspect. Therefore based on these considerations mini-focused follow up libraries were generated relating to these molecules and structure-activity relationship analysis was performed. *In vitro* screening of the analogues revealed novel hits with similar or improved activity, thereby further validating the initial pharmacophore model and the three initial hit compounds T'138, T'585 and T'837.

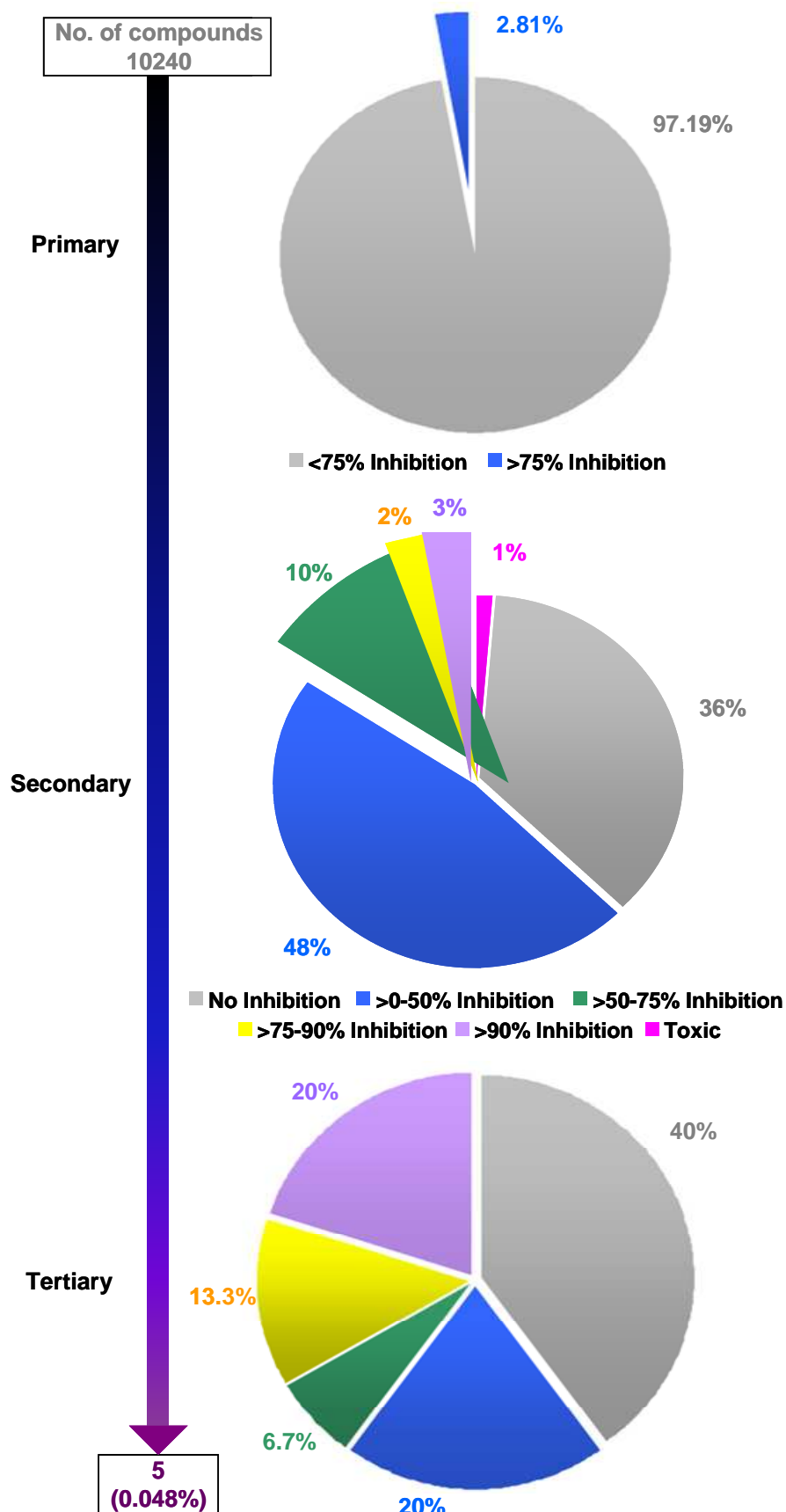


Figure 5.37. Graphical review of the HTS.

Of the 10,240 compounds screened in the primary screen, five validated hits were identified from the HTS process.

Several attempts were made to decipher the mechanism of action of the six most promising hits; T'138, T'136, T'585, T'402, T'837 and T'956. These compounds did not directly interfere with Ad5 binding to FX, instead they primarily caused a post-binding stage block of the transduction pathway and all affected optimal intracellular transport to the microtubule organising centre, as demonstrated by SPR, flow cytometry and confocal microscopy. Investigation of a direct interaction between Ad5 and the compounds could be performed by employing SPR techniques; coating Ad5 to a biosensor chip and passing 10 μM of each compound or DMSO over the chip to monitor compound:Ad5 binding. Additionally, efforts to dissect the point of the Ad5 transduction pathway being targeted by the compounds could be made, by performing time-addition experiments, i.e. add the compounds 0, 15, 30 or 60 min post-infection. Several early points in the FX-mediated pathway are well documented (Bradshaw *et al.*, 2010), and this could help assess whether the compound was having a critical effect prior to viral internalisation, endosomal escape or nuclear import etc.

Potent compound effects *in vitro* do not necessarily translate in the *in vivo* setting. However in this instance, *in vivo*, 10 μM T'138 substantially reduced Ad5 liver accumulation 48 h post-injection and, in addition to its closely related analogue T'136, dramatically reduced transgene expression at 48 h post-intravenous administration of a high viral dose (1×10^{11} vp/mouse). This dose of virus was chosen as it was previously demonstrated to cause high levels of liver transduction in mice, thereby providing a clear measure of compound effect (Alba *et al.*, 2010). The activity shown by T'138 and T'136 *in vivo* was a very promising result and this biological effect signifies the translational potential of the compounds. In this experiment a single dose of 10 μM compound was tested, whilst it may be the case that the other four compounds, T'585, T'402, T'837 and T'956, all of which have pharmacologically favourable profiles and none of which resulted in clear toxicities *in vivo*, may show activity at higher doses or against lower viral load.

A major factor for consideration in the potential use of these molecules in the gene therapy setting is that all six compounds ablate Ad5 transduction both in the presence and absence of FX, as assessed by assays in A549 cells. An inhibitor which specifically blocks FX-mediated transduction may hold great benefit for systemically administered Ad5 gene therapy applications, when combined with vector retargeting strategies. However, as these inhibitors appear to block Ad5 gene transfer via CAR and FX:HSPGs, they may not be suitable for such applications. This assay was designed to find inhibitors of Ad5 transduction, therefore this was always a possible outcome. Perhaps to look more

specifically at FX-mediated Ad transduction, identifying a small molecule which prevented the direct Ad5:FX interaction could be more suitable. There are several ways such an assay could be designed, such as employing SPR to screen compounds for those which blocked Ad5 binding to FX, or if a cell-based assay was preferable measuring the effect of compounds on fluorescently-labelled Ad5 binding in SKOV3 cells. Instead the inhibitors identified in this study may be of more value as anti-adenoviral agents.

As previously mentioned (section 5.1), in the immune compromised host, human Ad infections can culminate in disseminated and life threatening disease (Chakrabarti *et al.*, 2002; Munoz *et al.*, 1998). Although human Ads initially infect defined target tissues such as the lung, eye and gastrointestinal system, disseminated infections can occur, manifesting in serious clinical syndromes and are often fatal (Chuang *et al.*, 2003; Strausberg *et al.*, 2001). There are however, no currently approved, selective anti-adenovirus treatments on the market. Compounds T'138 and T'136, in particular, identified in this study may be suitable lead compounds for such an application, causing a potent effect *in vitro* and a substantial reduction in Ad5 transduction *in vivo*. Several other potential experiments could be performed to investigate this further. Firstly, by assessing whether the inhibitors of Ad5 transduction can prevent viral replication. In this thesis, all work was performed using a replication incompetent Ad5 vector. As 293 cells possess the E1 genes and machinery required for replication of this vector *in vitro*, it would be of interest to investigate if the compounds when incubated with 293 cells infected with Ad5, could prevent viral replication and viral spread as assessed by the induction of the cytopathic effect after 24 h or performing MTT assays (Graham *et al.*, 1977). Assessing the effects of WT Ad5 replication in A549 cells, would also be of great relevance. Ultimately the anti-viral potential of these inhibitors would be investigated *in vivo* in a suitable animal model. As human Ad replication is species specific, the use of appropriate animal models is important. Whilst mice are non-permissive to Ad5 replication, Syrian hamsters are permissive to replication and therefore a good model in which to examine the effects of the small molecules (Dhar *et al.*, 2012).

Whilst some pan-antiviral agents such as cidofovir and ribavirin have demonstrated efficacy against Ad infections, there is currently no antiviral specific to Ad available (Nishikawa *et al.*, 2011; Taniguchi *et al.*; Ulrych *et al.*, 2011). It would be worth investigating if the compounds identified in this study are selective to Ad5 or whether they prevent transduction of other Ad serotypes. Testing a panel of Ads from each of the seven species A to G to investigate the compounds effect on Ad infection *in vitro* would be of

interest, as Ads from species A, B, C and D are most common to infection in transplant recipients (Kojaoghlanian *et al.*, 2003; Kroes *et al.*, 2007). It has been reported that in pediatric allogeneic stem cell transplantation patients, of the 33 individuals positive for Ad infection in one study, more than one serotype was detected in 12 of the patients (Kroes *et al.*, 2007). Moreover, testing the effect of the compounds on other types of viruses, to ascertain Ad specificity would also be of importance.

A recent study by Andersson *et al.* developed a cell-based screen employing a GFP expressing replication competent Ad vector to screen 9,800 commercially available small organic compounds to identify one that directly or indirectly affected adenoviral protein expression *in vitro* (Andersson *et al.*, 2010). One compound, namely 2-((2-benzoylamino)benzoyl)amino)-benzoic acid, inhibited viral replication *in vitro* and showed efficacy against Ads from species A to F. However there was no *in vivo* data reported with this compound (Andersson *et al.*, 2010). Whilst several nucleoside analogues inhibit Ad replication *in vitro*, few appear to work against disease and infection *in vivo*. Therefore, the active *in vivo* inhibitors T'138 and T'136 identified in the current study may be very promising as lead compounds to treat Ad5 infection, particularly in the case of disseminated Ad disease.

The compounds screened throughout this project fall into three major categories; those which inhibit Ad5 transgene expression in the absence and presence of FX, those which enhance FX-mediated Ad5 infectivity and those which cause no effect. The two types of compounds showing efficacy may have strong market appeal. In the gene therapy setting, compounds capable of enhancing Ad5 infection in the presence of FX may be an attractive option for improved treatment of solid tumours via localised injection. Cancer accounts for nearly 65% of the gene therapy trials to date, this is followed by cardiovascular disease which account for a further 8.5%. This type of strategy could also be adapted for the treatment of cardiovascular diseases, via coating stents with the Ad:FX:compound complex to improve virus uptake in the vessel wall. Investigation of potential Ad transduction enhancers identified from this screen certainly warrants further study. As discussed, there is a clear gap in the market for an effective anti-Ad agent. Additionally, such an anti-adenoviral agents may also serve as a potential 'safety valve' in the gene therapy clinical setting e.g. in case of unwanted viral replication following administration of an oncolytic Ad, an anti-viral could be given to combat viral spread and be used as an additional measure of protection (Bauzon *et al.*, 2009).

This study describes the development, optimisation and implementation of a cell-based HTS, in a miniaturised 384-well format, to find small molecule inhibitors of Ad5 gene transfer in the presence of FX. Six promising hits were identified, T'138, T'136, T'837, T'956, T'585 and T'402 as being potent blockers of Ad5 gene transfer *in vitro* and two of the compounds, T'138 and T'136, successfully reduced Ad5 gene transduction following intravenous delivery of the vector *in vivo*. These pharmacologically favourable small molecules represent lead compounds for the development of anti-Ad agents.

Chapter 6

General Discussion

This thesis has focused on investigating and manipulating Ad5 interactions with host factors, in particular coagulation FX, a key *in vivo* tropism determining event following intravascular delivery of the vector. A greater understanding of Ad5:FX complex binding to hepatocytes was gained through genetic manipulation of key amino acid residues in the FX SP domain, which ablated FX-mediated Ad5 binding and transduction *in vitro* and *ex vivo*. The use of pharmacological agents, kinase inhibitors and small molecules to interfere with Ad5 gene transfer in the presence of FX was also investigated. A screen of 80 diverse kinase inhibitors and a robust high throughput screening platform to assay 10,240 compounds from the Pharmacological Diversity Drug-like Set library were developed. Through several rounds of screening, compounds effecting cell binding, optimal intracellular transport and potent inhibitors of Ad5 transduction in the absence and presence of FX were discovered. Therefore, novel agents to manipulate Ad5 gene transfer *in vitro* and *in vivo* were successfully identified from this work.

A major hurdle to the development of gene therapy is the lack of efficient vector targeting strategies following intravascular administration, the optimal route for many applications such as disseminated cancers and minimally invasive for cardiovascular diseases including heart failure or ischemic cardiomyopathy (Boecker *et al.*, 2004; Franz *et al.*, 1997). Viral vectors are used in almost 70% of clinical trials in gene therapy, approximately 24% of which are based on Ads (www.wiley.com/legacy/wileychi/genmed/clinical/). Ads, which exhibit high *in vivo* transduction efficiency, expression of transgenes, a large DNA payload capacity, manufacturing feasibility and the ability to propagate replication-defective vectors in complementing cell lines, have shown strong promise for gene therapy applications. These concepts have also led to Ads being used as molecular vaccine agents (reviewed by Matthews and Barouch (Barouch, 2010; Matthews, 2010)). In the gene therapy setting, Ad5 the most commonly used Ad vector has shown therapeutic potential, principally following local administration. However, this efficacy is largely determined by the route of administration, much of which is lost once the vector enters the bloodstream. Recent studies described an important pathway that Ads utilise once in the blood, that is, the high affinity interaction between the virus hexon protein and circulating coagulation FX (Kalyuzhniy *et al.*, 2008; Vigant *et al.*, 2008; Waddington *et al.*, 2008). A broad range of human Ad species have the capability to bind to FX (Waddington *et al.*, 2008). FX mediates substantial liver gene transfer, decreasing the availability of the vector to target tissues. Since this discovery, the interaction with FX has played a significant role in the design of gene therapy vectors (Alba *et al.*, 2010; Alba *et al.*, 2009; Kelkar *et al.*, 2004; Waddington *et al.*, 2008). It is therefore important to understand and characterise this

pathway in detail for the efficient optimisation and development of such vectors for clinical applications.

The haemostatic system provides physiological host defence and the coagulation cascade modulates inflammatory activity and limits tissue damage (Petäjä, 2011). However, this regulatory system can also be exploited by various pathogens for infection (Lenman *et al.*, 2011; Sutherland *et al.*, 2012; Waddington *et al.*, 2008). Several species of Ads bind FX (Waddington *et al.*, 2008), while coagulation FIX enhances species A Ad18 and Ad31 infection via a high affinity interaction with the hexon (Jonsson *et al.*, 2009; Lenman *et al.*, 2011). In the case of wildtype Ad5, respiratory tract infection commonly occurs following inhaled droplet transmission. Various stimuli, including inflammatory responses at the respiratory mucosa, may trigger exudation of plasma components (e.g. proteins involved in coagulation, complement, fibrinolysis) from subepithelial microvessels (Persson *et al.*, 1991). FX has been shown to be an efficient enhancer of Ad transduction *in vitro*, even at 1/100th the physiological level found blood suggesting the Ad:FX pathway may have evolved to enhance natural Ad infection *in vivo* (Jonsson *et al.*, 2009). In addition herpes simplex virus type-1 employs thrombin or a combination of coagulation FXa and FVII for increased infectivity (Sutherland *et al.*, 2007; Sutherland *et al.*, 2012). In the case of Ad5, the FX Gla domain docks within the cup formed by each hexon trimer and the SP domain tethers the Ad5:FX complex to hepatocytes through binding HSPGs, resulting in subsequent receptor-mediated virus internalisation (Bradshaw *et al.*, 2010; Kalyuzhniy *et al.*, 2008; Waddington *et al.*, 2008). Whilst it is evident that several types of viruses can utilise components of the coagulation cascade in order to enhance transduction, several other viral pathogens have also taken advantage of HSPGs as primary attachment receptors in different tissues and cell types. These include human immunodeficiency virus-1 (Endress *et al.*, 2008), AAV (Summerford *et al.*, 1998), human papilloma virus (Johnson *et al.*, 2009) and herpes simplex virus (Shukla *et al.*, 1999).

In this study, the critical HSPG-interacting residues of FX for Ad5:FX complex attachment to hepatocytes were identified. FX plasmid constructs were generated with mutations in the seven basic residues of the HBPE, previously defined as R93, K96, R125, R165, K169, K236, and R240 (Rezaie, 2000). SPR demonstrated that mutations did not affect binding to Ad5. FX-mediated, HSPG-associated cell binding and transduction were abolished. Unfortunately due to the complex synthesis of FX, difficulties in rFX production and scale-up, *in vivo* studies were not performed. Several methods to improve production could be tested, such as increasing the concentration of vitamin K or serum in the media, using

suspension cells or co-transfection of the WT FX or FX mutated constructs with an intracellular processing enzyme, such as the endoprotease furin, required for efficient biosynthesis (Drews *et al.*, 1995; Preininger *et al.*, 1999). Ideally, *in vivo* analysis would be performed, in which 10 µg/ml of the WT or rFX mutants would be injected into warfarin-treated mice 30 min prior to administration of Ad5 and liver transgene expression assessment after 48 h. Nonetheless, both *in vitro* and *ex vivo* data generated indicated that the cluster of basic amino acids in the SP domain mediated surface interaction of the Ad5:FX complex. Therefore this study has broadened the existing knowledge of the FX-mediated Ad5 transduction pathway.

Future success in the development of safe, targeted vectors for systemically delivered gene therapy will rely on the detailed understanding of complex interactions of Ads with host proteins. Aside from the Ad5:FX interaction, a range of other endogenous proteins lead to viral sequestration and prevent gene transfer to the desired cells or tissues. These include KCs, neutralising antibodies, complement components, erythrocytes and platelets, amongst others. Therefore it is evident that *in vivo* kinetics and Ad5 biodistribution are defined by a range of host interactions. While many years of research have been focused on altering the tropism of Ad5 vectors, many of these studies have attempted to translate the knowledge gained from CAR-mediated *in vitro* mechanisms to relevant *in vivo* pathways. The recent change in research focus from classical *in vitro* CAR-mediated infection to FX:HSPG-dependent mechanisms, requires additional studies to be performed to assess the role of different signalling pathways in the early stages of FX-mediated Ad5 infection.

Post-binding events that occur following FX-mediated Ad5 binding and the role of kinases involved in virus internalisation, intracellular trafficking and successful transduction were also investigated in this thesis. Similar to their involvement in the CAR-mediated pathway, PKA, PI3K and p38MAPK were found to be crucial for the optimal intracellular trafficking in the presence of FX in a CAR^{low} cell line *in vitro* (Li *et al.*, 1998b; Suomalainen *et al.*, 2001). Here, from screening a panel of other kinase inhibitors, a compound thought to have Syk kinase inhibitor activity was found to have a profound effect on FX-mediated Ad5 infectivity (Moriya *et al.*, 1997). ER-27319 disrupted efficient intracellular transport and decreased Ad5 transduction. Due to the lack of Syk in the cell lines tested, it was concluded that this effect was independent of this kinase. Syk has not previously been reported to have an involvement in Ad5 gene transfer *in vitro*. Instead ER-27319 was postulated to be acting via ITAM expressing cellular proteins. The ITAM containing ERM family, which act as cross-linkers between the plasma membrane and the

actin cytoskeleton were speculated to mediate the potent effects of the inhibitor on Ad5 transduction. However, in the time frame imposed by this study this speculation could not be verified but warrants further investigation. Additional experimentation could be performed to knockout the effects of ezrin, radixin and moesin proteins using an siRNA approach, as previously shown to be effective for individual or combined knockdown (Kano *et al.*, 2011), in SKOV3 or A549 cells and examine the effects on Ad5 trafficking. This would give insight into their importance in the Ad5 infectivity pathway. Whilst the effects of ER-27319 are interesting and it may be used *in vitro* as a tool to manipulate Ad5 gene transfer, as to our knowledge there are no other compounds available which cause a similar affect, its use in animals may be hindered by toxicity issues. *In vitro* the compound results in ~35% cytotoxicity following 48 h incubation, indicating that it may not be suitable for *in vivo* application.

A wide range of methods of Ad targeting have been developed with varying success. These include genetic engineering of the viral capsid (Alba *et al.*, 2009), polymer-conjugated Ad complexes (Yao *et al.*, 2011), adaptor molecules (Reynolds *et al.*, 2000), carrier-cell-mediated delivery (Pereboeva *et al.*, 2003), cell-specific Ad expression cassettes (Fukazawa *et al.*, 2010), promoters and microRNA-mediated tissue-specific transgene silencing (Cawood *et al.*, 2009). The use of warfarin to decrease circulating levels of functional blood factors (Parker *et al.*, 2006) or heparin to block HSPGs (Bradshaw *et al.*, 2010), have ablated unwanted Ad5 liver transduction. Both innate and adaptive immune responses against the Ads are efficient methods of sequestering the virus, greatly reducing the circulating half-life of the vector for gene therapy applications. Gadolinium chloride (Lieber *et al.*, 1997), clodronate encapsulated liposomes (Wolff *et al.*, 1997) and several other methods to deplete KCs led to evasion, at least in part, of an innate immune response. These drugs however are sub-optimal for administering to patients about to undergo a therapeutic gene therapy procedure due to safety issues related to their anticoagulant properties and toxicity profiles (Kumagai *et al.*, 2007; Ropposch *et al.*, 2012). Therefore, seeing the potential of a drug intervention approach, the third study in this thesis attempted to identify a novel and safe small molecule to manipulate the FX-mediated Ad5 infection pathway and prevent gene transfer. Such an inhibitor may also hold promise as an anti-Ad agent.

Ad infections can be asymptomatic or cause localised disease, such as respiratory tract infections following inhalation via droplet transmission of species C Ads (Hong *et al.*, 2001). However, the humoral response also plays an important role in controlling Ad

infection and in individuals in which the immune system is disabled, infection can become invasive (Echavarría, 2008; Hierholzer, 1992). Clinical manifestations can be aggressive leading to hepatitis, hemorrhagic cystitis, pancreatitis, meningoencephalitis and disseminated disease (de Mezerville *et al.*, 2006; Khoo *et al.*, 1995). They depend on the underlying disease, affected organ, virus serotype and patient age, being particularly severe in children (Echavarría, 2008; Lion *et al.*, 2003). Ad infection has also been detected in peripheral blood from immunocompromised patients, a significant proportion of whom (82% of paediatric patients in one study (Lion *et al.*, 2003)) then go on to develop life-threatening disseminated adenoviral disease (Lion *et al.*, 2003). In the immunocompromised host, disseminated Ad disease is lethal in most instances (Chakrabarti *et al.*, 2002).

While it is uncertain whether FX binding by Ad upon contact with bloodstream is used for viral dissemination, it was hypothesised that blocking this pathway may be advantageous for limiting disseminated Ad hepatitis and for gene therapy applications where avoidance of liver gene transfer is desirable. Therefore a high throughput screening platform to identify small molecule inhibitors of the Ad5:FX pathway was developed. Using a fluorescence and cell-based *in vitro* HTS 10,240 small molecules from the Pharmacological Diversity Drug-like Set library were evaluated. Primary and secondary screening identified 15 compounds that reduced FX-mediated Ad5 gene transfer by > 75% without causing cytotoxicity. Upon further analysis, three compounds, T'837, T'585 and T'138 were identified as consistently ablating Ad5 transduction both in the absence and presence of FX. As virtually all CAR and FX-mediated gene transfer was prevented by these compounds, such inhibitors may be more suitable as anti-viral agents rather than for gene therapy applications. However, it would also be of interest to investigate if the small molecules identified here also block integrin-mediated infection. This could be performed by coinoculation of 10 μ M of each compound with an integrin targeted vector such as Ad5RGD4C, which has been genetically engineered to contain a α v integrin binding ligand in the HI loop (Dmitriev *et al.*, 1998; Majhen *et al.*, 2009), to assess effects on vector transduction.

Without formally approved antiviral drugs against Ads available, there is a gap in the market for such a pharmacological agent (Dropulic *et al.*, 2010). Several drugs including ribavirin, cidofovir and ganciclovir, have been tested in clinical settings or in animal models and the results are variable (Lindemans *et al.*, 2010; Taniguchi *et al.*, 2012; Ulrych *et al.*, 2011; Yabiku *et al.*, 2011). Cidofovir is most commonly used to treat Ad infections,

but treatment outcome is often disappointing (Omar *et al.*, 2010; Taniguchi *et al.*, 2012). In a retrospective study of Ad infection in patients undergoing haploidentical stem cell transplantation, approximately 43% of individuals receiving cidofovir alone to treat disseminated Ad infection died (Taniguchi *et al.*, 2012). Additionally, many currently licensed drugs target the same viral protein, the viral DNA polymerase, and drug resistance is an emerging problem (Dropulic *et al.*, 2010). Furthermore the toxicity associated with some antiviral agents limits their use (Dropulic *et al.*, 2010). Safer and more effective drugs directed against new viral targets are required.

Candidate small molecules identified in this thesis were investigated in further detail. They did not directly interfere with Ad5 binding to FX, instead they primarily caused a “post-binding” stage block of the Ad infection pathway and disrupted optimal trafficking to the MTOC, as demonstrated by SPR, flow cytometry and confocal microscopy. The three lead compounds T’837, T’585 and T’138 shared common structural features and additional *in vitro* screening of compound analogues revealed novel hits with similar or improved activity. Whilst several compounds have previously been demonstrated to block Ad transduction *in vitro*, very few have shown efficacy *in vivo* (Andersson *et al.*, 2010; Öberg *et al.*, 2012). Here, intravascular administration of 10 μ M T’138 and its analogue T’136 substantially reduced Ad5 gene transfer *in vivo* at 48 h post-administration. Therefore, this study successfully identifies novel and potent small molecule inhibitors of Ad infection pathways which may be attractive for the development of anti-Ad agents.

Additional studies will be performed to investigate if the small molecule inhibitors identified in this study prevent Ad replication. Such an inhibitor may also be useful in the gene therapy clinical setting and its administration may act as a safety control for unwanted replication of oncolytic Ads (Bauzon *et al.*, 2009; Diaconu *et al.*, 2010). The requirement for more potent effects of oncolytic Ads equates to a higher risk of replication-associated side effects, such as innate immune reactions and toxicity (Diaconu *et al.*, 2010). The novel compounds found in this study may be suitable for the Ad replication-associated symptoms in the clinic and improve their safety profiles. In addition to the inhibitors of Ad infection, the small molecule enhancers of Ad5 transduction identified in this study warrant future study. Such compounds may have potential, in conjunction with FX for increasing Ad5 transduction efficiency following localised delivery e.g. intra-tumoural injection of the vector.

In summary, the work presented here increases the understanding and potential exploitations of the FX-mediated Ad5 infection pathway. In addition, potent inhibitors of this important pathway both *in vitro* and *in vivo* were identified, which represent promising lead candidates for anti-adenoviral drug development and gene therapy applications.

List of References

- Abbink P, Lemckert AAC, Ewald BA, Lynch DM, Denholtz M, Smits S, *et al.* (2007). Comparative Seroprevalence and Immunogenicity of Six Rare Serotype Recombinant Adenovirus Vaccine Vectors from Subgroups B and D. *J. Virol.* **81**(9): 4654-4663.
- Abzug MJ, Levin MJ (1991). Neonatal Adenovirus Infection: Four Patients and Review of the Literature. *Pediatrics* **87**(6): 890-896.
- Acharya C, Coop A, Polli JE, Mackerell AD, Jr. (2011). Recent advances in ligand-based drug design: relevance and utility of the conformationally sampled pharmacophore approach. *Curr Comput Aided Drug Des* **7**(1): 10-22.
- Adams WC, Bond E, Havenga MJE, Holterman L, Goudsmit J, Karlsson Hedestam GB, *et al.* (2009). Adenovirus serotype 5 infects human dendritic cells via a coxsackievirus–adenovirus receptor-independent receptor pathway mediated by lactoferrin and DC-SIGN. *Journal of General Virology* **90**(7): 1600-1610.
- Akanitapichat P, Lowden CT, Bastow KF (2000). 1,3-Dihydroxyacridone derivatives as inhibitors of herpes virus replication. *Antiviral Research* **45**(2): 123-134.
- Alba R, Bradshaw AC, Coughlan L, Denby L, McDonald RA, Waddington SN, *et al.* (2010). Biodistribution and retargeting of FX-binding ablated adenovirus serotype 5 vectors. *Blood* **116**(15): 2656-2664.
- Alba R, Bradshaw AC, Mestre-Frances N, Verdier JM, Henaff D, Baker AH (2012). Coagulation factor X mediates adenovirus type 5 liver gene transfer in non-human primates (*Microcebus murinus*). *Gene Ther* **19**(1): 109-113.
- Alba R, Bradshaw AC, Parker AL, Bhella D, Waddington SN, Nicklin SA, *et al.* (2009). Identification of coagulation factor (F)X binding sites on the adenovirus serotype 5 hexon: effect of mutagenesis on FX interactions and gene transfer. *Blood* **114**(5): 965-971.
- Aleman R, Curiel DT (2001). CAR-binding ablation does not change biodistribution and toxicity of adenoviral vectors. *Gene Ther* **8**(17): 1347-1353.
- Amalfitano A, Chamberlain JS (1997). Isolation and characterization of packaging cell lines that coexpress the adenovirus E1, DNA polymerase, and preterminal proteins: implications for gene therapy. *Gene Ther* **4**(3): 258-263.
- Amieva MR, Wilgenbus KK, Furthmayr H (1994). Radixin Is a Component of Hepatocyte Microvilli in Situ. *Experimental Cell Research* **210**(1): 140-144.
- Anderson CW, Young ME, Flint SJ (1989). Characterization of the adenovirus 2 virion protein, Mu. *Virology* **172**(2): 506-512.
- Andersson EK, Strand M, Edlund K, Lindman K, Enquist PA, Spjut S, *et al.* (2010). Small-molecule screening using a whole-cell viral replication reporter gene assay identifies 2-[[2-(benzoylamino)benzoyl]amino]-benzoic acid as a novel antiadenoviral compound. *Antimicrob Agents Chemother* **54**(9): 3871-3877.

- Atoda H, Ishikawa M, Mizuno H, Morita T (1998). Coagulation Factor X-Binding Protein from *Deinagkistrodon acutus* Venom Is a Gla Domain-Binding Protein†. *Biochemistry* **37**(50): 17361-17370.
- Au T, Thorne S, Korn WM, Sze D, Kirn D, Reid TR (2006). Minimal hepatic toxicity of Onyx-015: spatial restriction of coxsackie-adenoviral receptor in normal liver. *Cancer Gene Ther* **14**(2): 139-150.
- Baba M, Mori S, Shigeta S, De Clercq E (1987). Selective inhibitory effect of (S)-9-(3-hydroxy-2-phosphonylmethoxypropyl)adenine and 2'-nor-cyclic GMP on adenovirus replication in vitro. *Antimicrobial Agents and Chemotherapy* **31**(2): 337-339.
- Baell JB, Holloway GA (2010). New Substructure Filters for Removal of Pan Assay Interference Compounds (PAINS) from Screening Libraries and for Their Exclusion in Bioassays. *Journal of Medicinal Chemistry* **53**(7): 2719-2740.
- Baldick CJ, Wichroski MJ, Pendri A, Walsh AW, Fang J, Mazzucco CE, *et al.* (2010). A Novel Small Molecule Inhibitor of Hepatitis C Virus Entry. *PLoS Pathog* **6**(9): e1001086.
- Barouch DH (2010). Novel adenovirus vector-based vaccines for HIV-1. *Curr Opin HIV AIDS* **5**(5): 386-390.
- Barouch DH, Liu J, Li H, Maxfield LF, Abbink P, Lynch DM, *et al.* (2012). Vaccine protection against acquisition of neutralization-resistant SIV challenges in rhesus monkeys. *Nature* **482**(7383): 89-93..
- Barret C, Roy C, Montcourrier P, Mangeat P, Niggli V (2000). Mutagenesis of the Phosphatidylinositol 4,5-Bisphosphate (Pip2) Binding Site in the Nh2-Terminal Domain of Ezrin Correlates with Its Altered Cellular Distribution. *The Journal of Cell Biology* **151**(5): 1067-1080.
- Barrow AD, Trowsdale J (2006). You say ITAM and I say ITIM, let's call the whole thing off: the ambiguity of immunoreceptor signalling. *European Journal of Immunology* **36**(7): 1646-1653.
- Barton KN, Stricker H, Elshaikh MA, Pegg J, Cheng J, Zhang Y, *et al.* (2011). Feasibility of Adenovirus-Mediated hNIS Gene Transfer and 131I Radioiodine Therapy as a Definitive Treatment for Localized Prostate Cancer. *Mol Ther* **19**(7): 1353-1359.
- Basu A, Li B, Mills DM, Panchal RG, Cardinale SC, Butler MM, *et al.* (2011). Identification of a Small-Molecule Entry Inhibitor for Filoviruses. *Journal of Virology* **85**(7): 3106-3119.
- Bauzon M, Jin F, Kretschmer P, Hermiston T (2009). In vitro analysis of cidofovir and genetically engineered TK expression as potential approaches for the intervention of ColoAd1-based treatment of cancer. *Gene Ther* **16**(9): 1169-1174.
- Benson SD, Bamford JKH, Bamford DH, Burnett RM (1999). Viral Evolution Revealed by Bacteriophage PRD1 and Human Adenovirus Coat Protein Structures. *Cell* **98**(6): 825-833.
- Bergelson JM, Cunningham JA, Droguett G, Kurt-Jones EA, Krithivas A, Hong JS, *et al.* (1997). Isolation of a common receptor for Coxsackie B viruses and adenoviruses 2 and 5. *Science* **275**(5304): 1320-1323.

- Berryman M, Franck Z, Bretscher A (1993). Ezrin is concentrated in the apical microvilli of a wide variety of epithelial cells whereas moesin is found primarily in endothelial cells. *Journal of Cell Science* **105**(4): 1025-1043.
- Bischoff JR, Kirn DH, Williams A, Heise C, Horn S, Muna M, *et al.* (1996). An Adenovirus Mutant That Replicates Selectively in p53- Deficient Human Tumor Cells. *Science* **274**(5286): 373-376.
- Blaese RM, Culver KW, Miller AD, Carter CS, Fleisher T, Clerici M, *et al.* (1995). T Lymphocyte-Directed Gene Therapy for ADA- SCID: Initial Trial Results After 4 Years. *Science* **270**(5235): 475-480.
- Bleicher KH, Bohm H-J, Muller K, Alanine AI (2003). Hit and lead generation: beyond high-throughput screening. *Nat Rev Drug Discov* **2**(5): 369-378.
- Boecker W, Bernecker OY, Wu JC, Zhu X, Sawa T, Grazette L, *et al.* (2004). Cardiac-specific gene expression facilitated by an enhanced myosin light chain promoter. *Mol Imaging* **3**(2): 69-75.
- Bom VJ, Bertina RM (1990). The contributions of Ca²⁺, phospholipids and tissue-factor apoprotein to the activation of human blood-coagulation factor X by activated factor VII. *Biochem J* **265**(2): 327-336.
- Boyle M, Enke R, Reynolds J, Mogayzel P, Guggino W, Zeitlin P (2006). Membrane-associated heparan sulfate is not required for rAAV-2 infection of human respiratory epithelia. *Virology Journal* **3**(1): 29.
- Bradley RR, Lynch DM, Iampietro MJ, Borducchi EN, Barouch DH (2012a). Adenovirus Serotype 5 Neutralising Antibodies Target both Hexon and Fiber following Vaccination and Natural Infection. *Journal of Virology* **86**(1): 625-629.
- Bradley RR, Maxfield LF, Lynch DM, Iampietro MJ, Borducchi EN, Barouch DH (2012b). Adenovirus Serotype 5-Specific Neutralising Antibodies Target Multiple Hexon Hypervariable Regions. *Journal of Virology* **86**(2): 1267-1272.
- Bradshaw AC, Parker AL, Duffy MR, Coughlan L, van Rooijen N, Kähäri V-M, *et al.* (2010). Requirements for Receptor Engagement during Infection by Adenovirus Complexed with Blood Coagulation Factor X. *PLoS Pathog* **6**(10): e1001142.
- Bremner KH, Scherer J, Yi J, Vershinin M, Gross SP, Vallee RB (2009). Adenovirus Transport via Direct Interaction of Cytoplasmic Dynein with the Viral Capsid Hexon Subunit. *Cell host & microbe* **6**(6): 523-535.
- Brideau C, Gunter B, Pikounis B, Liaw A (2003). Improved Statistical Methods for Hit Selection in High-Throughput Screening. *Journal of Biomolecular Screening* **8**(6): 634-647.
- Brunetti-Pierri N, Nichols TC, McCorquodale S, Merricks E, Palmer DJ, Beaudet AL, *et al.* (2005). Sustained phenotypic correction of canine hemophilia B after systemic administration of helper-dependent adenoviral vector. *Hum Gene Ther* **16**(7): 811-820.
- Buddai SK, Touloukhonova L, Bergum PW, Vlasuk GP, Krishnaswamy S (2002). Nematode Anticoagulant Protein c2 Reveals a Site on Factor Xa That Is Important for

- Macromolecular Substrate Binding to Human Prothrombinase. *Journal of Biological Chemistry* **277**(29): 26689-26698.
- Burckhardt Christoph J, Suomalainen M, Schoenenberger P, Boucke K, Hemmi S, Greber Urs F (2011). Drifting Motions of the Adenovirus Receptor CAR and Immobile Integrins Initiate Virus Uncoating and Membrane Lytic Protein Exposure. *Cell host & microbe* **10**(2): 105-117.
- Burnett J.R., Hooper A.J. (2009). Alipogene tiparvovec, an adeno-associated virus encoding the Ser(447)X variant of the human lipoprotein lipase gene for the treatment of patients with lipoprotein lipase deficiency. *Curr Opin Mol Ther* **11**(6):681-91.
- Burnett, R. M. (1985). The structure of the adenovirus capsid. II. The packing symmetry of hexon and its implications for viral architecture. *J Mol Biol* **185**: 125–143
- Calderwood DA, Yan B, de Pereda JM, Alvarez B Ga, Fujioka Y, Liddington RC, *et al.* (2002). The Phosphotyrosine Binding-like Domain of Talin Activates Integrins. *Journal of Biological Chemistry* **277**(24): 21749-21758.
- Camire RM, Larson PJ, Stafford DW, High KA (2000). Enhanced γ -Carboxylation of Recombinant Factor X Using a Chimeric Construct Containing the Prothrombin Propeptide. *Biochemistry* **39**(46): 14322-14329.
- Campagnola G, Gong P, Peersen OB (2011). High-throughput screening identification of poliovirus RNA-dependent RNA polymerase inhibitors. *Antiviral Research* **91**(3): 241-251.
- Cappello M, Vlasuk GP, Bergum PW, Huang S, Hotez PJ (1995). Ancylostoma caninum anticoagulant peptide: a hookworm-derived inhibitor of human coagulation factor Xa. *Proceedings of the National Academy of Sciences* **92**(13): 6152-6156.
- Carlisle RC, Di Y, Cerny AM, Sonnen AF-P, Sim RB, Green NK, *et al.* (2009). Human erythrocytes bind and inactivate type 5 adenovirus by presenting Coxsackie virus-adenovirus receptor and complement receptor 1. *Blood* **113**(9): 1909-1918.
- Catherine OR (2002). Chapter 13 - Humoral Immune Response. In: David TC, Joanne TD (ed)^(eds). *Adenoviral Vectors for Gene Therapy*, edn. San Diego: Academic Press 375-407.
- Cavazzana-Calvo M, Hacein-Bey S, Basile GdS, Gross F, Yvon E, Nusbaum P, *et al.* (2000). Gene Therapy of Human Severe Combined Immunodeficiency (SCID)-X1 Disease. *Science* **288**(5466): 669-672.
- Cawood R, Chen HH, Carroll F, Bazan-Peregrino M, van Rooijen N, Seymour LW (2009). Use of Tissue-Specific MicroRNA to Control Pathology of Wild-Type Adenovirus without Attenuation of Its Ability to Kill Cancer Cells. *PLoS Pathog* **5**(5): e1000440.
- Chakrabarti S, Mautner V, Osman H, Collingham KE, Fegan CD, Klapper PE, *et al.* (2002). Adenovirus infections following allogeneic stem cell transplantation: incidence and outcome in relation to graft manipulation, immunosuppression, and immune recovery. *Blood* **100**(5): 1619-1627.

- Chattopadhyay D, Ghosh MK, Mal A, Harter ML (2001). Inactivation of p21 by E1A Leads to the Induction of Apoptosis in DNA-Damaged Cells. *Journal of Virology* **75**(20): 9844-9856.
- Chen CY, May SM, Barry MA (2010). Targeting adenoviruses with factor x-single-chain antibody fusion proteins. *Hum Gene Ther* **21**(6): 739-749.
- Chen HH, Cawood R, El-Sherbini Y, Purdie L, Bazan-Peregrino M, Seymour LW, *et al.* (2011). Active Adenoviral Vascular Penetration by Targeted Formation of Heterocellular Endothelial-epithelial Syncytia. *Mol Ther* **19**(1): 67-75.
- Cheng C, Gall JGD, Nason M, King CR, Koup RA, Roederer M, *et al.* (2010). Differential Specificity and Immunogenicity of Adenovirus Type 5 Neutralising Antibodies Elicited by Natural Infection or Immunization. *Journal of Virology* **84**(1): 630-638.
- Chrétien I, Marcuz A, Courtet M, Katevuo K, Vainio O, Heath JK, *et al.* (1998). CTX, a Xenopus thymocyte receptor, defines a molecular family conserved throughout vertebrates. *European Journal of Immunology* **28**(12): 4094-4104.
- Chuang YY, Chiu CH, Wong KS, Huang JG, Huang YC, Chang LY, *et al.* (2003). Severe adenovirus infection in children. *J Microbiol Immunol Infect* **36**(1): 37-40.
- Cichon G, Boeckh-Herwig S, Kuemin D, Hoffmann C, Schmidt HH, Wehnes E, *et al.* (2003). Titer determination of Ad5 in blood: a cautionary note. *Gene Ther* **10**(12): 1012-1017.
- Ciruela A, Dixon AK, Bramwell S, Gonzalez MI, Pinnock RD, Lee K (2003). Identification of MEK1 as a novel target for the treatment of neuropathic pain. *British Journal of Pharmacology* **138**(5): 751-756.
- Coan KED, Maltby DA, Burlingame AL, Shoichet BK (2009). Promiscuous Aggregate-Based Inhibitors Promote Enzyme Unfolding. *Journal of Medicinal Chemistry* **52**(7): 2067-2075.
- Cohen A, Hirschhorn R, Horowitz SD, Rubinstein A, Polmar SH, Hong R, *et al.* (1978). Deoxyadenosine triphosphate as a potentially toxic metabolite in adenosine deaminase deficiency. *Proceedings of the National Academy of Sciences* **75**(1): 472-476.
- Corjon S, Gonzalez G, Henning P, Grichine A, Lindholm L, Boulanger P, *et al.* (2011). Cell Entry and Trafficking of Human Adenovirus Bound to Blood Factor X Is Determined by the Fiber Serotype and Not Hexon:Heparan Sulfate Interaction. *PLoS ONE* **6**(5): e18205.
- Coughlan L, Alba R, Parker AL, Bradshaw AC, McNeish IA, Nicklin SA, *et al.* (2010). Tropism-Modification Strategies for Targeted Gene Delivery Using Adenoviral Vectors. *Viruses* **2**(10): 2290-2355.
- Crawford-Miksza L, Schnurr DP (1996). Analysis of 15 adenovirus hexon proteins reveals the location and structure of seven hypervariable regions containing serotype-specific residues. *Journal of Virology* **70**(3): 1836-1844.

- Cristalli G, Costanzi S, Lambertucci C, Lupidi G, Vittori S, Volpini R, *et al.* (2001). Adenosine deaminase: Functional implications and different classes of inhibitors. *Medicinal Research Reviews* **21**(2): 105-128.
- Croyle MA, Yu Q-C, Wilson JM (2000). Development of a Rapid Method for the PEGylation of Adenoviruses with Enhanced Transduction and Improved Stability under Harsh Storage Conditions. *Human Gene Therapy* **11**(12): 1713-1722.
- Damania B, Li M, Choi J-K, Alexander L, Jung JU, Desrosiers RC (1999). Identification of the R1 Oncogene and Its Protein Product from the Rhadinovirus of Rhesus Monkeys. *Journal of Virology* **73**(6): 5123-5131.
- Dave VP, Cao Z, Browne C, Alarcon B, Fernandez-Miguel G, Lafaille J, *et al.* (1997). CD3[delta] deficiency arrests development of the [alpha][beta] but not the [gamma][delta] T cell lineage. *EMBO J* **16**(6): 1360-1370.
- Davidson CJ, Hirt RP, Lal K, Snell P, Elgar G, Tuddenham EG, *et al.* (2003). Molecular evolution of the vertebrate blood coagulation network. *Thromb Haemost* **89**(3): 420-428.
- Davie EW, Ratnoff OD (1964). Waterfall Sequence for Intrinsic Blood Clotting. *Science* **145**: 1310-1312.
- De Clercq E (2003). Clinical Potential of the Acyclic Nucleoside Phosphonates Cidofovir, Adefovir, and Tenofovir in Treatment of DNA Virus and Retrovirus Infections. *Clinical Microbiology Reviews* **16**(4): 569-596.
- de Mezerville MH, Tellier R, Richardson S, Hebert D, Doyle J, Allen U (2006). Adenoviral infections in pediatric transplant recipients: a hospital-based study. *Pediatr Infect Dis J* **25**(9): 815-818.
- de Mol NJ, Catalina MI, Dekker FJ, Fischer MJE, Heck AJR, Liskamp RMJ (2005). Protein Flexibility and Ligand Rigidity: A Thermodynamic and Kinetic Study of ITAM-Based Ligand Binding to Syk Tandem SH2. *ChemBioChem* **6**(12): 2261-2270.
- Debbas M, White E (1993). Wild-type p53 mediates apoptosis by E1A, which is inhibited by E1B. *Genes Dev* **7**(4): 546-554.
- Dehecchi MC, Melotti P, Bonizzato A, Santacatterina M, Chilosi M, Cabrini G (2001). Heparan Sulfate Glycosaminoglycans Are Receptors Sufficient To Mediate the Initial Binding of Adenovirus Types 2 and 5. *Journal of Virology* **75**(18): 8772-8780.
- Dehecchi MC, Tamanini A, Bonizzato A, Cabrini G (2000). Heparan Sulfate Glycosaminoglycans Are Involved in Adenovirus Type 5 and 2-Host Cell Interactions. *Virology* **268**(2): 382-390.
- Dedieu JF, Vigne E, Torrent C, Jullien C, Mahfouz I, Caillaud JM, *et al.* (1997). Long-term gene delivery into the livers of immunocompetent mice with E1/E4-defective adenoviruses. *Journal of Virology* **71**(6): 4626-4637.
- Dehghani H, Brown CR, Plishka R, Buckler-White A, Hirsch VM (2002). The ITAM in Nef Influences Acute Pathogenesis of AIDS-Inducing Simian Immunodeficiency Viruses SIVsm and SIVagm without Altering Kinetics or Extent of Viremia. *Journal of Virology* **76**(9): 4379-4389.

Dhar D, Toth K, Wold WSM (2012). Syrian Hamster Tumor Model to Study Oncolytic Ad5-Based Vectors
Oncolytic Viruses. In: Kirn DH, Liu T-C, Thorne SH (ed)^(eds), edn, Vol. 797: Humana Press. p[^]pp 53-63.

Di Paolo NC, Miao EA, Iwakura Y, Murali-Krishna K, Aderem A, Flavell RA, *et al.* (2009a). Virus Binding to a Plasma Membrane Receptor Triggers Interleukin-1 \pm -Mediated Proinflammatory Macrophage Response In Vivo. *Immunity* **31**(1): 110-121.

Di Paolo NC, van Rooijen N, Shayakhmetov DM (2009b). Redundant and Synergistic Mechanisms Control the Sequestration of Blood-born Adenovirus in the Liver. *Mol Ther* **17**(4): 675-684.

Diaconu I, Cerullo V, Escutenaire S, Kanerva A, Bauerschmitz GJ, Hernandez-Alcoceba R, *et al.* (2010). Human adenovirus replication in immunocompetent Syrian hamsters can be attenuated with chlorpromazine or cidofovir. *The Journal of Gene Medicine* **12**(5): 435-445.

Dmitriev I, Krasnykh V, Miller CR, Wang M, Kashentseva E, Mikheeva G, *et al.* (1998). An Adenovirus Vector with Genetically Modified Fibers Demonstrates Expanded Tropism via Utilization of a Coxsackievirus and Adenovirus Receptor-Independent Cell Entry Mechanism. *Journal of Virology* **72**(12): 9706-9713.

Dobson CM (2004). Chemical space and biology. *Nature* **432**:824–828

Doronin K, Shashkova EV, May SM, Hofherr SE, Barry MA (2009). Chemical Modification with High Molecular Weight Polyethylene Glycol Reduces Transduction of Hepatocytes and Increases Efficacy of Intravenously Delivered Oncolytic Adenovirus. *Human Gene Therapy* **20**(9): 975-988.

Dranoff G, Jaffee E, Lazenby A, Golumbek P, Levitsky H, Brose K, *et al.* (1993). Vaccination with irradiated tumor cells engineered to secrete murine granulocyte-macrophage colony-stimulating factor stimulates potent, specific, and long-lasting anti-tumor immunity. *Proceedings of the National Academy of Sciences* **90**(8): 3539-3543.

Dransfield DT, Bradford AJ, Smith J, Martin M, Roy C, Mangeat PH, *et al.* (1997). Ezrin is a cyclic AMP-dependent protein kinase anchoring protein. *EMBO J* **16**(1): 35-43.

Drews R, Paleyanda RK, Lee TK, Chang RR, Rehemtulla A, Kaufman RJ, *et al.* (1995). Proteolytic maturation of protein C upon engineering the mouse mammary gland to express furin. *Proceedings of the National Academy of Sciences* **92**(23): 10462-10466.

Dropulic LK, Cohen JI (2010). Update on New Antivirals Under Development for the Treatment of Double-Stranded DNA Virus Infections. *Clin Pharmacol Ther* **88**(5): 610-619.

Echavarría M (2008). Adenoviruses in Immunocompromised Hosts. *Clinical Microbiology Reviews* **21**(4): 704-715.

Eckner R, Ewen ME, Newsome D, Gerdes M, DeCaprio JA, Lawrence JB, *et al.* (1994). Molecular cloning and functional analysis of the adenovirus E1A-associated 300-kD

- protein (p300) reveals a protein with properties of a transcriptional adaptor. *Genes Dev* **8**(8): 869-884.
- Einfeld DA, Schroeder R, Roelvink PW, Lizonova A, King CR, Kovesdi I, *et al.* (2001). Reducing the Native Tropism of Adenovirus Vectors Requires Removal of both CAR and Integrin Interactions. *Journal of Virology* **75**(23): 11284-11291.
- Endress T, Lampe M, Briggs JA, Krausslich HG, Brauchle C, Muller B, *et al.* (2008). HIV-1-cellular interactions analyzed by single virus tracing. *Eur Biophys J* **37**(8): 1291-1301.
- Esko JD, Lindahl U (2001). Molecular diversity of heparan sulfate. *The Journal of Clinical Investigation* **108**(2): 169-173.
- Evans DL, Marshall CJ, Christey PB, Carrell RW (1992). Heparin binding site, conformational change, and activation of antithrombin. *Biochemistry* **31**(50): 12629-12642.
- Fabry CMS, Rosa-Calatrava M, Conway JF, Zubieta C, Cusack S, Ruigrok RWH, *et al.* (2005). A quasi-atomic model of human adenovirus type 5 capsid. *EMBO J* **24**(9): 1645-1654.
- Farmer C, Morton PE, Snippe M, Santis G, Parsons M (2009). Coxsackie adenovirus receptor (CAR) regulates integrin function through activation of p44/42 MAPK. *Experimental Cell Research* **315**(15): 2637-2647.
- Fievet BT, Gautreau A, Roy C, Del Maestro L, Mangeat P, Louvard D, *et al.* (2004). Phosphoinositide binding and phosphorylation act sequentially in the activation mechanism of ezrin. *The Journal of Cell Biology* **164**(5): 653-659.
- Fischer A (2000). Severe combined immunodeficiencies (SCID). *Clinical & Experimental Immunology* **122**(2): 143-149.
- Francischetti IMB, Valenzuela JG, Andersen JF, Mather TN, Ribeiro JMC (2002). Ixolaris, a novel recombinant tissue factor pathway inhibitor (TFPI) from the salivary gland of the tick, *Ixodes scapularis*: identification of factor X and factor Xa as scaffolds for the inhibition of factor VIIa/tissue factor complex. *Blood* **99**(10): 3602-3612.
- Franz W-M, Rothmann T, Frey N, Katus HA (1997). Analysis of tissue-specific gene delivery by recombinant adenoviruses containing cardiac-specific promoters. *Cardiovascular Research* **35**(3): 560-566.
- Freytag SO, Movsas B, Aref I, Stricker H, Peabody J, Pegg J, *et al.* (2007a). Phase I Trial of Replication-competent Adenovirus-mediated Suicide Gene Therapy Combined with IMRT for Prostate Cancer. *Mol Ther* **15**(5): 1016-1023.
- Freytag SO, Stricker H, Movsas B, Kim JH (2007b). Prostate Cancer Gene Therapy Clinical Trials. *Mol Ther* **15**(6): 1042-1052.
- Friedlos F, Quinn J, Knox RJ, Roberts JJ (1992). The properties of total adducts and interstrand crosslinks in the DNA of cells treated with CB 1954: Exceptional frequency and stability of the crosslink. *Biochemical Pharmacology* **43**(6): 1249-1254.

- Fruehling S, Longnecker R (1997). The Immunoreceptor Tyrosine-Based Activation Motif of Epstein–Barr Virus LMP2A Is Essential for Blocking BCR-Mediated Signal Transduction. *Virology* **235**(2): 241-251.
- Fueyo J, Gomez-Manzano C, Alemany R, Lee PS, McDonnell TJ, Mitlianga P, *et al.* (2000). A mutant oncolytic adenovirus targeting the Rb pathway produces anti-glioma effect in vivo. *Oncogene* **19**(1): 2-12.
- Fujikawa K, Coan MH, Legaz ME, Davie EW (1974). Mechanism of activation of bovine factor X (Stuart factor) by intrinsic and extrinsic pathways. *Biochemistry* **13**(26): 5290-5299.
- Fukazawa T, Matsuoka J, Yamatsuji T, Maeda Y, Durbin ML, Naomoto Y (2010). Adenovirus-mediated cancer gene therapy and virotherapy (Review). *Int J Mol Med* **25**(1): 3-10.
- Funayama N, Nagafuchi A, Sato N, Tsukita S (1991). Radixin is a novel member of the band 4.1 family. *The Journal of Cell Biology* **115**(4): 1039-1048.
- Furcinitti PS, van Oostrum J, Burnett RM (1989). Adenovirus polypeptide IX revealed as capsid cement by difference images from electron microscopy and crystallography. *EMBO J* **8**(12): 3563-3570.
- Furie B, Furie BC (1988). The molecular basis of blood coagulation. *Cell* **53**(4): 505-518.
- Furumoto Y, Nunomura S, Terada T, Rivera J, Ra C (2004). The Fc ϵ RI β Immunoreceptor Tyrosine-based Activation Motif Exerts Inhibitory Control on MAPK and I κ B Kinase Phosphorylation and Mast Cell Cytokine Production. *Journal of Biological Chemistry* **279**(47): 49177-49187.
- Gabrilovich DI (2006). INGN 201 (Advexin $\text{\textcircled{R}}$): adenoviral p53 gene therapy for cancer. *Expert Opinion on Biological Therapy* **6**(8): 823-832.
- Gahéry-Ségard H, Farace F, Godfrin D, Gaston J, Lengagne R, Tursz T, *et al.* (1998). Immune Response to Recombinant Capsid Proteins of Adenovirus in Humans: Antifiber and Anti-Penton Base Antibodies Have a Synergistic Effect on Neutralising Activity. *Journal of Virology* **72**(3): 2388-2397.
- Gahéry-Ségard H, Juillard V, Gaston J, Lengagne R, Pavirani A, Boulanger P, *et al.* (1997). Humoral immune response to the capsid components of recombinant adenoviruses: Routes of immunization modulate virus-induced Ig subclass shifts. *European Journal of Immunology* **27**(3): 653-659.
- Gary R, Bretscher A (1995). Ezrin self-association involves binding of an N-terminal domain to a normally masked C-terminal domain that includes the F-actin binding site. *Molecular Biology of the Cell* **6**(8): 1061-1075.
- Gazumyan A, Reichlin A, Nussenzweig MC (2006). Ig β tyrosine residues contribute to the control of B cell receptor signaling by regulating receptor internalization. *The Journal of Experimental Medicine* **203**(7): 1785-1794.
- Gil D, Gutiérrez D, Alarcón B (2001). Intracellular Redistribution of Nucleolin upon Interaction with the CD3 ϵ Chain of the T Cell Receptor Complex. *Journal of Biological Chemistry* **276**(14): 11174-11179.

- Goodell JR, Madhok AA, Hiasa H, Ferguson DM (2006). Synthesis and evaluation of acridine- and acridone-based anti-herpes agents with topoisomerase activity. *Bioorg Med Chem* **14**(16): 5467-5480.
- Goodrum FD, Ornelles DA (1999). Roles for the E4 orf6, orf3, and E1B 55-Kilodalton Proteins in Cell Cycle-Independent Adenovirus Replication. *Journal of Virology* **73**(9): 7474-7488.
- Gould KL, Bretscher A, Esch FS, Hunter T (1989). cDNA cloning and sequencing of the protein-tyrosine kinase substrate, ezrin, reveals homology to band 4.1. *EMBO J* **8**(13): 4133-4142.
- Gräble M, Hearing P (1992). cis and trans requirements for the selective packaging of adenovirus type 5 DNA. *Journal of Virology* **66**(2): 723-731.
- Graham FL, Smiley J, Russell WC, Nairn R (1977). Characteristics of a Human Cell Line Transformed by DNA from Human Adenovirus Type 5. *Journal of General Virology* **36**(1): 59-72.
- Granés F, Berndt C, Roy C, Mangeat P, Reina M, Vilaró S (2003). Identification of a novel Ezrin-binding site in syndecan-2 cytoplasmic domain. *FEBS letters* **547**(1-3): 212-216.
- Greber UF, Suomalainen M, Stidwill RP, Boucke K, Ebersold MW, Helenius A (1997). The role of the nuclear pore complex in adenovirus DNA entry. *EMBO J* **16**(19): 5998-6007.
- Greber UF, Willetts M, Webster P, Helenius A (1993). Stepwise dismantling of adenovirus 2 during entry into cells. *Cell* **75**(3): 477-486.
- Greig JA, Buckley SMK, Waddington SN, Parker AL, Bhella D, Pink R, *et al.* (2009). Influence of Coagulation Factor X on In Vitro and In Vivo Gene Delivery by Adenovirus (Ad) 5, Ad35, and Chimeric Ad5/Ad35 Vectors. *Mol Ther* **17**(10): 1683-1691.
- Günther PS, Mikeler E, Hamprecht K, Schneider-Schaulies J, Jahn G, Dennehy KM (2011). CD209/DC-SIGN mediates efficient infection of monocyte-derived dendritic cells by clinical adenovirus 2C isolates in the presence of bovine lactoferrin. *Journal of General Virology* **92**(8): 1754-1759.
- Hacein-Bey-Abina S, Garrigue A, Wang GP, Soulier J, Lim A, Morillon E, *et al.* (2008). Insertional oncogenesis in 4 patients after retrovirus-mediated gene therapy of SCID-X1. *J Clin Invest* **118**(9): 3132-3142.
- Hacein-Bey-Abina S, Le Deist F, Carlier F, Bouneaud C, Hue C, De Villartay J-P, *et al.* (2002). Sustained Correction of X-Linked Severe Combined Immunodeficiency by ex Vivo Gene Therapy. *New England Journal of Medicine* **346**(16): 1185-1193.
- Haisma HJ, Kamps JAAM, Kamps GK, Plantinga JA, Rots MG, Bellu AR (2008). Polyinosinic acid enhances delivery of adenovirus vectors in vivo by preventing sequestration in liver macrophages. *Journal of General Virology* **89**(5): 1097-1105.

- Haks MC, Pépin E, van den Brakel JHN, Smeele SAA, Belkowski SM, Kessels HWHG, *et al.* (2002). Contributions of the T Cell Receptor-associated CD3 γ -ITAM to Thymocyte Selection. *The Journal of Experimental Medicine* **196**(1): 1-13.
- Hamid O, Varterasian ML, Wadler S, Hecht JR, Benson A, Galanis E, *et al.* (2003). Phase II Trial of Intravenous CI-1042 in Patients With Metastatic Colorectal Cancer. *Journal of Clinical Oncology* **21**(8): 1498-1504.
- Harada JN, Shevchenko A, Shevchenko A, Pallas DC, Berk AJ (2002). Analysis of the Adenovirus E1B-55K-Anchored Proteome Reveals Its Link to Ubiquitination Machinery. *Journal of Virology* **76**(18): 9194-9206.
- Hardonk MJ, Dijkhuis FW, Hulstaert CE, Koudstaal J (1992). Heterogeneity of rat liver and spleen macrophages in gadolinium chloride-induced elimination and repopulation. *Journal of Leukocyte Biology* **52**(3): 296-302.
- Hay RT, Freeman A, Leith I, Monaghan A, Webster A (1995). Molecular interactions during adenovirus DNA replication. *Curr Top Microbiol Immunol* **199** (Pt 2): 31-48.
- Hayashi K, Yonemura S, Matsui T, Tsukita S (1999). Immunofluorescence detection of ezrin/radixin/moesin (ERM) proteins with their carboxyl-terminal threonine phosphorylated in cultured cells and tissues. *Journal of Cell Science* **112**(8): 1149-1158.
- Heise C, Hermiston T, Johnson L, Brooks G, Sampson-Johannes A, Williams A, *et al.* (2000). An adenovirus E1A mutant that demonstrates potent and selective systemic anti-tumoral efficacy. *Nat Med* **6**(10): 1134-1139.
- Heise C, Sampson-Johannes A, Williams A, McCormick F, Von Hoff DD, Kirn DH (1997). ONYX-015, an E1B gene-attenuated adenovirus, causes tumor-specific cytolysis and antitumoral efficacy that can be augmented by standard chemotherapeutic agents. *Nat Med* **3**(6): 639-645.
- Henaff D, Salinas S, Kremer EJ (2011). An adenovirus traffic update: from receptor engagement to the nuclear pore. *Future Microbiology* **6**(2): 179-192.
- Henry LJ, Xia D, Wilke ME, Deisenhofer J, Gerard RD (1994). Characterization of the knob domain of the adenovirus type 5 fiber protein expressed in *Escherichia coli*. *Journal of Virology* **68**(8): 5239-5246.
- Hidaka C, Milano E, Leopold PL, Bergelson JM, Hackett NR, Finberg RW, *et al.* (1999). CAR-dependent and CAR-independent pathways of adenovirus vector-mediated gene transfer and expression in human fibroblasts. *The Journal of Clinical Investigation* **103**(4): 579-587.
- Hierholzer JC (1992). Adenoviruses in the immunocompromised host. *Clinical Microbiology Reviews* **5**(3): 262-274.
- Hirschhorn R (1983). Genetic deficiencies of adenosine deaminase and purine nucleoside phosphorylase: overview, genetic heterogeneity and therapy. *Birth Defects Orig Artic Ser* **19**(3): 73-81.
- Hirsh J, Anand SS, Halperin JL, Fuster V (2001). Mechanism of Action and Pharmacology of Unfractionated Heparin. *Arteriosclerosis, Thrombosis, and Vascular Biology* **21**(7): 1094-1096.

Hilleman MR, Werner JH (1954). Recovery of New Agent from Patients with Acute Respiratory Illness. *Proceedings of the Society for Experimental Biology and Medicine. Society for Experimental Biology and Medicine (New York, N.Y.)* **85**(1): 183-188.

Hodgson J (2001). ADMET[mdash]turning chemicals into drugs. *Nat Biotech* **19**(8): 722-726.

Hoffmann H-H, Kunz A, Simon VA, Palese P, Shaw ML (2011). Broad-spectrum antiviral that interferes with de novo pyrimidine biosynthesis. *Proceedings of the National Academy of Sciences* **108**(14): 5777-5782.

Hofherr SE, Shashkova EV, Weaver EA, Khare R, Barry MA (2008). Modification of Adenoviral Vectors With Polyethylene Glycol Modulates In Vivo Tissue Tropism and Gene Expression. *Mol Ther* **16**(7): 1276-1282.

Hong J-Y, Lee H-J, Piedra PA, Choi E-H, Park K-H, Koh Y-Y, *et al.* (2001). Lower Respiratory Tract Infections due to Adenovirus in Hospitalized Korean Children: Epidemiology, Clinical Features, and Prognosis. *Clinical Infectious Diseases* **32**(10): 1423-1429.

Hong SS, Habib NA, Franqueville L, Jensen S, Boulanger PA (2003). Identification of Adenovirus (Ad) Penton Base Neutralising Epitopes by Use of Sera from Patients Who Had Received Conditionally Replicative Ad (Add1520) for Treatment of Liver Tumors. *Journal of Virology* **77**(19): 10366-10375.

Howe JA, Mymryk JS, Egan C, Branton PE, Bayley ST (1990). Retinoblastoma growth suppressor and a 300-kDa protein appear to regulate cellular DNA synthesis. *Proc Natl Acad Sci U S A* **87**(15): 5883-5887.

Howe SJ, Mansour MR, Schwarzwaelder K, Bartholomae C, Hubank M, Kempinski H, *et al.* (2008). Insertional mutagenesis combined with acquired somatic mutations causes leukemogenesis following gene therapy of SCID-X1 patients. *J Clin Invest* **118**(9): 3143-3150.

Huard J, Lochmuller H, Acsadi G, Jani A, Massie B, Karpati G (1995). The route of administration is a major determinant of the transduction efficiency of rat tissues by adenoviral recombinants. *Gene Ther* **2**(2): 107-115.

Humphrey MB, Lanier LL, Nakamura MC (2005). Role of ITAM-containing adapter proteins and their receptors in the immune system and bone. *Immunological Reviews* **208**(1): 50-65.

Inglese J, Johnson RL, Simeonov A, Xia M, Zheng W, Austin CP, *et al.* (2007). High-throughput screening assays for the identification of chemical probes. *Nat Chem Biol* **3**(8): 466-479.

Itoigawa M, Ito C, Wu T-S, Enjo F, Tokuda H, Nishino H, *et al.* (2003). Cancer chemopreventive activity of acridone alkaloids on Epstein–Barr virus activation and two-stage mouse skin carcinogenesis. *Cancer Letters* **193**(2): 133-138.

Ivetic A, Ridley AJ (2004). Ezrin/radixin/moesin proteins and Rho GTPase signalling in leucocytes. *Immunology* **112**(2): 165-176.

- Jacobs F, Wisse E, De Geest B (2010). The Role of Liver Sinusoidal Cells in Hepatocyte-Directed Gene Transfer. *The American Journal of Pathology* **176**(1): 14-21.
- Jegede O, Khodyakova A, Chernov M, Weber J, Menéndez-Arias L, Gudkov A, *et al.* (2011). Identification of low-molecular weight inhibitors of HIV-1 reverse transcriptase using a cell-based high-throughput screening system. *Antiviral Research* **91**(2): 94-98.
- Jessup M, Greenberg B, Mancini D, Cappola T, Pauly DF, Jaski B, *et al.* (2011). Calcium Upregulation by Percutaneous Administration of Gene Therapy in Cardiac Disease (CUPID) / Clinical Perspective. *Circulation* **124**(3): 304-313.
- Jiang H, Wang Z, Serra D, Frank MM, Amalfitano A (2004). Recombinant Adenovirus Vectors Activate the Alternative Complement Pathway, Leading to the Binding of Human Complement Protein C3 Independent of Anti-Ad Antibodies. *Mol Ther* **10**(6): 1140-1142.
- Johansson C, Jonsson M, Marttila M, Persson D, Fan X-L, Skog J, *et al.* (2007). Adenoviruses Use Lactoferrin as a Bridge for CAR-Independent Binding to and Infection of Epithelial Cells. *J. Virol.* **81**(2): 954-963.
- Johnson KM, Kines RC, Roberts JN, Lowy DR, Schiller JT, Day PM (2009). Role of Heparan Sulfate in Attachment to and Infection of the Murine Female Genital Tract by Human Papillomavirus. *Journal of Virology* **83**(5): 2067-2074.
- Johnston PA, Johnston PA (2002). Cellular platforms for HTS: three case studies. *Drug Discovery Today* **7**(6): 353-363.
- Jonsson MI, Lenman AE, Frängsmyr L, Nyberg C, Abdullahi M, Arnberg N (2009). Coagulation Factors IX and X Enhance Binding and Infection of Adenovirus Types 5 and 31 in Human Epithelial Cells. *Journal of Virology* **83**(8): 3816-3825.
- Kalyuzhniy O, Di Paolo NC, Silvestry M, Hofherr SE, Barry MA, Stewart PL, *et al.* (2008). Adenovirus serotype 5 hexon is critical for virus infection of hepatocytes in vivo. *Proceedings of the National Academy of Sciences* **105**(14): 5483-5488.
- Kano T, Wada S, Morimoto K, Kato Y, Ogihara T (2011). Effect of knockdown of ezrin, radixin, and moesin on P-glycoprotein function in HepG2 cells. *Journal of Pharmaceutical Sciences* **100**(12): 5308-5314.
- Katz E, Lareef MH, Rassa JC, Grande SM, King LB, Russo J, *et al.* (2005). MMTV Env encodes an ITAM responsible for transformation of mammary epithelial cells in three-dimensional culture. *The Journal of Experimental Medicine* **201**(3): 431-439.
- Kelkar SA, Pfister KK, Crystal RG, Leopold PL (2004). Cytoplasmic Dynein Mediates Adenovirus Binding to Microtubules. *J. Virol.* **78**(18): 10122-10132.
- Khare R, May SM, Vetrini F, Weaver EA, Palmer D, Rosewell A, *et al.* (2011). Generation of a Kupffer Cell-evading Adenovirus for Systemic and Liver-directed Gene Transfer. *Mol Ther* **19**(7): 1254-1262.
- Khare R, Reddy VS, Nemerow GR, Barry MA (2012). Identification of Adenovirus Serotype 5 Hexon Regions That Interact with Scavenger Receptors. *Journal of Virology* **86**(4): 2293-2301.

- Khoo SH, Bailey AS, de Jong JC, Mandal BK (1995). Adenovirus infections in human immunodeficiency virus-positive patients: clinical features and molecular epidemiology. *J Infect Dis* **172**(3): 629-637.
- Kiang A, Hartman ZC, Everett RS, Serra D, Jiang H, Frank MM, *et al.* (2006). Multiple Innate Inflammatory Responses Induced after Systemic Adenovirus Vector Delivery Depend on a Functional Complement System. *Mol Ther* **14**(4): 588-598.
- Kim DJ, James HL (1994). Expression of human factor X with normal biological activity in human embryonic kidney cells. *Biotechnology Letters* **16**(6): 549-554.
- Kim I-H, Józkwicz A, Piedra PA, Oka K, Chan L (2001). Lifetime correction of genetic deficiency in mice with a single injection of helper-dependent adenoviral vector. *Proceedings of the National Academy of Sciences* **98**(23): 13282-13287.
- Kim M, Zinn KR, Barnett BG, Sumerel LA, Krasnykh V, Curiel DT, *et al.* (2002). The therapeutic efficacy of adenoviral vectors for cancer gene therapy is limited by a low level of primary adenovirus receptors on tumour cells. *European Journal of Cancer* **38**(14): 1917-1926.
- Koizumi N, Mizuguchi H, Sakurai F, Yamaguchi T, Watanabe Y, Hayakawa T (2003). Reduction of Natural Adenovirus Tropism to Mouse Liver by Fiber-Shaft Exchange in Combination with both CAR- and αv Integrin-Binding Ablation. *Journal of Virology* **77**(24): 13062-13072.
- Kojaoghlanian T, Flomenberg P, Horwitz MS (2003). The impact of adenovirus infection on the immunocompromised host. *Reviews in Medical Virology* **13**(3): 155-171.
- Koresawa M, Okabe T (2004). High-throughput screening with quantitation of ATP consumption: a universal non-radioisotope, homogeneous assay for protein kinase. *Assay Drug Dev Technol* **2**(2): 153-160.
- Kramer MJ, Cleeland R, Grunberg E (1976). Antiviral activity of 10 carboxymethyl 9 acridanone. *Antimicrobial Agents and Chemotherapy* **9**(2): 233-238.
- Kraus M, Pao LI, Reichlin A, Hu Y, Canono B, Cambier JC, *et al.* (2001). Interference with Immunoglobulin (Ig) α Immunoreceptor Tyrosine-Based Activation Motif (Itam) Phosphorylation Modulates or Blocks B Cell Development, Depending on the Availability of an Ig β Cytoplasmic Tail. *The Journal of Experimental Medicine* **194**(4): 455-470.
- Kritz AB, Nicol CG, Dishart KL, Nelson R, Holbeck S, Von Seggern DJ, *et al.* (2007). Adenovirus 5 Fibers Mutated at the Putative HSPG-binding Site Show Restricted Retargeting with Targeting Peptides in the HI Loop. *Mol Ther* **15**(4): 741-749.
- Kroes ACM, de Klerk EPA, Lankester AC, Malipaard C, de Brouwer CS, Claas ECJ, *et al.* (2007). Sequential emergence of multiple adenovirus serotypes after pediatric stem cell transplantation. *Journal of clinical virology : the official publication of the Pan American Society for Clinical Virology* **38**(4): 341-347.
- Kuhn I, Harden P, Bauzon M, Chartier C, Nye J, Thorne S, *et al.* (2008). Directed Evolution Generates a Novel Oncolytic Virus for the Treatment of Colon Cancer. *PLoS ONE* **3**(6): e2409.

- Kuhn I, Harden P, Bauzon M, Hermiston T (2005). 319. ColoAd1, a Chimeric Ad11p/Ad3 Oncolytic Virus for the Treatment of Colon Cancer. *Mol Ther* **11**(S1): S124-S124.
- Kumagai K, Kiyosawa N, Ito K, Yamoto T, Teranishi M, Nakayama H, *et al.* (2007). Influence of Kupffer cell inactivation on cycloheximide-induced hepatic injury. *Toxicology* **241**(3): 106-118.
- Kumaran S, Grucza RA, Waksman G (2003). The tandem Src homology 2 domain of the Syk kinase: A molecular device that adapts to interphosphotyrosine distances. *Proceedings of the National Academy of Sciences* **100**(25): 14828-14833.
- Lai NC, Roth DM, Gao MH, Tang T, Dalton N, Lai YY, *et al.* (2004). Intracoronary Adenovirus Encoding Adenylyl Cyclase VI Increases Left Ventricular Function in Heart Failure. *Circulation* **110**(3): 330-336.
- Lander ES, Linton LM, Birren B, Nusbaum C, Zody MC, Baldwin J, *et al.* (2001). Initial sequencing and analysis of the human genome. *Nature* **409**(6822): 860-921.
- Lanier LL, Bakker ABH (2000). The ITAM-bearing transmembrane adaptor DAP12 in lymphoid and myeloid cell function. *Immunology Today* **21**(12): 611-614.
- Lankes W, Griesmacher A, Grunwald J, Schwartz-Albiez R, Keller R (1988). A heparin-binding protein involved in inhibition of smooth-muscle cell proliferation. *Biochem J* **251**(3): 831-842.
- Lankes WT, Furthmayr H (1991). Moesin: a member of the protein 4.1-talin-ezrin family of proteins. *Proceedings of the National Academy of Sciences* **88**(19): 8297-8301.
- Larson RA, Dai D, Hosack VT, Tan Y, Bolken TC, Hruby DE, *et al.* (2008). Identification of a Broad-Spectrum Arenavirus Entry Inhibitor. *Journal of Virology* **82**(21): 10768-10775.
- Law CL, Chandran KA, Sidorenko SP, Clark EA (1996). Phospholipase C-gamma1 interacts with conserved phosphotyrosyl residues in the linker region of Syk and is a substrate for Syk. *Molecular and Cellular Biology* **16**(4): 1305-1315.
- Lee H, Guo J, Li M, Choi J-K, DeMaria M, Rosenzweig M, *et al.* (1998). Identification of an Immunoreceptor Tyrosine-Based Activation Motif of K1 Transforming Protein of Kaposi's Sarcoma-Associated Herpesvirus. *Molecular and Cellular Biology* **18**(9): 5219-5228.
- Lenaerts L, De Clercq E, Naesens L (2008). Clinical features and treatment of adenovirus infections. *Reviews in Medical Virology* **18**(6): 357-374.
- Lenaerts L, Naesens L (2006). Antiviral therapy for adenovirus infections. *Antiviral Research* **71**(2-3): 172-180.
- Lenman A, Müller S, Nygren MI, Frängsmyr L, Stehle T, Arnberg N (2011). Coagulation Factor IX Mediates Serotype-Specific Binding of Species A Adenoviruses to Host Cells. *Journal of Virology* **85**(24): 13420-13431.

- Leroy C, Fialin C, Sirvent A, Simon V, Urbach S, Poncet J, *et al.* (2009). Quantitative Phosphoproteomics Reveals a Cluster of Tyrosine Kinases That Mediates Src Invasive Activity in Advanced Colon Carcinoma Cells. *Cancer Research* **69**(6): 2279-2286.
- Li E, Stupack D, Bokoch GM, Nemerow GR (1998a). Adenovirus Endocytosis Requires Actin Cytoskeleton Reorganization Mediated by Rho Family GTPases. *J. Virol.* **72**(11): 8806-8812.
- Li E, Stupack D, Klemke R, Cheresch DA, Nemerow GR (1998b). Adenovirus endocytosis via alpha(v) integrins requires phosphoinositide-3-OH kinase. *J Virol* **72**(3): 2055-2061.
- Lieber A, He C, Meuse L, Schowalter D, Kirillova I, Winther B, *et al.* (1997). The role of Kupffer cell activation and viral gene expression in early liver toxicity after infusion of recombinant adenovirus vectors. *J. Virol.* **71**(11): 8798-8807.
- Lindemans CA, Leen AM, Boelens JJ (2010). How I treat adenovirus in hematopoietic stem cell transplant recipients. *Blood* **116**(25): 5476-5485.
- Lion T, Baumgartinger R, Watzinger F, Matthes-Martin S, Suda M, Preuner S, *et al.* (2003). Molecular monitoring of adenovirus in peripheral blood after allogeneic bone marrow transplantation permits early diagnosis of disseminated disease. *Blood* **102**(3): 1114-1120.
- Liu H, Jin L, Koh SBS, Atanasov I, Schein S, Wu L, *et al.* (2010). Atomic Structure of Human Adenovirus by Cryo-EM Reveals Interactions Among Protein Networks. *Science* **329**(5995): 1038-1043.
- Liu LW, Ye J, Johnson AE, Esmon CT (1991). Proteolytic formation of either of the two prothrombin activation intermediates results in formation of a hirugen-binding site. *Journal of Biological Chemistry* **266**(35): 23633-23636.
- Liu Y, Wang H, Yumul R, Gao W, Gambotto A, Morita T, *et al.* (2009). Transduction of liver metastases after intravenous injection of Ad5/35 or Ad35 vectors with and without factor X-binding protein pretreatment. *Hum Gene Ther* **20**(6): 621-629.
- Lonberg-Holm K, Crowell RL, Philipson L (1976). Unrelated animal viruses share receptors. *Nature* **259**(5545): 679-681.
- Lowden CT, Bastow KF (2003). Cell culture replication of herpes simplex virus and, or human cytomegalovirus is inhibited by 3,7-dialkoxylated, 1-hydroxyacridone derivatives. *Antiviral Research* **59**(3): 143-154.
- Lowe SW, Ruley HE (1993). Stabilization of the p53 tumor suppressor is induced by adenovirus 5 E1A and accompanies apoptosis. *Genes Dev* **7**(4): 535-545.
- Lozier JN, Csako G, Mondoro TH, Krizek DM, Metzger ME, Costello R, *et al.* (2002). Toxicity of a First-Generation Adenoviral Vector in Rhesus Macaques. *Human Gene Therapy* **13**(1): 113-124.
- Lu M, Freytag SO, Stricker H, Kim JH, Barton K, Movsas B (2011). Adaptive seamless design for an efficacy trial of replication-competent adenovirus-mediated suicide gene therapy and radiation in newly-diagnosed prostate cancer (ReCAP Trial). *Contemporary Clinical Trials* **32**(3): 453-460.

Lusky M, Christ M, Rittner K, Dieterle A, Dreyer D, Mourot B, *et al.* (1998). In Vitro and In Vivo Biology of Recombinant Adenovirus Vectors with E1, E1/E2A, or E1/E4 Deleted. *Journal of Virology* **72**(3): 2022-2032.

Lusky M, Grave L, Dieterlé A, Dreyer D, Christ M, Ziller C, *et al.* (1999). Regulation of Adenovirus-Mediated Transgene Expression by the Viral E4 Gene Products: Requirement for E4 ORF3. *Journal of Virology* **73**(10): 8308-8319.

Lyons M, Onion D, Green NK, Aslan K, Rajaratnam R, Bazan-Peregrino M, *et al.* (2006). Adenovirus Type 5 Interactions with Human Blood Cells May Compromise Systemic Delivery. *Mol Ther* **14**(1): 118-128.

Lysechko TL, Ostergaard HL (2005). Differential Src Family Kinase Activity Requirements for CD3 ζ Phosphorylation/ZAP70 Recruitment and CD3 ϵ Phosphorylation. *The Journal of Immunology* **174**(12): 7807-7814.

Macfarlane RG (1964). An Enzyme Cascade in the Blood Clotting Mechanism, and its Function as a Biochemical Amplifier. *Nature* **202**(4931): 498-499.

Maeda M, Matsui T, Imamura M, Tsukita S (1999). Expression level, subcellular distribution and rho-GDI binding affinity of merlin in comparison with Ezrin/Radixin/Moesin proteins. *Oncogene* **18**(34): 4788-4797.

Majhen D, Nemet J, Richardson J, Gabrilovac J, Hajsig M, Osmak M, *et al.* (2009). Differential role of $\alpha\beta$ 3 and $\alpha\beta$ 5 integrins in internalization and transduction efficacies of wild type and RGD4C fiber-modified adenoviruses. *Virus Research* **139**(1): 64-73.

Manickan E, Smith JS, Tian J, Eggerman TL, Lozier JN, Muller J, *et al.* (2006). Rapid Kupffer Cell Death after Intravenous Injection of Adenovirus Vectors. *Mol Ther* **13**(1): 108-117.

Martin K, Brie A, Saulnier P, Perricaudet M, Yeh P, Vigne E (2003). Simultaneous CAR- and alpha V integrin-binding ablation fails to reduce Ad5 liver tropism. *Mol Ther* **8**(3): 485-494.

Masson PL, Heremans JF, Dive CH (1966). An iron-binding protein common to many external secretions. *Clinica Chimica Acta* **14**(6): 735-739.

Matsui T, Maeda M, Doi Y, Yonemura S, Amano M, Kaibuchi K, *et al.* (1998). Rho-Kinase Phosphorylates COOH-terminal Threonines of Ezrin/Radixin/Moesin (ERM) Proteins and Regulates Their Head-to-Tail Association. *The Journal of Cell Biology* **140**(3): 647-657.

Matthews QL (2010). Capsid-Incorporation of Antigens into Adenovirus Capsid Proteins for a Vaccine Approach. *Molecular Pharmaceutics* **8**(1): 3-11.

McEver RP (1995). Regulation of function and expression of P-selectin. *Agents Actions Suppl* **47**: 117-119.

McGovern SL, Caselli E, Grigorieff N, Shoichet BK (2002). A Common Mechanism Underlying Promiscuous Inhibitors from Virtual and High-Throughput Screening. *Journal of Medicinal Chemistry* **45**(8): 1712-1722.

- McMullen BA, Fujikawa K, Kisiel W (1983). The occurrence of β -hydroxyaspartic acid in the vitamin K-dependent blood coagulation zymogens. *Biochemical and Biophysical Research Communications* **115**(1): 8-14.
- Medina-Kauwe LK (2003). Endocytosis of adenovirus and adenovirus capsid proteins. *Advanced Drug Delivery Reviews* **55**(11): 1485-1496.
- Micheva-Viteva S, Kobayashi Y, Edelstein LC, Pacchia AL, Lee H-LR, Graci JD, *et al.* (2011). High-throughput Screening Uncovers a Compound That Activates Latent HIV-1 and Acts Cooperatively with a Histone Deacetylase (HDAC) Inhibitor. *Journal of Biological Chemistry* **286**(24): 21083-21091.
- Miller N (2012). Glybera and the future of gene therapy in the European Union. *Nature Reviews Drug Discovery* **11**(5): 419.
- Mizuguchi H, Kay MA, Hayakawa T (2001). Approaches for generating recombinant adenovirus vectors. *Advanced Drug Delivery Reviews* **52**(3): 165-176.
- Mocsai A, Abram CL, Jakus Z, Hu Y, Lanier LL, Lowell CA (2006). Integrin signaling in neutrophils and macrophages uses adaptors containing immunoreceptor tyrosine-based activation motifs. *Nat Immunol* **7**(12): 1326-1333.
- Mócsai A, Humphrey MB, Van Ziffle JAG, Hu Y, Burghardt A, Spusta SC, *et al.* (2004). The immunomodulatory adapter proteins DAP12 and Fc receptor γ -chain (FcR γ) regulate development of functional osteoclasts through the Syk tyrosine kinase. *Proceedings of the National Academy of Sciences of the United States of America* **101**(16): 6158-6163.
- Mócsai A, Ruland J, Tybulewicz VLJ (2010). The SYK tyrosine kinase: a crucial player in diverse biological functions. *Nat Rev Immunol* **10**(6): 387-402.
- Monteiro RQ, Rezaie AR, Bae JS, Calvo E, Andersen JF, Francischetti IM (2008). Ixolaris binding to factor X reveals a precursor state of factor Xa heparin-binding exosite. *Protein Sci* **17**(1): 146-153.
- Monteiro RQ, Rezaie AR, Ribeiro JM, Francischetti IM (2005). Ixolaris: a factor Xa heparin-binding exosite inhibitor. *Biochem J* **387**(Pt 3): 871-877.
- Moriya K, Rivera J, Odom S, Sakuma Y, Muramoto K, Yoshiuchi T, *et al.* (1997). ER-27319, an acridone-related compound, inhibits release of antigen-induced allergic mediators from mast cells by selective inhibition of Fc ϵ receptor I-mediated activation of Syk. *Proceedings of the National Academy of Sciences* **94**(23): 12539-12544.
- Morsy MA, Gu M, Motzel S, Zhao J, Lin J, Su Q, *et al.* (1998). An adenoviral vector deleted for all viral coding sequences results in enhanced safety and extended expression of a leptin transgene. *Proceedings of the National Academy of Sciences* **95**(14): 7866-7871.
- Mosterd JJ, Thijssen HH (1992). The relationship between the vitamin K cycle inhibition and the plasma anticoagulant response at steady-state S-warfarin conditions in the rat. *Journal of Pharmacology and Experimental Therapeutics* **260**(3): 1081-1085.

- Mou DL, Wang YP, Jiang H, Xiao SY, Yu X, Li GY, *et al.* (2007). [Identification of a functional ITAM-like sequence within G1 cytoplasmic tail of Hantaan virus]. *Bing Du Xue Bao* **23**(6): 424-428.
- Mueller NH, Pattabiraman N, Ansarah-Sobrinho C, Viswanathan P, Pierson TC, Padmanabhan R (2008). Identification and biochemical characterization of small-molecule inhibitors of west nile virus serine protease by a high-throughput screen. *Antimicrob Agents Chemother* **52**(9): 3385-3393.
- Munoz RE, Piedra PA, Demmler GJ (1998). Disseminated Adenovirus Disease in Immunocompromised and Immunocompetent Children. *Clinical Infectious Diseases* **27**(5): 1194-1200.
- Murakami MT, Rios-Steiner J, Weaver SE, Tulinsky A, Geiger JH, Arni RK (2007). Intermolecular Interactions and Characterization of the Novel Factor Xa Exosite Involved in Macromolecular Recognition and Inhibition: Crystal Structure of Human Gladomainless Factor Xa Complexed with the Anticoagulant Protein NAPc2 from the Hematophagous Nematode *Ancylostoma caninum*. *Journal of Molecular Biology* **366**(2): 602-610.
- Muruve DA, Barnes MJ, Stillman IE, Libermann TA (1999). Adenoviral Gene Therapy Leads to Rapid Induction of Multiple Chemokines and Acute Neutrophil-Dependent Hepatic Injury in Vivo. *Human Gene Therapy* **10**(6): 965-976.
- Muul LM, Tuschong LM, Soenen SL, Jagadeesh GJ, Ramsey WJ, Long Z, *et al.* (2003). Persistence and expression of the adenosine deaminase gene for 12 years and immune reaction to gene transfer components: long-term results of the first clinical gene therapy trial. *Blood* **101**(7): 2563-2569.
- Nakano MY, Boucke K, Suomalainen M, Stidwill RP, Greber UF (2000). The First Step of Adenovirus Type 2 Disassembly Occurs at the Cell Surface, Independently of Endocytosis and Escape to the Cytosol. *J. Virol.* **74**(15): 7085-7095.
- Nathwani AC, Tuddenham EGD, Rangarajan S, Rosales C, McIntosh J, Linch DC, *et al.* (2011). Adenovirus-Associated Virus Vector-Mediated Gene Transfer in Hemophilia B. *New England Journal of Medicine* **365**(25): 2357-2365.
- Nelsestuen GL, Broderius M, Martin G (1976). Role of gamma-carboxyglutamic acid. Cation specificity of prothrombin and factor X-phospholipid binding. *Journal of Biological Chemistry* **251**(22): 6886-6893.
- Neofytos D, Ojha A, Mookerjee B, Wagner J, Filicko J, Ferber A, *et al.* (2007). Treatment of Adenovirus Disease in Stem Cell Transplant Recipients with Cidofovir. *Biology of blood and marrow transplantation : journal of the American Society for Blood and Marrow Transplantation* **13**(1): 74-81.
- Nicklin SA, Wu E, Nemerow GR, Baker AH (2005). The Influence of Adenovirus Fiber Structure and Function on Vector Development for Gene Therapy. *Mol Ther* **12**(3): 384-393.
- Nicol CG, Graham D, Miller WH, White SJ, Smith TAG, Nicklin SA, *et al.* (2004). Effect of Adenovirus Serotype 5 Fiber and Penton Modifications on in vivo Tropism in Rats. *Mol Ther* **10**(2): 344-354.

Nilsson EC, Storm RJ, Bauer J, Johansson SMC, Lookene A, Angstrom J, *et al.* (2011). The GD1a glycan is a cellular receptor for adenoviruses causing epidemic keratoconjunctivitis. *Nat Med* **17**(1): 105-109.

Nishikawa T, Nakashima K, Fukano R, Okamura J, Inagaki J (2011). Successful treatment with plasma exchange for disseminated cidofovir-resistant adenovirus disease in a pediatric SCT recipient. *Bone Marrow Transplant.*

Nogami K, Freas J, Manithody C, Wakabayashi H, Rezaie AR, Fay PJ (2004). Mechanisms of Interactions of Factor X and Factor Xa with the Acidic Region in the Factor VIII A1 Domain. *Journal of Biological Chemistry* **279**(32): 33104-33113.

O'Donnell J (2012). Anticoagulants: Therapeutics, Risks, and Toxicity--Special Emphasis on Heparin-Induced Thrombocytopenia (HIT). *J Pharm Pract* **25**(1): 22-29.

O'Donnell J, Taylor KA, Chapman MS (2009). Adeno-associated virus-2 and its primary cellular receptor—Cryo-EM structure of a heparin complex. *Virology* **385**(2): 434-443.

O'Riordan CR, Lachapelle A, Delgado C, Parkes V, Wadsworth SC, Smith AE, *et al.* (1999). PEGylation of Adenovirus with Retention of Infectivity and Protection from Neutralising Antibody in Vitro and in Vivo. *Human Gene Therapy* **10**(8): 1349-1358.

O'Shea CC, Johnson L, Bagus B, Choi S, Nicholas C, Shen A, *et al.* (2004). Late viral RNA export, rather than p53 inactivation, determines ONYX-015 tumor selectivity. *Cancer Cell* **6**(6): 611-623.

Öberg CT, Strand M, Andersson EK, Edlund K, Tran NPN, Mei Y-F, *et al.* (2012). Synthesis, Biological Evaluation, and Structure–Activity Relationships of 2-[2-(Benzoylamino)benzoylamino]benzoic Acid Analogues as Inhibitors of Adenovirus Replication. *Journal of Medicinal Chemistry* **55**(7): 3170-3181.

Öberg D, Yanover E, Adam V, Sweeney K, Costas C, Lemoine NR, *et al.* (2010). Improved Potency and Selectivity of an Oncolytic E1ACR2 and E1B19K Deleted Adenoviral Mutant in Prostate and Pancreatic Cancers. *Clinical Cancer Research* **16**(2): 541-553.

Olson ST, Björk I, Sheffer R, Craig PA, Shore JD, Choay J (1992). Role of the antithrombin-binding pentasaccharide in heparin acceleration of antithrombin-proteinase reactions. Resolution of the antithrombin conformational change contribution to heparin rate enhancement. *Journal of Biological Chemistry* **267**(18): 12528-12538.

O'Malley, R. P., R. F. Duncan, J. W. Hershey, and M. B. Mathews (1989). Modification of protein synthesis initiation factors and the shut-off of host protein synthesis in adenovirus-infected cells. *Virology* **168**:112-118.

O'Malley, R. P., T. M. Mariano, J. Siekierka, and M. B. Mathews (1986). A mechanism for the control of protein synthesis by adenovirus VA RNAI. *Cell* **44**:391-400.

Omar H, Yun Z, Lewensohn-Fuchs I, Pérez-Bercoff L, Örvell C, Engström L, *et al.* (2010). Poor outcome of adenovirus infections in adult hematopoietic stem cell transplant patients with sustained adenovirus viremia. *Transplant Infectious Disease* **12**(5): 465-469.

- Osterud B, Rapaport SI (1977). Activation of factor IX by the reaction product of tissue factor and factor VII: additional pathway for initiating blood coagulation. *Proc Natl Acad Sci U S A* **74**(12): 5260-5264.
- Othman M, Labelle A, Mazzetti I, Elbatarny HS, Lillicrap D (2007). Adenovirus-induced thrombocytopenia: the role of von Willebrand factor and P-selectin in mediating accelerated platelet clearance. *Blood* **109**(7): 2832-2839.
- Padmanabhan K, Padmanabhan KP, Tulinsky A, Park CH, Bode W, Huber R, *et al.* (1993). Structure of Human Des(1-45) Factor Xa at 2.2 Å Resolution. *Journal of Molecular Biology* **232**(3): 947-966.
- Parker AL, McVey JH, Doctor JH, Lopez-Franco O, Waddington SN, Havenga MJE, *et al.* (2007). Influence of Coagulation Factor Zymogens on the Infectivity of Adenoviruses Pseudotyped with Fibers from Subgroup D. *J. Virol.* **81**(7): 3627-3631.
- Parker AL, Waddington SN, Buckley SMK, Custers J, Havenga MJE, van Rooijen N, *et al.* (2009). Effect of Neutralising Sera on Factor X-Mediated Adenovirus Serotype 5 Gene Transfer. *J. Virol.* **83**(1): 479-483.
- Parker AL, Waddington SN, Nicol CG, Shayakhmetov DM, Buckley SM, Denby L, *et al.* (2006). Multiple vitamin K-dependent coagulation zymogens promote adenovirus-mediated gene delivery to hepatocytes. *Blood* **108**(8): 2554-2561.
- Pasqualini R, Koivunen E, Ruoslahti E (1997). [alpha]v Integrins as receptors for tumor targeting by circulating ligands. *Nat Biotech* **15**(6): 542-546.
- Patel P, Young JG, Mautner V, Ashdown D, Bonney S, Pineda RG, *et al.* (2009). A phase I/II clinical trial in localized prostate cancer of an adenovirus expressing nitroreductase with CB1954 [correction of CB1984]. *Mol Ther* **17**(7): 1292-1299.
- Pawlotsky J-M, Dahari H, Neumann AU, Hezode C, Germanidis G, Lonjon I, *et al.* (2004). Antiviral action of ribavirin in chronic hepatitis C. *Gastroenterology* **126**(3): 703-714.
- Peng Z (2005). Current Status of Gendicine in China: Recombinant Human Ad-p53 Agent for Treatment of Cancers. *Human Gene Therapy* **16**(9): 1016-1027.
- Pereboeva L, Komarova S, Mikheeva G, Krasnykh V, Curiel DT (2003). Approaches to Utilize Mesenchymal Progenitor Cells as Cellular Vehicles. *STEM CELLS* **21**(4): 389-404.
- Persson CG, Erjefält I, Alkner U, Baumgarten C, Greiff L, Gustafsson B, Luts A, Pipkorn U, Sundler F, Svensson C, *et al.* (1991). Plasma exudation as a first line respiratory mucosal defence. *Clin Exp Allergy* **21**(1):17-24.
- Petäjä J (2011). Inflammation and coagulation. An overview. *Thrombosis Research* **127**, **Supplement 2**(0): S34-S37.
- Plaimauer B, Mohr G, Wernhart W, Himmelspach M, Dorner F, Schlokot U (2001). 'Shed' furin: mapping of the cleavage determinants and identification of its C-terminus. *Biochem J* **354**(Pt 3): 689-695.
- Porollo A, Meller J (2007). Versatile Annotation and Publication Quality Visualization of Protein Complexes Using POLYVIEW-3D, *BMC Bioinformatics* **8**: 316.

- Preininger A, Schlokot U, Mohr G, Himmelspach M, Stichler V, Kyd-Rebenburg A, *et al.* (1999). Strategies for recombinant Furin employment in a biotechnological process: complete target protein precursor cleavage. *Cytotechnology* **30**(1): 1-16.
- Prill J-M, Espenlaub S, Samen U, Engler T, Schmidt E, Vetrini F, *et al.* (2011). Modifications of Adenovirus Hexon Allow for Either Hepatocyte Detargeting or Targeting With Potential Evasion From Kupffer Cells. *Mol Ther* **19**(1): 83-92.
- Querido E, Marcellus RC, Lai A, Charbonneau R, Teodoro JG, Ketner G, *et al.* (1997). Regulation of p53 levels by the E1B 55-kilodalton protein and E4orf6 in adenovirus-infected cells. *Journal of Virology* **71**(5): 3788-3798.
- Querido E, Morisson MR, Chu-Pham-Dang H, Thirlwell SW-L, Boivin D, Branton PE (2001). Identification of Three Functions of the Adenovirus E4orf6 Protein That Mediate p53 Degradation by the E4orf6-E1B55K Complex. *Journal of Virology* **75**(2): 699-709.
- Radhakrishnan S, Miranda E, Ekblad M, Holford A, Pizarro MT, Lemoine NR, *et al.* (2010). Efficacy of oncolytic mutants targeting pRb and p53 pathways is synergistically enhanced when combined with cytotoxic drugs in prostate cancer cells and tumor xenografts. *Hum Gene Ther* **21**(10): 1311-1325.
- Ramesh N, Ge Y, Ennist DL, Zhu M, Mina M, Ganesh S, *et al.* (2006). CG0070, a Conditionally Replicating Granulocyte Macrophage Colony-Stimulating Factor–Armed Oncolytic Adenovirus for the Treatment of Bladder Cancer. *Clinical Cancer Research* **12**(1): 305-313.
- Raper SE, Chirmule N, Lee FS, Wivel NA, Bagg A, Gao G-p, *et al.* (2003). Fatal systemic inflammatory response syndrome in a ornithine transcarbamylase deficient patient following adenoviral gene transfer. *Molecular Genetics and Metabolism* **80**(1–2): 148-158.
- Raper SE, Yudkoff M, Chirmule N, Gao GP, Nunes F, Haskal ZJ, *et al.* (2002). A pilot study of in vivo liver-directed gene transfer with an adenoviral vector in partial ornithine transcarbamylase deficiency. *Hum Gene Ther* **13**(1): 163-175.
- Rauma T, Tuukkanen J, Bergelson JM, Denning G, Hautala T (1999). rab5 GTPase Regulates Adenovirus Endocytosis. *Journal of Virology* **73**(11): 9664-9668.
- Reddy VS, Natchiar SK, Stewart PL, Nemerow GR (2010). Crystal Structure of Human Adenovirus at 3.5 Å Resolution. *Science* **329**(5995): 1071-1075.
- Reichert M, Winnicka A, Willems L, Kettmann R, Cantor GH (2001). Role of the Proline-Rich Motif of Bovine Leukemia Virus Transmembrane Protein gp30 in Viral Load and Pathogenicity in Sheep. *Journal of Virology* **75**(17): 8082-8089.
- Rekosh DMK, Russell WC, Bellet AJD, Robinson AJ (1977). Identification of a protein linked to the ends of adenovirus DNA. *Cell* **11**(2): 283-295.
- Reynolds PN, Zinn KR, Gavriilyuk VD, Balyasnikova IV, Rogers BE, Buchsbaum DJ, *et al.* (2000). A Targetable, Injectable Adenoviral Vector for Selective Gene Delivery to Pulmonary Endothelium in Vivo. *Mol Ther* **2**(6): 562-578.

Rezaie AR (2000). Identification of Basic Residues in the Heparin-binding Exosite of Factor Xa Critical for Heparin and Factor Va Binding. *Journal of Biological Chemistry* **275**(5): 3320-3327.

Roberts DM, Nanda A, Havenga MJE, Abbink P, Lynch DM, Ewald BA, *et al.* (2006). Hexon-chimaeric adenovirus serotype 5 vectors circumvent pre-existing anti-vector immunity. *Nature* **441**(7090): 239-243.

Robinson AJ, Younghusband HB, Bellett AJD (1973). A circular DNA—Protein complex from adenoviruses. *Virology* **56**(1): 54-69.

Roelvink PW, Lizonova A, Lee JGM, Li Y, Bergelson JM, Finberg RW, *et al.* (1998). The Coxsackievirus-Adenovirus Receptor Protein Can Function as a Cellular Attachment Protein for Adenovirus Serotypes from Subgroups A, C, D, E, and F. *J. Virol.* **72**(10): 7909-7915.

Ropposch T, Nemetz U, Braun EM, Lackner A, Walch C (2012). Low molecular weight heparin therapy in pediatric otogenic sigmoid sinus thrombosis: A safe treatment option? *Int J Pediatr Otorhinolaryngol.*

Ross SR, Schmidt JW, Katz E, Cappelli L, Hultine S, Gimotty P, *et al.* (2006). An Immunoreceptor Tyrosine Activation Motif in the Mouse Mammary Tumor Virus Envelope Protein Plays a Role in Virus-Induced Mammary Tumors. *Journal of Virology* **80**(18): 9000-9008.

Rowe WP, Huebner RJ, Gilmore LK, Parrott RH, Ward TG (1953). Isolation of a cytopathogenic agent from human adenoids undergoing spontaneous degeneration in tissue culture. *Proc Soc Exp Biol Med* **84**(3): 570-573.

Rozsnyay Z, Sarmay G, Zöller M, Gergely J (1996). Membrane-bound ezrin is involved in B-cell receptor-mediated signaling: Potential role of an ITAM-like ezrin motif. *Immunology Letters* **54**(2-3): 163-169.

Rudolph AE, Mullane MP, Porche-Sorbet R, Miletich JP (1997). Expression, Purification, and Characterization of Recombinant Human Factor X. *Protein Expression and Purification* **10**(3): 373-378.

Ruppelt A, Mosenden R, Grönholm M, Aandahl EM, Tobin D, Carlson CR, *et al.* (2007). Inhibition of T Cell Activation by Cyclic Adenosine 5'-Monophosphate Requires Lipid Raft Targeting of Protein Kinase A Type I by the A-Kinase Anchoring Protein Ezrin. *The Journal of Immunology* **179**(8): 5159-5168.

Ruschel A, Ullrich A (2004). Protein tyrosine kinase Syk modulates EGFR signalling in human mammary epithelial cells. *Cellular Signalling* **16**(11): 1249-1261.

Russell WC (2009). Adenoviruses: update on structure and function. *Journal of General Virology* **90**(1): 1-20.

Russell WC (2000). Update on adenovirus and its vectors. *Journal of General Virology* **81**(11): 2573-2604.

Rux JJ, Kuser PR, Burnett RM (2003). Structural and Phylogenetic Analysis of Adenovirus Hexons by Use of High-Resolution X-Ray Crystallographic, Molecular Modeling, and Sequence-Based Methods. *Journal of Virology* **77**(17): 9553-9566.

Ryu C-K, Kang H-Y, Lee SK, Nam KA, Hong CY, Ko W-G, *et al.* (2000). 5-Arylamino-2-methyl-4,7-dioxobenzothiazoles as inhibitors of cyclin-dependent kinase 4 and cytotoxic agents. *Bioorganic & Medicinal Chemistry Letters* **10**(5): 461-464.

Saban SD, Silvestry M, Nemerow GR, Stewart PL (2006). Visualization of α -Helices in a 6-Ångstrom Resolution Cryoelectron Microscopy Structure of Adenovirus Allows Refinement of Capsid Protein Assignments. *Journal of Virology* **80**(24): 12049-12059.

Sadler JE (1998). BIOCHEMISTRY AND GENETICS OF VON WILLEBRAND FACTOR. *Annual Review of Biochemistry* **67**(1): 395-424.

Safaiyan F, Kolset SO, Prydz K, Gottfridsson E, Lindahl U, Salmivirta M (1999). Selective effects of sodium chlorate treatment on the sulfation of heparan sulfate. *J Biol Chem* **274**(51): 36267-36273.

Sakurai D, Yamasaki S, Arase K, Park SY, Arase H, Konno A, *et al.* (2004). Fc ϵ RI γ -ITAM Is Differentially Required for Mast Cell Function In Vivo. *The Journal of Immunology* **172**(4): 2374-2381.

Schiedner G, Morral N, Parks RJ, Wu Y, Koopmans SC, Langston C, *et al.* (1998). Genomic DNA transfer with a high-capacity adenovirus vector results in improved in vivo gene expression and decreased toxicity. *Nat Genet* **18**(2): 180-183.

Seiradake E, Henaff D, Wodrich H, Billet O, Perreau M, Hippert C, *et al.* (2009). The Cell Adhesion Molecule “CAR” and Sialic Acid on Human Erythrocytes Influence Adenovirus In Vivo Biodistribution. *PLoS Pathog* **5**(1): e1000277.

Seregin SS, Aldhamen YA, Appledorn DM, Hartman ZC, Schuldt NJ, Scott J, *et al.* (2010). Adenovirus capsid-display of the retro-oriented human complement inhibitor DAF reduces Ad vector-triggered immune responses in vitro and in vivo. *Blood* **116**(10): 1669-1677.

Seregin SS, Aldhamen YA, Appledorn DM, Zehnder J, Voss T, Godbehere S, *et al.* (2011). Use of DAF-Displaying Adenovirus Vectors Reduces Induction of Transgene- and Vector-Specific Adaptive Immune Responses in Mice. *Human Gene Therapy* **22**(9): 1083-1094.

Sharlow ER, Leimgruber S, Yellow-Duke A, Barrett R, Wang QJ, Lazo JS (2008). Development, validation and implementation of immobilized metal affinity for phosphochemicals (IMAP)-based high-throughput screening assays for low-molecular-weight compound libraries. *Nat. Protocols* **3**(8): 1350-1363.

Shashkova EV, May SM, Doronin K, Barry MA (2009). Expanded Anticancer Therapeutic Window of Hexon-modified Oncolytic Adenovirus. *Mol Ther* **17**(12): 2121-2130.

Shaw AR, Ziff EB (1980). Transcripts from the adenovirus-2 major late promoter yield a single early family of 32 coterminal mRNAs and five late families. *Cell* **22**(3): 905-916.

Shayakhmetov DM, Gaggar A, Ni S, Li Z-Y, Lieber A (2005). Adenovirus Binding to Blood Factors Results in Liver Cell Infection and Hepatotoxicity. *J. Virol.* **79**(12): 7478-7491.

- Sheehan JP, Sadler JE (1994). Molecular mapping of the heparin-binding exosite of thrombin. *Proceedings of the National Academy of Sciences* **91**(12): 5518-5522.
- Short JJ, Rivera AA, Wu H, Walter MR, Yamamoto M, Mathis JM, *et al.* (2010). Substitution of Adenovirus Serotype 3 Hexon onto a Serotype 5 Oncolytic Adenovirus Reduces Factor X Binding, Decreases Liver Tropism, and Improves Antitumor Efficacy. *Molecular Cancer Therapeutics* **9**(9): 2536-2544.
- Shukla D, Liu J, Blaiklock P, Shworak NW, Bai X, Esko JD, *et al.* (1999). A Novel Role for 3-O-Sulfated Heparan Sulfate in Herpes Simplex Virus 1 Entry. *Cell* **99**(1): 13-22.
- Shun TY, Lazo JS, Sharlow ER, Johnston PA (2011). Identifying Actives from HTS Data Sets. *Journal of Biomolecular Screening* **16**(1): 1-14.
- Sills MA, Weiss D, Pham Q, Schweitzer R, Wu X, Wu JJ (2002). Comparison of Assay Technologies for a Tyrosine Kinase Assay Generates Different Results in High Throughput Screening. *Journal of Biomolecular Screening* **7**(3): 191-214.
- Sittampalam GS, Iversen PW, Boadt JA, Kahl SD, Bright S, Zock JM, *et al.* (1997). Design of Signal Windows in High Throughput Screening Assays for Drug Discovery. *Journal of Biomolecular Screening* **2**(3): 159-169.
- Small EJ, Carducci MA, Burke JM, Rodriguez R, Fong L, van Ummersen L, *et al.* (2006). A Phase I Trial of Intravenous CG7870, a Replication-Selective, Prostate-Specific Antigen-Targeted Oncolytic Adenovirus, for the Treatment of Hormone-Refractory, Metastatic Prostate Cancer. *Mol Ther* **14**(1): 107-117.
- Smith T, Idamakanti N, Kylefjord H, Rollence M, King L, Kaloss M, *et al.* (2002). In vivo hepatic adenoviral gene delivery occurs independently of the coxsackievirus-adenovirus receptor. *Mol Ther* **5**(6): 770-779.
- Snoeys J, Lievens J, Wisse E, Jacobs F, Duimel H, Collen D, *et al.* (2007). Species differences in transgene DNA uptake in hepatocytes after adenoviral transfer correlate with the size of endothelial fenestrae. *Gene Ther* **14**(7): 604-612.
- Sommers CL, Dejarnette JB, Huang K, Lee J, El-Khoury D, Shores EW, *et al.* (2000). Function of Cd3 ϵ -Mediated Signals in T Cell Development. *The Journal of Experimental Medicine* **192**(6): 913-920.
- Spjut S, Qian W, Bauer J, Storm R, Frängsmyr L, Stehle T, *et al.* (2011). A Potent Trivalent Sialic Acid Inhibitor of Adenovirus Type 37 Infection of Human Corneal Cells. *Angewandte Chemie International Edition* **50**(29): 6519-6521.
- Stankiewicz-Drogoń A, Dörner B, Erker T, Boguszewska-Chachulska AM (2010). Synthesis of New Acridone Derivatives, Inhibitors of NS3 Helicase, Which Efficiently and Specifically Inhibit Subgenomic HCV Replication. *Journal of Medicinal Chemistry* **53**(8): 3117-3126.
- Stankiewicz-Drogon A, Palchykovska LG, Kostina VG, Alexeeva IV, Shved AD, Boguszewska-Chachulska AM (2008). New acridone-4-carboxylic acid derivatives as potential inhibitors of Hepatitis C virus infection. *Bioorganic & Medicinal Chemistry* **16**(19): 8846-8852.

- Stanley TB, Jin D-Y, Lin P-J, Stafford DW (1999). The Propeptides of the Vitamin K-dependent Proteins Possess Different Affinities for the Vitamin K-dependent Carboxylase. *Journal of Biological Chemistry* **274**(24): 16940-16944.
- Stanton C, Wallin R (1992). Processing and trafficking of clotting factor X in the secretory pathway. Effects of warfarin. *Biochem J* **284** (Pt 1): 25-31.
- Stassens P, Bergum PW, Gansemans Y, Jespers L, Laroche Y, Huang S, *et al.* (1996). Anticoagulant repertoire of the hookworm *Ancylostoma caninum*. *Proceedings of the National Academy of Sciences* **93**(5): 2149-2154.
- Stewart PL, Burnett RM, Cyrklaff M, Fuller SD (1991). Image reconstruction reveals the complex molecular organization of adenovirus. *Cell* **67**(1): 145-154.
- Stewart PL, Fuller SD, Burnett RM (1993). Difference imaging of adenovirus: bridging the resolution gap between X-ray crystallography and electron microscopy. *EMBO J* **12**(7): 2589-2599.
- Stone D, Liu Y, Shayakhmetov D, Li Z-Y, Ni S, Lieber A (2007). Adenovirus-Platelet Interaction in Blood Causes Virus Sequestration to the Reticuloendothelial System of the Liver. *J. Virol.* **81**(9): 4866-4871.
- Storch E, Kirchner H, Brehm G, Huller K, Marcucci F (1986). Production of interferon-beta by murine T-cell lines induced by 10-carboxymethyl-9-acridanone. *Scand J Immunol* **23**(2): 195-199.
- Straussberg R, Harel L, Levy Y, Amir J (2001). A Syndrome of Transient Encephalopathy Associated With Adenovirus Infection. *Pediatrics* **107**(5): e69.
- Strunze S, Engelke Martin F, Wang IH, Puntener D, Boucke K, Schleich S, *et al.* (2011). Kinesin-1-Mediated Capsid Disassembly and Disruption of the Nuclear Pore Complex Promote Virus Infection. *Cell host & microbe* **10**(3): 210-223.
- Subr V, Kostka L, Selby-Milic T, Fisher K, Ulbrich K, Seymour LW, *et al.* (2009). Coating of adenovirus type 5 with polymers containing quaternary amines prevents binding to blood components. *Journal of Controlled Release* **135**(2): 152-158.
- Sumida SM, Truitt DM, Lemckert AAC, Vogels R, Custers JHHV, Addo MM, *et al.* (2005). Neutralising Antibodies to Adenovirus Serotype 5 Vaccine Vectors Are Directed Primarily against the Adenovirus Hexon Protein. *The Journal of Immunology* **174**(11): 7179-7185.
- Summerford C, Samulski RJ (1998). Membrane-Associated Heparan Sulfate Proteoglycan Is a Receptor for Adeno-Associated Virus Type 2 Virions. *Journal of Virology* **72**(2): 1438-1445.
- Suomalainen M, Nakano MY, Boucke K, Keller S, Greber UF (2001). Adenovirus-activated PKA and p38/MAPK pathways boost microtubule-mediated nuclear targeting of virus. *EMBO J* **20**(6): 1310-1319.
- Suomalainen M, Nakano MY, Keller S, Boucke K, Stidwill RP, Greber UF (1999). Microtubule-dependent Plus- and Minus End-directed Motilities Are Competing Processes for Nuclear Targeting of Adenovirus. *The Journal of Cell Biology* **144**(4): 657-672.

Sutherland MR, Friedman HM, Pryzdial ELG (2007). Thrombin enhances herpes simplex virus infection of cells involving protease-activated receptor 1. *Journal of Thrombosis and Haemostasis* **5**(5): 1055-1061.

Sutherland MR, Ruf W, Pryzdial ELG (2012). Tissue factor and glycoprotein C on herpes simplex virus type 1 are protease-activated receptor 2 cofactors that enhance infection. *Blood* **119**(15): 3638-3645.

Suttie JW, Hoskins JA, Engelke J, Hopfgartner A, Ehrlich H, Bang NU, *et al.* (1987). Vitamin K-dependent carboxylase: possible role of the substrate "propeptide" as an intracellular recognition site. *Proceedings of the National Academy of Sciences* **84**(3): 634-637.

Swart R, Ruf IK, Sample J, Longnecker R (2000). Latent Membrane Protein 2A-Mediated Effects on the Phosphatidylinositol 3-Kinase/Akt Pathway. *Journal of Virology* **74**(22): 10838-10845.

Tang P, Cao C, Xu M, Zhang L (2007). Cytoskeletal protein radixin activates integrin α M β 2 by binding to its cytoplasmic tail. *FEBS Letters* **581**(6): 1103-1108.

Taniguchi K, Yoshihara S, Tamaki H, Fujimoto T, Ikegame K, Kaida K, *et al.* (2012). Incidence and treatment strategy for disseminated adenovirus disease after haploidentical stem cell transplantation. *Ann Hematol.*

Tao N, Gao G-P, Parr M, Johnston J, Baradet T, Wilson JM, *et al.* (2001). Sequestration of Adenoviral Vector by Kupffer Cells Leads to a Nonlinear Dose Response of Transduction in Liver. *Mol Ther* **3**(1): 28-35.

Thompson S, Messick T, Schultz DC, Reichman M, Lieberman PM (2010). Development of a High-Throughput Screen for Inhibitors of Epstein-Barr Virus EBNA1. *Journal of Biomolecular Screening* **15**(9): 1107-1115.

Thuillier L, Hivroz C, Fagard R, Andreoli C, Mangeat P (1994). Ligation of CD4 Surface Antigen Induces Rapid Tyrosine Phosphorylation of the Cytoskeletal Protein Ezrin. *Cellular Immunology* **156**(2): 322-331.

Tim M (1983). Rapid colorimetric assay for cellular growth and survival: Application to proliferation and cytotoxicity assays. *Journal of Immunological Methods* **65**(1-2): 55-63.

Tollefson AE, Ryerse JS, Scaria A, Hermiston TW, Wold WSM (1996). The E3-11.6-kDa Adenovirus Death Protein (ADP) Is Required for Efficient Cell Death: Characterization of Cells Infected with adp Mutants. *Virology* **220**(1): 152-162.

Tomko RP, Xu R, Philipson L (1997). HCAR and MCAR: The human and mouse cellular receptors for subgroup C adenoviruses and group B coxsackieviruses. *Proceedings of the National Academy of Sciences* **94**(7): 3352-3356.

Trask OJ, Nickischer D, Burton A, Williams RG, Kandasamy RA, Johnston PA, *et al.* (2009). High-Throughput Automated Confocal Microscopy Imaging Screen of a Kinase-Focused Library to Identify p38 Mitogen-Activated Protein Kinase Inhibitors Using the GE InCell 3000 Analyzer

- High Throughput Screening. In: Janzen WP, Bernasconi P (ed)^(eds), edn, Vol. 565: Humana Press 159-186.
- Trotman LC, Mosberger N, Fornerod M, Stidwill RP, Greber UF (2001). Import of adenovirus DNA involves the nuclear pore complex receptor CAN/Nup214 and histone H1. *Nat Cell Biol* **3**(12): 1092-1100.
- Tsai V, Varghese R, Ravindran S, Ralston R, Vellekamp G (2008). Complement component C1q and anti-hexon antibody mediate adenovirus infection of a CAR-negative cell line. *Viral Immunol* **21**(4): 469-476.
- Tsuchida S, Yanagi S, Inatome R, Ding J, Hermann P, Tsujimura T, *et al.* (2000). Purification of a 72-kDa Protein-Tyrosine Kinase from Rat Liver and Its Identification as Syk: Involvement of Syk in Signaling Events of Hepatocytes. *Journal of Biochemistry* **127**(2): 321-327.
- Tsujimura T, Yanagi S, Inatome R, Takano T, Ishihara I, Mitsui N, *et al.* (2001). Syk protein-tyrosine kinase is involved in neuron-like differentiation of embryonal carcinoma P19 cells. *FEBS letters* **489**(2): 129-133.
- Ulanova M, Puttagunta L, Marcet-Palacios M, Duszyk M, Steinhoff U, Duta F, *et al.* (2005). Syk tyrosine kinase participates in β 1-integrin signaling and inflammatory responses in airway epithelial cells. *American Journal of Physiology - Lung Cellular and Molecular Physiology* **288**(3): L497-L507.
- Ulrych E, Dzieciatkowski T, Przybylski M, Zduńczyk D, Boguradzki P, Torosian T, *et al.* (2011). Disseminated Adenovirus Disease in Immunocompromised Patient Successfully Treated with Oral Ribavirin: A Case Report. *Archivum Immunologiae et Therapiae Experimentalis* **59**(6): 473-477.
- van Oostrum J, Burnett RM (1985). Molecular composition of the adenovirus type 2 virion. *Journal of Virology* **56**(2): 439-448.
- Van Rooijen N, Sanders A (1996). Kupffer cell depletion by liposome-delivered drugs: comparative activity of intracellular clodronate, propamidine, and ethylenediaminetetraacetic acid. *Hepatology* **23**(5): 1239-1243.
- van Rooijen N, van Kesteren-Hendriks E (2003). "In vivo" depletion of macrophages by liposome-mediated "suicide". *Methods Enzymol* **373**: 3-16.
- Vandenberghe LH, Bell P, Maguire AM, Cearley CN, Xiao R, Calcedo R, *et al.* (2011). Dosage Thresholds for AAV2 and AAV8 Photoreceptor Gene Therapy in Monkey. *Science Translational Medicine* **3**(88): 88ra54.
- Varnavski AN, Calcedo R, Bove M, Gao G, Wilson JM (2005). Evaluation of toxicity from high-dose systemic administration of recombinant adenovirus vector in vector-naive and pre-immunised mice. *Gene Ther* **12**(5): 427-436.
- Venkateswarlu D, Perera L, Darden T, Pedersen LG (2002). Structure and dynamics of zymogen human blood coagulation factor X. *Biophys J* **82** (3): 1190-1206.

- Verdino P, Witherden DA, Havran WL, Wilson IA (2010). The Molecular Interaction of CAR and JAML Recruits the Central Cell Signal Transducer PI3K. *Science* **329**(5996): 1210-1214.
- Vigant F, Descamps D, Jullienne B, Esselin S, Connault E, Opolon P, *et al.* (2008). Substitution of Hexon Hypervariable Region 5 of Adenovirus Serotype 5 Abrogates Blood Factor Binding and Limits Gene Transfer to Liver. *Mol Ther* **16**(8): 1474-1480.
- Vigne E, Mahfouz I, Dedieu J-F, Brie A, Perricaudet M, Yeh P (1999). RGD Inclusion in the Hexon Monomer Provides Adenovirus Type 5-Based Vectors with a Fiber Knob-Independent Pathway for Infection. *J. Virol.* **73**(6): 5156-5161.
- Von Seggern DJ, Kehler J, Endo RI, Nemerow GR (1998). Complementation of a fibre mutant adenovirus by packaging cell lines stably expressing the adenovirus type 5 fibre protein. *Journal of General Virology* **79**(6): 1461-1468.
- Vrancken Peeters MJ, Perkins AL, Kay MA (1996). Method for multiple portal vein infusions in mice: quantitation of adenovirus-mediated hepatic gene transfer. *Biotechniques* **20**(2): 278-285.
- Waddington SN, McVey JH, Bhella D, Parker AL, Barker K, Atoda H, *et al.* (2008). Adenovirus Serotype 5 Hexon Mediates Liver Gene Transfer. *Cell* **132**(3): 397-409.
- Waddington SN, Parker AL, Havenga M, Nicklin SA, Buckley SMK, McVey JH, *et al.* (2007). Targeting of Adenovirus Serotype 5 (Ad5) and 5/47 Pseudotyped Vectors In Vivo: Fundamental Involvement of Coagulation Factors and Redundancy of CAR Binding by Ad5. *J. Virol.* **81**(17): 9568-9571.
- Walters RW, Freimuth P, Moninger TO, Ganske I, Zabner J, Welsh MJ (2002). Adenovirus Fiber Disrupts CAR-Mediated Intercellular Adhesion Allowing Virus Escape. *Cell* **110**(6): 789-799.
- Wan Y, Kurosaki T, Huang X-Y (1996). Tyrosine kinases in activation of the MAP kinase cascade by G-protein-coupled receptors. *Nature* **380**(6574): 541-544.
- Wang H, Beyer I, Persson J, Song H, Li Z, Richter M, *et al.* (2012). A new human DSG2-transgenic mouse model for studying the tropism and pathology of human adenoviruses. *Journal of Virology*.
- Wang H, Li Z-Y, Liu Y, Persson J, Beyer I, Moller T, *et al.* (2011). Desmoglein 2 is a receptor for adenovirus serotypes 3, 7, 11 and 14. *Nat Med* **17**(1): 96-104.
- Wang H, Liu Y, Li Z, Tuve S, Stone D, Kalyushniy O, *et al.* (2008). In Vitro and In Vivo Properties of Adenovirus Vectors with Increased Affinity to CD46. *J. Virol.* **82**(21): 10567-10579.
- Wang Q, Greenburg G, Bunch D, Farson D, Finer MH (1997). Persistent transgene expression in mouse liver following in vivo gene transfer with a delta E1/delta E4 adenovirus vector. *Gene Ther* **4**(5): 393-400.
- Wang X, Bergelson JM (1999). Coxsackievirus and Adenovirus Receptor Cytoplasmic and Transmembrane Domains Are Not Essential for Coxsackievirus and Adenovirus Infection. *J. Virol.* **73**(3): 2559-2562.

- Warnock JN, Daigre C, Al-Rubeai M (2011). Introduction to Viral Vectors
Viral Vectors for Gene Therapy. In: Merten O-W, Al-Rubeai M (ed)^(eds), edn, Vol. 737:
Humana Press. p[^]pp 1-25.
- Webster A, Russell S, Talbot P, Russell WC, Kemp GD (1989). Characterization of the
Adenovirus Proteinase: Substrate Specificity. *Journal of General Virology* **70**(12): 3225-
3234.
- Weigel S, Dobbelstein M (2000). The Nuclear Export Signal within the E4orf6 Protein of
Adenovirus Type 5 Supports Virus Replication and Cytoplasmic Accumulation of Viral
mRNA. *Journal of Virology* **74**(2): 764-772.
- Wickham TJ, Mathias P, Cheresch DA, Nemerow GR (1993). Integrins α v β 3 and
 α v β 5 promote adenovirus internalization but not virus attachment. *Cell* **73**(2):
309-319.
- Wisse E, de Zanger RB, Charels K, van der Smissen P, McCuskey RS (1985). The liver
sieve: Considerations concerning the structure and function of endothelial fenestrae, the
sinusoidal wall and the space of disse. *Hepatology* **5**(4): 683-692.
- Wisse E, Jacobs F, Topal B, Frederik P, De Geest B (2008). The size of endothelial
fenestrae in human liver sinusoids: implications for hepatocyte-directed gene transfer.
Gene Ther **15**(17): 1193-1199.
- Witherden DA, Verdino P, Rieder SE, Garijo O, Mills RE, Teyton L, *et al.* (2010). The
Junctional Adhesion Molecule JAML Is a Costimulatory Receptor for Epithelial $\gamma\delta$ T Cell
Activation. *Science* **329**(5996): 1205-1210.
- Wodrich H, Henaff D, Jammart B, Segura-Morales C, Seelmeir S, Coux O, *et al.* (2010). A
Capsid-Encoded PPxY-Motif Facilitates Adenovirus Entry. *PLoS Pathog* **6**(3): e1000808.
- Wolff G, Worgall S, van Rooijen N, Song W, Harvey B, Crystal R (1997). Enhancement
of in vivo adenovirus-mediated gene transfer and expression by prior depletion of tissue
macrophages in the target organ. *J. Virol.* **71**(1): 624-629.
- Worgall S, Wolff G, Falck-Pedersen E, Crystal RG (1997). Innate Immune Mechanisms
Dominate Elimination of Adenoviral Vectors Following In Vivo Administration. *Human
Gene Therapy* **8**(1): 37-44.
- Xia D, Henry LJ, Gerard RD, Deisenhofer J (1994). Crystal structure of the receptor-
binding domain of adenovirus type 5 fiberprotein at 1.7 Å resolution. *Structure* **2**(12):
1259-1270.
- Xiang Z, Li Y, Cun A, Yang W, Ellenberg S, Switzer WM, *et al.* (2006). Chimpanzee
adenovirus antibodies in humans, sub-Saharan Africa. *Emerg Infect Dis* **12**(10): 1596-
1599.
- Xu Z, Tian J, Smith JS, Byrnes AP (2008). Clearance of Adenovirus by Kupffer Cells Is
Mediated by Scavenger Receptors, Natural Antibodies, and Complement. *J. Virol.* **82**(23):
11705-11713.

- Yabiku ST, Yabiku MM, Bottós KM, Araújo AL, Freitas Dd, Belfort Jr. R (2011). Uso de ganciclovir 0,15% gel para tratamento de ceratoconjuntivite adenoviral. *Arquivos Brasileiros de Oftalmologia* **74**: 417-421.
- Yamada T, Fujieda S, Yanagi S, Yamamura H, Inatome R, Sunaga H, *et al.* (2001). Protein-Tyrosine Kinase Syk Expressed in Human Nasal Fibroblasts and Its Effect on RANTES Production. *The Journal of Immunology* **166**(1): 538-543.
- Yamamoto N, Takeshita K, Shichijo M, Kokubo T, Sato M, Nakashima K, *et al.* (2003). The Orally Available Spleen Tyrosine Kinase Inhibitor 2-[7-(3,4-Dimethoxyphenyl)-imidazo[1,2-c]pyrimidin-5-ylamino]nicotinamide Dihydrochloride (BAY 61-3606) Blocks Antigen-Induced Airway Inflammation in Rodents. *Journal of Pharmacology and Experimental Therapeutics* **306**(3): 1174-1181.
- Yanagi S, Inatome R, Ding J, Kitaguchi H, Tybulewicz VLJ, Yamamura H (2001). Syk expression in endothelial cells and their morphologic defects in embryonic Syk-deficient mice. *Blood* **98**(9): 2869-2871.
- Yang Y, Ertl HCJ, Wilson JM (1994a). MHC class I-restricted cytotoxic T lymphocytes to viral antigens destroy hepatocytes in mice infected with E1-deleted recombinant adenoviruses. *Immunity* **1**(5): 433-442.
- Yang Y, Nunes FA, Berencsi K, Furth EE, Gönczöl E, Wilson JM (1994b). Cellular immunity to viral antigens limits E1-deleted adenoviruses for gene therapy. *Proceedings of the National Academy of Sciences* **91**(10): 4407-4411.
- Yao X, Yoshioka Y, Morishige T, Eto Y, Narimatsu S, Kawai Y, *et al.* (2011). Tumor Vascular Targeted Delivery of Polymer-conjugated Adenovirus Vector for Cancer Gene Therapy. *Mol Ther* **19**(9): 1619-1625.
- Yarrow JC, Feng Y, Perlman ZE, Kirchhausen T, Mitchison TJ (2003). Phenotypic Screening of Small Molecule Libraries by High Throughput Cell Imaging. *Combinatorial Chemistry & High Throughput Screening* **6**(4): 279-286.
- Youil R, Toner TJ, Su Q, Chen M, Tang A, Bett AJ, *et al.* (2002). Hexon Gene Switch Strategy for the Generation of Chimeric Recombinant Adenovirus. *Human Gene Therapy* **13**(2): 311-320.
- Yudushkin IA, Vale RD (2010). Imaging T-cell receptor activation reveals accumulation of tyrosine-phosphorylated CD3 ζ in the endosomal compartment. *Proceedings of the National Academy of Sciences* **107**(51): 22128-22133.
- Zaiss AK, Lawrence R, Elashoff D, Esko JD, Herschman HR (2011). Differential Effects of Murine and Human Factor X on Adenovirus Transduction via Cell-surface Heparan Sulfate. *Journal of Biological Chemistry* **286**(28): 24535-24543.
- Zaiss AK, Machado HB, Herschman HR (2009). The influence of innate and pre-existing immunity on adenovirus therapy. *Journal of Cellular Biochemistry* **108**(4): 778-790.
- Zarubaev VV, Slita AV, Krivitskaya VZ, Sirotkin AK, Kovalenko AL, Chatterjee NK (2003). Direct antiviral effect of cycloferon (10-carboxymethyl-9-acridanone) against adenovirus type 6 in vitro. *Antiviral Research* **58**(2): 131-137.

Zhang J-H, Chung TDY, Oldenburg KR (1999). A Simple Statistical Parameter for Use in Evaluation and Validation of High Throughput Screening Assays. *Journal of Biomolecular Screening* **4**(2): 67-73.

Zhijin Wu, Dongmei Liu, Yunxia Sui (2008). Quantitative Assessment of Hit Detection and Confirmation in Single and Duplicate High-Throughput Screenings. *Journal of Biomolecular Screening* **13**(2): 159-167.

Zhu J, Huang X, Yang Y (2007). Innate Immune Response to Adenoviral Vectors Is Mediated by both Toll-Like Receptor-Dependent and -Independent Pathways. *Journal of Virology* **81**(7): 3170-3180.

Zinn KR, Szalai AJ, Stargel A, Krasnykh V, Chaudhuri TR (2004). Bioluminescence imaging reveals a significant role for complement in liver transduction following intravenous delivery of adenovirus. *Gene Ther* **11**(19): 1482-1486.

Zubieta C, Schoehn G, Chroboczek J, Cusack S (2005). The Structure of the Human Adenovirus 2 Penton. *Molecular cell* **17**(1): 121-135.

Appendices

Appendix 1

List of the 80 compounds from the Pharmacological Diversity Drug-like Set library chosen for initial screening in Chapter 5.

Appendix 2

Duffy MR, Parker AL, Bradshaw AC, Baker AH (2012). Manipulation of adenovirus interactions with host factors for gene therapy applications. *Nanomedicine* 7(2): 271-288

Appendix 3

Duffy MR, Bradshaw AC, Parker AL, McVey JH, Baker AH (2011). A Cluster of Basic Amino Acids in the Factor X Serine Protease Mediates Surface Attachment of Adenovirus/FX Complexes. *Journal of Virology* 85(20): 10914-10919

Appendix 1. 80 compound subset from the Pharmacological Diversity Drug-like Set library

Compound I.D.	Molecular weight
T6157156	479.60
T6147393	278.10
T6157679	209.3
T5797151	356.43
T6045662	256.34
T5938260	368.34
T5243644	280.37
T6005553	275.32
T5888802	413.34
T5895535	190.16
T5982390	378.78
T6090409	315.37
T5786618	204.25
T5786988	354.4
T5786231	273.26
T6195375	404.25
T6205233	215.72
T6205606	293.40
T6037038	264.24
T6538287	323.44
T6260188	125.12
T6296542	167.63
T6530803	272.78
T6531308	334.05
T6391409	189.21
T6394162	277.34
T5666758	317.36
T6467204	314.23
T6465064	254.46
T6464837	206.29
T6456691	205.64
T6449216	209.27
T6421771	193.19
T6426611	332.74
T6437770	289.81
T6466171	270.39
T6475407	234.25
T6486717	216.30
T6494910	205.75
T6226934	193.17
T6339082	258.1
T6330125	220.01
T6330009	236.33

T6159723	313.29
T6024950	374.44
T5971725	245.61
T5603728	442.54
T5617403	531.99
T5618922	367.40
T0506-1018	319.24
T5330666	517.60
T0503-2971	358.27
T0501-4889	325.37
T0510-1910	354.45
T0511-5084	476.56
T0514-6922	469.48
T5250021	364.46
T5676844	279.27
T5749380	354.39
T5509594	305.78
T5508544	219.24
T5359005	342.33
T0517-7883	294.42
T0500-2894	328.24
T5419299	306.16
T5240685	326.36
T0519-4248	361.91
T0519-9051	430.52
T0515-0234	173.21
T0516-4802	380.35
T0514-9644	327.47
T5343938	286.29
T5380460	252.17
T0500-5518	379.41
T0501-2198	303.40
T0501-7827	469.53
T0502-2012	276.38
T5473838	455.44
T5474623	230.30
T5476447	262.28